

Analysis of MHC-I homologues in Molluscum Contagiosum and Human Cytomegalovirus

A thesis submitted in candidature for the degree of
DOCTOR OF PHILOSOPHY (PhD) By

Hana A Mohamed Elasifer

December 2018

HCMV and Adenovirus Research Group, Division of Infection and
Immunity, School of Medicine,
Cardiff University,
CF14 4XN, UK

Declaration

STATEMENT 1 This thesis is being submitted in partial fulfilment of the requirements for the degree of ... (insert PhD, MD, MPhil, etc., as appropriate)

Signed _____ Date _____

STATEMENT 2

This work has not been submitted in substance for any other degree or award at this or any other university or place of learning, nor is it being submitted concurrently for any other degree or award (outside of any formal collaboration agreement between the University and a partner organisation)

Signed _____ Date _____

STATEMENT 3

I hereby give consent for my thesis, if accepted, to be available in the University's Open Access repository (or, where approved, to be available in the University's library and for inter-library loan), and for the title and summary to be made available to outside organisations, subject to the expiry of a University-approved bar on access if applicable.

Signed _____ Date _____

DECLARATION

This thesis is the result of my own independent work, except where otherwise stated, and the views expressed are my own. Other sources are acknowledged by explicit references. The thesis has not been edited by a third party beyond what is permitted by Cardiff University's Use of Third-Party Editors by Research Degree Students Procedure.

Signed _____ Date _____

WORD COUNT 35,580 words

(Excluding summary, acknowledgements, declarations, contents pages, appendices, tables, diagrams and figures, references, bibliography, footnotes and endnotes)

Acknowledgements

I would like to express my sincerest gratitude to my supervisors Prof. Gavin Wilkinson, Dr Rebecca Aicheler for the opportunity to study a PhD, and for their constant encouragement, patience and endeavours.

I wholeheartedly thank to Dr Eddie Wang and Dr Joachim Bugert for help and advice, also I am thankful to my colleagues at the Institute of Infection and Immunity for making this PhD a pleasurable experience. Special thanks to Dr Richard Stanton, Dr Mihil Patel and Mrs Dawn Roberts for their ever-present support in the laboratory, Dr James Davies for help with recombineering mc033 and mc080, Dr Simone Forbes and Dr Virginia-Maria Vlachava for NK lines, and Dr Ceri Fielding for HCMV US18 and US20 deletion mutants.

I wish to thank my husband Sean McMahon and my family for their relentless support throughout my studies at University.

Summary

Molluscum contagiosum virus (MOCV) and human cytomegalovirus (HCMV) each encode two MHC-I homologues: mc080 and mc033 in MOCV, UL18 and UL142 in HCMV. Codon optimised versions of the mc080 and mc033 genes were cloned in to a second-generation lentivirus system, vaccinia virus and a replication-deficient adenovirus (Ad) vector. MOCV mc033 and mc080 were expressed from the Ad vector as endoglycosidase H (EndoH) sensitive glycoproteins with apparent molecular weights of 64kDa and 44kDa respectively, both localised predominantly to the ER. MC033 had no effect on either MHC-I or HLA-E expression, nor did it impact NK cells or T cell function. MC080 downregulated cell surface expression of classical HLA-I and HLA-E in a TAP independent, although not MICA/B. This downregulation of HLA-1 correlated with protection against CD8⁺ T cell activation, thus MC080 is here identified as a novel viral T cell evasion function. MC080 was capable of suppressing or activating NK cell, depending on context and consistent with MC080's control of HLA-I and HLA-E.

UL142 expression was enhanced by optimising codon usage and through provision of an alternative leader sequence. Using an Ad vector, UL142 was expressed as a heavily glycosylated 105kDa protein that localised to the ER, cell surface and was released into the supernatant in an EndoH-resistant form. When over-expressed from the Ad vector UL142 suppressed full length MICA, but not in the context of a productive HCMV infection where that function was performed by the US12 gene family. Preliminary allogenic functional NK cell assays showed UL142 to suppress NK cell function in one of four donors. However, cell-associated and secreted UL142 both activated NK cell degranulation when the assay was moved to an autologous setting. The results suggest that UL142 can modulate NK cell function independently of MICA.

Table of contents

| | |
|---------------------------|------|
| Contents Declaration..... | i |
| Acknowledgements..... | ii |
| Summary | iii |
| Contents..... | iv |
| List of tables | vii |
| List of figures..... | viii |
| Abbreviations..... | x |

1- INTRODUCTION1

| | |
|---|----|
| 1.1 DNA VIRUSES: TAXONOMY AND CLASSIFICATION OF MOCV AND HCMV | 2 |
| 1.2 VACCINIA VIRUS FROM VACCINATION VECTOR TO IMMUNE EVASION | 7 |
| 1.3 MOCV GENOME OVERVIEW | 9 |
| 1.4 HCMV GENOME OVERVIEW | 15 |
| 1.5 HCMV AND MOCV IMMUNE EVASION MECHANISMS..... | 20 |
| 1.6 MOCV BIOLOGY..... | 24 |
| 1.6.1 <i>Epidemiology</i> | 27 |
| 1.6.2 <i>Host range and tissue and cell tropism</i> | 28 |
| 1.6.3 <i>Cell culture and animal system</i> | 28 |
| 1.7 HCMV BIOLOGY..... | 29 |
| 1.7.1 <i>HCMV Epidemiology</i> | 30 |
| 1.7.2 <i>Cellular tropism of HCMV in vivo</i> | 32 |
| 1.7.3 <i>HCMV replication</i> | 33 |
| 1.7.4 <i>HCMV propagation in vitro</i> | 35 |
| 1.8 HCMV DOWNREGULATION OF MHC-1..... | 39 |
| 1.9 HCMV NK EVASION FUNCTIONS | 44 |
| 1.10 HCMV MHC-I HOMOLOGUES UL18 & UL142..... | 48 |
| 1.11 MOCV MHC I HOMOLOGUES GENES -MC033 AND MC080..... | 50 |
| 1.12 AIMS | 50 |

2-METHODS AND MATERIALS52

| | |
|---|----|
| 2.1 SOLUTIONS | 53 |
| 2.2 ANTIBODIES..... | 55 |
| 2.3 CELLS..... | 57 |
| 2.3.1 <i>Cell lines</i> | 57 |
| 2.3.2 <i>Tissue culture media</i> | 58 |
| 2.3.3 <i>Cell counting</i> | 59 |
| 2.3.4 <i>Cryopreservation of cell lines</i> | 59 |
| 2.3.5 <i>Thawing cells</i> | 59 |
| 2.4 VIRUSES | 59 |
| 2.4.1 <i>Propagation of Recombinant Adenovirus (RAd) stocks</i> | 60 |
| 2.4.2 <i>Adenovirus purification by Caesium Chloride</i> | 61 |
| 2.4.3 <i>Adenovirus titration</i> | 62 |
| 2.4.4 <i>Growth of HCMV stocks</i> | 62 |
| 2.4.5 <i>HCMV titration by plaque assay</i> | 63 |
| 2.4.6 <i>Lentivirus</i> | 63 |
| 2.4.7 <i>Single infection of cells for assays</i> | 64 |
| 2.4.8 <i>Co-infection of cells for assays</i> | 65 |
| 2.5 MOLECULAR BIOLOGY | 65 |
| 2.5.1 <i>PCR</i> | 65 |

| | |
|---|------------|
| 2.5.2 Agarose gel electrophoresis..... | 66 |
| 2.5.3 Isolation of DNA form an Agarose gel..... | 66 |
| 2.5.4 Determination of DNA concentration..... | 66 |
| 2.5.6 Plasmid DNA minipreps..... | 67 |
| 2.5.7 Plasmid DNA maxiprep..... | 67 |
| 2.5.8 Restriction enzyme digest for pHAGE plasmid cloning..... | 68 |
| 2.5.9 Ligation..... | 68 |
| 2.5.10 Transformation..... | 69 |
| 2.5.11 Amplification and Purification of Plasmid DNA..... | 69 |
| 2.6 TRANSFECTION OF CLONED PLASMIDS..... | 69 |
| 2.7 RECOMBINEERING..... | 70 |
| 2.8 TRANSFECTION OF 293-TREX CELLS WITH ADENOVIRUS BAC DNA..... | 71 |
| 2.9 RESTRICTION ENZYME DIGEST OF BAC..... | 71 |
| 2.10 SANGER SEQUENCING..... | 72 |
| 2.11 ANALYSIS OF PROTEIN EXPRESSION..... | 72 |
| 2.11.1. Immunofluorescence..... | 72 |
| 2.11.2 Immunoblot detection of proteins..... | 73 |
| 2.12. FLOW CYTOMETRY..... | 74 |
| 2.13 INTRACELLULAR STAINING OF FIXED CELLS BY FLOWCYTOMETRY..... | 75 |
| 2.14 ISOLATION OF PBMC..... | 75 |
| 2.15 NK DEGRANULATION ASSAYS..... | 76 |
| 2.16 CD8 ⁺ T CELL CD107A MOBILIZATION ASSAYS:..... | 76 |
| 3-CLONING AND COMPARATIVE EXPRESSION OF MOCV GENES MC080 AND MC033 IN DIFFERENT VIRAL GENE EXPRESSION SYSTEMS..... | 78 |
| 3.1 INTRODUCTION..... | 79 |
| 3.2 ANALYSIS OF mc080 EXPRESSION USING VACCINIA AND ADENOVIRUS VECTOR..... | 80 |
| 3.2.1 Western Blot of cells infected with recombinant adeno and vaccinia viruses..... | 80 |
| 3.3 THE LENTIVIRUS VECTOR..... | 82 |
| 3.3.1 Cloning of mc033 and mc080 into a Lentivirus vector..... | 84 |
| 3.3.2 Cloning of pHAGE mc080 neo and pHAGE mc033 neo..... | 84 |
| 3.3.3 TRE controlled and rtTA constructs..... | 88 |
| 3.3.4 Expression using recombinant lentiviral virions..... | 90 |
| 3.4 CLONING AND EXPRESSION MC033 AND MC080 USING ADENOVIRUS VECTOR- 5 (AdZ-5)..... | 94 |
| 3.4.1 Cloning mc033 and mc080 into AdZ5..... | 95 |
| 3.4.2 Optimizing expression of recombinant deficient adenovirus of mc033 and mc080..... | 95 |
| 3.4.3 The time course expression of RAdmc033 and RAdmc080..... | 98 |
| 3.5 SUMMARY..... | 100 |
| 4- FUNCTIONAL ASSAY OF MC033 AND MC080..... | 101 |
| 4.1: INTRODUCTION..... | 102 |
| 4.2 INTRACELLULAR LOCALISATION OF MC033 AND MC080 AND THEIR EFFECT ON TOTAL MHC I..... | 103 |
| 4.3 EFFECT OF MC033 AND MC080 ON NK CELL ACTIVATION..... | 106 |
| 4.4 MC080 DOWN REGULATES CELL SURFACE MHC CLASS I EXPRESSION..... | 110 |
| 4.5 MC080 DOWNREGULATES HLA-E..... | 112 |
| 4.6 EFFECT OF MC080 ON MICA..... | 116 |
| 4.7 EFFECT OF MC080 ON T-CELL ACTIVATION..... | 118 |
| 4.8 SUMMARY..... | 120 |
| 5-CHARACTERISATION OF HCMV MHC-I HOMOLOGUES UL142..... | 121 |
| 5.1 INTRODUCTION..... | 122 |
| 5.2 EXPRESSION OF UL142 USING AN ADENOVIRUS VECTOR..... | 125 |
| 5.3 WESTERN BLOT ANALYSIS OF UL142 EXPRESSION..... | 129 |
| 5.4 GLYCOSYLATION OF SECRETED AND CELL-ASSOCIATED FORMS OF GPUL142..... | 133 |
| 5.5 UL142 AND SURFACE EXPRESSION OF MICA..... | 138 |
| TABLE 5.2: THE HCMV VIRUSES USED IN THIS CHAPTER..... | 138 |

| | |
|--|------------|
| 5.6 UL142 DOWNREGULATES NK CELL KILLING IN AN ALLOGENIC SETTING USING A DONOR 007 NK LINE..... | 142 |
| 5.7 SUMMARY..... | 146 |
| 6-DISCUSSION..... | 147 |
| 6.1 OPTIMISING EXPRESSION OF MC033L AND MC080R USING VIRAL VECTORS..... | 148 |
| 6.2 MC080 BUT NOT MC033 DOWNREGULATED MHC I AND HLA-E IN A TAP INDEPENDENT WAY..... | 150 |
| 6.3 MC080 MODULATES NK CELL ACTIVATION..... | 152 |
| 6.4 MC080 EXPRESSION IMPAIR CD 8 ⁺ T CELLS ACTIVATION..... | 154 |
| 6.5 OPTIMIZING EXPRESSION OF UL142..... | 154 |
| 6.6 GPUL142 IS EXPRESSED ON THE CELL SURFACE AND MAY BE RELEASED/SECRETED FROM THE CELLS..... | 156 |
| 6.7 UL142 HAS NO EFFECT ON MICA..... | 157 |
| 6.8 UL142 MODULATE NK CELL KILLING..... | 158 |
| 6.9 THE LIMITATIONS AND FUTURE PLANS OF THIS THESIS..... | 160 |
| 7-REFERENCES..... | 163 |
| 8-APPENDIX..... | 190 |
| THE OPTIMIZED MC080R..... | 191 |
| MC080 AMINO ACID SEQUENCE..... | 191 |
| THE OPTIMIZED MC033L..... | 192 |
| MC033 AMINO ACID SEQUENCE..... | 193 |
| PREDICTION OF TRANSMEMBRANE PART AND SIGNAL PEPTIDE..... | 193 |
| MC033 MHC-I HOMOLOGY USING BLASTT AND PHYRE..... | 194 |
| MC080 MHC-I HOMOLOGY USING BLASTT AND PHYRE..... | 196 |
| PRIMERS TO PRODUCE RADMC033 AND RADMC080..... | 198 |
| PCR USING PHUSION® HIGH-FIDELITY DNA POLYMERASE (M0530L, NEW ENGLAND BIOLABS) KIT..... | 198 |
| EXPAND HIGH FIDELITY (HIFI, 11732 641001, ROCHE)/TAQ POLYMERASE..... | 199 |
| UL142 MHC-I HOMOLOGY USING BLASTT AND PHYRE..... | 200 |
| | 200 |

List of tables

| | |
|--|-----|
| Table 1.1: MOCV genes 033 and 080 | 14 |
| Table 1.2: MOCV immune evasion genes | 20 |
| Table 1.3: HCMV immune evasion genes | 22 |
| Table 2.1: The used antibodies in this thesis | 55 |
| Table 2.2: Lasers, excitation wavelength and emission Spectra of fluorochromes used for Flow Cytometry | 57 |
| Table 2.3: HLA and MICA genotypes of the donors | 58 |
| Table 2.4: The viruses used in thesis | 59 |
| Table 2.5: Deglycosylation mixture | 74 |
| Table 3.1: Summary of pHAGE plasmid constructs | 92 |
| Table 5.1: The viruses used in this chapter | 124 |
| Table 5.2: The HCMV viruses used in this chapter | 138 |

List of figures

| | |
|---|-----|
| Figure 1.1: Species phylogenetic tree for the Herpesviridae | 5 |
| Figure 1.2: Gene sequence phylogeny of the family Poxviridae | 6 |
| Figure 1.3: The complete genome of MOCV type I | 11 |
| Figure 1.4: Genome annotation of the low-passage HCMV strain Merlin (GenBank accession NC_006273) | 16 |
| Figure 1.5: Clinical picture of molluscum contagiosum | 25 |
| Figure 1.6: Lifecycle of molluscum contagiosum and local immune responses in infected skin | 26 |
| Figure 1.7: HCMV Gene Expression divided to four or five classes | 36 |
| Figure 1.8: Life cycle of human cytomegalovirus | 37 |
| Figure 1.9: The assembly of MHC class I | 42 |
| Figure 1.10: Downregulation MHC I molecules by HCMV | 43 |
| Figure 3.1: Expression of mc080 from vaccinia and adenovirus vectors | 81 |
| Figure 3.2: The second-generation lentivirus system | 83 |
| Figure 3.3: vNTI virtual constructs of pHAGE plasmids | 85 |
| Figure 3.4: Cloning of mc033 and m080 into the retrovirus vector pHAGE | 85 |
| Figure 3.5: The expression of pHAGE plasmids ILR482 (mc080), ILR485 (mc033) and ILR489 rtTA | 86 |
| Figure 3.6: vNTI virtual constructs of pHAGE IRES neo plasmids | 86 |
| Figure 3.7: Expression of ILR 500 (mc033) and ILR498 (mc080) plasmids | 87 |
| Figure 3.8: The tetON system | 89 |
| Figure 3.9: vNTI virtual constructs of pHAGE (Neo IRES) plasmids | 89 |
| Figure 3.10: vNTI virtual constructs of pHAGE plasmid ILR489 | 91 |
| Figure 3.11: Analysis of expression from Lentivirus particles | 93 |
| Figure 3.12: Virtual construct of MOCV genes cloned into the AdZ vector | 96 |
| Figure 3.13: cloning mc033 and mc080 into AdZ vector | 97 |
| Figure 3.14: Expression of RAdmc033 and RAdmc080 | 97 |
| Figure 3.15: Time point expression of RAdmc033 and RAdmc080HF | 99 |
| Figure 3.16: Flowcytometric analysis of MC033 and MC080 expression | 99 |
| Figure 4.1: MC080 and MC033 are localized predominantly to the ER | 105 |

| | |
|---|-----|
| Figure 4.2: MC080 modulates NK cell activity | 108 |
| Figure 4.3: MC080 downregulates total MHC I | 111 |
| Figure 4.4: Flow cytometric analysis of effect of MC033 and MC080 on surface expression MHC-I | 111 |
| Figure 4.5: Flow cytometric analysis of effect of MC033 and MC080 on surface expression HLAE | 114 |
| Figure 4.6: MC080 downregulate MHC I and HLAE in a TAP independent way | 115 |
| Figure 4.7: MC080 has no effect in surface expression MICA | 117 |
| Figure 4.8: MC080 downregulate CD8 ⁺ T cells | 119 |
| Figure 5.1: Intracellular Expression of UL142 | 127 |
| Figure 5.2: Surface Expression of UL142. 122 | 128 |
| Figure 5.3: Western Blot of expression of UL142 expression from Ad recombinants | 130 |
| Figure 5.4: UL142 is highly glycosylated | 136 |
| Figure 5.5: Effect of RAd UL142 on cell surface expression of MICA | 139 |
| Figure 5.6: Effect of HCMV UL142 on surface expression of MICA | 139 |
| Figure 5.7: UL142 has no effect on surface expression of MICA in CHO cells | 141 |
| Figure 5.8: Effect of UL142 Expression of NK Cell Degranulation | 144 |

SYMBOLS/ACRONYMS/ABBREVIATIONS

| | |
|-------|--|
| °C | degrees Celsius |
| Δ | deletion |
| μM | micromolar |
| μL | microlitre |
| μm | micrometre |
| aa | amino acid |
| AC | Assembly compartment |
| Ad | Adenovirus |
| AIDS | Acquired immunodeficiency syndrome |
| Ab | Antibody |
| AdZ-5 | Adenovirus vector |
| ATP | Adenosine triphosphate |
| ATCC | American Tissue Culture Collection |
| BAC | Bacterial Artificial Chromosome |
| BLAST | Basic Local Alignment Search Tool BM – Bone Marrow |
| bp | base pairs |
| BSA | Bovine Serum Albumin |
| cAMP | Cyclic Adenosine monophosphate |
| CAV | Cell-Associated Virus CD – Cluster of Differentiation |
| CCMV | Chimpanzee Cytomegalovirus |
| CD | Cluster of differentiation |
| CID | Cytomegalic Inclusion Disease cm – centimetre |
| CMV | Cytomegalovirus |
| CPE | Cytopathic Effect |
| CTL | Cytotoxic T lymphocyte |
| Da | Dalton |
| DAB | 3, 3' diaminobenzidine |
| DAPI | 4, 6' diamino-2-phenylindole |
| DMEM | Dulbecco's Modified Eagle's Medium DMSO – Dimethyl Sulfoxide |
| DMSO | Dymethyl sulfoxide |
| DNA | Deoxyribonucleic Acid |
| DNase | Deoxyribonuclease |

| | |
|---------------|--|
| dNTP | Deoxynucleotide Triphosphate |
| DTT | Dithiothreitol |
| DC | Dendritic Cell |
| EC | Endothelial Cell |
| <i>E.Coli</i> | Escherichia coli |
| EDTA | EthyleneDiamineTetraacetic Acid |
| EGFR | Epidermal Growth Factor Receptor |
| EM | Electron Microscopy |
| ER | Endoplasmic Reticulum |
| FADD | Fas-Associated Death Domain |
| FBS | Fetal Bovine serum |
| g | Gravity |
| GM-CSF | Granulocyte Macrophage Colony-Stimulating Factor |
| gp | Glycoprotein |
| gH | Glycoprotein H |
| gL | Glycoprotein L |
| hCAR | Human Coxsackievirus-Adenovirus-Receptor |
| HCMV | Human Cytomegalovirus |
| HF | Human Fibroblast |
| HFFF | Human Foetal Foreskin Fibroblast |
| HHV | Human Herpesvirus |
| HRP | Horseradish Peroxidase |
| h(s) | Hour(s) |
| hTERT | Human Telomerase Reverse Transcriptase |
| IF | Immuno-Fluorescence |
| IFN- β | Interferon Beta |
| IFN- γ | Interferon Gamma |
| Ig | Immunoglobulin |
| IKK | Inhibitor of kappa B Kinase |
| IL2 | Interleukin 2 |
| IL6 | Interleukin 6 |
| IE/ α | Immediate Early |
| IPTG | Isopropyl β -D-1-thiogalactopyranoside |
| IRES | Internal Ribosome Entry Site |

| | |
|---------|--|
| IRF | Interferon Regulatory Factor |
| IRL/IRL | Internal Repeat Long |
| IRS/IRS | Internal Repeat Short |
| JAK | Janus kinase |
| Kb | Kilobase |
| Kbp | Kilobase pairs |
| KDa | Kilodalton |
| KV | Kilovolt |
| L | Litre |
| L/γ | Late |
| LB | Luria's Broth |
| M | Molar (moles per litre) |
| mAb | Monoclonal Antibody |
| MAVS | Mitochondrial Antiviral-Signalling |
| MCMV | Murine Cytomegalovirus |
| MEM | Minimal Eagle's Medium |
| mg | Milligram |
| MHC | Major Histocompatibility Complex |
| MICA | MHC class I polypeptide-related sequence A |
| MICB | MHC class I polypeptide-related sequence B |
| min(s) | Minutes |
| miRNA | Micro RNA |
| ml | Millilitre |
| mM | Millimolar |
| MOI | Multiplicity of Infection |
| mRNA | Messenger RNA |
| NK cell | Natural Killer cell |
| NKG2D | Natural killer group 2, member D |
| NKG2DL | Natural killer group 2, member D ligand |
| NP40 | Nonyl phenoxypolyethoxylethanol-40 |
| NPHS | National Public Health Service |
| nm | Nanometre |
| OD | Optical Density |
| ORF | Open Reading Frame |

| | |
|---------|--|
| PAGE | Polyacrylamide Gel Electrophoresis |
| PBMC | Peripheral blood mononuclear cell |
| PBS | Phosphate Buffered Saline |
| PBS-T | Phosphate Buffer Saline + tween 20 |
| PCR | Polymerase Chain Reaction |
| PEG | Polyethylene glycol |
| PFA | Paraformaldehyde |
| PFU | Plaque forming units |
| PHLS | Public Health Laboratory Service |
| p.i. | Post infection |
| PMNL | Polymorphonuclear Leukocyte |
| RAAd | Recombinant adenovirus |
| RB | Retinoblastoma |
| RCMV | Rat Cytomegalovirus |
| RhCMV | Rhesus Cytomegalovirus |
| RAAdZ | Recombinant Adenovirus Vector |
| RNA | Ribonucleic acid |
| RPM | Revolutions per minute |
| RT-PCR | Reverse Transcriptase PCR |
| SCMV | Simian Cytomegalovirus |
| SDS | Sodium dodecyl sulphate |
| SLAM | Signalling lymphocyte-activation molecule |
| siRNA | Small inhibitory RNA |
| STAT | Signal Transducers and Activators of Transcription |
| TAP | Transporter associated with antigen processing |
| TAE | Tris-acetate-EDTA |
| TBK | TANK-binding kinase |
| tet | Tetracycline |
| TM | Transmembrane |
| TNF | Tumour Necrosis Factor |
| TNFR | Tumour Necrosis Factor Receptor |
| TRL/TRL | Terminal Repeat Long |
| TRS/TRS | Terminal Repeat Short |
| TRAIL | TNF related apoptosis-inducing ligand |

| | |
|-------|---|
| TREX | Tetracycline repressor protein |
| ULBP | UL16-binding protein |
| UL/UL | Unique Long |
| US/US | Unique Short |
| UV | Ultraviolet V – Volts |
| VAC | Virus Assembly Compartment |
| VACV | Vaccinia virus |
| VARV | Variola virus |
| VEP | Virion Egress Protein |
| X-gal | 5-bromo-4-chloro-3-indolyl-beta-D-galacto-pyranoside. |

1- Introduction

1.1 DNA viruses: Taxonomy and Classification of MOCV and HCMV

Viruses have relatively small genomes and their genes tend to be mainly involved in functions essential for efficient replication, including receptor recognition to promote entry into cells, enzymes involved in the transcription and replication of the viral genome and structural proteins required for the formation of new virus particles. Some viruses, like papilloma virus, have very small genomes with less than 10 open reading frames, whilst relatively large mammalian viruses can encode well over a hundred gene products; most notably poxviruses and members of the *Herpesviridae*. The *Poxviridae* is a family of enveloped double stranded DNA viruses that have been isolated from a large number of vertebrate or invertebrate hosts (Fields et al. 2013). Poxviruses replicate in the cytoplasm and encode many proteins needed for macromolecular precursor pool regulation, biosynthetic processes. Also, these viruses have a complex morphogenesis, which involves the de novo synthesis of virus-specific membranes and inclusion bodies. Interestingly, these viruses encode many immune evasion proteins which interact with host processes at both the cellular and systemic levels. The most notorious member of the *Poxviridae* is the causative agent of smallpox, variola virus (VARV), which although now eradicated from human populations worldwide is still retained in two high containment facilities; one in the United States and the other Russian Federation. Poxviruses infections are generally acute, molluscum contagiosum virus (MOCV) is an exception, and commonly infect the epidermis directly (e.g. VARV, MOCV) but can also be transmitted by the oral route, e.g. ectromelia in mice (Buller and Palumbo 1991; Fields et al. 2013). Like Poxviruses, members of the *Herpesviridae* are also large enveloped double-stranded DNA viruses that are distributed across a wide range of vertebrates and invertebrates. However, herpesviruses genomic replication and encapsidation takes place in the nucleus. In contrast to poxviruses that are associated primarily with short term acute infections, herpesviruses invariably establish lifelong persistent or latent infections which the host immune response is unable to clear; the site of latency/persistence in the host does vary. MOCV is unusual in being a poxvirus that causes a benign skin tumour capable of persisting for months or years, although the infection is ultimately

eliminated. Some herpesviruses are also associated with malignancy (e.g. EBV, KSHV), yet even if the herpesvirus malignancy is controlled the virus infection will persist. (Buller and Palumbo 1991; Elliott and O'Hare 2000; Sinzger et al. 2000; Alba et al. 2001).

Herpesviruses (HV) have been classified into three subfamilies: the *Alphaherpesvirinae*, *Betaherpesvirinae*, and *Gammapherpesvirinae*, this classification based in differences in the cellular tropism, genome organization, and gene content. All herpesviruses families are thought to have a common ancestral HV species, as judged by extensive equivalences in their gene complements. The herpesvirus genome encodes between ~70 to 173 proteins. Although numbers vary depending on the analysis, the best estimate currently is that human cytomegalovirus (HCMV, HHV-5) contains about 173 canonical protein coding genes (Alba et al. 2001; Davison et al. 2003b; Murphy et al. 2003; Dolan et al. 2004; Gatherer et al. 2011) Phylogenetic analysis helps in the classification of viruses and assessing the relationships between different viruses and their genes. Phylogenetic trees can be constructed based upon numbers of shared genes between completely sequenced virus genomes, the functionally related proteins usually have shared conserved sequence motifs (Fitz-Gibbon and House 1999; Snel et al. 1999).

The family Herpesviridae consists of viruses belong to the *Alpha*-, *Beta*- and *Gammapherpesvirinae* subfamilies that can be classified on the basis of their sequence similarity and gene content; these comprise all characterized HVs identified in mammalian, avian and reptilian hosts (figure 1.1). A new family, the *Alloherpesviridae* will be assigned for a group of piscine and amphibian HVs, while the invertebrate HVs will be assigned to *Malacoherpesviridae*. A new higher-level taxon, the order *Herpesvirales* includes *Alpha*-, *Beta*- and *Gammapherpesvirinae* subfamilies. The wide sequence comparison between the genome of HV subfamilies reveals at least 26 conserved open reading frames (ORFs) (McGeoch et al. 2006) that encode a diverse range of functions required for packaging of the viral genome, replication, or transcription, also, the ORFs that involved in the formation of virus structure, like nucleocapsid and glycoprotein spikes. A third of known ORF of viral protein of Alpha and Gamma-herpes viruses are conserved, yet a lower proportion of the *Betaherpesvirinae* because of their larger genomes (Alba et al. 2001). *The*

Betaherpesvirinae is divided further to four genera: *Cytomegalovirus*, *Muromegalovirus*, *Roseolovirus* and *Proboscivirus*. The genus *Cytomegalovirus* includes human cytomegalovirus (HCMV; species, Human herpesvirus 5), rhesus cytomegalovirus (RhCMV; species, Macacine herpesvirus 3), and chimpanzee cytomegalovirus (CCMV; species, Panine herpesvirus 2). The genus *Muromegalovirus* comprises murine cytomegalovirus (MCMV; species, Murid herpesvirus 1) and rat cytomegalovirus (RCMV; species, Murid herpesvirus 2) (Davison et al. 2009). While the herpesviruses all establish life-long persistent infections, they have undergone divergent speciation during co-evolution with their respective hosts that can readily be tracked by a comparison of their genomes (McGeoch et al. 1995; McGeoch et al. 2000). HCMV naturally infects only humans, and its success in host species is closely associated with the acquisition of mechanisms to evade or subvert the human host immune response (Wilkinson et al. 2015)

Over fifty complete genome sequences of poxviruses are available in online databases. The *Poxviridae* are classified into two subfamilies according to host range. Viruses classified under the *Chordopoxvirinae* infect vertebrates and members of the *Entomopoxvirinae* infect insects. (Lefkowitz et al. 2006). The *Chordopoxvirinae* are divided into eight genera (*Orthopoxvirus*, *Parapoxvirus*, *Avipoxvirus*, *Capripoxvirus*, *Leporipoxvirus*, *Suipoxvirus*, *Molluscipoxvirus*, and *Yatapoxvirus*), while the *Entomopoxvirinae* are divided into three genera (*Entomopoxvirus A*, *Entomopoxvirus B* and *Entomopoxvirus C*) (figure 1.2). The members of the same genus are genetically and antigenically related, besides they have similar morphology. The genus *Orthopoxvirus* has been the subject of intense investigation as it includes both VARV and Vaccinia virus (VACV). *Ectromelia virus* and *Rabbitpox virus* (closely related to VACV) are been studied as animal models for smallpox; they are highly virulent for mice and rabbits respectively (Smee and Sidwell 2003; Schriewer et al. 2004).

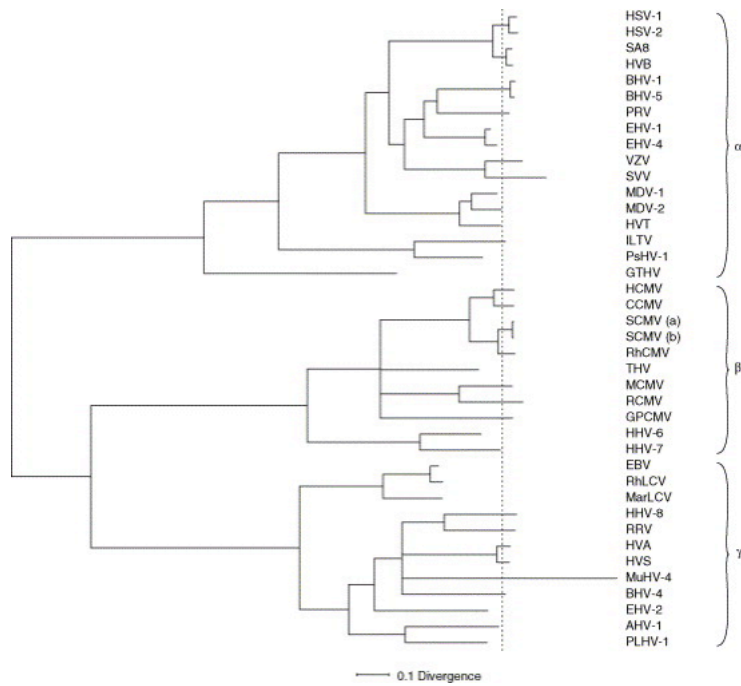


Figure 1.1: Species phylogenetic tree for the Herpesviridae. Based on alignment of amino acid sequences of six genes from 40 HV species, the phylogenetic tree was constructed. In the *Betaherpesvirinae*, HCMV is most closely related to Chimpanzee cytomegalovirus (CCMV) and the Simian CMVs (SCMV). 0.1 divergence means 10 % differences in amino acid sequences between two species. (McGeoch et al. 2006)

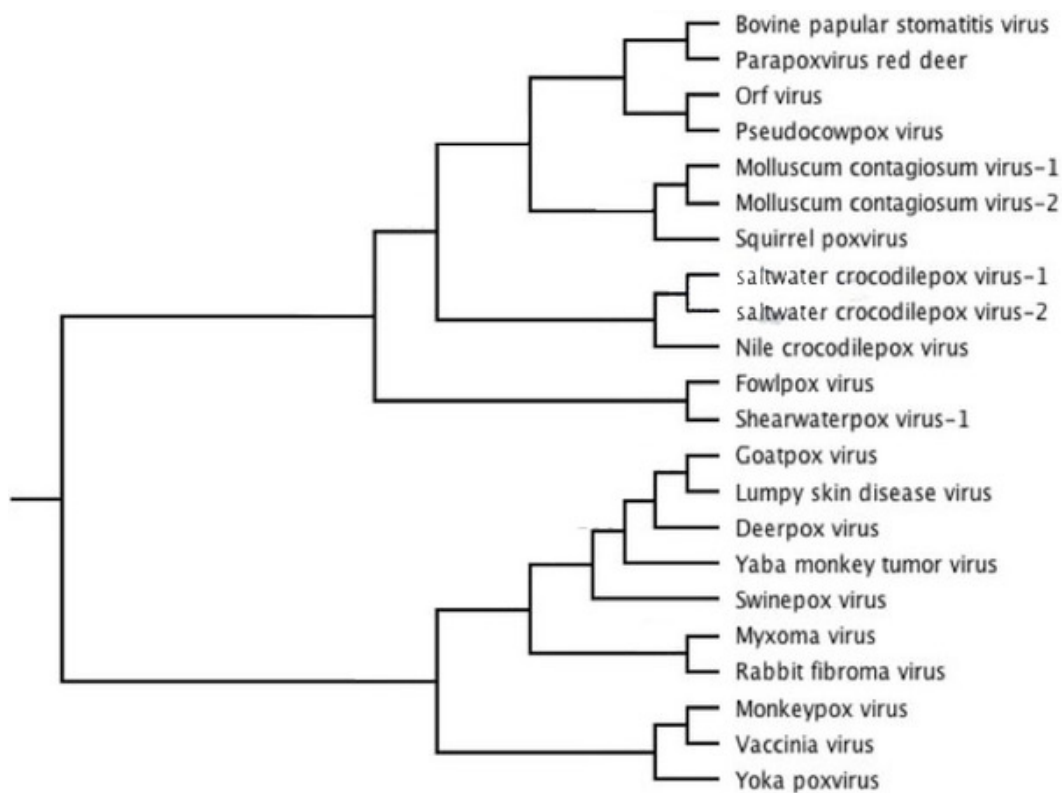


Figure 1.2: Gene sequence phylogeny of the family Poxviridae The phylogenetic analysis is based on the alignments of the complete genomic sequences of a range of poxvirus including MOCV type-1 and MOCV type-2. MOCV type-1 and MOCV type-2 are most closely related to each other yet relatively close to squirrel poxvirus (Sarker et al. 2018)

1.2 Vaccinia virus from vaccination vector to immune evasion

In 1796 Edward Jenner first deliberately used the cowpox virus to vaccinate successfully against smallpox. Over the next two centuries, vaccination was used to prevent smallpox disease and control VARV spread worldwide. Smallpox was the first disease that was prevented using vaccination, ultimately its eradicated being declared by the WHO in 1977 after worldwide vaccination. The virus used in the eradication program was known as vaccinia virus (VACV) but was of uncertain origin as it was grown in skin of calves or another large animal prior to the systematic WHO campaign; when its genomic sequence was defined VACV was shown to be an *orthopoxvirus* but not cowpox (LeDuc and Becher 1999; Smith 2011). Modified vaccinia virus Ankara (MVA) is a vaccinia strain that has been used as a vaccine. MVA vaccine was produced by the Bavarian State Vaccine Institute between 1968 and 1985, it was administered to around 120,000 people in large field trials in Germany. While MVA has a good safety record, its efficacy against smallpox itself could not be evaluated as VARV was already under control. MVA has been studied extensively as a viral vector as VACV does occasionally cause disease and the occasional fatality. MVA was attenuated by propagation in chicken embryo fibroblast, a process that lead to a loss of around 10% of the VACV genome and its ability to replicate in many mammalian cells; since it is replication deficient in human cells it can safely be used even in immunosuppressed individuals (Mayr et al. 1978; Gomez et al. 2011; Volz and Sutter 2013).

VACV is the prototypic and the most studied virus species of *orthopoxvirus*, a third of its genome and a half of its coding genes are dedicated to modulate immune system and establish infection. VACV virus has a linear double strand DNA genome which could be divided into around 100 kb encodes viral replication protein locate in the central region while the terminal part of genome encodes immune evasion proteins mainly affect innate immune system (Kotwal and Moss 1988; Smith et al. 2013a). The complement system, part of the innate immune response, consists of complex of well-regulated proteins that work in harmony to destroy viruses, virus-infected cells and other pathogens. Complement promotes opsonization of virions resulting in their elimination by phagocytosis. VACV complement protein (VCP) is able block

activation of classical and alternative complement pathways by binding to components C3b and C4b and enhances their cleavage. VCP also binds to the VACV A56 protein; A56 is expressed on the surface of extracellular enveloped vaccinia virus (EEV) and VACV-infected cells to shield both from the complement system (Kotwal and Moss 1988; McKenzie et al. 1992). EEV acquires host complement control protein CD46, CD55 and CD 59 in its envelope to help protect the virus particles from elimination by complement system (Vanderplasschen et al. 1998).

Interferons (INF) are generally considered to constitute the most potent innate immune defence against virus infections. The elimination of virus infections in the hosts usually relies on interferon type I response. IFN- α and IFN- β are families of type I IFN which are secreted as an alarm signal from cells infected with viruses whereas NF-gamma (type II IFN) is secreted by activated immune cells, notably cytotoxic T cells and NK cells, it is important in macrophage activation and it has antiviral activity mediated either by induction of effector molecules like IL-1, IL-6 or by enhancing antigen presentation by increasing expression of MHC I and MHCII. (van den Broek et al. 1995; Bartlett et al. 2005; Smith et al. 2013a). IFN-I (α and β) expression is activated during the early stages of virus infection often as a result of direct recognition of viral genetic material, transcripts or antigens by pattern recognition receptors (PRRs) triggering the IFN response. One of IFN-I functions is transmission of its signals to healthy cells surrounding the infected tissue. Binding to the type I IFN receptor (IFNAR) stimulates the Jak/STAT signalling pathway followed by further transcription of several interferon stimulated genes (ISGs), they are together acting as antiviral to control virus replication and spreading (Sen and Sarkar 2007; Schneider et al. 2014). Type I IFNs with ability to amplify antigen presentation and this promote recognition by antigen-specific T cells.

IFNs are corner stone in protection against *orthopoxvirus* infections, many poxviruses exploit multiple genes, to neutralise the antiviral action of IFN (Hernaiz et al. 2018). In VACV, E3L protein binds double strand RNA to prevents its recognition by the dsRNA-activated protein kinase R (PKR). VACV K3L is similar to eukaryotic initiation factor 2a (eIF2a), a host protein needed for initiation of translation. K3L inhibits eIF2a phosphorylation by PKR by acting as competitive substrate for PKR (Beattie et al. 1991; Chang et al. 1992). VACV VH1 also inhibits all INF receptors signalling by STAT 1 (signal transducer and activator of

transcription) and STAT2 whereas B18 is able to bind type I INFs to block its antiviral action in uninfected cells (Alcami et al. 2000; Mann et al. 2008; Montanuy et al. 2011; Smith et al. 2013a). VACV encodes C4, A49, A46, A52, E3, K7, K1, N1 and M2 proteins during early phase of infection, they are able to inhibit NF- κ B activation (Smith et al. 2013a)

Cytokines are small protein which important in cell signalling and regulation of innate and acquired immune response, they are classified into families according to their structures. VACV encodes multiple proteins to block cytokine function, e.g., F1, B15 and B13 all targets IL while B13 protein inhibits mature IL18, C12 protein binds soluble IL18 and suppress NF- κ B or IRF activation. VACV is able to sequester extracellular TNF and prevent its binding to cellular receptors. Moreover, VACV secretes chemokine binding protein able to bind CC chemokines. While HLA-E downregulation does render VACV-infected cells more susceptible to NK cells attack, the existence of VACV NK evasion genes is predicted but they have yet to be discovered (Smith et al. 2013a)

1.3 MOCV Genome Overview

The poxviruses have large DNA genomes ranging in size from 130 to 380 kbp (Fields et al. 2013). However, the VARV and molluscum contagiosum virus (MOCV) are the only poxviruses to known infect humans only. VARV is responsible for smallpox, two types are known: variola major viruses caused case fatalities ranging to 30%, and variola minor viruses (known as Alastrim variola minor virus), which caused less than 2% case fatalities (Shchelkunov et al. 2000). VARV is eradicated through immunization by using live vaccinia virus. MOCV is the sole member of the genus *molluscipoxvirus*. MOCV has a large double strand DNA genome with a high GC content (63%), especially when compared with only 34% in VARV and VACV (Senkevich et al. 1996), and four distinct genotypes (Dohil et al. 2006). The genome of MOCV type I (figure 1.3) has been sequenced and comprises of 190289bp with GenBank Accession No. U60315 (Senkevich et al. 1997).

MOCV is predicted to contain 182 open reading frames (ORF) that are likely to encode for functional proteins. When the MOCV genome is compared with that of the orthopoxviruses (OPV), 105 genes are homologous to proteins of OPV and 55

genes of these are more widely conserved poxvirus genes. The conserved gene set are responsible for replication or expression of the viral genome or are structural component of virion. All the VACV genes that are essential for virus growth in cell culture are conserved in MOCV; this correlation implies that the processes involved in productive MOCV replication is similar to that of the OPV. However, the MOCV genes known to modulates the host immune response lack homologues in the OPV, examples of those genes are: mc066L, mc080R, mc148R and mc033L (Senkevich et al. 1996; Senkevich et al. 1997).

The ORFs in the MOCV genome occurs in series of blocks transcribed in the same direction, rightward-oriented ORFs are located mainly in the middle and on the right side of the genome, whereas the leftward-oriented ORFs tend to be on the left side (figure 1.3). The first annotated gene on the left-hand end, mc001R, consists of 488 codons and begins proximal to the tandem repeats within the left ITR and the final gene, mc164L, sits adjacent to the right ITR and encodes 680 amino acids protein. 36 MOCV proteins were identified as having cellular homologues with conserved functional motifs. MC066L is a glutathione peroxidase homologue, MC148R is CC chemokine homologue and MC080R is an MHC I homologue; MC080R has 20 to 30% sequence identity with MHC-I molecules, while MC066L is 74% identical to selenocysteinyl glutathione peroxidase (Senkevich et al. 1997).

MOCV is predicted to encode a number of proteins that may help evade the immune system or be targets for antiviral agents. MC007L does not have homology to other poxvirus genes yet encodes a mitochondrial outer membrane (MOM) protein, the protein uses its N-terminal mitochondrial targeting sequence to attach to the MOM. MC007L inactivates retinoblastoma protein pRb by mis-localising and sequestering it at mitochondrial membranes, MC007L co-immunoprecipitates with the endogenous pRb/E2F-1 complex. Interestingly, MC007L has ability to transform primary rat kidney cells thus it likely plays a crucial role in MOCV-mediated cell transformation (Mohr et al. 2008). MC039L has homology to vaccinia virus DNA polymerase E9L gene and is a potential target the cidofovir and other polymerase inhibitors (Magee et al. 2005). MC054L is a homologue of human interleukin 18 binding protein (IL-18BP); IL-18 is a potent activator of macrophage through its

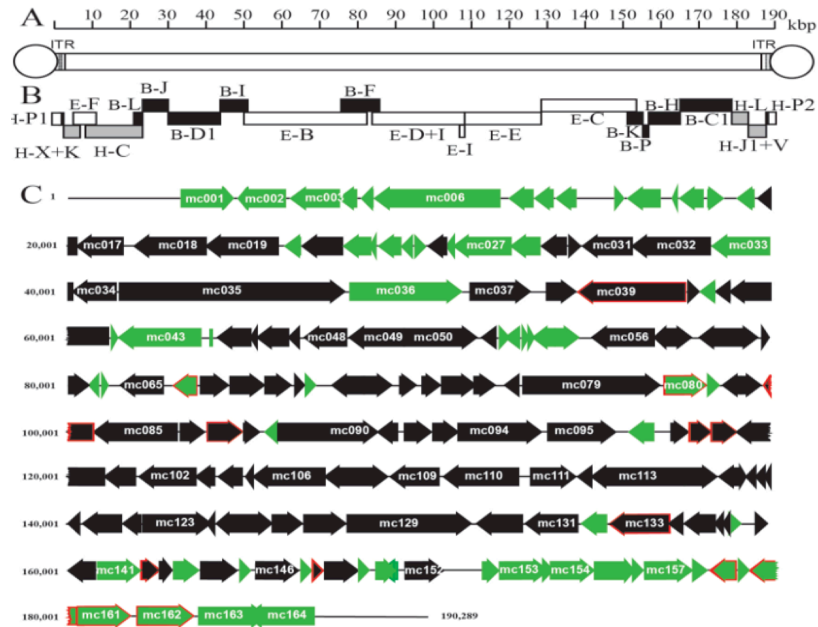


Figure 1.3: The complete genome of MOCV type I. MOCV type 1 genome encodes 182 hypothetical open reading frames. 95 MOCV ORFs have early promoters indicating they are involved in setting up the host cell for viral replication and extend the survival of the virus infection by suppressing elements of the immune system active in the human epidermis. These include two MHC homologs MC033 and MC080. The black represents the genes conserved between poxviruses, the genes depicted in green are unique to MOCV. Adapted from (Senkevich et al. 1997).

capacity to induce production of cytokines, including IFN γ . By acting as decoy receptor for IL18, MC054L acts to suppress the IL-18-mediated synthesis of gamma interferon, activation of NK cells and T helper cell response (Dinarello 1999). Interestingly, MC054 has two forms the full length MC054 which neutralise locally produced IL18 and the soluble N-terminal fragment which responsible for neutralising of IL18 systemically (Xiang and Moss 2001,2003). MC051L and MC053L are hypothetical proteins that also exhibit homology to human IL-18-binding protein and may act with MC054 to neutralise IL18. (Xiang and Moss 2001).

MC148R a secreted protein that shares amino acid sequence homology with the chemokine receptor CCR8 (Bugert et al. 1998). Two forms of mc148R have been studied, the mc148R1 from MOCV type-1 and mc148R2 from MOCV type-2. MC148R1 inhibited the migration of monocytes, lymphocytes and neutrophils by its action on multiple CC and CXC chemokine (Krathwohl et al. 1997; Damon et al. 1998). MC148R1 has the ability to block CXCL12 α and CCL3 whilst MC148R2 inhibits CCL3 only. The interaction of MC148R1 with CXCL12 α prevents the host chemokine from binding CXCR4 (Jin et al. 2011). Also, MC148R1 binds to CCR8 and blocks its function. (Luttichau et al. 2000). MC148R is expressed early in the MOCV lifecycle, and the CCR8 (the receptor blocked by MC148) is found on monocytes, natural killer (NK) cells and thymocytes. This suggests that MC148R has anti-inflammatory activity and may act to suppress the recruitment of an inflammatory cells to MOCV lesions in co-operation with other MOCV immunomodulating protein (Bugert et al. 1998; Luttichau et al. 2001). Also, MC148R1 shows homology to locus chemokine (ILC) that is strongly and selectively expressed in epidermis (Ishikawa-Mochizuki et al. 1999). mc066L exhibits homology to the eukaryotic gene encoding glutathione peroxidase, an enzyme that protects cells from oxidative damage. Consequently, MC066L is thought to help protect infected cells against UV-light and peroxide-induced cellular apoptosis. By inhibiting apoptosis, MC066L may allow the MOCV infected cells to survive longer in UV exposed skin (Shisler et al. 1998).

Apoptosis can act as a highly effective host defence mechanism when it triggers the destruction of virus-infected cells. Many DNA viruses, including MOCV, encode proteins that block apoptosis allowing virus-infected cells to survive long enough to

produce new virions. TNF and Fas ligand bind receptors TNFR and Fas respectively to initiate death receptor signalling, mediated through the recruitment of the adapter molecule Fas-associated death domain (FADD) to the death receptor and formation of the death-inducing signalling complex (DISC). DISC causes caspase-8 to be cleaved to its active form, the activated caspase 8 in turn activates effector caspases, such as caspase 3 and caspase 7, resulting in apoptosis. The cellular FLICE (FADD-like IL-1 β -converting enzyme) -inhibitory proteins (c-FLIP), has ability to compete with caspase-8 for FADD binding and they contain death effector domains as well. The results of recruitment of c-FLIP are inhibition of apoptosis and alteration in death-inducing signalling complex composition (Scaffidi et al. 1999; Lavrik and Krammer 2012). TNF α activates the transcription factor NF-kB (nuclear factor kappa-light-chain-enhancer of activated B cells) which promotes the expression of proteins involved in malignant transformation, cell adhesion, controlling cell growth, controlling apoptosis, in immune functions and even embryonic development. Moreover, NF-kB has important antiviral responses as activation of NF-kB leads to induction of expression of β IFN, HLA class I, and many inflammatory cytokines (Thanos and Maniatis 1995; Barkett and Gilmore 1999; Pahl 1999).

MC159 is a viral FLIPs, similar to other known cellular and viral FLIPs, MC159 has two tandem protein-protein interaction domains which called death effector domains (DEDs; DEDA, DEDB). MC159 blocks NF-kB activation by inhibiting TNF. Also, MC159 protein inhibits PMA-induced NF-kB activation or MyD88 over-expression that activates NF-kB, MC159 may inhibit TNFR1 signalosome. The MC159 N-terminal DED inhibits NF-kB and mediates MC159-TRAF2 interactions (Murao and Shisler 2005). Randall et al also found that MC159 enhance the expression of Mitochondrial antiviral-signalling protein (MAVS), TANK-binding kinase 1 (TBK1) or I κ B kinase ϵ (IKK ϵ) which leads to inhibition of Interferon regulatory factor 3 (IRF3) but by a constitutively active (Randall et al. 2014).

The MOCV ORF mc002L, mc161R and mc162L were grouped into a family of MOCV genes because of they have positional amino acid homology between the N terminal portions of the predicted proteins, and they are expressed at the early stage during infection. All of this family share predicted signal peptides, a carboxyterminal transmembrane domain and a marginal amino acid homology to the human SLAM

(Signalling lymphocytic activation molecule) proteins, a cellular membrane protein that has a truncated form lacking the transmembrane domain that can act as a self-ligand that has ability to induce the activation of T lymphocytes (Bugert et al. 2000). MC002 and MC162 both have consensus PY motifs in their cytoplasmic domains, the PY motif (PY motifs are proline-rich sequence, which the site of binding by proteins having a WW domain) normally interact with the Hrs endosomal switching protein and with cellular ubiquitin ligases AIP4 and NEDD4. The SLAM proteins have a dual role in both viral lifecycle and immune evasion role, and there is suggestion that SLAM gene family involves in T lymphocyte inhibition and surface receptors recycling. (Chen et al. 2013).

Senkevich et al identified two MHC homologues during the original analysis of the MOCV genomic sequence: mc080R has 24.5% amino acid homology to the human major histocompatibility class I antigen and mc033L has 28% homology to Xenopus class I histocompatibility antigen (Senkevich et al. 1997) (Table 1.1). MC080 protein was found to be glycosylated, localised to the ER and Golgi apparatus compartments, and formed a stable complex with β 2m but could not be detected on the cell surface. To function as an MHC-I mimic, MC080 would need to be expressed on the cell surface (Senkevich and Moss 1998). The role of MC033L has yet to be studied.

Table 1.1: MOCV genes 033 and 080

| MOCV gene | Location bp (codon length; calculated MW) | Identification criteria | Promotor type | Homology (%identity) | Prediction structure and feature |
|-----------|---|---|---------------|--|--|
| MC033L | Located between 38362-40098 with 579aa which has 62kDa | Sequence conserved GeneMark Prediction | Early | Xenopus classI histocompatibility antigen gi630859 28% | Signal Peptide, with transmembrane helix, C-terminal immunoglobulin domain |
| MC080 | Located between 96986-98170 with 395 aa 42kDa, 46kDa(with signal peptide) | Sequence conserved GeneMark | Early | Rat MHCI protein gi11521, 24.5% | 3-transmembrane helix, N-terminal, 1 transmembrane helix, N-terminal, MHCI heavy chain homolog |

1.4 HCMV Genome Overview

The herpesviruses have linear, double-stranded DNA genomes whose architecture is divided into six classes, A to F, as exemplified by HHV-6B, herpesvirus saimiri, EBV, VZV, HCMV, and tupaia herpesvirus, respectively (Fields et al. 2013). Accordingly, HCMV has a typical of class E herpesvirus genome consisting of two main regions of unique sequences the unique long [UL] and unique short [US] flanked by two sets of inverted repeats, *ab* (TR_L/IR_L) and *ac* (IR_S/TR_S) (figure 1.4). At approximately 230 kb, the HCMV genome is the largest reported for any herpesviruses and any human virus. In 1990, the first complete HCMV genomic sequence was reported for strain AD169 at 229,354 bp with the preliminary annotation describing 208 ORFs (Chee et al. 1990). Mutations in HCMV are known to accumulate in passage. The relatively low passage strain Toledo already exhibits evidence of adaptation to in vitro tissue culture, the most dramatic being a large sequence inversion (UL133-UL148) that is reflected in the reverse numerical order of the standard gene annotation in this region. The most commonly used laboratory strains AD169 and Towne have been serially passaged numerous times and this has resulted in substantial genetic alterations. The most notable genetic change observed being 15 kb and 13 kb deletion in the U_L/*b*' region of strains AD169 (encompassing UL132-UL150A) and Towne respectively relative to the low passage strain Toledo or Merlin (Cha et al. 1996; Davison et al. 2003b). A diagrammatic representation of the genetically intact Merlin HCMV strain genome with an up-to-date definition of the canonical gene set is given in figure 1.4.

HCMV is most commonly passaged in human foreskin fibroblast cells and, according to the extent of culture following isolation from clinical samples the HCMV, can be designated either high or low passage viruses. Typically, clinical virus replicates extremely inefficiently in vitro until tissue culture-adapted mutants have been selected. The epithelial cells tropism of high- and low-passaged HCMV strains are different. When clinical viruses are cultured in fibroblasts, they undergo genetic changes that substantially affect their growth characteristics and lose the capacity to infect myeloid, epithelial and endothelial cells. By 8 to 16 passages of HCMV clinical

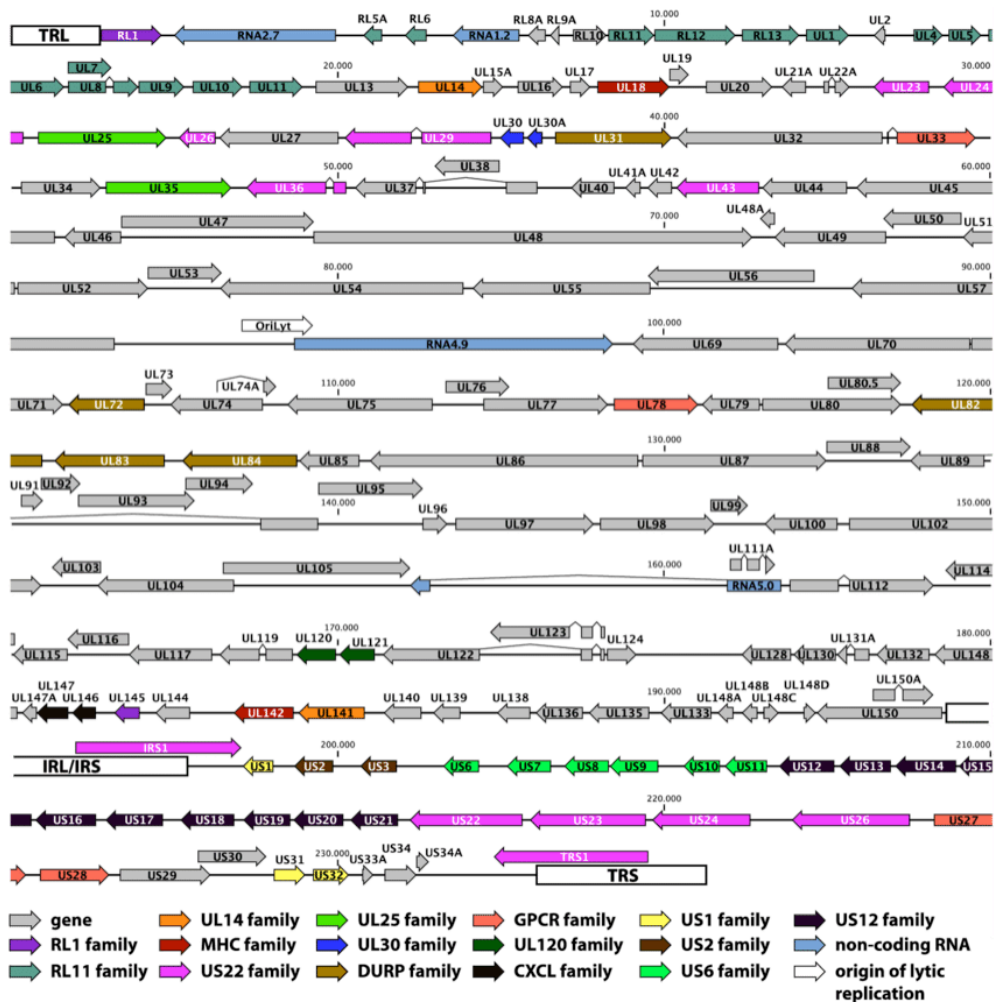


Figure 1.4: Genome annotation of the low-passage HCMV strain Merlin (GenBank accession NC_006273). The single line represents the dsDNA genome. HCMV has two terminal repeats (TRL, TRS) and two internal repeat regions (IRL, IRS) which represented in white boxes in the genome. The HCMV has 12 genes family which represent in the arrows which have different colour codes, below the genome is the gene family names. Figure reproduced from (Sijmons et al. 2014).

isolates in fibroblasts, mutations disabling the RL13 genes have been selected that permit more efficient plaque formation, and this change is followed by a further mutation in one of three genes contained in the UL128 locus (UL128L: UL128, UL130 or UL131A) by passage from 15 to 20. On further in vitro passage, additional defects can arise elsewhere on the genome. There is a tendency for a mutation in the *U_L/b'* region to occur focusing on the gene UL140–UL145 region to emerge by passage 32 to 63. The UL128L mutation was mainly associated with growing the virus using fibroblast cell lines (Dargan et al. 2010; Murrell et al. 2013). The UL128L encodes three proteins that, along with gH and gL, form the pentameric complex packaged into virion envelopes. The presence of pentameric complex in appropriate concentrations in virions appears to be required not only for efficient infection of cells other than fibroblasts but also for driving direct cell-to-cell infection, rather than spread by release of free virus in to the supernatant. These genetic changes all occur naturally. However, the researchers need also to be aware that during the cloning of HCMV genomes in to BACs, a deletion is often deliberately introduced into the virus genome to make space for the prokaryotic genome. To construct Towne, Toledo and AD169 BAC incorporated the prokaryotic vector cassette in a stably integrated element with in US region, where it replaced genes US2, US3, US6 and (in some cases) US11. As a result of that, the effect of MHC-I and MHC-II of the viruses derived from these BACs is different from clinical virus, consequently, this has profound effects on NK and T cell assays (Murphy et al. 2003; Murrell et al. 2013).

HCMV research has historically been based on the high passage AD169 and Towne laboratory strains. However, when the growth comparison between Toledo, Towne, and AD169 in the SCID-hu (thymus plus liver) mouse, it has been noticed that Toledo replicated at higher levels (at least 3 orders) than the other two strains. These differences could be related to the loss of genetic information by Towne and AD169 during propagation in cell culture (Cha et al. 1996).

The Merlin HCMV strain (ATCC VR-1590) is the main virus used in our laboratory, it was isolated from the urine sample of a congenitally infected neonate in Cardiff. To provide sufficient DNA initially to sequence the whole strain Merlin genome, the virus was expanded through three passages in fibroblast cell culture, after which HCMV genomic DNA was cloned into an M13 vector and analyse by Sanger

sequencing. Strain Merlin (clinical sample 742) was selected as the main virus used in our laboratory because its genome appeared to be relatively intact and the virus could be readily recovered from frozen ($-70\text{ }^{\circ}\text{C}$) stocks (Davison et al. 2003b; Dolan et al. 2004). At passage three the complete 235 646 bp genome of Merlin was sequenced and originally 170 protein-coding canonical genes identified during annotation (Dolan et al. 2004). The original clinical sample was retained for comparison, and with the advent of Next Generation sequencing the complete virus genome was subsequently determined direct from the urine and found to match the published sequence. Strain Merlin was designated the reference HCMV genome sequence by the National Centre for Biotechnology Information (GenBank AY446894; RefSeq NC_006273). It was the first World Health Organization (WHO) International Standard for HCMV (Davison et al. 2003b; Dolan et al. 2004; Fryer et al. 2016). The sequencing of the Merlin BAC clone revealed a nucleotide substitution in UL128 which is necessary for growth the virus in vitro. Additional defects in RL13 were revealed when sequencing of multiple clones; all Merlin BAC clones had a mutation in RL13 but that not all mutations were the same (Stanton et al. 2010).

Nine multigene families were identified in the original annotation of strain AD169, and three more families added subsequently (Chee et al. 1990; Davison et al. 2003a). The RL11 family is one of the largest consists of at least 12 genes (RL11, RL12, RL13, UL1, UL4, UL5, UL6, UL7, UL8, UL9, UL10 and UL11). As illustrated in figure 1.4, the 12 RL11 family genes are located close to each other near left terminus of the genome, and each contains a RL11D (CR1) domain which encodes a variable length key motif formed around three conserved amino acid residues. All but two members are predicted to contain N-linked glycosylation sites, the structure of individual RL11 genes vary between the RL11D regions and a similar domain has been identified in proteins encoded by some human adenovirus serotypes (Chee et al. 1990; Davison et al. 2003a; Davison et al. 2003b; Dolan et al. 2004). The entire RL11 gene family is dispensable for virus growth in cell culture.

An unusual feature US22 gene family is that is ancient, as evidence by it having homologues in rodent CMVs: the family consists of 12 members in both HCMV and MCMV and 11 in rat CMV. The US22 family is relatively dispersed through the HCMV genome, as indicated by the gene allocations UL23, UL24, UL28, UL29,

UL36, UL43, TRS1, IRS1, US22, US23, US24 and US26 (figure 1.4). Certain genes of US22 gene family have up to four conserved sequence motifs and many have stretches of hydrophobic and charged residues (Nicholas 1996). A number of US22 family encode proteins have regulatory functions. However, not all US22 gene family members have been studied. For example, the US22 gene itself is expressed with early kinetics and specifies a nuclear and cytoplasmic protein that is secreted into the extracellular medium but its function still unknown, (Mocarski et al. 1988). UL36 suppresses Fas-mediated apoptosis activation by interfering with caspase 8 activation (Skaletskaya et al. 2001).

US27, US28, UL33, and UL78 are members of the GPCR family and all chemokine receptor homologues. It has been suggested the family has been pirated from a mammalian-genome during virus evolution (Chee et al. 1990; Gompels and Macaulay 1995). US28 and US27 homologues have been identified only in primate CMVs, whereas UL33 and UL78 homologues are conserved throughout the β -herpesvirus family (Penfold et al. 1999). There have been many studies published about US28, it has ability to bind to different members of the CC family of chemokines, including CCL5, CCL2, and CX3CL1. US28 is internalized rapidly after chemokine binding, thus raising the possibility UL28 works as a chemokine sink in the viral life cycle (Randolph-Habecker et al. 2002).

The US2 family consists of two homologous genes, US2 and US3; it was found that the genes of the US2 and US6 gene families maybe evolved from a common precursor. According to genes alignments, and the functions of both gene family. The US2 and US6 family genes may arise by gene duplication, that is why sometimes they represent in a single family of proteins referred to US6 family (Ahn et al. 1996; Benz and Hengel 2000; Gewurz et al. 2001). The HLA class I antigen presentation pathway is inhibited by genes US2, US3, US6 and US11 by different mechanisms (Table 1.3), and accordingly these functions act in concert to protect HCMV infected cells against cytotoxic CD8⁺ T lymphocytes (Benz and Hengel 2000).

While the HCMV US12 gene family is also not essential for viral replication in cultured cells, it is highly conserved among clinical isolates. US12 family encodes a series of 7-transmembrane spanning proteins that share only limited homology with the cellular transmembrane bax-inhibitor one motif-containing proteins (TMBIM)

(Murphy et al. 2003; Das and Pellett 2007; Fielding et al. 2014). The US12 gene family composed of ten contiguous, tandemly arranged genes (US12 through US21). At least four members of US12 gene family have a role in suppressing NK cells killing of HCMV infected cells. Fielding et al showed that the expression of full-length MICA was inhibited US18 and US20; MICA is a stress ligand that binds the NK cell activating receptor NKG2D. Expression of B7-H6 is also induced by cellular stress (including virus infection) and also activate natural killer cells, B7-H6 is a ligand for the NK cell activating receptor NKp30. While B7-H6 is activated in productive HCMV infections, it fails to reach the cell surface due to the action of US18 and US20 (Fielding et al. 2014; Charpak-Amikam et al. 2017; Fielding et al. 2017).

1.5 HCMV and MOCV Immune Evasion Mechanisms

There are four MOCV genotypes, the genome of MOCV type I has been sequenced and comprises of 190289bp with 164 predicted genes, thirty-six MOCV proteins have recognizable cellular homologues (Senkevich et al. 1996; Senkevich et al. 1997; Dohil et al. 2006). MOCV encodes a number of proteins that help it evade the immune system (Table 1.2). MOCV infection is characterized by prolonged absence of inflammatory cells at the site of replication. MOCV has yet to be propagated in cell culture or in animals, though limited replication in human foreskin keratinocyte grafted mice has been reported (Buller et al. 1995; Fife et al. 1996). The inability to grow MOCV in cell culture have restricted investigation of virus-host interaction. Interestingly, infected keratinocytes in MOCV lesions were observed not to display β 2m on the cells surface (Viac and Chardonnet 1990), this observation implies the MOCV is capable of suppressing cells surface expression of MHC-1.

Table 1.2: MOCV immune evasion genes

| Gene | Target | Mechanism |
|---------------|-----------------------------------|---|
| mc066L | Glutathione peroxidase homologues | Inhibit apoptosis in infected cells by inhibiting peroxide radicals |

| | | |
|---------------|--|---|
| mc002L | homologues to human SLAM protein CD150 | Inhibit T lymphocyte activation |
| mc161R | Has homology to human SLAM protein CD150 | Inhibit activation of T lymphocyte |
| mc162R | homologues to human SLAM protein CD150 | Inhibit T lymphocyte activation |
| MC54L | Has similarity to human interleukin 18 binding protein | Antagonist of the proinflammatory cytokine IL18 (it inhibits the activates macrophages and several cytokines include $INF\gamma$, that is leads to inactivation of NK cells and Th1 responses) |
| MC148R | Chemokine receptor antagonist | Possess anti-inflammatory properties, it prevents chemotaxis in epidermis before the engagement of other mechanisms |
| mc007L | | Mislocalization and inactivation of mitochondrial membrane protein by cytosolic sequestering of retinoblastoma protein (pRb) |

An exceptionally wide variety of functions have been selected through evolution to allow cytomegaloviruses (CMVs) to both evade and modulate host immune responses and thereby permit the establishment of infection, persistence and onward transmission. Inflammatory cytokines, NK cells, adaptive CD4⁺ and CD8⁺ T cell responses and high avidity neutralizing antibodies released by B cells combine to combat HCMV infection. While many poxviruses immune evasion function are often clear homologues of host genes, this is much less common with the herpesviruses. Nevertheless, HCMV encodes a number of chemokines and chemokine receptor homologues, a number of which have been demonstrated to be functional, including UL146 (IL-8 like), the IL-10 homologue UL111a (vIL-10) (Kotenko et al. 2000) and the chemokine receptor homologues UL33, UL78, US27 and US28 (Randolph-Habecker et al. 2002)

NK cells play an important role in the early control of HCMV infections. NK cells are composed of many different subsets that express a distinct repertoire of inhibitory and activating receptors, which affect their mode of activation and their functional properties (Vivier et al. 2011). The capacity of HCMV to promote evasion of NK cells has been studied extensively and has provided a better understanding of how NK cells regulate HCMV pathogenesis (Wilkinson et al. 2008). HCMV evades NK cells by three main strategies: enhancement of expression of ligands for inhibitory NK cell receptors, suppressing cell surface expression of activating ligands and suppressing formation of the immune synapse. Some of the better characterised HCMV immune evasion genes are detailed in table 1.3.

Table 1.3: HCMV immune evasion genes

| Gene | Target | Mechanism |
|---------------|-------------------------|--|
| UL18 | MHC I homologue | UL18 forms a trimeric complex with β 2-macroglobulin that binds the inhibitor receptor LIR-1. UL18 inhibits LIR-1 ⁺ NK cells but stimulates LIR- ⁻ NK cells. |
| UL33 | CCR1 homologue | UL33 is homologous to chemokine receptor, located in HCMV envelope. |
| UL78 | CCR1 homologue | UL78 forms heteromers with CCR5 and CXCR4 chemokine receptors, it is similar to the fMLP receptor. Has a role in inflammatory response and leukocyte migration |
| UL111A | IL-10 homologue | UL111A encodes a secreted viral cytokine CMV IL10 which binds to IL10 binding receptor. |
| UL146 | CXCL8 (IL-8) homologues | UL146 is a chemokine homologue that mimics CXCL8. Stimulates chemotaxis |
| US27 | CCR1 homologue | US27 is a chemokine receptor-like protein, inhibits chemotaxis. |
| US28 | CCR1 homologues | US28 is a constitutively active CCR5-like chemokine receptor homologue that binds to CCL5, CCL2, and CX3CL1 – possibly as a chemokine ‘sink’ |
| US3 | HLA-I and HLA-II | US3 retains HLA-I in ER. Also binds to class II α/β heterodimers to interferes with the maturation of HLA class II |

| | | |
|--------------------------|--|--|
| US2 | HLA-I and HLA-II | US2 prevents HLA-I cell surface expression by promoting their retrograde transport to the cytosol where they are rapidly degraded by proteasomes. US2 is also responsible for downregulation of MHC II by degradation of HLA-DR-alpha and DM-alpha molecules. |
| US11 | HLA-I | US11 prevents HLA-I cell surface expression by promoting their retrograde transport from ER to the cytosol where they are rapidly degraded by proteasomes |
| US6 | HLA-I | US6 downregulates HLA-I and HLA-E by inhibition of TAP-dependent peptide translocation |
| SP^{UL40} | HLA-E, UL18 | The peptide derived from UL40 signal sequence (SP ^{UL40}) binds to and stabilises both HLA-E and gpUL18 to enable surface expression in a TAP-independent manner. HLA-E binds CD94/NKG2A (inhibitory receptor) and CD94/NKG2C (paired activating receptor) on NK cells |
| UL16 | MICB, ULBP1-4 and RAET1G | UL16 inhibits NK cell killing by downregulate multiple NKG2D ligands |
| miR-UL112 | MICB, TLR2 and Modulates TLR2/IRAK1/NF-κB Signalling Pathway | miR-UL112 inhibits NK cell killing by downregulating MICB |
| UL135 | Remodels actin cytoskeleton | UL135 suppresses formation of the immunological synapse |
| UL141 | CD112, CD155 and TRAIL-R2 | UL141 elicit robust protection against NK cell activation |
| UL142 | MICA alleles except MICA*008 | UL142 inhibits NK cell killing by downregulate NKG2D |
| UL148 | Downregulates CD58 (LFA3) | UL148 causes suppression of co-stimulation impairs T and NK cell responses |
| US12 family | Regulate array of cell surface immune ligands | The family acts in concert to regulate cell surface proteome. E.g US18 and US20 and both involved in suppressing cell surface expression of MICA (NKG2D ligand) and B7H6 (NKp30 ligand) in productive infection. |
| UL36-38 | | UL36-38 suppresses apoptosis |
| IRS1 and TRS1 | | IRS1 and TRS1 suppress interferon |

1.6 MOCV biology

MOCV is an interesting human skin pathogen that has been the only endogenous human poxvirus after eradication of smallpox. The sole member of *Molluscipoxvirus* genus has four distinct genotypes, a double-stranded DNA genome of some 190289 bp (GenBank accession U60315: MOCV type 1/80) and is predicted to possess 164 genes (Senkevich et al. 1997; Dohil et al. 2006). MOCV is an enveloped, pleomorphic (mainly ovoid to brick shaped) virus which, like the orthopoxviruses, has a dumbbell-shaped central core with lateral bodies similar and replicates in the cytoplasm of human epidermal cells (Birthistle and Carrington 1997). MOCV causes self-limited benign tumours of the skin, it mainly infects children and can be a sign of immunodeficiency. The lesions are limited to the epidermis (figure 1.5) and can persist for months, sometimes years, even when they show signs of inflammation. Attempts to treat MOCV infections are usually associated with spread of the infection and may cause greater distress.



Figure 1.5: Clinical picture of molluscum contagiosum. MOCV causes superficial skin infection which occurs most commonly on exposed skin, the lesion begins as a small papule and, when mature, is a discrete, waxy, smooth, dome-shaped pearly or flesh-colored nodule, often umbilicated. The number of individual lesions is usually fewer than 20, MOCV infects the skin with around 3 to 5mm in diameter (A to G, L and M); MC infects the eyelid causing follicular conjunctivitis (H, I). MCV lesions from an immunocompromised patient with Dedicator of cytokinesis 8 (DOCK8) deficiency, showing varying degrees of acute inflammation (J, K). NIH Clinical Center: Bugert and Turner, 1993. (Chen et al. 2013).

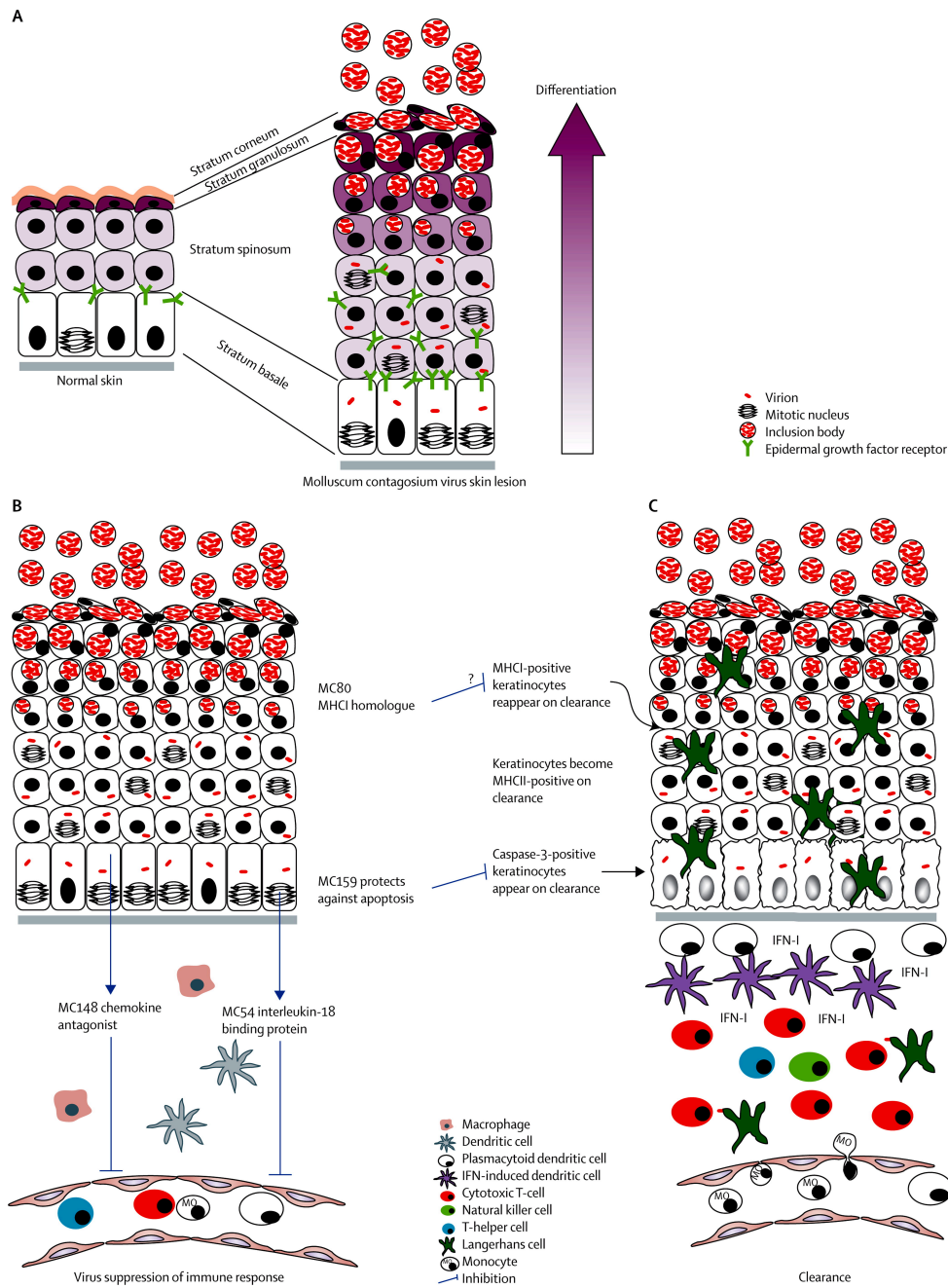


Figure 1.6: Lifecycle of molluscum contagiosum and local immune responses in infected skin. The maturation MOCV in human skin. (A) The virus infects the basal layer of epidermis, the mature virus released from differentiated keratinocytes. (B) MOCV suppresses immune response at the lesions, the immune effector cells are unrecognized at site of infection. (C) The lesions are surrounded by inflammatory cells which are an early sign of cure. The figure is reproduced from Chen et al., 2013.

1.6.1 Epidemiology

While molluscum contagiosum has a worldwide distribution, it is more common in areas with tropical and humid climates. The MOCV species contains of four clinically indistinguishable genotypes, types 1 and 2 being the commonest. Usually, the diagnoses are based on the appearance of the characteristic lesions with only a minority of cases being confirmed by analysing biopsies (Senkevich et al. 1996; Husar and Skerlev 2002; Leung et al. 2017). Humans are the only known host for MOCV. Epidemiologic data on the incidence of molluscum contagiosum is limited so the true prevalence of MC has probably been underestimated (Tyring 2003).

The MOCV genotype 1 is the most common and is responsible for 98% of cases reported in the United States. Other genotypes are significantly more common in immunocompromised patients, including HIV-infected persons, as well as in countries outside the United States (Dohil et al. 2006). All genotypes are clinically indistinguishable. The typical presentation of MC is multiple skin lesions, MC is mainly transmitted by direct skin contact which leads to typical cutaneous lesions. However, mucosal lesions are rarely recognized. Also, MC transmitted by fomites on bath sponges and bath towels with beauty parlours, school swimming pools, and Turkish baths all having been responsible for transmission of infection (Dohil et al. 2006).

MC is common in sexually active adults with sexual transmission and skin contact in sports being well documented modes of transmission. The incidence of MC infection in the United States has been increasing since the 1960s where the condition is recognized as a sexually transmitted disease. According to the results of surveys performed in two clinics for sexually transmitted disease over period 1966-1983, MC mainly infected persons in an age group between 15 and 29 years of age (Niizeki et al. 1984; Becker et al. 1986).

Agromayor et al examined 147 HIV-negative Spanish patients clinically and analysed their blood for the presence of MOCV and typed isolates. 66% were children and 49% had atopic dermatitis, the lesions were indistinguishable between different age groups. However, patients with atopic dermatitis had larger lesions in comparison with non-atopic patients. In adults, the lesions were mainly in genital

area, MOCV type I was predominant with the ratio of MOCVI to MOCVII was 146:1 (Agromayor et al. 2002).

A study on 93 patients in a London hospital based on endonuclease digest pattern of MOCV DNA found that MOCVI: MOCVII was 3.23:1 (Porter et al. 1989) whilst as analysis of 222 MOCV isolates from the Grampian region in Scotland found that MOCV type I was about 40 times more common than type II; MOCV genotypes did not change over time in the same patient, or when passed on in a contact group (Scholz et al. 1989).

1.6.2 Host range and tissue and cell tropism

Vertebrate poxviruses commonly cross species, MOCV is exceptional in being restricted to a single species. Moreover, MOCV replicates only in keratinocytes of the epidermis (Buller et al. 1995). The virus promotes cell mitosis to generate a slow benign skin tumour. The histopathology of the lesion characterised by acanthotic squamous epithelium (acanthoma) forming central crater filled with keratin and large eosinophilic intracytoplasmic known as Henderson Peterson bodies (figure 1.6). The basal layer of epidermis stays intact (Chen et al. 2013).

1.6.3 Cell culture and animal system

Many attempts to grow MOCV in primary cells and cell lines have been unsuccessful, the virus does not produce infectious progeny in standard cell culture systems (Bugert et al. 2001). Placa prepared virus suspensions from MC patient skin lesions, and inoculated extracts in to human amnion cell cultures. While such infection produced typical cytopathic changes, there was no evidence of virus multiplication (Placa 1966). MOCV suspensions alter amnion cells by a cytotoxic reaction rather than by replication of intracellular virus (Burnett 1968). Buller and co-workers were more successful using human foreskin grafts in to athymic mice, where MOCV infection induced morphological changes that were indistinguishable from patient biopsies and included the development and migration of molluscum bodies (Buller et al. 1995). Using a similar approach, pieces of foreskin were exposed to extracts from MC patients lesions then implanted under the renal capsule of athymic mice. The infected implants showed the presence of cytoplasmic

inclusions containing typical poxvirus particles within 2 – 3 weeks of implantation. However, attempts to pass the virus from one infected implant to another were unsuccessful (Fife et al. 1996; Paslin et al. 1997). MOCV infection of human fibroblasts and keratinocytes culture results in transcription only of MOCV early mRNAs and an abortive infection (Bugert et al. 1999; Melquiot and Bugert 2004).

1.7 HCMV biology

HCMV has a worldwide distribution with an estimated seroprevalence of 45–90% in adult populations depending on socioeconomic status. HCMV is an important pathogen in immunocompromised patients (e.g. AIDS or tumour patients) and individuals with immature (e.g. neonates) or compromised (e.g. pregnancy, patients with organ transplantation) immune responses. However, HCMV appears to be relatively harmless in most immunocompetent individuals. Following an acute infection, HCMV establishes lifelong persistence in its host. Exposure to HCMV results in the induction of a comprehensive humoral and cellular immune response that is not capable of completely suppressing reactivations or superinfection with a different strain (Gandhi and Khanna 2004; Cannon et al. 2010; Boeckh and Geballe 2011). HCMV has broad host-cell tropism during acute infection that include epithelial cells, fibroblasts, smooth muscle cells, endothelial cells and macrophages (Sinzger et al. 2000).

The development of efficient cell culture methods in the middle of the last century enabled the isolation and propagation of HCMV to be reported by three groups independently in 1956 and 1957 (Wilkinson et al. 2015). The detection of HCMV in clinical specimens initially required weeks of cultivation to isolate the virus. In the 1980s, rapid diagnosis was enabled by adopting immunofluorescence assays capable detecting HCMV antigens, in particular the major immediate early protein. Rapid diagnosis proved invaluable with the advent of antiviral therapies in the 1990s. Antiviral therapy and enhanced patient management has improved the outcome for solid organ and bone marrow transplant patients with HCMV disease. Further advances in diagnosis (notably PCR) has aided patient management over the past two decades. Nevertheless, HCMV still accounts for substantial morbidity, mortality, and cost (Boeckh and Geballe 2011).

1.7.1 HCMV Epidemiology

HCMV infection was originally detected in the 19th century when they studied organs in people who had died from unknown causes. Histologically the lesion contained cytomegalic cells with intranuclear inclusion bodies in epithelial and salivary glands that reflect the name ultimately given to the virus (Just-Nubling et al. 2003). Infection were widely reported in newborns during the early 20th century that were detected as large cells in the urine of children and associated with cytomegalic inclusion disease, a severe congenital disease associated with a characteristic owl's eye cytopathology

HCMV is transmitted from one person to another through contact with infected bodily fluids, such as urine or saliva, including sexual transmission. HCMV is the most common cause of congenital infection and can be transmitted to the foetus at any trimester of pregnancy (Cannon and Davis 2005; Kagan and Hamprecht 2017). HCMV infection is manifest as an exceptionally wide range of clinical conditions and thus, unlike MC, infections cannot be reliably diagnosed from its symptoms but requires laboratory tests. The vast majority of primary HCMV infections are subclinical, indeed most are thought to be mild or asymptomatic. Nevertheless, HCMV is capable of causing disease in the immunocompetent, it is a significant cause of infectious mononucleosis and hepatitis. However, serious disease is most evident among immunocompromised persons, most notably persons with HIV infection and organ transplant recipients on immunosuppressive treatment. Infants who born with HCMV can suffer from permanent disabilities including hearing loss, vision loss, and mental retardation (Scholz et al. 2003; Scholz et al. 2004).

Kenneson and Cannon reviewed studies that reported results of systematic cytomegalovirus screening on foetuses and/or live-born infants by comparing the incidence of live-born infants with HCMV in a series of 34 papers (Kenneson and Cannon 2007). Estimates of HCMV infection at birth ranged from 0 to 13.6%, with newborns from the Gambia having the highest prevalence (13.6%). However, they found the average of prevalence of congenital HCMV from 27 culture-based universal study groups was 0.64%. Another study carried in Germany found 0.2% of newborns had HCMV infection and one study from Brazil had a birth prevalence of 0.10%. However, in this study the screening was conducted by testing for IgM in

dried bloodspot cards, a method known to have a lower sensitivity than PCR or culture. (Dollard et al. 2007; Kenneson and Cannon 2007). The extent of foetal damages depended on when virus was transmitted during pregnancy. When the mother was infected for first time (primary infection) during pregnancy the disease in the foetus tends to be more severe infection than following HCMV reactivation in the mother. Congenital infection can cause hepatomegaly, the CNS sequelae like cerebral calcification, vision and hearing losses, mental retardation etc, and hydrops fetalis. HCMV disease is also less severe when the virus is acquired later, indeed perinatal and early postnatal HCMV infection is ten times more common than congenital infection (Lubeck et al. 2010).

The prevalence of HCMV in developing world higher than in developed world. The acquisition of HCMV in the developing world is nearly universal in early childhood, in South America, Sub-Saharan Africa, East Asia, and India more than 90% of preschool children are HCMV antibody positive (>90%). In contrast, in Great Britain and in certain populations in the United States less than 20% of children of similar age are seropositive. 60% of children 4 to 7 years of age in Chengdu, China were HCMV seropositive. In Taipei, Taiwan, 58% of children 4 to 12 years of age are HCMV seropositive. 61% of low-income population of hospitalised paediatric patients in Rio de Janeiro, Brazil are HCMV seropositive (Boppana and Fowler 2007). Similarly, 56% of children aged 1 to 4 years in Jamaica were HCMV antibody positive. The HCMV prevalence rate in Finland increased from 27% in children 7 months of age to 41% in children 8 years of age in 8 years study. In a population survey in Parma, Italy HCMV seroprevalence increased from 28% in two-year olds to 96% in 45–54-year-old. Similarly, in Spain, the HCMV seroprevalence rate in children 2 to 5 years of age was 42% increasing to 79% in adults 31 to 40 years of age. In studies included only blood donors in Asia and Africa continue to have HCMV seropositivity rates of 95%–100%, whereas, HCMV seropositivity rates in blood donors in Germany had lower ranging from 30% in 18 to 20-year olds to >70% in adults >65 years of age (Boppana and Fowler 2007). The prevalence of HCMV in the community is significant as it has a direct impact on the ratio of congenital infections that come from either a primary infection or a reactivation in the mother.

1.7.2 Cellular tropism of HCMV in vivo

HCMV infects only humans. It can infect virtually any tissue because of its wide cellular tropisms. There are no animal models to study HCMV, studying patient samples and autopsy materials are the only source to interpret HCMV pathogenesis. Dynamic aspects of viral replication and spread have generally only been addressable within the blood compartment (Rice et al. 1984; Emery et al. 1999).

When the route of transmission of infection by saliva in primary HCMV infection, the first cells to be infected are epithelial cells of the rhinopharynx. With sexual transmission the epithelium of the genital tract is infected first. Historically, HCMV was sometimes transmitted in blood transfusion where endothelial cells of the vascular tree and circulating myeloid cells would be first exposed to infection. The haematogenous dissemination may be initiated by leukocytes recruited to the primary site of infection, which then take up virus spread through the blood and lymphatic systems. HCMV can establish systemic infections that can implicate virtually all organs in the body, the virus can commonly be recovered in the salivary glands, kidneys, liver and mammary glands. Accordingly, HCMV diagnosis can be achieved by detection (historically isolation) of the virus in secretion products from these organs including saliva, urine or milk. HCMV disease is routinely assessed by monitoring virus load in the blood by PCR (DNAemia), although measuring the pp65 antigen (ppUL83) in peripheral blood polymorphonuclear leukocytes and monocytes (antigenemia), immediate early (IE) or late mRNA (RNAemia) provides direct evidence of active virus replication. Once the acute phase of primary infection is controlled by the immune response, HCMV enters a period of clinical latency where the virus is difficult detect and even more difficult to isolate (Gerna et al. 1990; Boeckh et al. 1992; Gerna et al. 1992; Boeckh and Boivin 1998).

By using leukocyte-depleted blood in blood transfusion HCMV transmission by blood transfusion was significantly decreased (Yeager et al. 1981; Gilbert et al. 1989); this provided an early indication that the virus could persist in peripheral blood leukocytes (PBL). Following up on this observation using recently developed sensitive PCR assay, it was revealed that a CD14⁺ monocyte population rather than a T cells, B cells or PMNL fraction of peripheral blood carried HCMV DNA (Taylor-

Wiedeman et al. 1991; Taylor-Wiedeman et al. 1993). The monocytes derive from CD34⁺ haematopoietic cell precursors been shown to be carriers of the virus (Mendelson et al. 1996; Sindre et al. 1996). Infection of monocytes can be considered as ‘latent carriage’ as virus production is not observed until the cells differentiate into macrophages, DCs of Langerhan’s cells. Long-term latency of HCMV DNA may be the bone marrow progenitors of the monocyte and myeloid lineage or an associated bone marrow stromal cell (Hahn et al. 1998; Sinclair and Sissons 2006).

Endothelial cells (EC) and epithelial cells are important targets for HCMV infection. HCMV exploits EC as a means to disseminate the infection. EC are present in the microvascular of capillaries and venules of many organs which include the entire gastrointestinal tract, lungs, kidneys, liver, salivary glands and brain (Sinzger et al. 1995). The macrovascular EC were also shown to be susceptible to HCMV lytic infection. (Maidji et al. 2002; Jarvis and Nelson 2007) . In addition to circulating cytomegalic EC, the HCMV can be circulating in blood by peripheral blood leukocyte, including PMNL and monocyte/ macrophages (M/M) (van der Bij et al. 1988).

1.7.3 HCMV replication

HCMV can establish a lytic (productive) virus replication cycle that follows a set pattern of attachment, entry, DNA replication, capsid assembly, DNA encapsidation, nuclear egress, secondary envelopment and release or latent carriage where it is not readily susceptible to antivirals yet poised to reactivate (Reeves and Sinclair 2008). According to convention, the cascade of HCMV gene expression during productive infection is divided into three phases. The IE genes are expressed in from the virus in the absence of de novo gene expression and are thus dependent on pre-existing host cell transcription factor and viral proteins that enter alongside virions. Early phase gene expression occurs in the absence of viral DNA replication whereas late genes are activated following replication of the virus genome. Infections can be performed in the presence of an inhibitor of protein synthesis (e.g. cycloheximide) to limit expression to IE genes and in the presence of an inhibitor of DNA replication (e.g. Ganciclovir) to limit expression to early genes. A less artificial means of following the cascade of virus (and cellular) gene expression was achieved using

temporal proteomics to follow gene expression through the full course of a productive infection. This pattern in human fibroblast of all expressed genes could be each be classified into one of 5 temporal classes (TP1-5) based on proteomic analysis and illustrated in figure 1.7 (Weekes et al. 2014).

HCMV is like many alphaherpesviruses, it initiates infection by attachment to cell surface by heparan sulphate (Compton et al. 1993). HCMV needs gB and gH/gL for entry to the cell. It was found that an HCMV gB-null mutant could assemble virus particles but was not able to enter cells, the defect could be overcome by treating virions with the chemical fusogen polyethylene glycol (PEG) (Isaacson and Compton 2009). The mode of entry is different according to cell type. HCMV enters fibroblasts by direct fusion with the plasma membrane and requires gH/gL but not the pentameric complex of gH, gL and pUL128-131. However, HCMV requires the pentameric complex to enter into epithelial and endothelial cells where the complex promotes macropinocytosis and endosomal fusion. (Vanarsdall and Johnson 2012). Feire et al found that during HCMV entry, cellular morphological changes and signalling cascades are activated that are consistent with engagement of cellular integrins. An integrin-binding disintegrin-like domain within gB that is conserved throughout Herpesviridae, HCMV may use $\alpha 2\beta 1$, $\alpha 6\beta 1$, and $\alpha V\beta 3$ integrins as entry receptors and to activate signalling during the penetration stage of the entry pathway (Feire et al. 2004).

After attachment of viral envelope glycoproteins with cellular receptors on fibroblasts, the virion merges with cell membrane, in the cytoplasm, the HCMV releases its capsid and tegument proteins. After endocytosis in epithelial and endothelial cells the HCMV uses its envelop glycoprotein to survive in low pH endosomes. The nucleocapsid bind to microtubules travel to the nucleus while tegument proteins (e.g. pp65 and pp71) are released into the cytosol. Some tegument proteins remain in the cytoplasm while others access to the nucleus through nuclear pore along with viral genomic DNA (Kalejta 2008; Smith et al. 2014). The herpesvirus genome transcription and replication occur in the nucleus followed by assembly of the capsid, the encapsidated virion buds through the nuclear envelope. The virus finally assembled by adding additional tegument proteins and the final

virion envelope in the assembly compartment (AC) prior to egress using the cellular secretory apparatus (Smith et al. 2014).

1.7.4 HCMV propagation in vitro

The first in vitro propagation of virus from two neonates who had cytomegalic inclusion disease (CID) was in 1954 by Margaret Smith. The Davis strain was isolated by Thomas Weller from culture of liver biopsy with embryonic muscle cells from a patient with suspected toxoplasmosis, after that the strains Esp and Kerr were grown from patients with CID. The agent in the end was called human cytomegalovirus. While Wallace Rowe was culturing adenoid tissue when the 169th sample, from a seven-year-old girl, the infection characterized by intranuclear inclusion bodies, this leads to isolation of the HCMV strain and they designated AD169 (Wilkinson et al. 2015). Plotkin and co-workers subsequently isolated HCMV strain Towne from the urine of infected infant, they deliberately sequentially passaged the virus 125 times in WI-38 fibroblasts in order to attenuated the virus to use as a potential live vaccine (Plotkin et al. 1975).

Strain AD169 was the first HCMV genome to be sequenced completely (Chee et al. 1990). Comparing the data of AD169 with other strain later revealed frameshift mutation in three genes (RL5A, RL13 and UL131A) and a deletion of 19 genes at the right end U_L region (the U_L/b region: UL133-UL150) that was substituted by an inverted duplication of a sequence from near the end of left genome, that leads to a substantial expansion of RL sequence (Cha et al. 1996). Furthermore, some stocks contain a deletion in genes UL42 and UL43 (Cha et al. 1996; Davison et al. 2003b). An effect of passaging HCMV strain Towne (ATCC VR-977) was to produce two variants, one exhibiting the loss of the U_L/b' and the other intact in this region. Nevertheless, both variants have mutations in genes RL13, UL1, UL40, UL130, US1 and US9 (Bradley et al. 2009). Cultured AD169, Towne, and Davis strains of cytomegalovirus (CMV) are able to infect fibroblasts, but not endothelial cells. In contrast, the low passage Toledo strain can infect endothelial cells. However, the endothelial tropism was lost on passaged Toledo strain through fibroblasts yet retained on passage through endothelial cells. Although the Toledo strain retains U_L/b' sequences, it was inverted in passage. Since this was not obvious

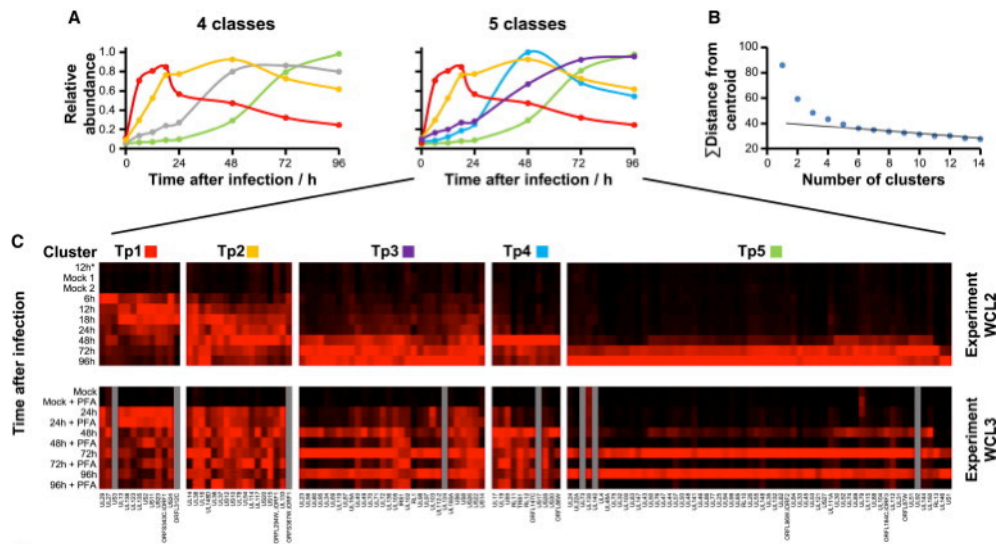


Figure 1.7: HCMV Gene Expression divided to four or five classes. The analysis is of temporal expression of all HCMV proteins detected in a time course of virus infection. (A) a computer analysis in which HCMV encoded proteins are classified into four or five temporal profiles. The protein groups have parallels with the classical IE, early (E), delayed E, late (L) and true L classification. Division into 5 temporal profiles (TP1-5) was considered optimal. (B) According to the distance of each protein from its cluster centroid number the temporal classes divided into two to fourteen classes, provides rational that 5 was the minimum number of classes that provided definition (C) Heat map illustrating the temporal regulation of expression of all HCMV proteins detected by proteomics and assigning their kinetics in fibroblasts (TP1-5). Figure reproduced from (Weekes et al. 2014)

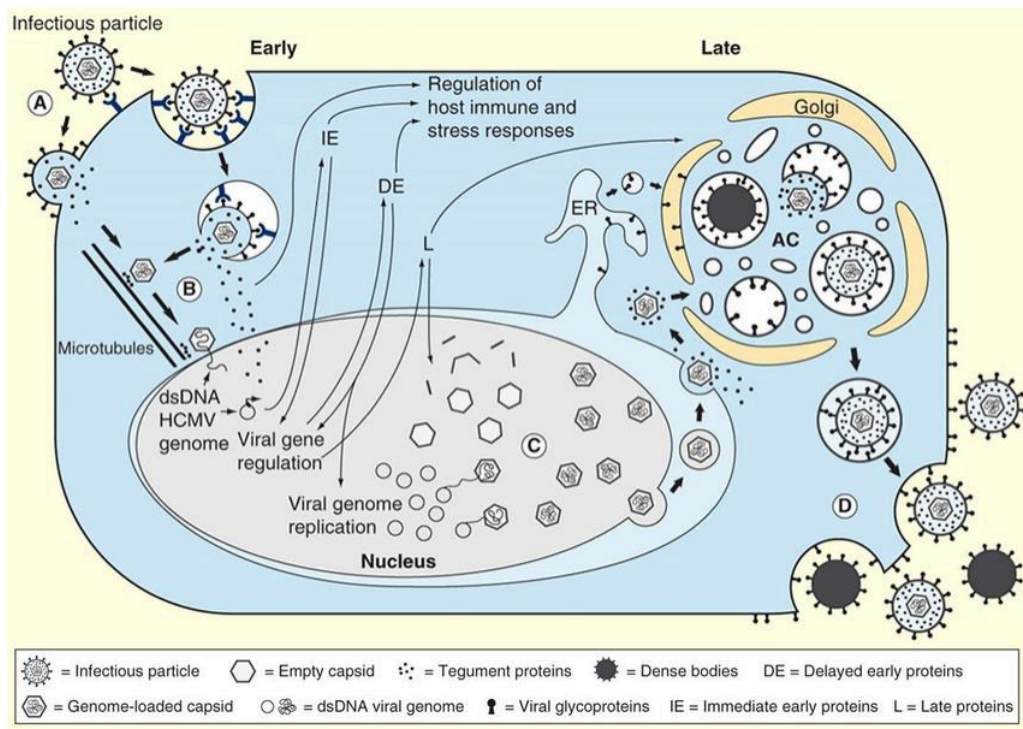


Figure 1.8: Life cycle of human cytomegalovirus. (A) First the virions attach the cellular receptors, then it gives access for tegument and capsid to enter the cells. (B) In the nucleus where the capsid travel to, the IE genes are expressed, after that the delayed early genes (DE) are expressed followed by late (L) genes. (C) In the nucleus, the capsid is assembled, and then reaches the cytoplasm, it followed by budding of the virion which acquire tegument and viral envelope into intracellular vesicles at the assembly compartment (AC). (D) It ends by egression of the enveloped virion from the cell. Figure and figure legends are adapted from (Jean Beltran and Cristea 2014).

when used to annotate these additional genes, it was responsible for genes between UL132-UL149 being annotated in reverse numerical order on genetically intact viruses. When HCMV strains are propagated in cell culture they change, losing properties of the HCMV clinical isolates. Prolonged passage will result in a loss of virulence, as revealed by vaccine trials using strain AD169 and Towne, and decreased resistance of infected cells to NK cells (Quinnan et al. 1984; Plotkin et al. 1989)

In our laboratory the Merlin strain is in use, it was isolated from HCMV doing PCR-positive urine sample from a neonatal, the sample kindly provided by Public Health Laboratories (Cardiff PHLS/NPHS). To generate sufficient DNA, the viruses were amplified using fibroblast cell culture and cloned into an M13 vector and fully sequenced using Sanger sequencing. Merlin strain was passaged three times, each passage of Merlin involved infection of an uninfected fibroblast monolayer with cell-free supernatant. The Merlin strain genome sequenced completely at passage 3 and saved in the GenBank with accession number AY446894, it is first World Health Organization (WHO) International Standard for HCMV (Davison et al. 2003b; Dolan et al. 2004; Wilkinson et al. 2015). The Merlin virus strain had mutations at two genetic loci, in RL13 and UL128, that occurred after limited replication in vitro proceeded by cloning. The premature stop codon in UL128 abrogated gH/gL/gpUL128/gpUL130 /gpUL131A. Stanton and co-workers test the complete wild-type HCMV gene complement was made by retaining back to the original clinical sample from which Merlin strain was made, they found that RL13 efficiently repressed HCMV replication in many cell types. Also, they found that RL13 mutants helped the reproducibility of the virus. The other virus mutation is in the UL128 locus that acquired mutations in genes UL128, UL130, or UL131A, it was noticed the virus growth was inhibited in fibroblast cells in wild-type form (Stanton et al. 2010).

The use bacterial artificial chromosome (BAC) clones has major impact in studying HCMV. When Shizuya and co-workers developed BAC vector technology, they found it capable of capturing and stably maintaining human genomic DNA fragments of >300 kilobases (Shizuya et al. 1992). Messerle and co-workers were the first research group to adapt the BAC system to CMV studies by cloning mouse cytomegalovirus genome as BAC in *E.coli* then transfecting BAC plasmid into eukaryotic cells to generate infectious virus from the bacterial clone (Messerle et al.

1997). Borst et al were then able to apply BAC technology to clone the human cytomegalovirus (HCMV) strain AD169 (Borst et al. 1999).

HCMV can be regenerated from BACs containing the virus genome, including the Merlin BAC (Stanton et al. 2010). BAC vectors are based on studying *Escherichia coli* F factor. The Replication of the F factor in *E. coli* is controlled to keep it at in low copy number and retained in bacterial cells (Borst et al. 1999). For cloning HCMV genomes into BAC constructs, BAC vectors are first engineered to contain arms of homology to viral genome sequences flanking the site of BAC insertion. Then, linearized BAC vectors are delivered into HCMV infected cells where they may capture integrated into the HCMV genome by homologous recombination. By maintaining HCMV genome in *E. coli*, it avoids in vitro selection of HCMV gene mutations, and the infectious virus can then be recovered by DNA transfection of permissive cells. The BAC vector-based cloning facilitates manipulation of viral genome and provides genetically defined virus (Borst et al. 1999).

BAC clones are stable when propagated or manipulated in *E. coli* and not prone to spontaneous deletions or rearrangements. However, the manipulation of viral genome in BACs, can lead to large-scale engineered deletions, insertions, or other rearrangements which may have impact on the virus replication efficiency or genome stability has often been overlooked (Cui et al. 2009). With modern sequencing technologies it is now feasible to routinely sequence HCMV genomes to monitor sequence fidelity in BACs, following transfection and through passage.

1.8 HCMV downregulation of MHC-1

MHC class I molecules are found on the cell surface of most nucleated cells, but not on the red blood cells. The MHC encodes the human leukocyte antigen (HLA) gene complex and is found on the short arm of chromosome 6, band p21.3 (Kulski et al. 2002). MHC class I molecules are heterodimers a 45 kDa heavy chain consists of $\alpha 1$, $\alpha 2$, and $\alpha 3$, and the smaller 12kDa $\beta 2$ -microglobulin ($\beta 2m$) subunit. The two chains are linked non-covalently via an interaction between $\alpha 3$ domain and $\beta 2m$. The α chain is polymorphic and encoded by a HLA gene, while the $\beta 2m$ subunit is constant. On the upper surface of the MHC class I molecule, the $\alpha 1$ and $\alpha 2$ domains form a

groove, the peptide-binding site, which binds antigenic peptides of 8–10 amino acids in length. Most peptides presented by HLA-I molecules are derived from translation products that have been degraded in the cytoplasm by the multisubunit proteasome complex (Jones 1997) (figure 1.9).

MHC class I molecules consists of the classical (class Ia) HLA-A, -B, and -C and non-classical MHC molecules HLA-E, -F and -G, antigens. By comparing non-classical HLA molecules, to classical HLA, the non-classical HLA molecules have a low genetic variability, their own expression pattern, particular structural organization and function (Koller et al. 1988; Bjorkman and Parham 1990; Geraghty et al. 1990). The assembly and folding of MHC class I occurs within the endoplasmic reticulum (ER) lumen and peptide binding is needed for assembly process. The transporter associated with antigen processing (TAP) is responsible for translocating peptide from cytosol, where they are generated, into the ER lumen by where they can bind HLA-I (Abele and Tampe 1999). In ER, the chaperones facilitate the folding of nascent HLA-I molecules heavy chain and β 2m. The immature HLA-I HC and β 2m dimeric complex binds to TAP along with the chaperones calreticulum and ERP57 (Pamer and Cresswell 1998; Antoniou et al. 2003). Tapasin is important for HLA-I assembly, it acts as a bridging molecule between the HLA-I/chaperone complex and TAP. Also, it is crucial for high affinity peptide to bind to HLA- I molecules. Once the peptide is loaded onto the HLA-I HC, the complex dissociates and the newly formed trimeric HLA-I complex then traffics through the Golgi apparatus to the plasma membrane (Spiliotis et al. 2000; Williams et al. 2002). The summary HLA - I antigen presentation pathway is showed on figure 1.9.

The MHC class I chain-related (MIC) genes are located in chromosome 6 within the MHC class I region. The MIC genes have seven loci (MICA–MICG) but only MICA and MICB are transcribed. MICA and MICB have molecular mass of 43kDa from 383 amino acids polypeptide. MICA/B have 18–30% similarity to classical HLA class I and whilst also normally possessing three external domains (α 1–3), a transmembrane domain and (usually) a cytoplasmic domain, MICA/B does not bind β 2m or peptide. MICA/B expression is thus TAP independent (Groh et al. 1996). MICA/B is expressed by monocytes, keratinocytes, fibroblasts, endothelial cells, epithelial cell lines and most epithelial tissues. (Bahram et al. 1994; Bahram et al. 1996; Groh et al. 1996; Zwirner et al. 1999; Bahram 2000). MICA/B is a ligand to NK2GD, an activating receptor expressed on all NK cells, all $\gamma\delta$ T cells and some $\alpha\beta$

CD8⁺ T cells. The activation of NKG2D in NK cell receptor occurs through the transmembrane adapter protein DAP10 (Bauer et al. 1999; Wu et al. 1999).

MICA is polymorphic with more than 50 recognized human MICA alleles (Robinson et al. 2001). In comparison with MICA, MICB is less polymorphic with only 17 different alleles (Fischer et al. 2000). Due to stop codon MICA*008, MICA*023 and MICA*028 alleles have truncated cytoplasmic tail. Studies have established that MICA*008 is the most common allele in North American with a frequency of 66.9% (Robinson et al. 2001; Zhang et al. 2001).

The HCMV US6 gene family downregulates of HLA-I from the cell surface these inhibitors include US2, US3, US6 and US11. HCMV US3 is expressed during IE period of viral replication around 1–4 h post-infection and alters HLA-I antigen presentation. There are three transcripts produced by the US3 open reading frame through alternative splicing (Ahn et al. 1996; Liu et al. 2002). The largest transcript, producing a 22 kDa protein, it is able to retain the fully assembled MHC class I complexes in the ER (Ahn et al. 1996). The transmembrane and ER-luminal domains of US3 is needed to downregulate MHC I by binding chaperon tapasin and inhibiting peptide loading. Also, US3 uses US2 gene product to enhance degradation of MHC I. Interestingly US3 binds newly synthesized class II α/β heterodimers and prevent its assembly interfering with MHC II antigen presentation (Hegde et al. 2002; Chevalier and Johnson 2003; Noriega and Tortorella 2009). US2 and US11 genes are also expressed early in infection and prevent HLA-I cell surface expression by promoting their retrograde transport to the cytosol where they are rapidly degraded by proteasomes (Wiertz et al. 1996a; Wiertz et al. 1996b; Jones and Sun 1997). A single glutamine residue within the transmembrane domain of US11 is responsible for ubiquitination and degradation of HLA-I heavy chain, interestingly the cytoplasmic tail residues of US2 are important for HLA-I instability (Lilley et al. 2003; Noriega and Tortorella 2008). Also, US2 downregulates MHC II by degrading the HLA-DR-alpha and DM-alpha molecules (Tomazin et al. 1999). US2 downregulates HLA-A2, HLA-B27, and HLA-G gene products. However, it has no effect on HLA-B, -C or -E alleles or soluble HLA-G1. It was found that US11 induced the degradation of HLA-A2 but not HLA-G (Barel et al. 2003a; Barel et al. 2003b). This supports the hypothesis that US2 and US11 work in different ways even though their degradation pathways are similar (Soetandyo and Ye 2010).

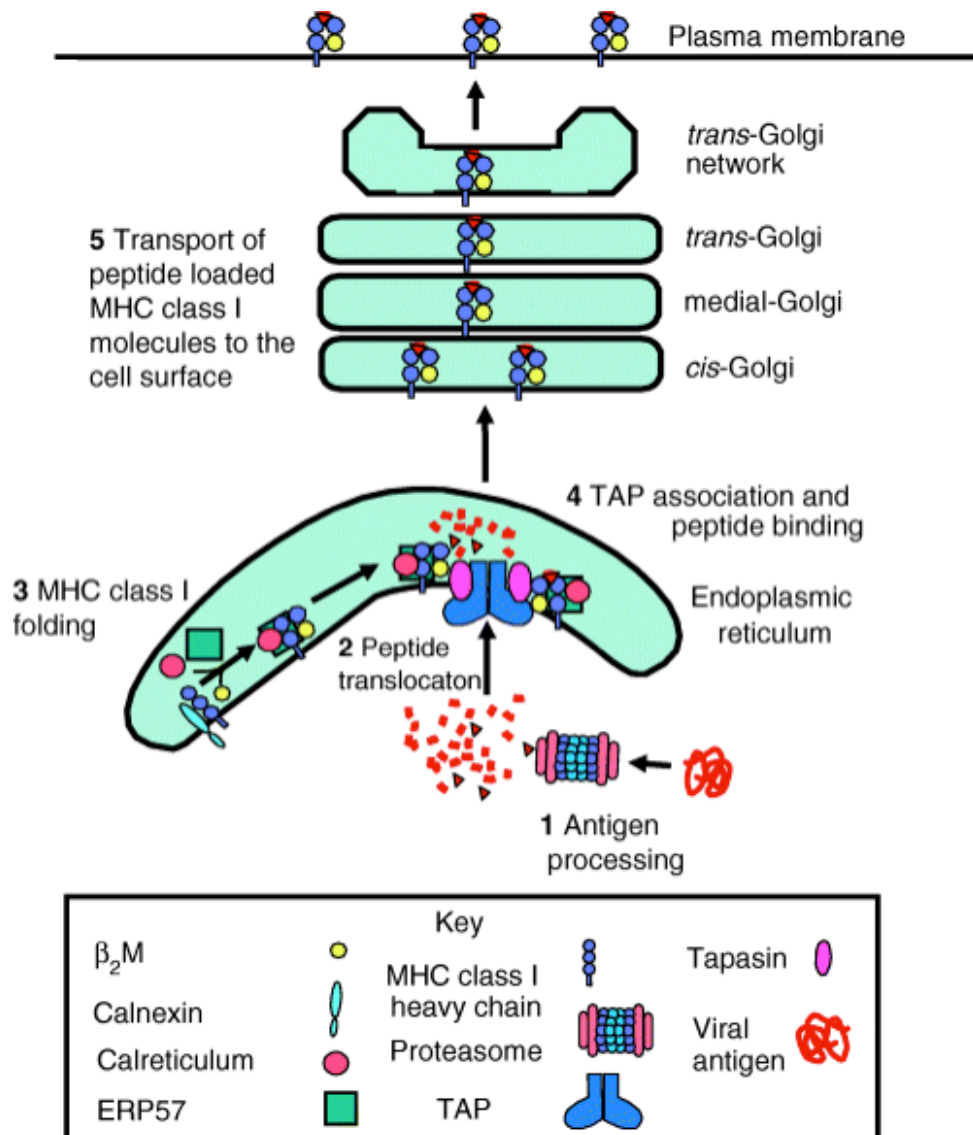


Figure 1.9: The assembly of MHC class I. (1) In the cytoplasm protein is degraded to peptides by the proteasome. (2) By using TAP, the peptides are transported into the ER. (3) The heavy chain of HLA class I molecules binds to β_2m in the ER lumen with help of the ER chaperones calnexin, calreticulum and ERP57. (4) The calreticulum and ERP57-HLA class I complex with TAP. The tapasin aids peptide binding. (5) After peptide binding to HLA class I molecules the TAP dissociated from the HLA-class I complex which then transported through the secretory pathway to presented on surface of plasma membrane. The diagram is adapted from (Hewitt 2003).

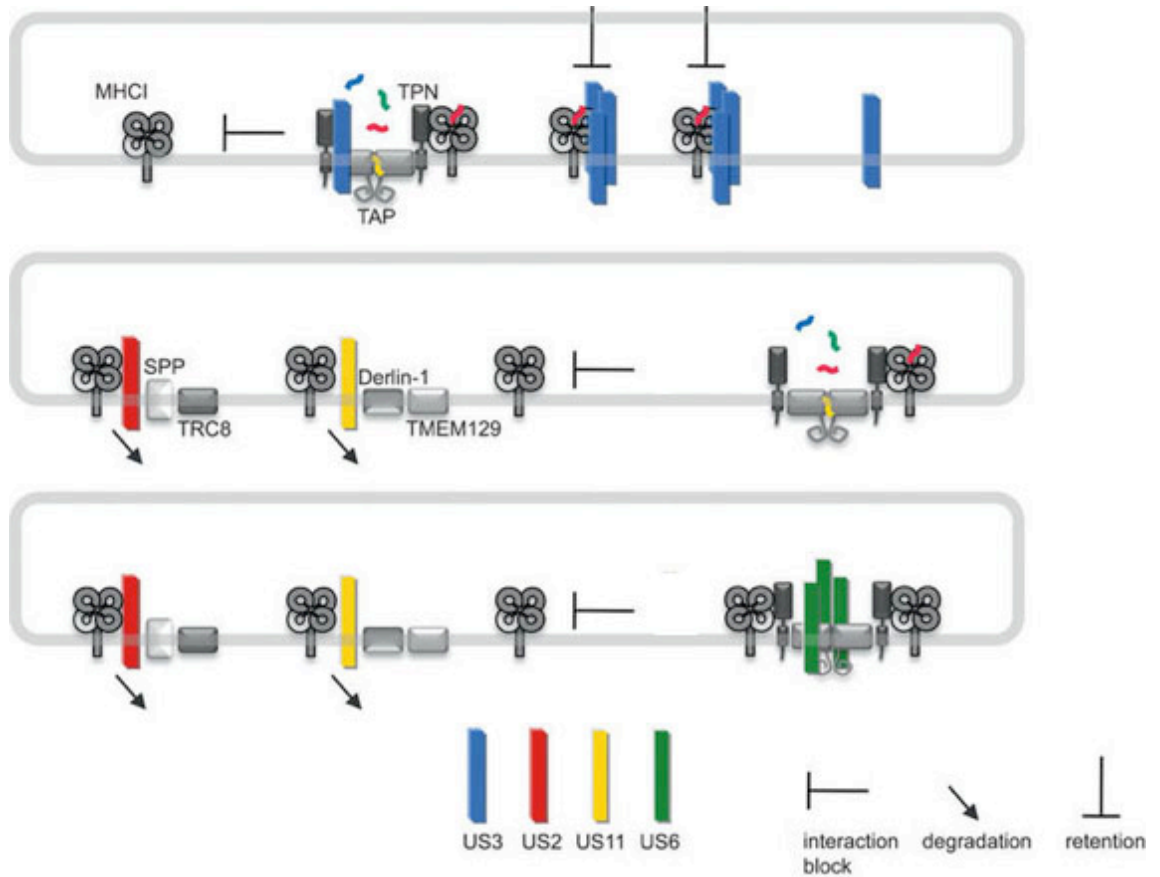


Figure 1.10: Downregulation MHC I molecules by HCMV. The cartoon details the inhibition of HLA-I antigen presentation during HCMV replication. US3 (blue) retains HLA-class I in ER by making a complex with it. US3 blocks PLC complex interaction by binding to TAP1 and tapasin. US2 (red) uses SPP/TRC8 pathways and US11 (yellow) uses Derlin-1/TMEM129 ERAD pathways to translocate HLA class I molecules to ERAD pathways which lead to its degradation in proteosomes. US6 (green) blocks TAP -dependent peptide translocation into the ER. ER, endoplasmic reticulum; ERAD, ER-associated degradation; TRC8, translocation in renal carcinoma, chromosome 8 gene; SPP, signal peptide peptidase; PLC, peptide loading complex (Halenius et al. 2015).

The mode-of-action of HCMV US6 is quite distinct from US2, US3 and US11 in that it prevents cytosolic peptides being transported to the ER by the TAP complex (Lehner et al. 1997). GpUS6 binding to the ER luminal side of TAP1 causes a conformational change that prevents the binding of ATP (Ahn et al. 1997). It was found that just the peptide from 89 to 108 is sufficient to inhibit antigen presentation (Dugan and Hewitt 2008). US6 inhibits classical HLA- I alleles and non-classical alleles HLA-G (Jun et al. 2000). The effect of US6 family on MHC I is summarized in figure 1.10.

UL142 encodes an MHC-I-related glycoprotein that inhibits the surface expression of full-length MICA but not the truncated MICA*008 allele (Chalupny et al. 2006; Ashiru et al. 2009). The luminal and transmembrane domains of UL142 sequesters the full-length MICA alleles in the ER and cis-Golgi apparatus. However, it has effects only on nascent MICA but not mature cell surface MICA (Ashiru et al. 2009). Fielding and co-workers recently showed that the US12 gene family played a major role in regulating MICA. Although both US18 and US20 were capable of acting independently to promote lysosomal degradation of MICA, they were more efficient when working together and in the context of a productive HCMV infection (Fielding et al. 2014; Fielding et al. 2017).

1.9 HCMV NK evasion functions

NK cells are derived from CD34⁺ hematopoietic progenitor cells, in the bone marrow and were first defined as large granular lymphocyte (non-T cells, lacking CD3) that were able to lyse tumour cell without any priming or prior activation (Frag et al. 2003). NK cells are an innate immune cell capable of combating infections. NK cells unlike B or T cells do not require receptor rearrangement in order to recognise virus infected cells or tumour cells. Rather, NK cells are heterogenous group of cells that differentially express a wide range of activating and inhibitory receptors that determine their individual specificity (Long 1999; Bottino et al. 2005). NK cells are responsive to cytokines and interferons and become activated when their surface receptors recognise an excess of activating over inhibitory ligands on the surface of infected cells (Santoli et al. 1978; Trinchieri et al. 1978; Lanier 2005).

NK cells, neutrophils, dendritic cells, and macrophages, act in concert to suppress virus infections, the neutrophils interact with natural killer cells, they help each other

in maturation, activation, and effector functions (Mocsai 2013; Scapini and Cassatella 2014). The NK cell stimulated with IL-15 and IL-18 use IFN- γ and granulocyte macrophage colony-stimulating factor (GM-CSF) to sustain immune response and modulate neutrophils activation and survival (Costantini et al. 2010). Apoptosis of neutrophils is enhanced by NKp46 and Fas-dependant human NK cell functions, and this NK cells can restrain inflammation (Thoren et al. 2012). Interestingly, the neutrophils also modulate NK cell maturation and activation and have effect on NK cells function and homeostasis beside cytokine production and NK cell licensing (Jaeger et al. 2012).

Macrophages control NK cells by the expression of ligands and cytokines secretion, at same time NK cells kill the virus infected macrophages to cease the virus infection (Michel et al. 2012). NK cells are regulated by interactions with dendritic cells. Interestingly, NK cells can activate dendritic cells (DC) and they influence on subsequent effector functions on DC. The mature DCs release IL-12 and IL-15 cytokines that activate NK cells and induce their proliferation, the activated NK cells induce DCs maturation by secreting IFN- γ , tumour necrosis factor- α (TNF- α) and GM-CSF then NK cells eliminate autologous immature DCs (Gerosa et al. 2002; Ferlazzo et al. 2004; Morandi et al. 2006; Goldszmid et al. 2012)

NK cells are particularly important in the control of herpesvirus infections. Genetic deficiencies in NK cell function are rare but often associated with increased incidence of herpesvirus infection, in particular by HCMV and EBV (Biron et al. 1989; Gazit et al. 2004). NK cells are one of the innate immune cells which react to a decreased levels of HLA class I expression on target cells, also they are sensitive to the release of proinflammatory cytokines. However, NK cell activation is the result of a summation of activation and inhibitory receptors. KIR constitute a family of NK receptor that primarily recognise MHC class I. Although the majority of KIRs are inhibitory, they are paired with a subset of activating receptors. Depending on signalling molecules recruited by their cytoplasmic domains, KIRs can provide either an activating or an inhibitory signal. LIR1 (LILRB1/ILT2/CD85j/PIRB) is another inhibitory NK cell receptors that recognises HLA class I, thus, normal self-recognition acts to suppress killing by NK cells. As mentioned previously, the HCMV US6 family downregulates MHC I using multiple mechanisms, the consequence of MHC I downregulation is to release the repression on NK cells, a

well-recognised phenomenon known as ‘missing self’ (Wilkinson et al. 2008; Hoglund and Brodin 2010; Yokoyama et al. 2010; Pegram et al. 2011).

HLA-E is non-classical HLA class-I molecules which binds the inhibitory receptors CD94/NKG2A, to inhibit NK cell-killing. However, HLA-E also binds to CD94/NKG2C, which is an activating receptor expressed on the surface of NK and T cells, albeit binding to the paired activating receptor is 6 times weaker than binding to the inhibitory receptor (Borrego et al. 1998; Braud et al. 1998; Kaiser et al. 2008). HLA-E is expressed on the surface of the cells of most tissues that express classical HLA-I, it binds to nonamers of conserved peptide that is derived from leader sequence of signal peptide of HLA class I and HLA-G (Braud et al. 1997). The signal peptide peptidase enzyme cleaves the signal peptide from HLA-I peptide and, following its release, the signal peptide is further processed by intramembrane protease (Lemberg et al. 2001; Weihofen et al. 2003). Following release into the cytosol, the residual peptide is further processed in the proteasome to produce shorter peptide that are transferred to the lumen of the ER by TAP where it can bind HLA-E and promote its transport to the cell surface (Lee et al. 1998). US6 downregulates HLA-I by blocking TAP, but as a result of it also downregulates HLA-E. Both these properties of US6 can be expected to stimulate NK cell recognition. However, the signal peptide of gpUL40 is responsible for rescuing HLA-E cell surface expression by providing a nine amino acid sequence (VMAPRTLIL) to HLA-E in a TAP independent way, accordingly the UL40 protects HCMV infected cells from and lysis by CD94/NKG2A⁺ NK cells (Tomasec 2000; Ulbrecht et al. 2000).

HCMV UL141 glycoprotein (gpUL141) is able to downregulate NK cell killing. gpUL141 downregulates surface expression of CD155 (nectin-like molecule 5; poliovirus receptor), which is a ligand for the NK cell activating receptors DNAM-1 and TACTILE, also known as CD226 and CD96 respectively (Tomasec et al. 2005). gpUL141 acts by sequestering CD155 in the ER. CD155 is involved in cellular adhesion, motility, transendothelial migration, focal adhesions and endocytosis and only becomes exposed on the cell surface when normal cell-to-cell interactions are disrupted by virus infection or cell transformation. HCMV infection is able to disrupt normal intercellular interactions (Stanton et al. 2007). CD112, also known as nectin 2, is normally involved in adherent junctions but also becomes exposed when normal

intercellular interactions break down. Like CD155, CD112 is also a ligand for the NK cell activating receptor DNAM-1. HCMV gpUL141 downregulates CD112 from the cell surface then recruiting US2 to target the cellular protein for proteasomal degradation, gpUL141 thus removes two activating ligands for DNAM-1 from the surface of HCMV infected cells. (Prod'homme et al. 2010; Hsu et al. 2015).

HCMV-encodes UL142 glycoprotein that is able to neutralize NK cell killing in HCMV infected cell, gpUL142 has a homology to HLA class I and in silico analysis reveals secondary structure prediction delineation of HLA class I alpha-1 and alpha-2 domains that in HLA class I which may have the ability to bind peptide (Wills et al. 2005). It was found that UL142 down regulates cell surface expression of MICA NKG2D ligands of NK cells, by retaining MICA in the ER and the cis-Golgi apparatus. GpUL142 down-modulated surface expression full-length MICA alleles. However, the truncated allele MICA*008 is immune from attention of UL142 (Chalupny et al. 2006; Ashiru et al. 2009).

The US12 gene family of HCMV consists of a sequential array of 10 genes extending from US12 to US21 in a tandem arrangement (figure 1.4). Their encoded proteins each contain a seven-transmembrane domain (7TMD) and homology with the BAX Inhibitor-1 (BI-1) protein, that function as apoptotic enhancer (Lesniewski et al. 2006). Fielding and co-workers found that the US18 and US20, inhibit NK cell mediated cytotoxicity by downregulating full length MICA in HCMV infection, (Fielding et al. 2014). Another study performed by Fielding et al demonstrated that the HCMV upregulates the surface expression of B7-H6. However, NK cell killing is inhibited by HCMV US18 and US20 encoded protein by downregulating B7-H6 surface expression, by sending them to endosomal degradation (Fielding et al. 2017)

The UL18 glycoprotein has similarity to HLA class I molecules, that has ability to bind β_2m and presenting peptide (Beck and Barrell 1988). GpUL18 is able to bind LIR-1 receptors 1000 times more efficiently than HLA class I (Beck and Barrell 1988; Leong et al. 1998; Kaiser et al. 2008). Prod'homme and co-workers found that the gpUL18 able to inhibit cytotoxicity LIR1⁺ NK cells. However, it stimulates LIR-1⁻ NK cells (Prod'homme et al. 2007).

HCMV also express a small, non-coding microRNAs, to date twenty-four miRNAs have been described to be encoded by HCMV during the lytic and the latent infection phase, they target certain viral and cellular transcripts which helps HCMV to evade

immune responses. They also affect viral replication, cell cycle, and mediate latency (Grey et al. 2007; Hook et al. 2014; Kim et al. 2015; Meshesha et al. 2016). miR-UL112-1 is one viral miRNA that is expressed during latency in primary myeloid cells and during lytic infection, where it inhibits the activation of a stress ligand of the NK cell activating receptor NKG2D by targeting MICB transcript (Stern-Ginossar et al. 2007; Meshesha et al. 2016).

The glycoprotein UL16 is able to retain ULBP1, ULBP2, and MICB in ER, that is enables HCMV to evade immune response by inhibiting stress activating receptor of NK cells NKG2D (Cosman et al. 1997; Kubin et al. 2001; Spreu et al. 2006).

1.10 HCMV MHC-I homologues UL18 & UL142

The UL18 gene encodes UL18 glycoprotein which has homology to HLA class I, it was first discovered when AD169 genome was analysed. GpUL18 is a type I transmembrane, which is sensitive to endoglycosidase H with a 67-kDa protein molecular weight, it forms a trimeric complex with β 2-microglobulin and is able to bind peptides (Beck and Barrell 1988; Browne et al. 1990). UL18 gene encodes another form of the UL18 glycoprotein which is Endo H resistant protein with a 160-kDa molecular weight. In comparison with HLA class I, which has 1-3 glycosylation sites, UL18 is heavily glycosylated with 13 N-linked glycosylation sites. Also, it is unlike the MHC I as it binds only LIR-1 (Beck and Barrell 1988; Cosman et al. 1997). GpUL18 binds to LIR-1 with 1000 times higher affinity than HLA class I molecules, gpUL18 also binds to CD94/NKG2C, with 1,000-times less affinity when compared to LIR1 (Chapman et al. 1999; Kaiser et al. 2008). The crystal structure of LIR-1 indicates that binding to gpUL18 is mediated through similar interfaces as LIR-1 uses to interact with HLA class I molecules (Willcox et al. 2003).

Whilst UL18 is relatively well studied, its function and regulation are not yet fully defined. Initially, based on the similarity between gpUL18 and MHC class I molecules, Fahnestock et al proposed that the viral glycoprotein could function as a molecular decoy for NK cells, inhibiting NK cell lysis (Fahnestock et al. 1995). Reyburn et al found that gpUL18 was expressed in MHC class I negative cell line and it elicited protection against killing by NK cells (Reyburn et al. 1997). In

another study, gpUL18 was reported to enhance NK cell killing compared to control cells (Leong et al. 1998). These apparently contradictory findings were explained by Prod'homme et al, who studied NK cell degranulation from multiple donors targets and found that gpUL18 inhibit LIR1⁺ NK cells but stimulates LIR-1⁻ NK cells (Prod'homme et al. 2007). The capacity of gpUL18 to stimulate LIR-1⁻ NK cells has yet to be explained satisfactorily. The explanation proposed is that gpUL18 may also stimulate an activating receptor. Since the effect was observed in all donors, such a receptor would not be expected to be donor specific. Moreover, the observation that gpUL18 also selectively binds the HLA-E binding peptide donated by the UL40 signal peptide was unexpected (Prod'homme et al. 2007; Prod'homme et al. 2012). What purpose may be served in binding this peptide? UL40 does provide the peptide in a TAP-independent manner, so it does provide a source of peptide that is immune to the effects of US6. However, the peptide-binding region of gpUL18 is not involved in LIR1 binding so its role may lie elsewhere, possibly in recognition by an activating receptor. In this context it is interesting to note that KIR recognition of MHC-1 does tend to involve the peptide binding domain of MHC-1, and can be dependent on the nature of the peptide bound.

UL142 ORF is encoded by one of genes within the *U_L/b'* region that is present in HCMV clinical isolates and low passaged strains virus which absent from the laboratory strains AD169 and Towne. The sequencing of UL142 reveals similarity between gpUL142 and gpUL18, both of them comprise the HCMV MHC gene family (Davison et al. 2003b). In silico analysis of UL142 reveals that UL142 encodes MHC-I-related α 1 and α 2 domains, but not α 3 domain. UL142 glycoprotein is a heavily glycosylated protein with 17 potential N-linked glycosylation sites, gpUL142 inhibits NK cell killing when expressed in isolation but not with all donors (Wills et al. 2005; Prod'homme et al. 2007). Chalupny and co-workers found that the gpUL142 has the capacity to evade immune response by inhibiting NK killing by downregulate the cell surface expression of full-length MICA. However, it fails to downregulate the truncated allele of MICA, MICA*008 (Chalupny et al. 2006). Another study was performed by Ashiru et al demonstrated that UL142 was mainly localized to the ER and cis-Golgi apparatus. Also, they demonstrated that the ER localization of gpUL142 was mediated by also transmembrane domain, while its cis-Golgi localization was mediated by the luminal domain. In agreement with the study

performed by Chalupny et al, they demonstrated that UL142 downregulated surface expression of full-length MICA alleles while having no effect on the truncated allele MICA*008. In addition, their data demonstrate that the UL142 retains full-length MICA alleles in the cis-Golgi apparatus and gpUL142 luminal and transmembrane parts were involved in recognition and intracellular sequestration of MICA. They suggested that UL142 has no effect on mature MICA on the cell surface, but interacts with nascent MICA and sequestered in the ER (Ashiru et al. 2009). Whilst the effect of UL142 on MICA is potentially extremely important, it is also somewhat redundant as the US12 family has now been shown to be highly effective at targeting full length MICA(Fielding et al. 2014; Fielding et al. 2017).

1.11 MOCV MHC I homologues genes -MC033 and MC080.

The mc033L and mc080R are MHC-I homologues encoded by MOCV (Senkevich et al. 1997). mc080R was studied by Senkevich and Moss in 1998, who demonstrated in this study that MC080R protein was glycosylated and localised predominantly within the ER and Golgi compartments. MC080R was predicted to have a transmembrane domain and shown to bind to β 2m in ER, however, it could not be detected on the cell surface (Senkevich and Moss 1998). The role of MC033L has not been previously studied.

1.12 Aims

The mc33L, mc80R, UL18 and UL142 are all recognised MHCI homologues encoded by large DNA viruses. Both HCMV genes have been functionally implicated in regulating NK cell recognition. There is indirect evidence that MOCV may downregulate cell surface expressions of MHC I as cell surface expression of β 2-m is reduced on MC lesions. It is also recognised that the downregulation of MHC-I renders HCMV infected cells more vulnerable to NK cell attack, and thus a similar situation may hold with MOCV. Thus, building on findings with HCMV, it was hypothesised that the MOCV MHC-I homologues may also be involved in modulating NK cell function. Moreover, whilst UL142 appears to downregulate full length MICA, that function has also been assigned to the US12 gene family. In

studying the MHC-I homologues of two large yet unrelated DNA viruses, the aims of this thesis were to:

1. Generate reagents to characterise the expression and function of MC033 and MC080
2. Investigate whether MC033 and MC080 modulate the cellular immune response.
3. Investigate the effect of optimally-expressed UL142 on NK cell recognition both when expressed in isolation and in the context of a productive HCMV infection.

2-METHODS AND MATERIALS

2.1 SOLUTIONS

All formulated bacterial culture media was sterilized by autoclaving. Prior to addition of supplements, media was tempered to 50°C.

Double-distilled ultra-pure water (ddH₂O) used for the preparation of solutions, buffers, and media was delivered from a Purelab Ultra water system (Elgin).

The tissue culture reagents used were from the Gibco product line of Invitrogen/Life Technologies (Fisher Scientific, Loughborough, UK) and the analytical grade chemicals and bacterial culture reagents used were from Sigma and/or Fisher unless otherwise stated.

Ampicillin stock: Ampicillin (Sigma-Aldrich, Poole, UK) was dissolved in H₂O at 50mg/ml and stored at -20°C.

Bicarbonate Buffer: 2% (w/v) sodium bicarbonate in H₂O.

Block solution: PBS-T containing 5% dry milk powder

3.5 M CsCL solution: 1.45g/ml CsCl in 5mM Tris HCl, pH7.8

1.6M CsCl solution: 1.33g/ml CsCl in 1mM EDTA, 5mM Tris HCl, pH7.8

Chloramphenicol stock: Chloramphenicol was dissolved in ethanol at 12.5mg/ml and stored at -20°C.

Dialysis buffer for 5 liters: 1mM MgCl₂, 135mM NaCl, 10mM TRIS HCl pH7.8, 10% glycerol, Make up to 5 litres with water

DNA loading buffer (6X): 30% glycerol in de-ionised water with 0.25% (w/v) bromophenol blue (Sigma-Aldrich) in 0.25% (w/v) xylene cyanol FF (Sigma-Aldrich).

Freezing media: 90% foetal calf serum (FCS) and 10% (v/v) dimethyl sulphoxide (DMSO).

2x Hepes Buffered Saline (HBS) for 100mL: 274 mM of NaCl, 10 mM KCl, 1.4 mM Na₂HPO₄, 15 mM D-glucose, 42 mM HEPES (free acid), at pH 7.05-7.06 (by using NaOH)

Immunofluorescence (IF) wash/block buffer: PBS, 1% (w/v) BSA. Depending on use, IF buffers differed on the inclusion or exclusion of sodium azide. For IE1 immuno-staining, 0.01 % (w/v) sodium azide was added to IF buffer.

Immunoblot block/stain buffer: PBS-T, 5% (w/v) fat-free milk proteins (Marvel)

Isopropyl β-D-1-thiogalactopyranoside (IPTG): 23.8mg Isopropyl P-D-1-thiogalactopyranoside (IPTG) (Melford, Ipswich) dissolved in 1ml water to generate a 100mM stock solution.

Luria Bertani (LB) broth: 1% (w/v) tryptone, 1% (w/v) sodium chloride 0.5% yeast extract dissolved in H₂O then autoclaved.

LB agar: As for LB broth but with 1.5% (w/v) agar added before autoclaving. Antibiotics were added before setting in plates.

LB sucrose selection plates: 1% (w/v) tryptone, 0.5% (w/v) yeast extract, 5% (w/v) sucrose 1.5% (w/v) agar dissolved in water then autoclaved. 1:1000 chloramphenicol stock, 1:500 X-gal stock and 1:500 IPTG stock were added before setting in plates.

2x medium (Per 100 ml): 50 ml sterile water, 20 ml 10x DMEM (Gibco 21430), 20 ml FCS (Invitrogen, 10500), 6 ml sodium bicarbonate (Gibco 25080), 4 ml Pen/Strep (Gibco15070063), 2 ml glutamine (Gibco 25030024).

NK media: 10% of FCS and 5% of Human AB serum were added to RPMI media, the media was supplemented with 100 U/mL penicillin, and 100 µg/mL streptomycin, and 1% L-glutamine, then 100U/ml of IL-2 and 10ng/ml of IL-15 were added to the mix.

Phosphate buffered saline (PBS): One PBS tablet (Oxoid, Hampshire, UK) was dissolved in 100ml dH₂O for making the buffer. It contains 8% (w/v) sodium chloride, 0.2% (w/v) potassium chloride, 1.15% (w/v) disodium hydrogen phosphate and 0.2% (w/v) potassium dihydrogen phosphate at pH 7.3.

PBS-T (per 1 L): PBS, 0.5 ml TritonX-100 (Fisher, BP151- 500), 0.5 ml Tween 20 (Fisher, BP337500) in water

4% Paraformaldehyde (PFA) solution: PBS, 4% (w/v) paraformaldehyde.

TBE (10X): 108 g Tris, 55 g boric acid dissolved in deionised H₂O to a final volume of 920 ml and then 80 ml 0.5 M EDTA pH 8.0 added.

TE: 10 mM Tris (pH 7.5), 1 mM EDTA sterilized and DNAases inactivated by autoclaving.

Transfer buffer: (per 500 ml): 50ml 20x NuPAGE[®] Transfer Buffer, 50 ml methanol, 400 ml deionised water

TRIS buffer: 10ml of 1M Tris-Cl pH7.4 was mixed with 2ml 0.5M EDTA, pH8.0 with water added to a final volume of 1 liter

1M TRIS-HCl: 121.1g Tris base was dissolved in 1 liter of d H₂O and adjusted to pH 7.8 with hydrogen chloride.

X-gal stock: 5-bromo-4-chloro-3-indoyl-p-D-galactopyranoside (X-gal) was dissolved in N, N-dimethyl formamide (DMF) to generate a 40mg/ml stock solution. Aliquots were stored at -20°C.

2.2 Antibodies

The used antibodies are listed in table 2.1

Table 2.1: The used antibodies in this thesis.

| Antibody | Supplier | Clone | Cataloug number |
|------------------------|-----------------|--------------|------------------------|
| A- Western Blot | | | |

| | | | |
|---|------------------------------------|------------|--------------------|
| 1- V5 (mouse, monoclonal) | BioRad | SV5-Pk5 | MCA2895GA |
| 2- HC10 (mouse) | Kindly provided by Dr Hidde Ploegh | hybridoma | (Stam et al. 1986) |
| 3- Actine (rabbite) | Sigma | Polyclonal | A2066 |
| B- Flowcytometry | | | |
| 1- V5 (mouse, monoclonal) | BioRad | SV5-Pk5 | MCA2895GA |
| 2- Human HLA-E (PE conjugated) | Biolegend | 3D12 | 342604 |
| 3- human HLA A, B, C (Alexia flour @ 647) | Biolegend | W6/32 | 311414 |
| 4- FITC-conjugated CD107 | BD Biosciences | H4A3 | 555800 |
| 5- PE-Cy7-conjugated CD3 | Biolegend | 17A2 | 100220 |
| 6- APC-conjugated CD8 | Biolegend | HIT8a | 300911 |
| 7- PE- conjugated CD56 | Beckman Coulter | N901 | IM2073U |
| 8- Isotype antibodies: - PE conjugated mouse IgG1 k | BD Bioscience pharmingen | MOPC-21 | 555749 |
| - Mouse IgG2a k alexea flour @ 647 | Biolegend | MOPC-173 | 400234 |
| - Mouse IgG | Sigma | | 15381 |
| - FITC-conjugated IgG1 | BD Biosciences | MOPC-21 | 555748 |
| C- Immunofluorescence | | | |
| 1- V5 (rabbite) | Abcam | ab 9116 | GR116421-19 |
| 2- Calnexin (mouse) | Millipore | C8.B6 | 2274261 |
| 3- Giantin (rabbit) | Abcam | Polyclonal | Ab24586 |
| 4- V5 (mouse, monoclonal) | BioRad | SV5-Pk5 | MCA2895GA |
| D- Secondary antibody | | | |

| | | | |
|---|-----------------|-------------------|---------|
| 1- Alexia flour @488 (goat anti-rabbit) | Invitrogen | F(ab)2, IgG(H+L) | A11070 |
| 2- Alexia flour @594 (goat anti-mouse) | Life technology | F(ab)2, IgG9H+L) | A 1102 |
| 3- Alexia flour @647 (goat anti-mouse) | Life technology | F(ab)2, IgG (H+L) | A-21235 |
| 4- Anti mouse HRP | BioRad | | |
| 5- Anti-rabbit HRP | BioRAD | | |

Table 2.2: Lasers, excitation wavelength and emission spectra of fluorochromes used for flow Cytometry

| Fluorochrome | Laser (nm) | Emission |
|--------------|-------------------|----------|
| FITC | Argon Laser 488nm | 525nm |
| PE | Argon Laser 488nm | 575nm |
| PE-Cy7 | Argon Laser 488nm | 767nm |
| APC | Diode Laser 633nm | 660nm |

2.3 Cells

2.3.1 Cell lines

The human cervical epithelial cell line, HeLa, were obtained from the American Type Culture Collection (ATCC). Human foetal foreskin fibroblasts (HFFFs) were kindly provided by Dr Graham Farrar (Porton Down). HF-TERT were made by immortalising HFFF cells by transducing them with the human telomerase reverse transcriptase (hTERT), provided by Sian Llewelyn-Lacey (McSharry et al. 2001), HF-CAR cells were made from HFFF-hTERTs after engineering them to express the human Cocksackie adenovirus receptor (hCAR) that facilitates adenovirus infection, provided by Dr J. DeGregori (University of Colorado Health Sciences Centre, Denver, USA) (Stanton et al. 2008). 293 cells expressing the tetracycline repressor protein (293-TREX) were purchased from Invitrogen (Invitrogen, R71007). HEK293 cells transduced to express the Adenovirus E1 genome region (Graham et

al. 1977), were used for the propagation of AdZ-5 vectors. NPi cells are fibroblast cell line derived from a TAP deficient patient (N.P) that are MHC class I and HLA-E deficient (provided by V. Cerundolo, University of Oxford). Chinese Hamster Ovary cells expressing CAR (CHO-CAR) were obtained from ATCC.

Table 2.3: HLA and MICA genotypes of the donors

| The Donor | HLA-A genotype | HLA-B genotype | HLA-C genotype | MICA genotype |
|------------------|-----------------------|-----------------------|-----------------------|------------------------|
| D007 | HLA: -A2 -A24 | HLA: -B44 - B44 | HLA: - Cw10 - Cw10 | MIC-A*00801 A*00804 |
| D008 | HLA: -A2 -A24 | HLA: -B60 - B60 | HLA: - Cw5 - Cw5 | MIC-A*00801 A*00804 |
| D009 | HLA: -A1 -A24 | HLA: -B8 - B44 | HLA: - Cw5 - Cw7 | MIC-A*00801 A*00804 |
| HFFF | HLA: -A1 -A24 | HLA: -B8 - B13 | Have not done | MIC-A*016 A*027 |

2.3.2 Tissue culture media

The standard tissue culture conditions for the growth of human cells were 37°C, in an environment of 5% CO₂. Dulbecco's modified Eagle's medium (DMEM, Invitrogen) were used to grow the cells. Media was supplemented with 100 U/ml penicillin, and 100 µg/ml streptomycin, and 10% FCS, referred as complete medium in text. The cells were routinely maintained in 150 cm² flasks, they were allowed to reach around 70 to 90% confluency before cells were passaged. Adherent cells were passaged by first removing media, then the cells monolayer was washed by using 10 ml of PBS, then 5ml of trypsin (Trypsin-EDTA (0.05%), phenol red, Gibco by life technology) was added and incubated at 37°C with 5% CO₂ until the cells detached. After that 5ml of complete medium were added to the detached cells, then the cells suspension was divided into fresh flasks.

2.3.3 Cell counting

The cells were counted using a glass haemocytometer (Fisher, MNK-790-M). The counting chamber was loaded with 10 μ l of homogenous cell suspensions, and the number of cells within grids that held 0.1 μ l (1×10^{-4} ml) was counted. Cells counted under x10 magnification, and the average number from three grids was obtained. The averaged cell count was multiplied by a factor of 10,000 (10^4) to determine the number of cells in 1 ml of the original suspension.

2.3.4 Cryopreservation of cell lines

The suspension of adherent cells was made as described in section 2.3.2, then the cells were centrifuged and resuspended in 1 ml of freezing media and transferred immediately to a cryovial tube and placed in freezing container contain isopropanol (Nalgene 5100 Cryo 1°C freezing container) (Merck, West Drayton). After that the container was transferred to a -80°C freezer for overnight before transfer the cryovial tubes to liquid nitrogen freezer.

2.3.5 Thawing cells

To resurrect cells from liquid nitrogen, the cryovial was transferred in dry ice, then thawed rapidly in a 37°C H₂O bath. The thawed cells were suspended in 10 ml of complete medium. Then they were centrifuged at 470 x g for 5 minutes, then the cells were resuspended for counting before using them.

2.4 Viruses

Table 2.4: The viruses used in thesis

| Viruses | Source /Reference |
|----------------|--|
| RAd-mc080 | Genotype 1 molluscum contagiosum mc-080-codon optimized with C terminal V5 tag. Made by Hana Elasifer |
| RAd-mc033 | Genotype 1 molluscum contagiosum mc-033-codon optimized with C terminal V5 tag. Made by Hana Elasifer |
| vWR293-mc080 | Genotype 1 molluscum contagiosum mc080 cloned into the replication-competent vaccinia virus Western Reserve (WR) strain and designated v293. Made by by Dr Subuhi Sherwani |

| | |
|-------------------|---|
| RAd-UL18 | Strain Merlin UL18 ORF with a C-terminal V5 tag amplified by PCR and cloned in to AdZ vector system. Constructed by Dr Sepehr Seirafian and Dr James Davies |
| RAd-1253 | AdZ-5 vector without insert. Made by Dr Richard Stanton |
| RAd-UL142 | Strain Merlin UL142 ORF with a C-terminal V5 tag amplified by PCR and cloned in to AdZ vector system. Constructed by Dr Sepehr Seirafian and Dr James Davies |
| RAd961-mc080 | Genotype 1 molluscum contagiosum non-codon optimized mc080. Made by Virginie Dr Prod'homme and Dr Rich Stanton |
| 1812 | The HCMV strain Merlin genome (1111) deleted UL142. Made by Dr Peter Tomasac |
| 1656 | The HCMV strain Merlin genome (1111) deleted US18+US20. Made by Dr Ceri Fielding |
| 1111 | The HCMV strain Merlin genome was cloned in to a BAC at passage 5. Derived from the prototype RL13 ⁻ , UL128 ⁻ Merlin BAC described in Stanton et al (2010) |
| RAd-UL141 | Strain Merlin UL141 ORF with a C-terminal V5 tag amplified by PCR and cloned in to AdZ vector system Constructed by Dr Sepehr Seirafian and Dr James Davies |
| RAd-UL142-1A | Strain Merlin UL142 synthesised <i>de novo</i> to contain UL142 ORF with the signal peptide in the N terminus removed and replaced with a signal peptide from preprotrypsin (PPT). It has N terminal V5- epitope tag;. Constructed by Dr Rebecca Aicheler |
| RAd-UL142-2A | Strain Merlin UL142 synthesised <i>de novo</i> to contain UL142 ORF with the signal peptide in the N terminus removed and replaced with a signal peptide from preprotrypsin (PPT). It has C terminal V5- epitope tag. Constructed by Dr Rebecca Aicheler |
| RAd-UL142-3C | Strain Merlin UL142 synthesised <i>de novo</i> to contain the UL142 ORF with HCMV endogenous signal peptide. It has C terminal V5- epitope tag. Constructed by Dr Rebecca Aicheler |
| RAd-Soluble UL142 | Strain Merlin UL142 synthesised <i>de novo</i> to contain UL142 ORF, the transmembrane part was cut and it has C terminal V5- epitope tag linked to Bir A Construct. Constructed by Dr Sepehr Seirafian |

2.4.1 Propagation of Recombinant Adenovirus (RAd)

stocks

RAd stocks were propagated in 293T_{REX} cells, the used RAd viruses are shown in table 2.4. 150cm² tissue culture flask with 70% confluent 293T_{REX} cells were infected by adding virus at an MOI of 0.1 in 1ml of complete medium and incubated

at 37°C in 5% CO₂. The virus was monitored for Cytopathic effect (CPE), the complete medium was changed when it needed. The infected cells were detached from the flask and resuspended in complete medium then they were centrifuged at 470 x g for 5 minutes then the cell pellet was suspended in PBS and centrifuged at 470 x g for 5 minutes, after that the cell pellet was transferred to -80°C freezer.

2.4.2 Adenovirus purification by Caesium Chloride

As the virus collected in section 2.4.1 contained cellular debris, a Caesium-Chloride (CsCl, Sigma, C3011-500G) gradient was used to purify the virus.

5ml of PBS was added to the adenovirus infected cell pellet and same volume of tetrachloroethylene then was added, the mixture was shaken vigorously then centrifuged at 836 x g for 25 minutes to release the virus from infected cells. The mixture was separated into three layers, the upper layer contains the virus, the middle layer contains the cell debris and the lower layer contains tetrachloroethylene, the upper layer was collected in 15ml falcon tube. To make CsCl gradient, 1.6 ml of 3.6M CsCl solution was pipetted into a 14x 89 mm ultra-clear Beckman centrifuge tube (331372, Beckman Coulter), overlaid with 3 ml of 1.6M CsCl solution drop by drop, to cause minimal disturbance in the bottom layer. The collected virus then was added to the CsCl gradient. The tubes were centrifuged at 90,000 x g for 2 hours (SW41 Ti rotor, Ultra Beckman L8-M ultracentrifuge), after centrifugation the opalescent virus band in the middle of the tubes was collected using a 19G needles and syringes. To remove CsCl from collected virus, it dialysed against a buffer solution, the sterile dialysed buffer was added to collected virus to up 2 ml total volume which then added to dialysed tubes (Medicell International Ltd, DTV12000.01.000). Then it was clipped from both sides and placed in 1 to 2 L of dialysed buffer then it rocked at 4°C, the dialysed buffer was changed after 4 hours with fresh dialysed buffer, then it rocked at 4°C for overnight. Next morning the dialysed pure adenovirus was collected and sterile dialysed buffer was added up to 5ml total volume and then aliquoted into 500 µl volume in each tube and stored in -80°C freezer

2.4.3. Adenovirus titration

5×10^5 293 TREX cells were seeded into one well of a 12 well plate (Fisher, TKT-520-070H). The following day 10^{-4} and 10^{-5} virus dilutions were made. 100 μ l of each dilution was pipetted drop by drop in wells in duplicates. After 48 hs incubation at 37°C in 5% CO₂ the media were removed from infected well, and the cells dried by keeping them in the hood for 10 mins. 500 μ l of ice cold 1:1 methanol and acetone were added to each well and incubated at -20°C for 10 minutes to fix the cells. The cells then were washed using PBS containing 1% BSA for 3 times then polyclonal goat-adenovirus antibody (Abcam, AB1056) was diluted 1:5,000 in PBS containing 1% BSA then 0.5ml added to each well and incubated for 1hr at 37°C under constant rocking. The cells then were washed using PBS containing 1% BSA 3 times, then donkey anti-goat HRP (Santa Cruz Biotechnology, SC- 2056), 1:1000 dilution was added and incubated for 30 minutes at 37°C under constant rocking. The cells then were washed using PBS containing 1% BSA 3 times, the infected cells detected by the ImmunoPure metal enhanced DAB Substrate kit (Thermo Scientific, 34065). DAB substrate was used according to manufacturer's instructions. Substrate was applied to cells that were then incubated for sufficient time for signal development before counting stained cells. Titres were calculated using the below formula:

$$\text{Titre (pfu/ml)} = \frac{(\text{average of infected cells per field}) \times (\text{number of fields per well})}{(\text{Virus volume (ml)}) \times (\text{dilution factor})}$$

2.4.4 Growth of HCMV stocks

To grow HCMV from the stock with known titre, 70% to 90% confluent HF-TERT cells in Cell Factories (TKT-175-020M, Fisher scientific) were infected with 50 ml of complete medium containing HCMV at an MOI 0.1. The infected cells were monitored for CPE and when 70% to 80% of CPE was observed the media was collected in 250 ml polycarbonate centrifuge bottles (Fisher, CFS-300-520C) and then centrifuged at 30,000 x g for 2 h. Fresh media was added to cell factory and then the media was collected again every 48 h, until the monolayer cells had detached. After centrifugation the supernatant was discarded and the 1ml of DMEM was added to the dislodged pellet and collected in a sterile tube, 0.5 ml of DMEM was added to

remaining pellet then it was added to previous collection. The collected virus was dissociated using a 19G needle and syringe, the collected virus was centrifuged at 16060 x g (Biofuge Fresco, Heraeus) for a minute, then the supernatant was transferred to sterile tubes and stored at -80°C freezer.

2.4.5 HCMV titration by plaque assay

3x10⁵ of HF-TERT were seeded into a single well of a 6 well plate, the next day the 10⁻⁶, 10⁻⁷ and 10⁻⁸ virus dilutions were made. The media were removed from the wells and 1ml of virus dilution was added to each well in duplicates, then they rocked for 2 hs at 37°C in 5% CO₂. After removing the virus, the 10ml of overlay media was added to infected cells which is a mixture of 1:1 of 2% avicel and 2x media then incubated at 37°C and 5% CO₂ for 2 weeks. The overlay used to restrict free transfer of released virus from the infected cells and prevent cell to cell infection transmission. After 2 weeks the overlay media was removed, and the cells were washed for 2-4 times with PBS. Plaques were counted in each duplicate using a light microscope, titres were calculated using the below formula:

$$\text{Titre (pfu/ml)} = \frac{\text{Average number of plaques per well}}{\text{Dilution factor} \times \text{virus volume (ml)}}$$

2.4.6 Lentivirus

2.4.6.1 Making lentivirus expressing mc080 and mc033 by transfection by calcium phosphate DNA precipitation

45µg of mc033 or mc080 pHAGE plasmids, 32 µg of p8.91 plasmid and 13µg of pMDG plasmid (p8.91 and pMDG plasmids were kindly provided by Dr Katja Finsterbusch) were added into HEPES buffered dH₂O (2.5mM) to a final volume of 750µl then they were mixed gently and incubated at room temperature for 5 minutes. Then the DNA-water mix was added to 750µl of 500mM CaCl₂, the DNA-CaCl₂ mixture was added drop by drop, into a tube containing 1.5ml of 2x HBS, while continuing to vortex the tube. The mixture was incubated at room temperature for 30 minutes, 3mls of DNA-CaCl₂-HBS mixture was added drop by drop using a transfer

pipette, for each culture flask of HEK293 cells then placed in the 37°C 5% CO₂ incubator. The medium was removed from each flask 6 hours post transfection then they were washed gently with 20mls sterile PBS, and then 25mls of fresh, warm complete DMEM was added to each flask and incubated at 37°C and 5% CO₂.

2.4.6.2 Lentivirus packaging

The second-generation lentiviruses were made by using the plasmids p8.91 and pMDG along with pHAGE plasmids (Kindly provided by Dr Richard Mulligan) expressing MC033 or MC080. Early passaged 293T_{REX} cells were counted and seeded at 15×10^6 cells per T150 cm² culture flask in 15mls of complete DMEM. The next day the cells were transfected by calcium phosphate DNA precipitation (section 2.4.6.1), 28 hs post transfection the cell supernatants were harvested and filtered using a 0.45µm sterile filter. The collected filtered virus was kept in the fridge (2-8°C) and complete DMEM was added to the cells and incubated at 37°C, 5% CO₂. The second harvest of viral particles was collected at 72 hs post transfection, filtered and added to the first virus harvest. 3ml 20% sucrose in PBS was placed in an ultracentrifuge tube then the filtered supernatant was added gently to the sucrose solution. The tubes were spun at 90,000 x g at 4°C for 90mins (SW41 Ti rotor, Ultra Beckman L8-M ultracentrifuge), the viral pelleted in the bottom, the supernatant and sucrose layer was aspirated, the tubes were inverted for 10 minutes to dry the pellet. The pellet was suspended in 100µl of complete DMEM and stored in the -80°C freezer

2.4.7 Single infection of cells for assays

The cells were counted and seeded the day before infection (5×10^5 cells for a 25 cm² flask, 2.5×10^5 cells per well for a 6-well plate, 5×10^4 cells per well for a 24-well plate) and incubated at 37°C in 5% CO₂ overnight to allow cell adherence. The virus (adenovirus or HCMV) was removed from -80°C, then transferred to a 37°C H₂O bath. The defrosted virus was mixed by pipetting it gently, the cells were infected with virus at the required MOI in complete media for adenovirus and only DMEM for HCMV (2 ml for a 25 cm² flask, 1 ml per well for a 6-well plate, 250 µl per well for a 24-well plate). The infected cells were incubated for 2 hs at 37°C in 5% CO₂ in a rocking incubator. The virus was removed, and complete medium was added to

infected cells (5 ml for a 25 cm² flask, 4 ml per well for a 6-well plate, 1 ml per well for a 24-well plates) and the cells were incubated at 37°C in 5% CO₂ for a required time

2.4.8 Co-infection of cells for assays

The cells were counted and seeded the day before infection and were allowed to adhere overnight. The viruses were removed from -80°C, and transferred to a 37°C water bath, the defrosted virus mixed by gentle pipetting. For NPi cells HLA-E experiments, the cells were infected on day 1 with RAd-HLA-E at an MOI 350 PFU/cell, and RAd mc080 or RAd US6 at an MOI 350 PFU/cell then on day 2 the cells were infected with RAd-UL40 at an MOI 350 PFU/cell, the infected cells incubated for a further 48 hs prior to analysis. In HLA-A2 experiment the NPi cells infected with RAd mc080 or RAd US6 at an MOI 350 PFU/cell, next day the cells infected with RAd-HLA-A2 at an MOI 350 PFU/cell and incubated for a further 48 hs prior to analysis. For MICA assay in CHO-CAR cells, the cells were co-infected with RAd expressing MICA*008 or RAd expressing MICA*002 at an MOI 50 PFU/cell and RAd mc080, RAd vector or RAd expressing UL142 at an MOI 50 PFU/cell and incubated for 72 hs prior analysis.

2.5 MOLECULAR BIOLOGY

2.5.1 PCR

The gene was amplified by PCR from the plasmid, the primers designed then they delivered from Eurofin, the Biometra T3000 Thermal cycler was programmed. The temperature, number of cycles, and concentration of template DNA and time are adjusted according the amplified DNA length, the DNA amount and polymerase type. All reagents were defrosted in water bath except dNTP which was defrosted at room temperature, PCR programs are presented in appendix.

2.5.2 Agarose gel electrophoresis

In order to assess that the correct DNA was present at each stage of the cloning or recombineering process, the samples were separated by gel electrophoresis. 0.8% to 1% of agarose containing gel was used, the separation of PCR products based on their size, the visualisation of the bands on the gel were enhanced with ethidium bromide. The band visualized by UV light using an Autochemi Bioimaging system (UVP) and LabWorks software (Perkin Elmer), or a bench-top transilluminator (Spectroline). Gels were cast using trays taped at either end and accompanying well-forming combs, and allowed to set prior to submersion in excess TAE running buffer. 0.2 volumes of 6X DNA loading buffer was added to each sample, 10µl of molecular weight marker and test samples were pipetted into the wells of the gel and electrophoresis was run for 2-3 hours at 100 V.

2.5.3 Isolation of DNA from an Agarose gel

UV light (Spectroline transilluminator, model TVC-312A) was used to visualize the DNA bands, then DNA bands were cut, and then DNA purified from PCR reactions using the Illustra GFX DNA and Gel Band purification Kit (28-9034-70, GE Healthcare) following manufacturer's instructions. In brief, nucleic acids and other macromolecules were first denatured in the presence of a chaotropic buffer (supplied) and by using the heat blocker heated to 60°C, the solution was transferred to a column and placed in Eppendorf tube after 30 seconds it was centrifuged at 16060 x g for 30 seconds. After discard of flow-through, 500µl of washing buffer was pipetted onto the column then it was centrifuged at 16060 x g for 30 seconds. The column was transferred to a fresh Eppendorf tube and 30µl of sterile deionized H₂O was pipetted onto the column and after 30 seconds incubation the tube was centrifuged for 1 minutes at 16060 x g.

2.5.4 Determination of DNA concentration

The DNA concentration of the samples were determined using a Nano-drop ND-1000 spectrophotometer (ThermoScientific). The spectrophotometer was initialised with 2µl dH₂O the loading pedestal was wiped. The instrument was then blanked by

loading 2µl of the relevant solvent buffer and performance of a measurement. The loading pedestal was again wiped before loading 2 µl of analyte sample to be measured. The concentration was obtained in ng/µl.

2.5.6 Plasmid DNA minipreps

The Qiagen 27104 miniprep kit was used, the colonies were inoculated and grown overnight in 5 ml of LB containing ampicillin (50µg/ml). The bacteria cells were harvested by centrifugation at 5400 x g for 5 minutes. The supernatants were discarded and 250µl of buffer P1 (Qiagen, 27104) was used to resuspend the cells, 250µl of buffer P2 was added, the tubes were inverted 4-6 times to lyse the cells and denature their DNA. 350µl N3 buffer was added to neutralise the reaction. The samples were mixed by inversion and centrifuged at 17,900 x g for 10 minutes at room temperature. The supernatants were transferred to the QIAprep spin column by decanting and centrifuged at 17,900 x g for a minute, the flow-through was discarded. To remove the trace of nuclease activity the QIAprep spin column was washed twice by 0.5ml of PB buffer and centrifuged at 17,900 x g for a minute and the flow-through was discarded. Then the QIAprep spin column was centrifuged at 17,900 x g for a minute to remove the residual of washing buffer. The QIAprep column was placed in a clean 1.5 ml Eppendorf tube and DNA was eluted by adding 50 µl dH₂O to the centre of each QIAprep spin column, and it was let to stand for 1 min, and centrifuged at 17,900 x g for 1 min.

2.5.7 Plasmid DNA maxiprep

In order to obtain transfection quality DNA, recombinant DNA was purified following the protocol of low copy plasmid purification (Max/Bac) plasmid DNA purification nucleo-Bond by Machery-Nagel. The bacteria colonies containing the plasmid of interest was inoculated into 250 ml LB media containing antibiotics and incubated overnight at 37°C with shaking. Cultures were centrifuged at 6,000 x g for 15 minutes at 4°C. 24 ml of S1 buffer was added to bacteria pellets. Then 24 ml lysed buffer (S2 buffer) was added to the tubes which then was inverted 6–8 times, the tubes were incubated for 3 minutes at room temperature. 24 ml of cooled neutralising buffer was added to the mixture, the tubes inverted 6-8 times, then the tubes were

incubated in ice for 5 minutes which then centrifuged at 6000 x g for 15 minutes at 4°C. In mean time the equilibration buffer (6 ml) was added to a NucleoBond® Column, and the column allowed to empty by gravity flow. Then the supernatant was added onto column which had emptied by gravity flow. 18 ml of buffer N3 was added twice to the column and the DNA was eluted by adding 15 ml of elution buffer heated to 50°C to the column and the DNA was collected in fresh tubes. 11 ml of isopropanol was added to the eluted DNA then the tube was centrifuged at 4,500 x g at 4°C for 30 minutes. The DNA precipitate was washed with 70% ethanol and centrifuged at 4,500 x g, at 15 minutes. After ethanol evaporation the DNA was resuspended in 100 µl sterilised dH₂O, the solution DNA was stored -20°C

2.5.8 Restriction enzyme digest for pHAGE plasmid cloning

The restriction enzyme digestion was used to generate compatible ends capable of being ligated together. 5 µl of PCR product and 5 µl of plasmid vector were each purified from an agarose gel using a Qiagen gel extraction kit (section 2.5.3). Both the PCR product and plasmid vector were digested with the compatible restriction enzymes (2 µl each; 10 U/µl) in 10X SURECUT buffer A (5 µl; ROCHE) in a total volume of 50 µl, they were incubated at 37°C for 2 h. This was mixed with 15 µl loading buffer and analysed on a gel. The bands were again gel purified (section 2.5.3), to remove small DNA fragments, and ligated following the protocol in section 2.5.9.

2.5.9 Ligation

To ligate the digested PCR product and the vector, 5 µL of the digested PCR product was mixed with 1 µl of the digested plasmid vector, and 2 µl glycogen with 100 µl -20°C ethanol. Then the mixture was centrifuged for 15 minutes at 16060 x g, to pellet the DNA and bring the vector and insert into close proximity. The supernatant was discarded and the pellet was incubated at 50°C for 5 minutes to dry, then it was resuspended in 10 µl ligation mix which consisted of 1 µl T4 DNA ligase

(Invitrogen), 2 µl 5X T4 DNA ligase buffer (Invitrogen) and 7 µl sterile injection water. The ligation reaction was stored at 4°C for overnight.

2.5.10 Transformation

The chemically competent Top10 bacteria (One Shot TOP10 chemically competent *E.Coli*; Life Technologies) were transformed using heat shock to carry the ligated product (section 2.5.9). The bacteria were thawed slowly on ice, then 5 µl of ligated DNA (section 2.5.9) was added to the cells on ice. After that the tube was placed on a heat block at 37°C for 5 minutes and transferred to ice for 5 minutes. 250 µl of SOC media was added to the cells which were left to recover on the heat block at 37°C for one hour. 100 µl of transformed bacteria were spread onto an Ampicillin LB agar plate (Sigma; 1 µl/ml of 100mg/ml stock). The plates were incubated overnight at 37°C, next day, colonies were picked from the plate and grown up in 10 ml of LB containing Ampicillin at 37°C overnight. Plasmid from the remaining 9 ml of bacteria was purified using the MiniPrep kit (Qiagen) and one ml of the transformed bacteria having the right ligation were frozen for storage at -20°C.

2.5.11 Amplification and Purification of Plasmid DNA

All plasmids were purified using the Qiagen[®] MiniPrep kit (section 2.5.6), the diagnostic restriction digest was done to verify the integrity of vector and also the presence/size of genes cloned into related vector. Bacteria were cultured in LB containing Ampicillin at 37°C overnight in a shaking incubator and purified using miniprep kit as described in section 2.5.6.

2.6 Transfection of cloned plasmids

The plasmid was used to transfect HeLa cells in 12 well plates with coverslips, for transfection, 50µl of OptiMEM (Life technologies) was used to dilute 0.3mg of plasmid DNA. 2µl Lipofectamine 2000 (Life technologies) was then added to diluted DNA. The transfection mix was incubated at room temperature in the dark for 15 minutes, the medium was removed from HeLa cells and 100µl of transfection mix is

added to each well and incubated at 37°C in 5% CO₂ for overnight. The following day the transfection mix was replaced by complete DMEM.

2.7 Recombineering

Recombination mediated genetic engineering (Recombineering) of BAC-cloned AdZ-5 genomes, for the insertion of transgenes into the AdZ-5 vector was performed as previously described (Stanton et al. 2008). The SW102 bacteria was used in recombineering which has the lambda red genes expressed from a defective phage which mediate homologous recombination between DNA sequences as short as 50bp homology. The lambda gene is under temperature control expression, it is induced by raise the temperature from 32 °C to 42°C for 15 minutes. The bacteria were induced on the day of experiment because they do not survive freeze-thawing process. The recombineering start by PCR the mc033 and mc080 from plasmids (pEX mc080 myc opt and pEX mc033 ha opt (ordered from Eurofins MWG)) using primers had homology to the CMV promoter & polyA (see the appendix). The SW102 *E.coli* colonies which have BAC-cloned RAZ-5 genomes inoculated in 5 ml LB contained 50µg/ml ampicillin and 12.5µg/ml chloramphenicol. The day after 500 µl of grown bacteria were added to 25 ml of LB contained 50µg/ml ampicillin and 12.5µg/ml chloramphenicol. The bacteria incubated at 32°C in shaking incubator for around 3 hs which needed for bacteria to reach the optical density (OD) of 0.6 at 600nm (Ultraspec 3000, Pharmacia Biotech spectrophotomer). The lambda phage genes were induced by incubating the bacteria on ice for 15 minutes then the bacteria were centrifuged at 3,345 x g for 5 minutes at 0°C. After that the pellet was suspended in 1 ml of sterile ice-cold H₂O. The sterile ice-cold H₂O was added to bacteria up to 25 ml and they were centrifuged at 3,345 x g for 5 minutes at 0°C, the washing step was repeated. Then 400 µl ice cold H₂O was added to the pellet and 25 µl of the suspension were mixed with 4 µl PCR DNA, the mix were transferred to 0.2 cm gap electroporation cuvettes (Bio-Rad, 165-2082) on ice. Then, they were incubated for 5 minutes before the mix was electroporated at 2.50 kV using the Biorad Micropulser, then 5ml of LB containing 12.5µg/ml chloramphenicol was added to electroporated bacteria and incubated for 4 hs in shaking incubator at 32°C. 50µl of bacteria were plated on selective media containing 5% sucrose at 32°C for 30 to 48 hs. Four colonies from each plate were minipreped (section 2.5.6) then tested for the right

insert by using BamHI as restriction enzyme (section 2.9). The inserted genes were sequenced as described in section 2.10 and they were 100% identical to original genes for both mc033 and mc080. For large scale plasmid preparation and for transfection-quality DNA, maxipreparation for both mc033 and mc080 were done using Qiagen kit (section 2.5.7). The mc033 and mc080 adenoviruses were made by transfection of circular maxiprep DNA using Polyfect (Qiagen) as described in section 2.8.

2.8 Transfection of 293-TREX cells with adenovirus BAC

DNA

It was not necessary to digest the Ad vectors genome before transfection, the circular maxiprep DNA was used in transfection. E1 gene was deleted from Ad-vector. However, 293-TREX cells express E1 gene in trans beside expression of the tet-repressor gene, that prevents transgene expression. Transfection was performed using Polyfect (301105, Qiagen), transfection kits. 2×10^6 293-TREX cells were seeded in a cell bind T25 cm² flask (Fisher, TKV-123-031L), the next day 4µg vector DNA was added to 100µl DMEM, 40µl polyfect was added to the DNA in DMEM and incubated for 10 minutes at room temperature. During the incubation, the media was changed on the cells and 3mls DMEM was added. 1ml DMEM was added to DNA complex and then they transferred to cells. After 24 hs the media was changed and then the media changed whenever went yellow, after 7-10 days the plaques were visible. When the cells were totally infected, the detached infected cells were collected in 2 ml of DMEM, the collected virus was used to infect 80% confluent of 293TREX cells in T150cm² cell bind flask.

2.9 Restriction enzyme digest of BAC

For verifying the integrity of adenovirus vector and testing if the transgenes (mc033 and mc080) were intact, a diagnostic restriction enzyme digest from miniprep DNA was performed.

By using BamHI restriction enzyme on the miniprep DNA of BAC of adenovirus vector, the integrity and presence of mc033 and mc080 was confirmed. When BamHI restriction enzyme used for restriction digest AdZ-5 vectors, it gave bands of 18, 11,

7.7, 2.5, 1.7, 0.8 and 0.6 Kbp. However, the 2.5 & 1.7 Kbp bands (from the Sac/LacZ/Amp cassette) were replaced with mc033 or mc 080 DNA band. The miniprep DNA (8 µl) was added to with buffer E (Promega, R005A) (1 µl) and BamHI enzyme (Promega, R6021) (1 µl), the mixture was incubated at 37°C for 2 hours. The mix was loading in agarose gel and the electrophoresis was performed at 150V for 90 minutes.

2.10 Sanger sequencing

Sequencing analysis of short genome regions or PCR products was performed by the Sanger sequencing services offered by Eurofins (MWG). Sequencing primers were designed to bind about 100 bp upstream of either end of the region to be validated. The concentration of DNA was also determined as previously described in section 2.5.4. All DNAs and primers were sent in volumes and at concentrations as required

2.11 Analysis of protein expression

2.11.1. Immunofluorescence

4×10^4 HF-CARs were seeded in 12 well plates with coverslips. The day after, the cells were infected with adenovirus as described in section 2.4.7. 48 hs after infection, the media was removed, and the cells were then fixed using 500µl of 4% PFA and incubated for 10 minutes at room temperature. The cells were washed with PBS and permeabilised using wash buffer (1% BSA and 0.2% saponin in PBS). All antibody incubations and washes were carried out in the wash buffer unless stated otherwise. Primary antibody incubation was performed for an hour at 37°C in 50 µl, in order to chase nascent protein in ER the cells incubated with primary antibodies, rabbit anti V5-tag, (Abcam, GR116421-19) and/or mouse anti-calnexin clone (Millipore,2274261). For Golgi complex double staining immunofluorescence was performed, by use mouse anti V5 tag (AbD Serotec, MCA1360) and/or rabbit anti Giantin. The cells in coverslips were then washed 5 times, then the appropriate secondary antibodies (table 2.1) were applied at 1/500 dilution for 30 minutes at 37°C in a total volume of 50 µl, the cells were then washed 5 times. 4,6-Diamidino-2-Phenylindole, Dihydrochloride (DAPI) (Thermo Fisher, D1306) was added to

coverslips and then they were left in dark overnight, then examined using Zeiss fluorescence microscope (Carl Zeiss Microscopy, Germany).

2.11.2 Immunoblot detection of proteins

Semi-quantitative detection of proteins was performed by immuno-blot techniques, with targeted proteins first resolved and isolated from mixed samples using the NuPage Novex protein isolation kit (Invitrogen/Life technologies).

2.11.2.1 Sample preparation

The media was removed from HF-CAR infected cells then washed using PBS, excess PBS was removed using pipette then 400µl of lithium dodecyl sulfate sample loading buffer (LDS) (100 of 4XLDS, 40µl of 10 mM DTT and 260µl ddH₂O) was added to each T25 cm² flask, the cells were resuspended in the buffer using a cell scraper, and then the mix was transferred to an Eppendorf tube. Proteins in all samples were denatured by incubation at 100°C for 10 mins using a heating block.

2.11.2.2 Western Blot

20 µl or 30 µl of the samples were loaded in 10% Nu-PAGE polyacrylamide gels (Invitrogen) by SDS-PAGE, and 10 µl of prestained protein markers (Invitrogen, LC5800) and electrophoresed for 2 hs at 100V. After that they were transferred to Hybond-C nitrocellulose (GE Life Science) by semi-dry blotting using Trans-Blot SD semidry transfer cell (Bio-Rad) for 2 hs at 10 Volts. They were then blocked in 5% milk in Phosphate-buffered saline containing 0.05% TWEEN-20 (PBS-T) overnight at 4°C. The membranes were then incubated with primary antibodies diluted in 5% milk in PBS-T at room temperature for an hour, followed by washing in PBS-T, and incubation with anti-mouse or anti-rabbit IgG-HRP conjugate for an hour at room temperature. Membranes were then washed in PBS-T and incubated in SuperSignal West Pico Chemiluminescent substrate (Fisher Scientific) before being imaged using Syngene imaging system (UK, Cambridge) with GeneSys software. Where appropriate, the blots were stripped in Pierce Stripper buffer (Fisher Scientific) for 10 min, washed in PBS-T, reblocked using block buffer, and reprobed.

2.11.2.3 Deglycosylations

The EndoH and PNGase deglycosylations was performed by incubation of EndoH (New England Biolabs, P0702S) or PNGaseF (New England Biolabs, P0704L) enzymes in presence of G3 buffer (New England Biolabs, B1702S) in the EndoH digestion, and G2 (New England Biolabs, B3704L) and 10% NP40 (New England Biolabs, B270S) buffers in PNGase reaction with samples for overnight at 37°C. The amounts of buffers and enzymes are included in table 2.5.

For running the samples using Western Blot (section 2.11.2.2), 5µl of 4x LDS sample buffer (Invitrogen, NP0008) was added to 1 µl of 1M DTT and 14 µl of digested sample and incubated for 10 minutes, and centrifuged for a minute at 16060 x g.

Table 2.5: Deglycosylation mixture

| | Mock digested (µl) | EndoH digested (µl) | PNGase digested (µl) |
|--------------------|--------------------|---------------------|----------------------|
| Sample | 22 | 22 | 22 |
| EndoH | | 2 | |
| PNGase | | | 2 |
| G2 | | | 3 |
| G3 | 3 | 3 | |
| NP40 | | | 3 |
| ddH ₂ O | 5 | 3 | |
| Total volume | 30 | 30 | 30 |

2.12. Flow cytometry

After seeding and infecting the cells in T25cm² flasks, the media were first aspirated, then the cells rinsed with PBS, one ml of trypsin was used to detach the cells, then 5 ml complete media was added to neutralise trypsin. The mixture was spun at 470 x g for 5 minutes. The cell pellet was suspended in 800-1000 µl of PBS with 1% BSA (wash buffer), then 100 µl of each sample was transferred to a V bottomed 96 well plate and centrifuged at 470 x g for 5 minutes, at 4°C. The pellet was washed with cold wash buffer and centrifuged at 4°C for 470 x g, for 5 minutes. The cells were incubated with primary antibody for 20-30 minutes, after that the samples were

centrifuged, and supernatants discarded. The cells were washed twice in wash buffer to remove excess primary antibody. The cells were incubated with the secondary antibody for 20-30 minutes, then they were washed twice using washing buffer. The cells then fixed in 2% of PFA at least for 10 minutes. The BD Accuri™ C6 flow cytometer (BD Biosciences) was used to detect fluorescence, and results were analysed using C-flow software (BD Biosciences, Oxford, UK).

2.13 Intracellular staining of fixed cells by flowcytometry

After 72 hours of infection of HF-CARs with desired virus the media was removed, and the cells rinsed with PBS and trypsinised then 10ml of DMEM was added to T25cm² flask. The mix of infected cells were spun at 301 x g for 3 minutes, the supernatant was discarded, and the pellet was resuspended in complete DMEM and aliquoted in V bottomed 96 well plate. The cells were washed with PBS then fixed using 4% PFA for 10 minutes, then they were washed twice with PBS. The cells were permeabilised using washing buffer (1% BSA and 0.2% saponin in PBS) for 30 minutes, all antibody incubations and washes were carried out in the wash buffer unless stated otherwise. The cells were incubated with primary antibody for an hour at 37°C after washing the cells were incubated with secondary antibody for 30 minutes, after that the cells were washed using PBS and fixed in 2% PFA and examined using BD Accuri™ C6 and analysed using C-flow software (BD Biosciences, Oxford, UK).

2.14 Isolation of PBMC

Blood was collected into tubes containing preservative-free heparin (Monoparin) (CP Pharmaceuticals Ltd., Clwydd) (5 IU/ml blood) and layered onto Histopaque-1077 in a 3:2 volume ratio (15 ml blood to 10 ml Histopaque) in a 30 ml universal container (Greiner). Tubes were centrifuged for 20 minutes at 1100 x g without braking. The interfacing layer of mononuclear cells was removed into a universal container and diluted with PBS. The cells were washed with PBS first at 1100 x g for 6 minutes followed by 2 washes of 350 x g for 4 minutes. The cells were re-suspended in

appropriate media, counted and diluted to the required concentration for use. Generally, 1×10^6 PBMC were collected per ml of blood from healthy donors.

2.15 NK degranulation assays

NK degranulation assays were performed in a similar manner to that described previously (Prod'homme et al. 2007b; Prod'homme et al. 2010) , PBMC were harvested as described in section 2.14 and incubated overnight with IFN- α (1000 IU/ml). PBMC (0.5×10^6) were incubated for 5hr with 5×10^4 fibroblast targets per well in a V bottomed 96 well (effector:target ration of 10:1) with the addition of 1 μ l per well FITC-conjugated anti-CD107 antibody or 1 μ l per well FITC-conjugated isotype control. 0.5 μ l/well BD GolgiStop (BD Biosciences) was added an hour after the beginning of the assay. After 5 hs incubation the 96 well plate was centrifuged at 470 x g for 5 minutes, at 4°C. The pellet was washed with cold wash buffer and centrifuged at 4°C for 470 x g, for 5 minutes. The cells were stained with PE-Cy7 conjugated antibodies against CD3 and PE conjugated CD56 then they were incubated for 30 minutes at 4°C. Then the pellet was washed twice with cold wash buffer and centrifuged at 470 x g, for 5 minutes at 4°C, after that the cells fixed in 2% PFA before analysis by flow cytometry AccuriTMC6 flow cytometer (BD Biosciences), C-flow software (BD Biosciences, Oxford, UK).

2.16 CD8⁺ T cell CD107a mobilization assays:

D007 human skin fibroblast (HSF) infected with RAd mc033, RAd mc80, RAd US6 or RAd control were coated with 1 μ g/ml, 0.2 μ g/ml or 0.04 μ g/ml concentration of HCMV VLE peptide or 1 μ g/ml, 0.2 μ g/ml, 0.04 μ g/ml or 0.008 μ g/ml concentration of HCMV pp65 peptide in 1ml of RPMI-10 for an hour at 37°C. Then, two washes with RPMI-10 were applied to remove excess peptide. 1×10^5 CD8⁺ T cells (kindly provided by Mihil Patel (Cardiff)) were incubated in quadruplicate with 1×10^4 target cells and anti-CD107a-FITC mAb (1 μ l/well) or one well with 1 μ l/well of an isotype control containing IgG1 κ -FITC was used. 0.5 μ l/well of BD GolgiStop (BD Biosciences) was added to the cells after an hour then they were incubated for 4 hs more. The plate was centrifuged at 470 x g for 5 minutes, at 4°C, the pellet was washed with cold wash buffer and centrifuged at 4°C for 470 x g buffer. The cells

were stained with PE-Cy7conjugated antibodies against CD3 and APC conjugated antibody against CD8 for 30 min at 4°C. Cells were washed twice in cold wash buffer, the pelleted cells were fixed in 2% PFA before analysis by flow cytometry Accuri™C6 flow cytometer (BD Biosciences), C-flow software (BD Biosciences, Oxford, UK).

**3-Cloning and comparative
expression of MOCV genes
mc080 and mc033 in different
viral gene expression systems**

3.1 Introduction

Molluscum contagiosum virus (MOCV) and Human Cytomegalovirus (HCMV) are two large human DNA viruses that both express MHC-I homologues. MOCV encodes two potential MHC class I homologues: hypothetical proteins MC080 and MC033. MC080 exhibits closest sequence similarity to human HLA A2 and rat MHC class I homologous while MC033 has homology to *Xenopus* class I histocompatibility antigen (Senkevich et al. 1997; Senkevich and Moss 1998). HCMV encodes MHC class I homologs UL18 and UL142 (section 1.10). UL18 has been shown not only to be a viral MHC I homologue but to act as a MHC-I mimic by suppressing the cytotoxic responses of NK cells through a direct interaction with the inhibitory receptor LIR1 (Prod'homme et al. 2007a). The second HCMV MHC I homologue, UL142, has similarity to UL18 and together they constitute the HCMV MHC I gene family (Davison et al. 2003b). UL142 glycoprotein (gpUL142) has been reported to downregulate the polymorphic full-length NK ligand MICA, but not truncated MICA*008 (Chalupny et al. 2006; Ashiru et al. 2009). The situation became more complicated when recent studies indicated that HCMV genes US18 and US20 may be primarily responsible for cell surface downregulation of MICA (Fielding et al. 2014; Fielding et al. 2017).

The goal of my PhD project is to compare and contrast the roles of these MOCV and HCMV MHC-I homologues using UL18 as the paradigm.

Our understanding of MOCV is limited by a lack of appropriate *in vitro* systems because the virus can not readily be propagated in cell culture. The inoculation of primate cells with MOCV taken from clinical lesions results in an abortive infection with the cells initially inducing a cytopathic effect manifesting as clumping and rounding, only to revert to normal growth after 48 hours (Barbanti-Brodano et al. 1974; McFadden et al. 1979). Buller *et al* have achieved replication of MOCV by engrafting human foreskin into athymic mice and inoculating the skin with extract from patient lesion (Buller et al. 1995). However, this complex system is not readily compatible with studies of gene function. Since it is not possible to grow MOCV *in vitro*, it was necessary to look at MOCV genes in isolation. Although clinical HCMV strains also cannot readily be propagated *in vitro*, the virus readily adapts in culture due to the selection of mutants in RL13 and the UL128 locus; thus, systems have been developed to propagate tissue culture adapted HCMV strains *in vitro* (Dargan

et al. 2010). Therefore, the potential exists to examine the function of HCMV genes both in isolation and in the context of virus replication.

In this thesis, vaccinia, lentiviral and adenoviral systems have been used as expression vectors to study the MOCV genes, mc033 and/or mc080.

3.2 Analysis of mc080 expression using Vaccinia and Adenovirus Vector

Vaccinia virus (VV), a prototype member of the Poxviridae family, has a large DNA genome with virus DNA replication and virion assembly taking place entirely in the cytoplasm of the host cell (Gallego-Gomez et al. 2003). VV has been widely employed as an expression vector capable of carrying large inserts of foreign genes and producing proteins that undergo the normal post translational modification associated with human cells (Perkus et al. 1985; Coupar et al. 1988). The shutoff of the host cell protein synthesis by VV early genes results in expression of cloned genes being favoured. The broad host range of vaccinia virus allows a wide array of primary and transformed tissue culture cell lines to be utilized (Broder and Earl 1999). Prior to initiating this study, mc080 gene had been cloned into the replication-competent VACV Western Reserve (WR) strain and designated v293 (vWR293-mc080; by Dr Subuhi Sherwani) and into a replication-deficient Adenovirus (RAd) vector and designated RAd961 (RAd961-080; by Dr Rich Stanton). Both viruses showed poor growth characteristics in infected cells, resulting in low titre virus stocks. The first goal was to test the suitability of existing reagents to investigate the function of MC080.

3.2.1 Western Blot of cells infected with recombinant adeno and vaccinia viruses

To test the expression of MC080 by the recombinant viruses, using Western blot, HeLa cells were infected with recombinant adenovirus RAd961 and vaccinia virus v293 at an MOI of 1. A peptide derived from MC080 (CDSWKSSWRARWEEGKRRVAT; Charles River 2518/10 1+2) was used as a

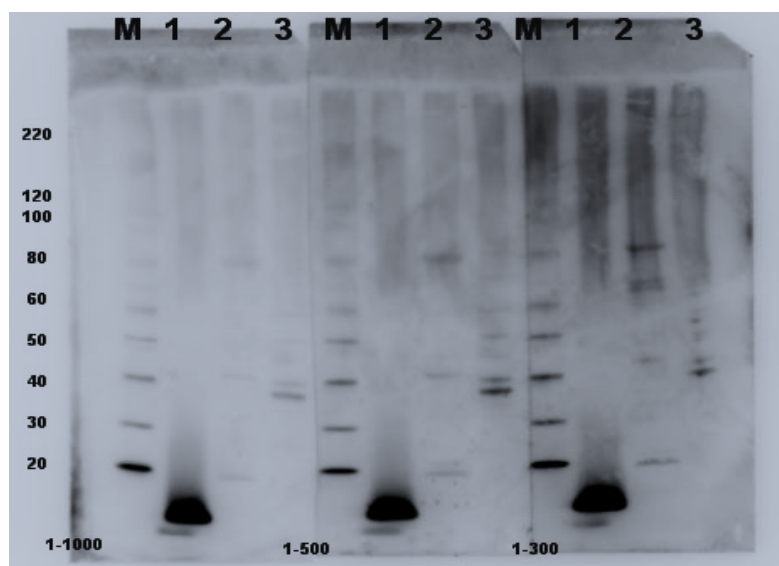


Figure 3.1: Expression of mc080 from vaccinia and adenovirus vectors. Western blot of cell lysates prepared from HeLa cells infected with an MOI 1 of either vWR293-080 or RAd961-080. 10 μ l of each lysate was subjected to electrophoresis by SDS PAGE then transferred electrophoretically to a nitrocellulose membrane. Samples were run in triplicate: M were molecular weight markers highlighted by Magic Mark and of the indicated sizes; (1) the MC080 peptide used to raise the polyclonal antibody; (2) vWR293-080 infected cell lysate and (3) RAd961-080 infected cell lysate. The membrane was cut into three parts and probed using different dilutions of rabbit polyclonal anti-MC080 (1:300, 1:500, 1:1000) as shown. The secondary antibody was anti rabbit Ab HRP (Chemiluminescent kit-AmershamTM, ECLTM PRIM) diluted 1:5000. The image was captured after 2min using a LAS- 3000 (FUJIFILM).

positive control (McGuigan, Hinsinger, Farleigh, Pathirana). There were no specific bands for mc080 (calculated molecular weight 42 kDa); the peptide control, running below the molecular weight marker for 20kDa, was detected with high affinity (figure 3.1). The apparent lack of expression of MC080 was noted, which was then ascribed to a possible toxic effect of mc080 on the HeLa cells.

After initial experiments with vaccinia expression systems, it was concluded that the gene mc080 was not well expressed, and may even have a toxic effect on cells, possibly due to the high GC content (~60%) of the original MOCV sequences used for the construction of the recombinant viruses v293 and RAd961, leading to low titre virus recombinants and no detection of recombinant proteins in Western blot (figure 3.1).

Following this line of thought, if mc080 gene expression has a toxic effect, the strong promoters used in poxviral and adenoviral constructs, or the location of gene transcription in these expression systems may exacerbate this effect. In order to test this possibility, it was decided to clone codon optimized MOCV MHC homologs into a lentiviral vector expression system, which has weaker promoters and may offer an advantage with a possibly toxic gene expression product.

3.3 The Lentivirus vector

Lentivirus vectors reverse transcribe their RNA genomes into a double-stranded DNA, which is stably integrated into the genome of the host cell so that it will also be passed to daughter cells (S. and R. 1997; Gillet et al. 2009). Human Immunodeficiency Virus 1 (HIV-1) is the most extensively studied human lentivirus and also provides the backbone to many lentiviral vectors. Second generation lentiviral vectors have improved safety compared to first generation vectors, because of the removal of the accessory genes *vif*, *vpr*, *vpu* and *nef* (Naldini et al. 1996) (figure 3.2). In addition, the vector is pseudotyped with the vesicular stomatitis virus glycoprotein (VSV-G) which enhances virion stability and broadens viral tropism (Miyoshi et al. 1997; Palu et al. 2000; Escors and Breckpot 2010). Three plasmids, a packaging plasmid, a transfer plasmid and an envelope-encoding plasmid are used to reduce the possibility of recombination to replication-competent virus (Wei et al. 1998; Freed 2015).

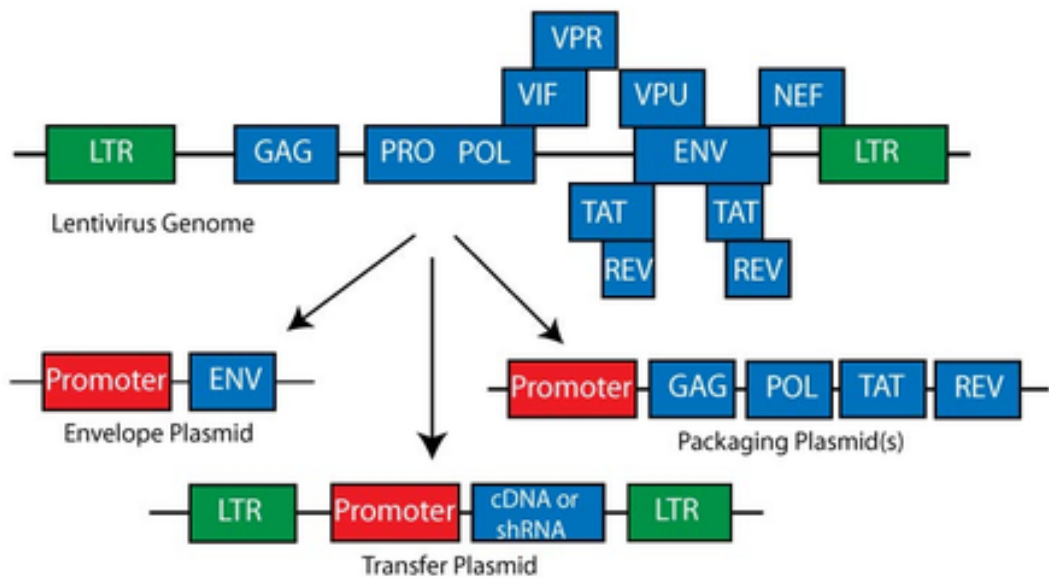


Figure 3.2: The second-generation lentivirus system. The graphic illustrates the second-generation lentiviral vector system. The lentiviral genome is divided into three plasmids, the packaging plasmid, encoding a number of non-structural lentiviral proteins including the polymerase (GAG, POL, TAT, REV), the transfer plasmid, with long terminal repeats and promoter (subsequently called pHAGE), and the envelope plasmid, encoding the envelope protein (ENV). Figure provided by Addgene. (<https://www.addgene.org/viral-vectors/lentivirus/lenti-guide/12/02/2018>)

3.3.1 Cloning of mc033 and mc080 into a Lentivirus vector

In an attempt to enhance expression levels of mc080 and reduce potential toxicity associated with the high GC content of MOCV, it was decided to synthesis a codon optimised version of mc033 and mc080 by MWG Eurofins-Gene.

The codon optimized genes were cloned into the plasmids pEXmc033 internal lab reference number (ILR) 476 and pEXmc080 (ILR 474) (figure 3.3). The genes were synthesised with C-terminal epitope tags to facilitate their detection and remove dependence on the polyclonal peptide antibody.

The lentiviral pHAGE transfer plasmid (ILR 445) was prepared by restriction digest with BamHI and NotI. Genes of interest with tag epitopes (mc033-ha; mc080-myc) were excised using the same restriction enzymes, then ligated into the pHAGE NotI-BamHI vector backbone, and transformed into TOP10 *E.coli*. Ampicillin resistant colonies were grown up, DNA extracted and digested. Plasmids with inserts of the appropriate size were selected for DNA sequencing, and their inserts found to be identical to the synthesized sequences (figure 3.4). The expression was confirmed by transfection of HeLa cell with pHAGE ILR482 (mc080) and pHAGE ILR485 (mc033). In the selected cells shown in figure 3.5, a strongly apple green signal in adherent and dividing cells, clearly distinguishable from background or artefacts, indicates expression of mc080 and mc033. The cells transfected with ILR482 (MC080) appear deformed which suggest that expression of MC080 is toxic (Figure 3.5).

3.3.2 Cloning of pHAGE mc080 neo and pHAGE mc033

neo

The lentiviral donor plasmid pHAGE was further modified, using a neomycin resistance cassette, to allow for efficient expression in stably transfected cell lines. The IRES - ZsGreen gfp cassettes were replaced by IRES Neo (derived by PCR from pIRES2EGFP- Clontech; ILR17) using restriction enzymes BamHI and ClaI (figure 3.6). Plasmids were produced and confirmed as described above. The expression was confirmed by transfection of HeLa cell with pHAGE ILR498 (mc080) and pHAGE ILR500 (mc033). In the selected cells shown in figure 3.7, a strongly apple green signal in adherent and dividing cells indicates expression of mc080 and mc033. These plasmids were used for lentivirus package (transgene plasmid).

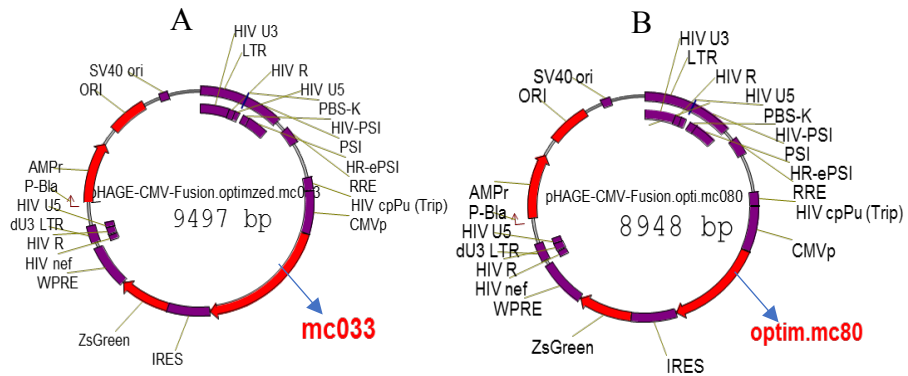


Figure 3.3: vNTI virtual constructs of pHAGE plasmids. (A) The codon optimized mc033-ha was placed under the control of CMV promoter (ILR485); (B) the codon optimized mc080-myc construct (ILR482). Both MOCV gene inserts are followed by an IRES controlled GFP cassette (ZsGreen) from the original pHAGE plasmid.

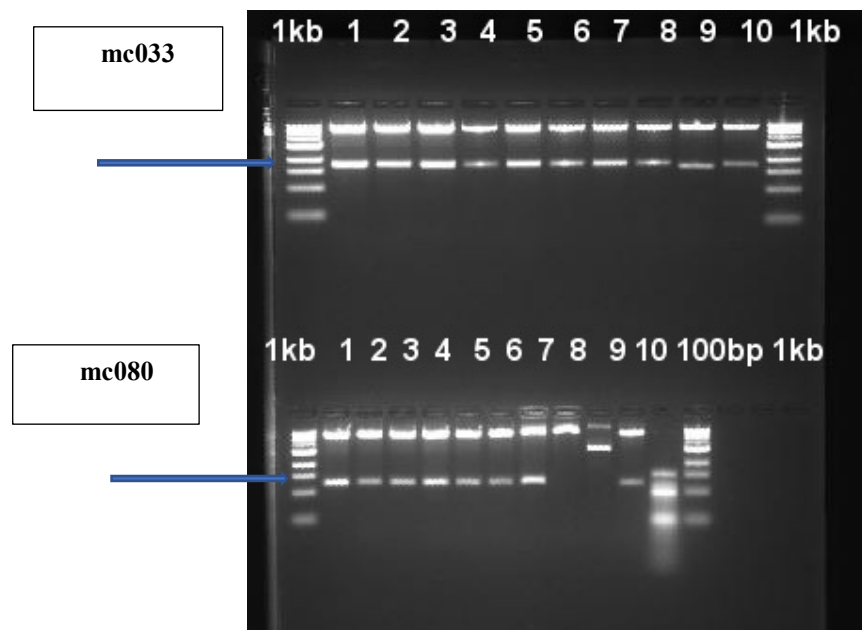


Figure 3.4: Cloning of mc033 and mc080 into the retrovirus vector pHAGE. Diagnostic restriction endonuclease digest of plasmids with *NotI* and *BamHI* derived from ligation (pHAGE opt mc033-ha) and (pHAGE opt mc080-myc: top pHAGE (7717)). Anticipated size of mc033-ha was 1780bp and mc080-myc was 1231bp. All clones had inserts of the appropriate size except mc080 clones 8, 9. The molecular weight standard was a 1kb ladder.

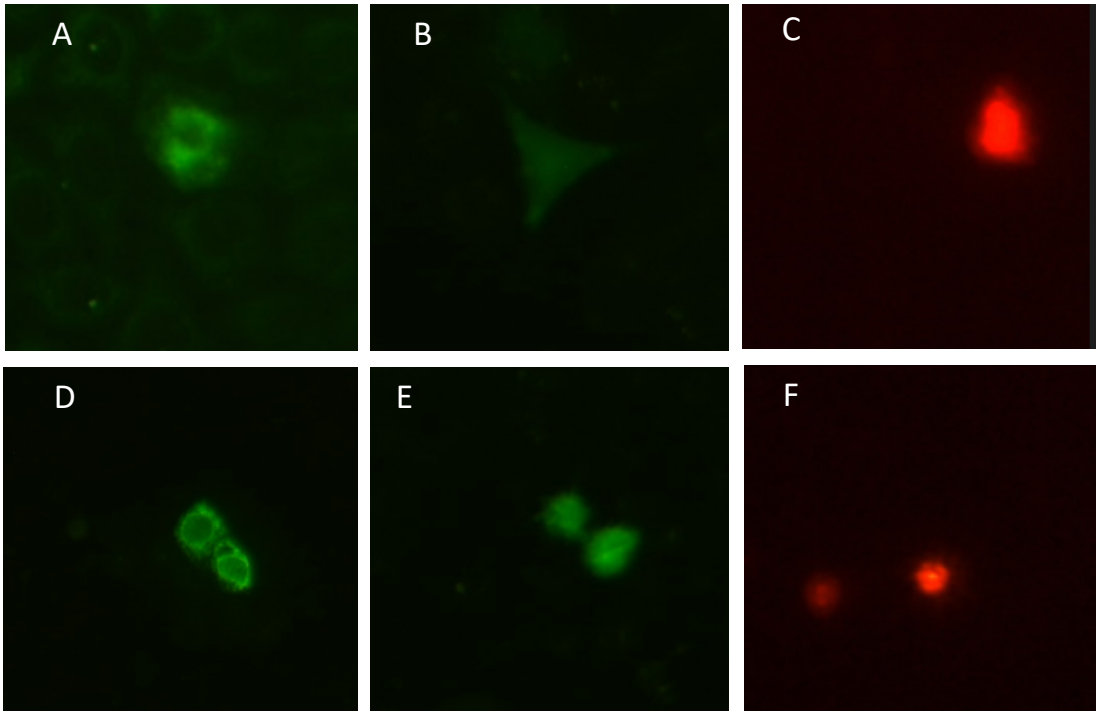


Figure 3.5: The expression of pHAGE plasmids ILR482 (mc080), ILR485 (mc033) and ILR489 rtTA. The figure showed immunofluorescent picture of HeLa cell transfected with pHAGE plasmid mc080(ILR482) (A, B); plasmid mc033 (ILR485) (D, E) or plasmid rtTA (ILR489) (C, F). At 48 hours posttransfection they were fixed and permeabilized then stained using 1:100 rabbit anti Ha antibody for ILR485; rabbit anti myc antibody for ILR482 or mouse anti ha antibody for ILR489, then immunostained with 1:1000 chicken anti-rabbit AlexaFluor - 488(green) or donkey anti-mouse AlexaFluor-594(red).

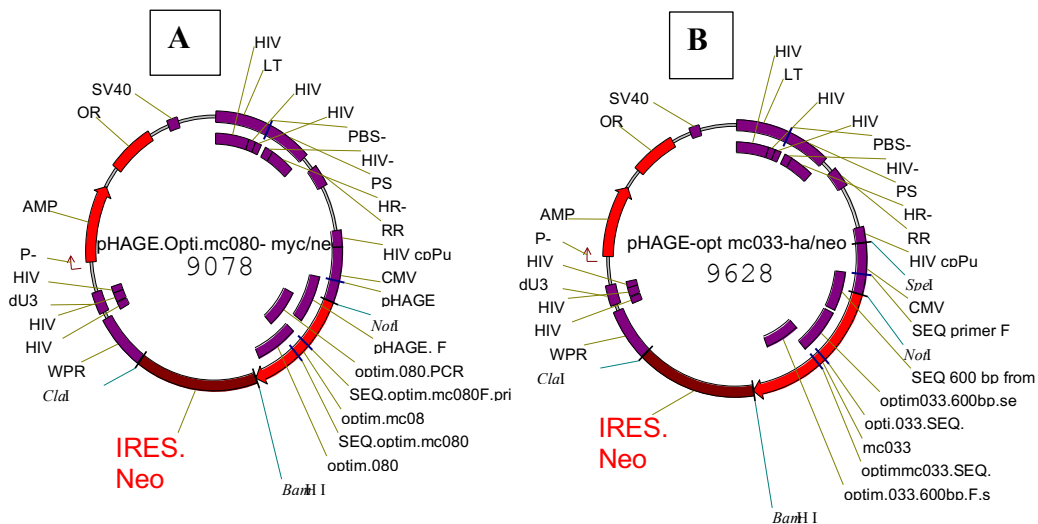


Figure 3.6: vNTI virtual constructs of pHAGE IRES neo plasmids. (A) using the pHAGE-opt mc033-ha plasmid, IRES ZsGreen (GFP) was replaced with IRES neo (ILR500); (B) same construct derived from pHAGE-opt mc080-myc (ILR498). Both MOCV gene inserts are now followed by an IRES controlled neo cassette from pIRES2EGFP.

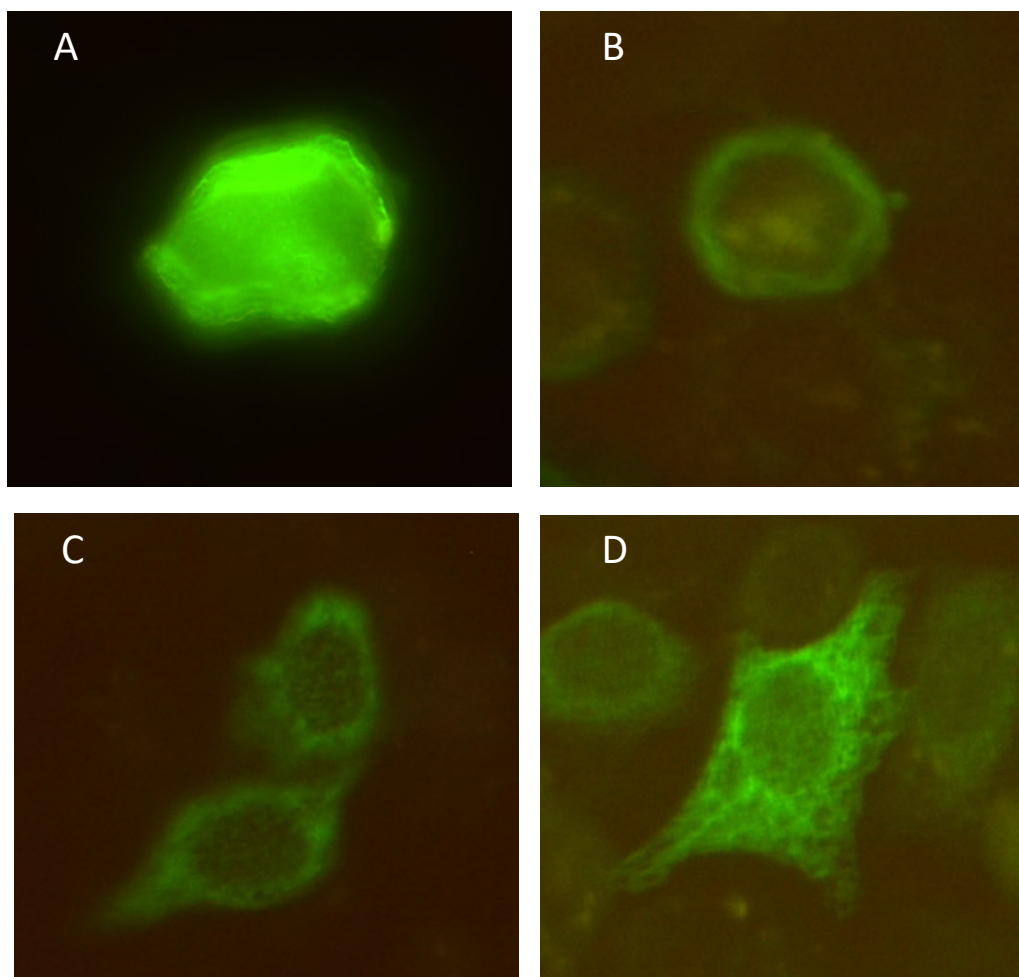


Figure 3.7: Expression of ILR 500 (mc033) and ILR498 (mc080) plasmids. The HeLa cells transfected with either ILR498 (mc080) (A, B) or ILR500 (m033) (C, D) plasmids. At 48 hours post transfection, the cells were fixed, permeabilized and stained with either anti Ha (ILR500 mc033) or anti myc (ILR598, mc080) then immunostained with chicken anti-rabbit AlexaFluor-488.

At this point in the project expression by recombinant lentiviral plasmid constructs, both in transient transfections and in stably expressing cell lines was weak, and toxicity seemed a possible explanation. Therefore, the tet- inducible expression of mc080/m033 coded proteins, using tetracycline induction of gene expression either in stably transfected cell lines, or following production of recombinant lentiviral particles without gene expression during the growing up of recombinant lentiviruses.

3.3.3 TRE controlled and rtTA constructs

To control gene expression in an inducing system, the genes need to be controlled by a minimal promoter that has a very low baseline expression and inducer elements that increase the promoter strength upon addition of the inducer substance. In the tetON tetracycline regulated expression system, this is tetracycline or related drugs, and it requires the rtTA regulator to be co-expressed with tetracycline responsive element (TRE) controlled proteins (figure 3.8). The TRE, including the minimal CMV promoter, was derived by PCR from pTRE2shuttle (Clontech; ILR19) adding restriction sites *SpeI-NotI*, resulting in a 443bp product. The PCR product was cloned into the respective restriction sites of pHAGE opt-mc033-ha/neo and mc080-myc/neo, deleting the full length CMV promoter in the process (figure 3.9). Plasmids were produced and confirmed as described above.

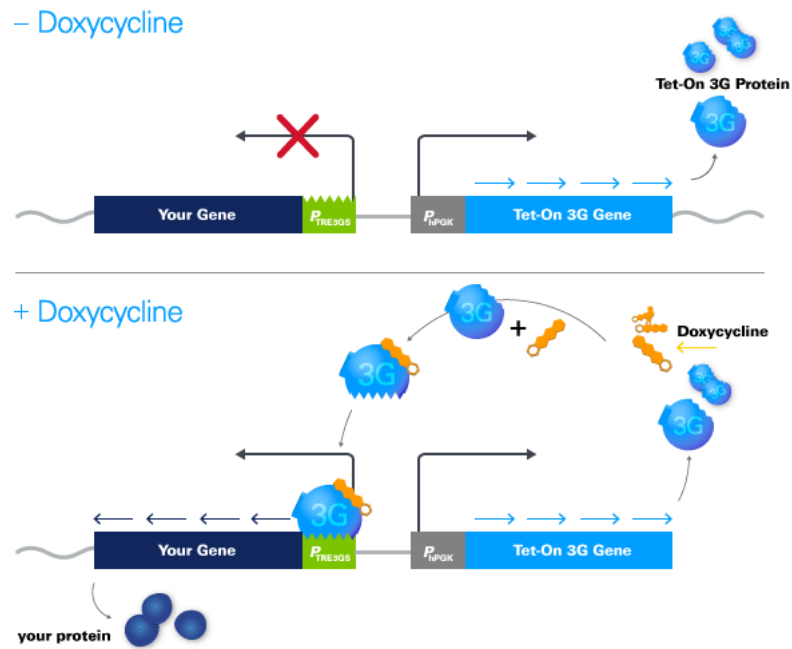


Figure 3.8: The tetON system. On the top panel, the transactivator is unable to bind to P_{TRE3GS} because of absence of doxycycline that necessitates binding. When doxycycline is supplied in the culture medium, it binds to transactivator, enabling it to bind to P_{TRE3GS} , and activate transcription of the transgene cloned downstream, panel (http://www.clontech.com/US/Products/Inducible_Systems/TetSystems_Product_Overview/Tet-One_Overview 12/02/2018)

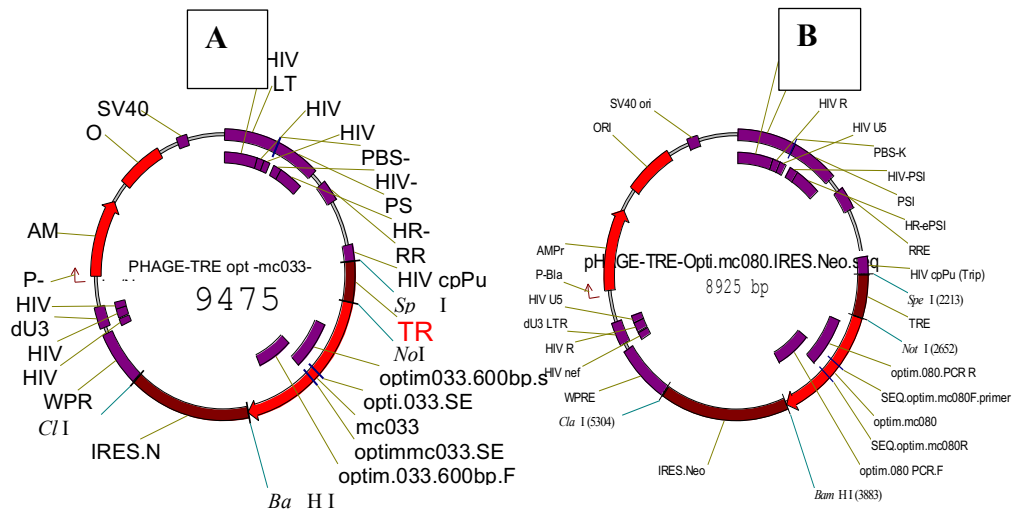


Figure 3.9: vNTI virtual constructs of pHAGE (Neo IRES) plasmids. (A) mc033 was tagged with ha epitope and produced under control of TRE promoter, CMV promoter was replaced with replaced with TRE promoter; (B) the mc080 was tagged with myc epitope and produced under control of TRE promoter, CMV promoter was replaced with replaced with TRE promoter (Table 3.1).

In order to provide for inducible expression, the tet regulator has to be provided *in trans* by the cell line. To achieve this, the rtTA cassette was derived by PCR from the AdOn adenovirus (Clontech) adding restriction sites NotI and BamH along with a C-terminal ha-epitope tag, resulting in a PCR product of 1040bp. pHAGE rtTA-ha (ILR 489) was made by ligation of rtTA into the pHAGE-original plasmid (ILR445), allowing selection by GFP expression, as the rtTA cassette is followed by IRES-ZsGreen (GFP) (figure 3.10). Plasmids were produced and confirmed as described above. The expression of rtTA plasmid (ILR489) was confirmed by immunofluorescence as shown in figure 3.5.

The expression of mc033/mc080 from the stably transfected plasmids upon addition of the tet inducer, was low and only small numbers of cells showed fluorescence in these experiments, indicating low induction efficiency or further toxicity in this system. A limitation of the lentiviral gene expression system is that expression tends to be limited to a small proportion of genes and the act of delivery can be cytopathic. Since the ultimate aim was to study these genes in immunological assays, it was decided to utilise Adenoviral and lentiviral vectors.

3.3.4 Expression using recombinant lentiviral virions

Second generation Lentiviruses vector particles were produced by using the plasmids p8.91; pmdg kindly provided by Katja Finsterbusch and transfer plasmids (ILR498 (mc080) and ILR500 (mc033)). Confluent T150 flasks of early passaged 293TRES cells were transfected using Calcium phosphate DNA perception, two days post transfection cell supernatants were filtered and concentrated using 20% sucrose as described in section 2.4.6

These experiments were only conducted in preliminary fashion. To test the expression of MC080/MC033 using lentiviruses, the HeLa cells were infected using lentivirus stocks, only very small numbers of cells showed fluorescence in these experiments, indicating low titre of lentiviral stocks. The selected cells shown in figure 3.11 were strongly apple green, in adherent and dividing cells, clearly distinguishable from background or artefacts.

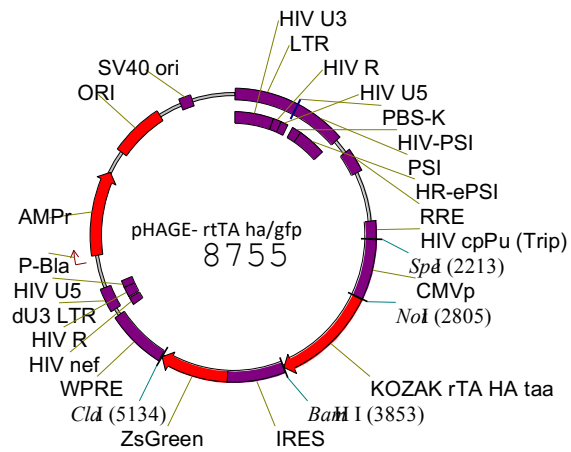


Figure 3.10: vNTI virtual constructs of pHAGE plasmid ILR489. the rtTA-ha was placed under the control of CMV promoter

Table 3.1: Summary of pHAGE plasmid constructs

| ILR number (gene number) | Ligation number (clone) TRE, tag, and selection marker | Sequencing results | Transfection of HeLa cell line |
|-------------------------------------|---|-------------------------------|---|
| 474 (080 opt) | pEX mc080 myc opt | Eurofins | |
| 476 (033 opt) | pEX mc033 ha opt | Eurofins | |
| 482 (080) | L322 (1) myc gfp | 100% identical | GFP positive |
| 483 (080) | L322 (4) myc gfp | 100% identical | |
| 485 (033) | L323 (1) ha gfp | 100% identical | GFP positive |
| 486 (033) | L323 (2) ha gfp | 100% identical | |
| 488 (rtTA) | L 325 (1) ha gfp | 100% identical | |
| 489 (rtTA) | L 325 (5) ha gfp | 100% identical | GFP positive |
| 498 (080) | L340 (1) (myc neo) | Seq over insert /tag | IF positive anti myc/ anti-80 |
| 499 (080) | L340 (2) (myc neo) | Seq over insert /tag | |
| 500 (033) | L341 (1) (ha neo) | Seq over insert /tag | IF positive anti ha |
| 501 (033) | L341 (2) (ha neo) | Seq over insert /tag | |
| 503 (080) | L345-3 (TRE myc neo) | 100% identical | IF positive anti myc/ anti-80 |
| 504 (080) | L345-6 (TRE myc- neo) | 100% identical | |
| 505 (033) | L346-1 (TRE ha- neo) | 100% identical | IF positive anti ha |
| 506 (033) | L346-2(TRE ha- neo) | 100% identical | |

Following discussions regarding functional assays available in Cardiff to test MHC class I homologs it was decided at this point to also clone the codon optimized mc080 and mc033 sequences into the adenoviral expression system. While expression in the lentiviral system was observed, it appeared rather weak in immunofluorescence assays. Also, the subsequent functional assays available in Cardiff are all established

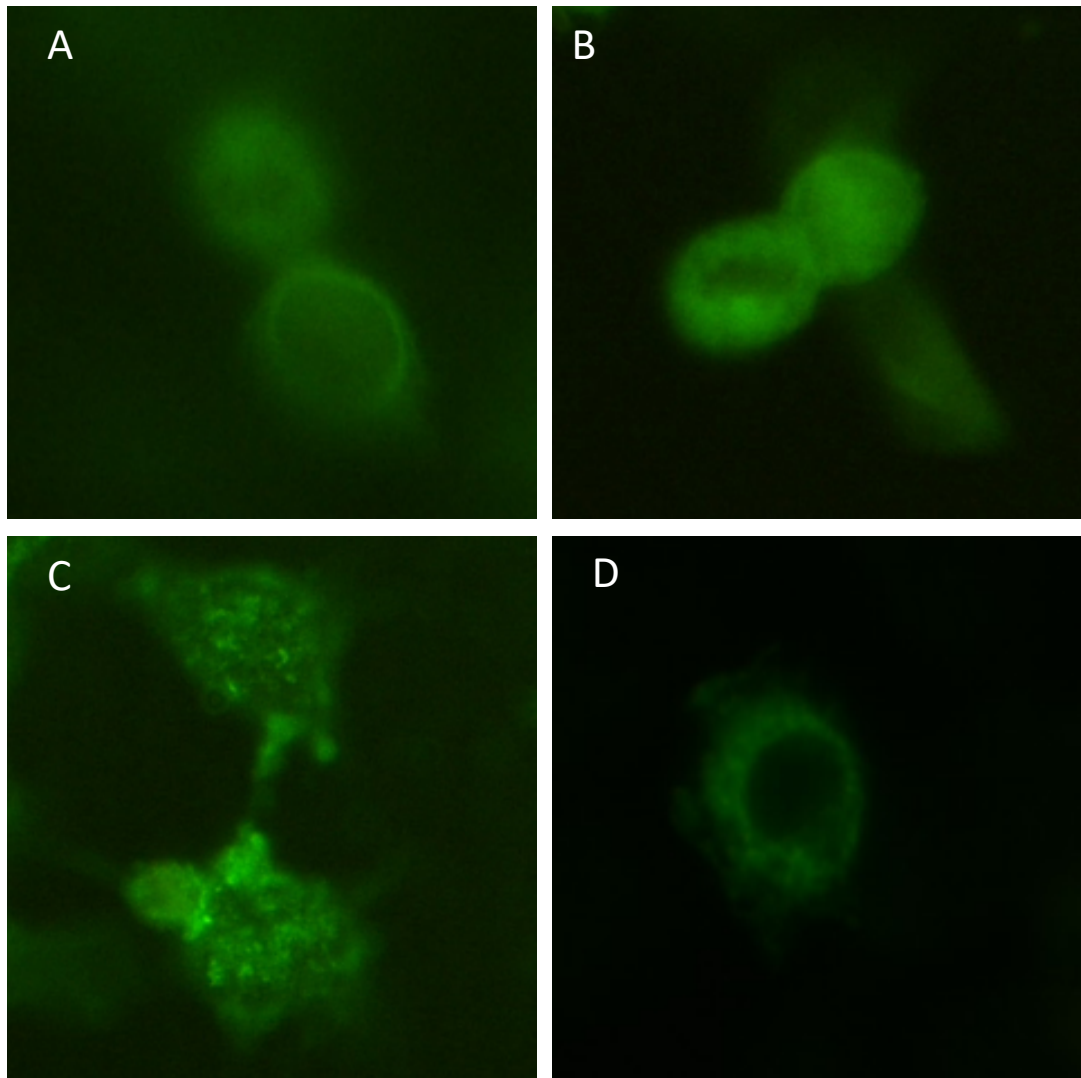


Figure 3.11: Analysis of expression from Lentivirus particles. The representative microscopy is image of immunofluorescent staining of lentivirus mc080 (A, B) and lentivirus mc033 (C, D). The HeLa cells were infected using lentiviruses described above, at 48 hours post infection the cells were permeabilized and stained using rabbit anti-ha (mc033) or rabbit anti-myc(mc080), then they were immunostained using chicken anti-rabbit AlexaFluor @488.

using adenoviral expression vectors (Tomasec 2000; Prod'homme et al. 2007), and HCMV genes to compare the MOCV homologs to are all only available in adenoviral vectors.

So, while the functional testing of mc080/033 expressed from lentiviral vectors may be academically interesting to confirm results obtained in the adenoviral system, for practical reasons and in order to allow direct comparisons to HCMV proteins characterized by the Wilkinson group, adenoviral constructs using the codon optimized mc080/mc033 gene sequences would be required.

3.4 Cloning and expression mc033 and mc080 using adenovirus vector- 5 (AdZ-5)

Over sixty years have now passed since adenoviruses were first isolated. Adenovirus is non-enveloped virus with a ~36 kb double strand DNA genome. At least 83 human serotypes have been discovered, they divided into seven different species (A- F) (McConnell and Imperiale 2004; Espinola et al. 2017). Prior to the initiation of this study, attempts to clone mc080 in to an AdEasy1 vector were unsuccessful, efficient expression on mc080 appeared to be incompatible with vector replication. Work was therefore switched to an 'inhouse' species C serotype 5 replication-deficient Ad vector designed to permit transgene insertion with 'zero' cloning steps (AdZ). AdZ was produced by Stanton et al (Stanton et al. 2008) by deleting both the E1 and the E3 regions of the Ad genome thereby allowing insertion of transgenes up to 8 kb in size. The E1 region is multifunctional and required for the activation of Ad late genes and thus essential for virus replication. The E3 encode immune evasions that are not essential for virus replication *in vitro*. Deletion of E1 means the AdZ vectors must be propagated on E1-expressing helper cells; 293 cells are the most commonly used (Stanton et al. 2008). The transgene is inserted directly into vector within *E. coli* strain SW102 utilizing recombination-mediated genetic engineering as described in section 2.7 (Graham et al. 1977; Stanton et al. 2008). A useful feature of the AdZ vector is that it contains two tetracycline responsive elements (TRE) downstream of the HCMV IE promoter. When the vector is propagated in 293 cells expressing the tet-repressor (293TRES), expression from the transgene is silenced, this device enabled cloning of the mc080 gene.

3.4.1 Cloning mc033 and mc080 into AdZ5

The codon optimized mc033 and mc080 genes were cloned into AdZ by recombineering in frame with a C-terminal V5-epitope tag already present in the vector, allowing their expression to be validated using an anti V5 antibody. Genes were amplified individually from pEX mc080 myc opt (ILR474) and pEX mc033 ha opt (ILR476) (synthesized by MWG Eurofins-Gene). The PCR-amplified DNA fragments were electroporated into *E. coli* SW102 then cultured on agar plates containing sucrose; the selective media ensures that bacteria where recombination did not happen failed to grow. Four white colonies of each plate were inoculated into 5ml LB media containing chloramphenicol, grown overnight before miniprep were performed and tested to see if they had an acquired insert of an appropriate size. Digestion of the AdZ-5 vector with *Bam*HI generates bands of 18, 11, 7.7, 2.5, 1.7, 0.8 and 0.6 kb; replacement of the 2.5 and 1.7 kb *Sac*/*LacZ*/ *Amp* bands with the mc033 and mc080s genes of ~1.7 kb and ~1.2 kb respectively. The second, third and fourth mc033 clones and all mc080 clones contained inserts of the appropriate size (figure 3.12 and figure 3.13). The inserted genes were sequenced and found to be 100% identical to original genes for both mc033 and mc080.

3.4.2 Optimizing expression of recombinant deficient adenovirus of mc033 and mc080

Western blot was performed using lysates of HF-CAR cells infected with recombinant adenoviruses RAd mc080 and RAd mc033 at an MOI 5. The MC033 protein was estimated to have an apparent molecular weight of 64 kDa, which is consistent with its predicted mass of 64.415 kDa. MC080 protein detected at 40 kDa, ran faster than the predicted primary translation products (44.55 kDa) (figure 3.14), this may be the caused by incomplete denaturation of protein by SDS (Rath et al. 2009)

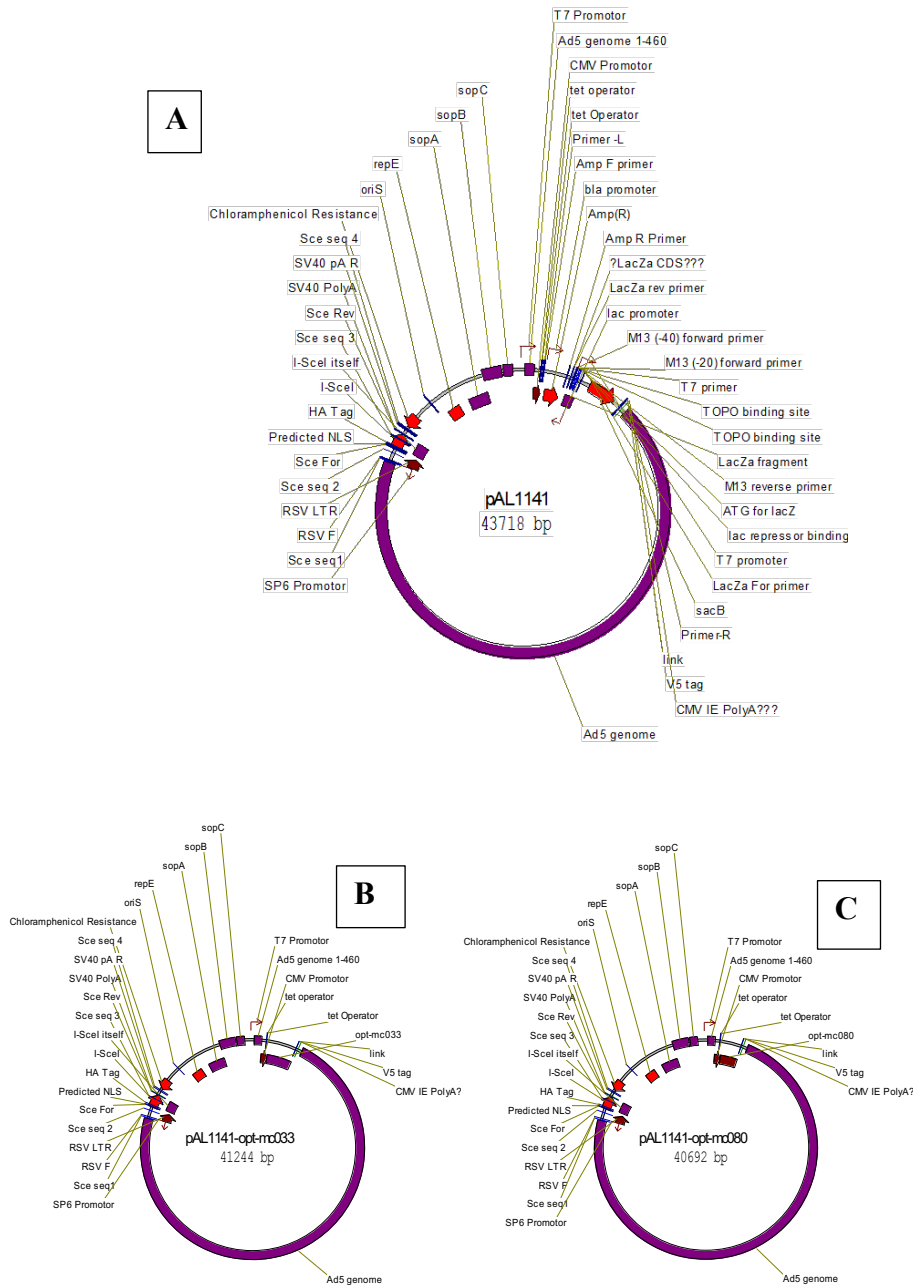


Figure 3.12: Virtual construct of MOCV genes cloned into the AdZ vector. (A) plasmid pAL1141; (B) pAL1141-opt-mc033 and (C) pAL1141-opt-mc080. The amp-lacZ-SacB selection cassette was replaced to put the opt-mc033 and opt-mc080 in to the replication deficient Ad vector under the control of the HCMV IE promoter and with a C-terminal V5 epitope tag.

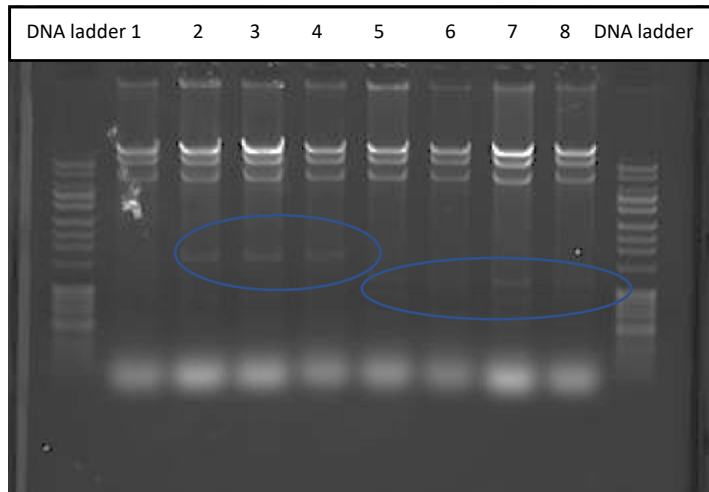


Figure 3.13:cloning mc033 and mc080 into AdZ vector. Diagnostic *Bam*HI restriction endonuclease digest of of pAL1141-opt-mc033 lane 1-4 (1.7 kb), and pAL1141-opt-mc080 lane 5-8 (1.2 kp). All clones had an insert of the appropriate size except the first clone of pAL1141-opt-mc033.

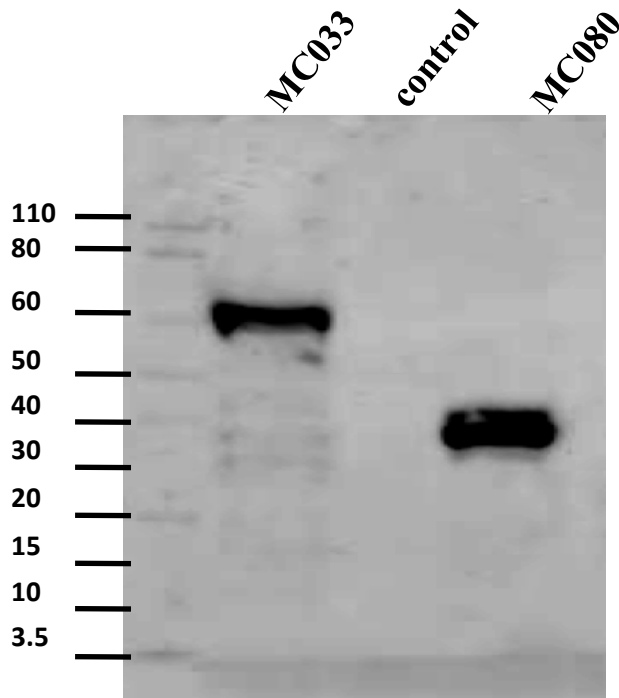


Figure 3.14: Expression of RAdmc033 and RAdmc080. Lysates were prepared from of HF-CAR cells infected with RAdmc033; RAdmc080 or an AdZ vector control (empty vector) (MOI 5) for 72h. 25 μ l of each sample was loaded onto 10% NuPAGE Bis-Tris gel, electrophoresis performed then transferred to nitrocellulose membrane. The blot was probed first with a mouse V5 monoclonal antibody then the anti-mouse IgG HRP (1:2000) was used. The MC033 band was calculated at 64.415 kDa and MC080 at 44.55 kDa using justbio.

3.4.3 The time course expression of RAdmc033 and RAdmc080

RAdmc033 and RAdmc080 encode the MOCV MHC-1 homologues under the control of the constitutive HCMV major IE promoter. The expression of MC033 and MC080 proteins from HF-CAR cells infected with the Ad recombinants were tested at 48, 72, 96 hours p.i. by using Western Blot analysis. MC033 ran as single band at around 64 kDa with its expression increasing gradually over time. In contrast, MC080 was observed to migrate as 2 band, the faster migrating species estimated at ~40 kDa and the heavier more diffuse band at around 42 kDa. MC080 expression was slightly lower at 96 h than at 72 h p.i. (figure 3.15). Moreover, some cellular cytotoxicity was observed at the later time point. In view of these observation, future experiments were performed at 72 h p.i. unless otherwise indicated.

Senkevich and Moss found that MC080 was not present on the cell surface (Senkevich and Moss 1998). To test for the intracellular expression of mc080 and mc030, HF-CARs were infected with RAdmc080, RAdmc033, RAdUS6 (positive control) or RAd control (negative control) at an MOI 5 PFU/Cell. Forty-eight hours post infection cells were fixed, permeabilized and stained for V5 then analysed by flow cytometry. The displacement of the peak for MC033 and MC080 to the right compared with the negative control (1253), shown in red signifies the expression mc033 and mc080. However, there was a displacement of the peak for RAd negative control to the right compared to isotype control, which potentially due to cross reaction between of V5 antibody and adenovirus protein. The expression levels of MC033 and MC080 exceeded the scale as shown in figure 3.16.

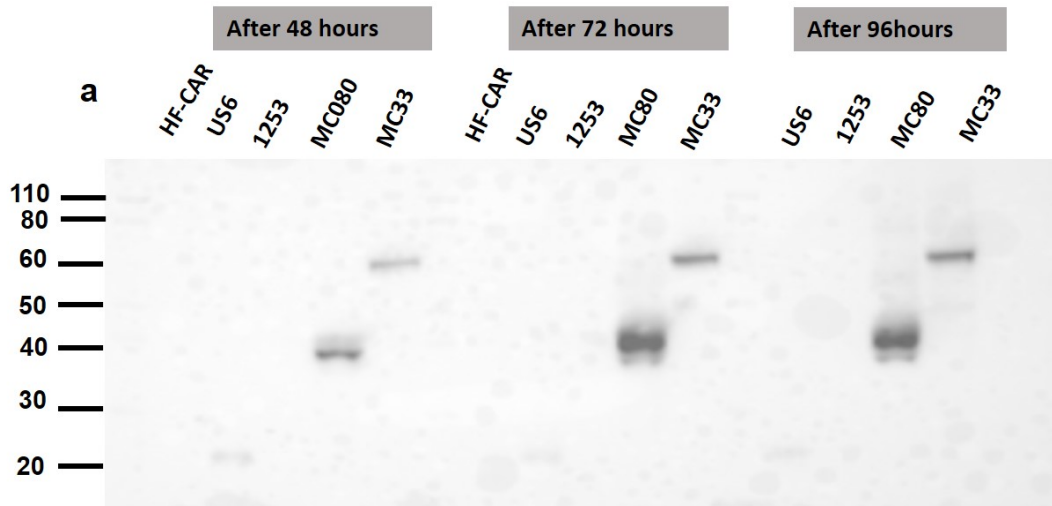


Figure 3.15: Time point expression of RADmc033 and RADmc080HF. HF-CAR cells were infected with RADmc033, RADmc080, RAdUS6 (positive control) or RAd1253 (negative control) at an MOI 5 for 48, 72 and 96 hours. Equivalent amount of samples were applied into 10% NuPAGE Bis-Tris gel, then they were electroblotted to nitrocellulose membranes and probed by mouse monoclonal V5 (1:10000) for corresponding V5 tagged protein then the anti-mouse IgG HRP (1:2000) was used.

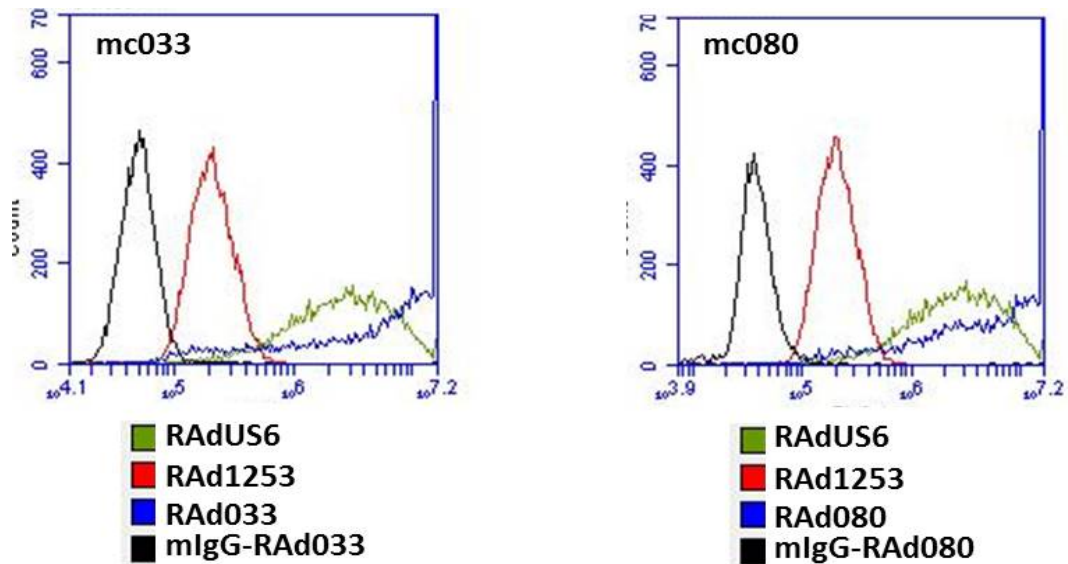


Figure 3.16: Flowcytometric analysis of MC033 and MC080 expression. For expression of MC033 and MC080 from the recombinant adenoviruses, HF-CAR cells were infected with RADmc033, RADmc080, RAdUS6 (positive control) or RAd1253 (negative control) at an MOI 5 for 72 hours followed by intracellular staining for V5 using mouse monoclonal V5 and IgG1 was used as isotype control

3.5 Summary

The expression of the codon optimized mc080 and mc033 was undertaken using RAd5Z vector, DNA transfection of HeLa cells using different pHAGE plasmids and a second-generation lentiviral vector. However, the lentiviral vectors grew to poor titre, giving low expression of mc080 and mc033 and for this reason they were not progressed. I failed to observe any expression from mc080 using vaccinia vector, potentially due to toxicity of the virus and possibly due to the high GC content of the original MOCV sequences, leading to low titre virus recombinants and no detection of recombinant proteins.

From previous experiments cellular cytotoxicity was observed at the later time point when using RAdmc080. In view of these observation, future experiments were performed at 72 h post infection unless otherwise indicated.

4- Functional assay of mc033 and mc080

4.1: Introduction

The only previous study on mc080R used a VACV virus vector to express the gene and found that it encoded a glycoprotein that formed a complex with $\beta 2$ microglobulin and was not presented on the cell surface but retained in the ER (Senkevich and Moss 1998). Neither the role or the expression of MC033L has previously been studied. Although the selection of another poxvirus vector to express mc080R was rational, the use of a lytic system hindered the detailed analysis the MOCV gene. Replication-deficient Ad vectors express only the gene of interest, provide efficient and reliable expression of the codon optimized MOCV genes and are compatible with functional assays already established in the laboratory. This thesis therefore preferentially used expression using replication-deficient Ad vectors as the basis for further studies.

HLA class I heavy chains form a trimeric complex with β -2m and peptide that are assembled in the ER before being processed through the Golgi apparatus and presented on the cell surface. A subset of endogenous cell proteins is degraded by proteasomes into short peptides which are actively transferred into the lumen of the ER by the transporter associated with antigen processing (TAP). During virus infection, a subset of viral proteins will also enter and be processed by this pathway. After binding peptide in ER, the peptide-MHC I complex are further processed in the Golgi apparatus before being presented on the cell surface (Androlewicz 2001). Virus-derived peptides may be recognised as foreign by TCR present on CD8⁺ cytotoxic T lymphocytes (CTL) and result in killing of virus infected targets. HCMV encodes at least four functions that act together to impede the MHC I antigen processing pathway and thereby to avoid activating CTLs. US6 one of those genes, inhibits the function of TAP, blocking the translocation of peptide from cytosol to ER lumen (section 1.8) (Lehner et al. 1997). Endogenous MHC-I molecules are however the chief inhibitory ligands for Natural Killer cells (section 1.8). Although suppressing cell surface expression of MHC-I renders HCMV-infected cells resistant to CTL attack, it has the potential to make them more vulnerable to NK cells (Wilkinson et al. 2008). This vulnerability is combated in part by HCMV gpUL18, acting as a class I mimic by binding the inhibitory receptor LIR-1. Furthermore, a peptide donated by the UL40 signal peptide upregulates HLA-E in a TAP-

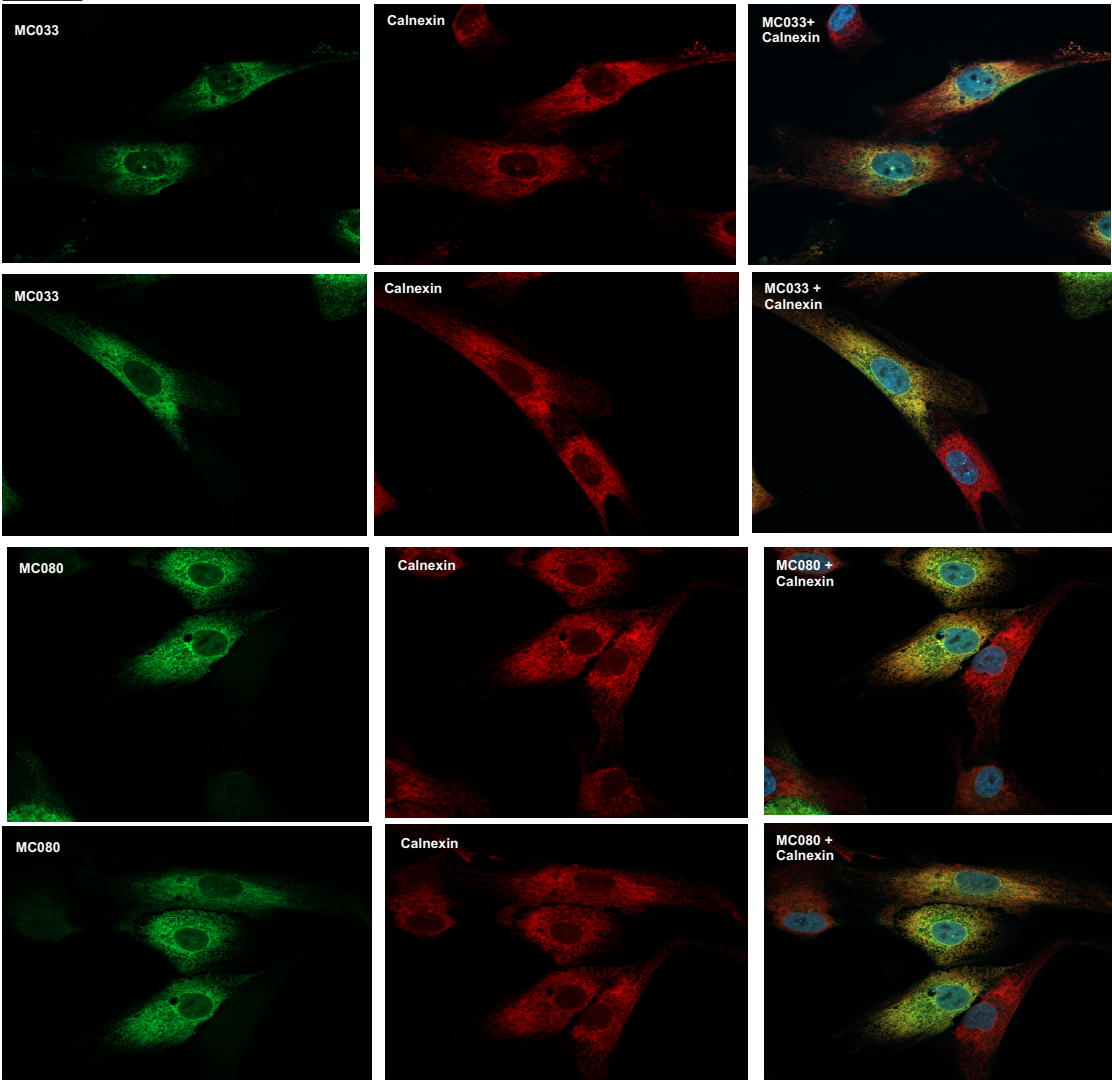
independent manner; HLA-E bind the NK cell inhibitory receptor CD94:NKG2A (Prod'homme et al. 2007). MOCV infection is also thought to downregulate MHC-I from the cells surface, as indicated by the loss of β -2m from the surface of MOCV lesions (Viac & Chardonnet - 1990). The goal of the study was to first characterise the MOCV mc033L and mc080R MHC-I homologs expressed from the Ad virus vector and then investigate whether MC033 and MC080 modulate the cellular immune response.

4.2 Intracellular localisation of mc033 and mc080 and their effect on total MHC I

The expression of MC033 and MC080 were each readily detected by immunofluorescence in HF-CAR cells infected with the Ad recombinants encoding mc033 or mc080, respectively. In analysing these data, it is prudent to remember MC033 and MC080 are being expressed in isolation; in the context of an MOCV infection, the proteins may interact with other virus-encoded proteins and the act of productive infection can be expected to impact on cellular organelles.

To investigate trafficking of the proteins, cells were co-stained with a second antibody specific for either calnexin (an ER marker) or giantin (a marker for the Golgi apparatus). DAPI was included in merged images to identify the cell nucleus. The overall distribution of the V5 tagged MC033 and MC080 was similar to calnexin and thus consistent with both proteins being localised to the ER (figure 4.1 A). (This correlation was supported by the dual exposure image where co-localisation produces a yellow colour.) The distribution of Golgi marker was quite distinct being found in a globular structure adjacent to the nucleus. While it is clear from the images that MC033 did not localise exclusively to the Golgi, there was some overlap (that results in some yellow colour associated with the Golgi) in the merged image with MC080 and giantin (figure 4.1 B). It is possible that MC080 may be in the Golgi, has to be confirmed by confocal microscopy.

A



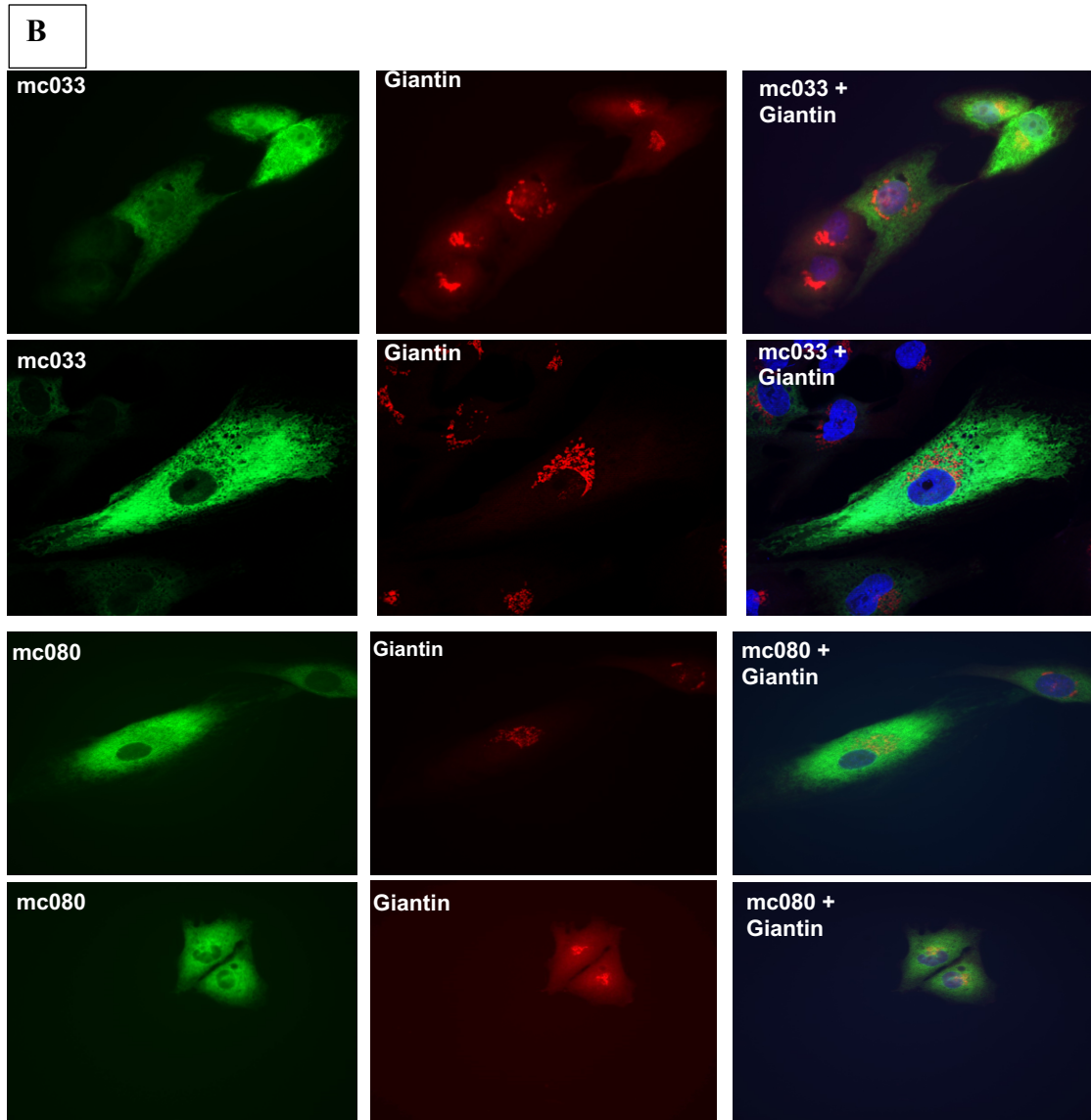


FIGURE 4.1: MC080 and MC033 are localized predominantly to the ER. HF-CAR cells were infected with RAdmc033 or RAdmc080, at an MOI 5 for 48 hours followed by cellular permeabilization and stained with (A) a rabbit monoclonal anti-V5 and Alexia Flour@488 goat anti-rabbit to detect either MC033 or MC080 (green). The ER was labelled using a mouse monoclonal anti-calnexin (1:200), they were immune-stained with and Alexia Flour@594 goat anti-mouse antibody(red) or both. (B) The Golgi was labelled with rabbit giantin antibody and Alexia Flour@594 goat anti-rabbit (red) and a mouse monoclonal anti-V5 and Alexia Flour@488 goat anti-mouse to detect either MC033 or MC080 (green) or both. DAPI was included in merged images to illustrate cell nuclei. Cells were examined by a Zeiss immunofluorescence microscope.

4.3 Effect of MC033 and MC080 on NK Cell Activation

The hypothesis was that MC033 and MC080 were acting as MHC-I mimic, i.e. they were expressed on the surface of infected cells and binding directly to inhibitory ligands on NK cells. Although the localisation of both MC033 and MC080 to the ER appears inconsistent with that model, both HCMV gpUL18 and gpUL142 were found predominantly in the ER when expressed from an Ad vector, yet both NK evasion functions can be detected on the cell surface and gpUL18 is known to bind directly with the NK inhibitory receptor LIR-1 (Griffin et al. 2005; Prod'homme et al. 2007). The first series of experiments sought to explore the effect of MC080 and MC033 on NK cell activation in a CD107a mobilisation assays that provides a direct measurement of NK cell degranulation assay. HCMV UL141 is recognised to elicit robust protection against NK cell activation not only through downregulating activating ligands CD112 and CD155 from the cell surface but also by targeting the death receptor TRAIL-R2 (Tomasec et al. 2005; Prod'homme et al. 2010; Smith et al. 2013b); UL141 was therefore included as a positive control.

NK assays are primarily performed from PBMC purified from the blood from volunteer donors or blood bags provided by the Welsh blood transfusion service. Overnight interferon stimulated PBMC were used in NK cell functional assays as an approach that minimises in vitro culture and thus provide as close to a physiological source of NK cell for in vitro assays as practical.

The PBMC from donor 008 and donor 009 and two NK lines from donor 007 (kindly provided by Dr Rebecca Aicheler) and from blood donor 5 (BD5) (kindly provided by Dr Simone Forbes and Dr Virginia-Maria Vlachava) were tested in autologous (when applicable) and allogenic setting.

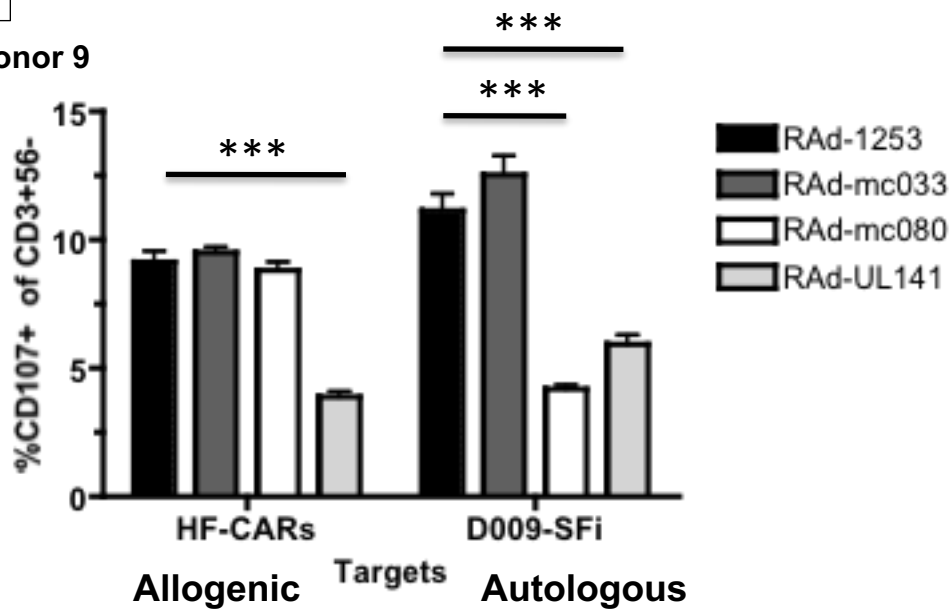
Peripheral blood mononuclear cells (PBMC) were freshly isolated from volunteer donor 008 and donor 009, and the BD5 NK line and donor 007 NK line, the PBMCs were incubated for 16h with α -interferon. Interferon-stimulated PBMC were incubated with HF-CARs or autologous HSF infected with RAd-mc080, RAd-mc033, RAd-UL141 or the control vector at an effector:target ratio of 10:1 and incubated for 5 h in a CD107a assay (section 2.15). NK cell degranulation was assessed by flowcytometry.

In an allogeneic setting, MC080 did not protect against NK cell degranulation in PBMC in D009 and D008. However, in NK lines D007 and BD5, mild inhibition of NK cells killing were noticed (figure 4.2). In an autologous setting MC080 was able to either activate in PBMC from donor 008 and NK line donor 007 or inhibit NK cell degranulation in cells of donor 009 (figure 4.2) this difference NK cell responsiveness may have related to KIR/HLA genotype difference between donors (Ahlenstiel et al. 2008). It was found that MC033 had no effect in either D009 allogenic or autologous setting, that is why it was not included in other NK experiments. It is suggested that MC080 is effective in suppressing NK cell activation in certain individuals and MC033 has no effect in NK cell activity (figure 4.2).

In seeking an explanation for the observed results, NK cells constitutively express the killer immunoglobulin-like receptors (KIR), which are specific and highly polymorphic, they are dividing into inhibitory and stimulatory depending upon the expression of either a long (L) or a short (S) cytoplasmic tail, respectively. The KIR gene content may vary between individuals, and to date there are more than a twelve KIR genes that have been described. KIR and leukocyte inhibitory receptor (LIR-1) are ligands for MHC class I (Moretta et al. 2001; Martin et al. 2004; Parham 2005).

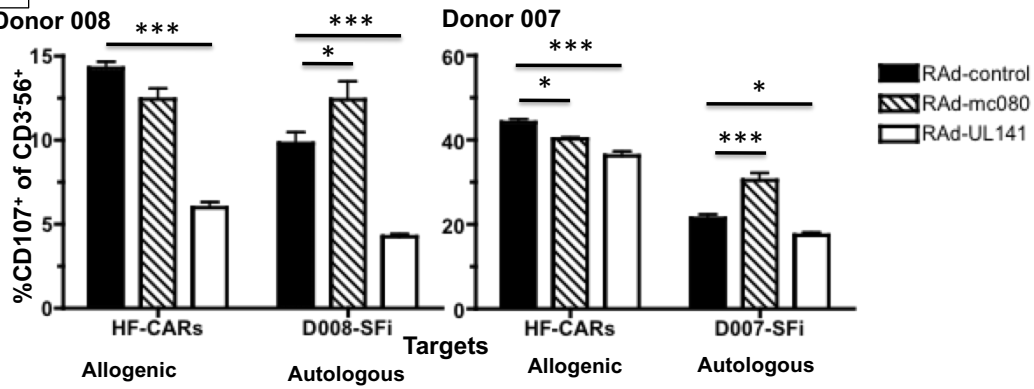
A

Donor 9

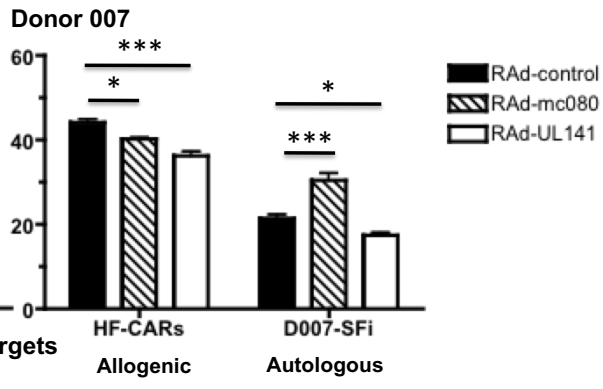


B

Donor 008



Donor 007



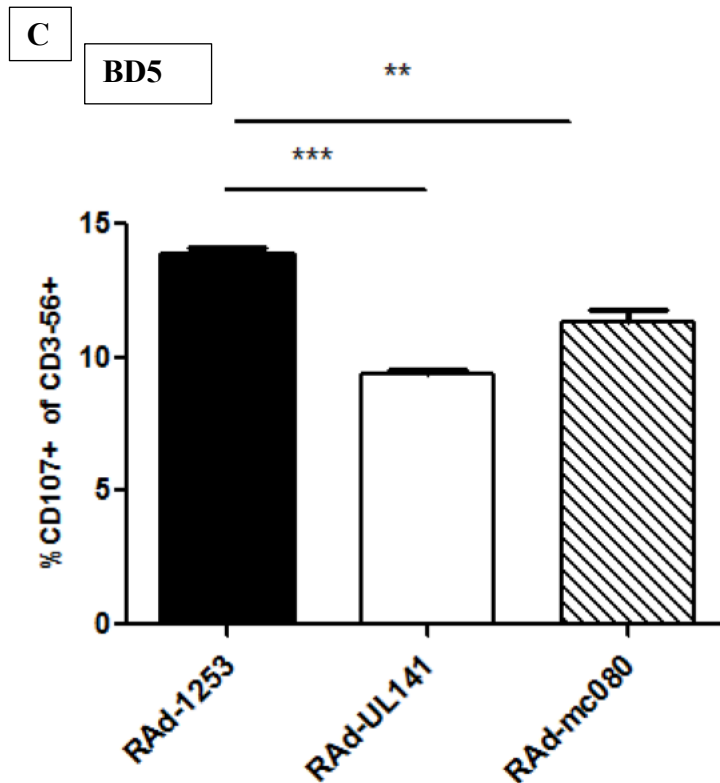


Figure 4.2: MC080 modulates NK cell activity. The effect of MC080 and MC033 on NK cells degranulation was assessed by measuring the proportion of CD107a+ cells within the CD3- and CD56+ population. UL141 is a recognised HCMV NK cell evasion function that was included in the assays as a positive control. (A) HF-CARs and autologous skin fibroblasts cells infected at an MOI 5 or 500 respectively with RAd-mc080, RAd-mc033, RAd UL141 or Ad vector (RAd-control) for 72 hs. Infected cells were incubated with D009 PBMC with effector:target 10:1 ratio for 5 h with FITC conjugated CD107a or FITC IgG1 isotype control in presence of Golgi stop. (B) HF-CARs and D007 or D008 fibroblast cells infected at an MOI 5 or 500 respectively with RAd-mc080; RAd-1253(vector control); or RAd-UL141. After 72 hs, the D007 NK cells or D008 PBMC and infected cells with 10:1 effectors:target, incubated for 5 hours with FITC conjugated CD107a or FITC IgG1 isotype control in presence of Golgi stop. NK degranulation assessed by %CD107a+ within the CD3- and CD56+. (C) HF-CARs cells infected at an MOI 5 with RAd-mc080, RAd-1253(control), or RAd-UL141 for 72 hs. Infected cells were incubated with BD5 NK cells with effector:target 10:1 for 5 hs in presence of FITC conjugated CD107a or FITC IgG1 isotype and Golgi stop. The data was analysed using one-way anova and the virus constructs were compared versus RAd control using Dunnett test (* $P < 0.05$, ** $P < 0.01$, *** $P < 0.001$).

4.4 MC080 down regulates cell surface MHC class I expression

The complex pattern of NK cell modulation encouraged further characterisation of MC033 and MC080 expression. To analyse the subcellular localisation of MC033, MC080 and gpUS6 lysates were treated with endoglycosidase H (Endo H) and Peptide-N-Glycosidase F (PNGase F) and analysed by immunoblotting. HCMV US6 is known to be ER resident and to downregulate MHC-I and was included as a positive control (Lehner et al. 1997). The MC033 mock treated sample ran as two bands, a high molecular form (64 kDa) that was sensitive to Endo H and PNGase F, consistent with retention of MC033 in the ER (figure 4.1). The resistance of the faster migration MC033 species implied it was not N-glycosylated. The MC080 mock treated sample ran as three bands; a slow migrating form (~46kDa), an intermediate form (~42kDa), and a faster migrating form (~40kDa). Both heaviest and intermediate forms are sensitive to Endo H and PNGase F which may indicate a prolonged glycosylation and/or a longer retention in the ER, the fast migrating form was not sensitive to de-glycosylation (figure 4.3). MC080 forms stable intracellular complexes with β 2-m, a protein required for the expression of mature MHC-I heavy chains (MHC-I HC) on the cell surface (Senkevich and Moss 1998). Therefore, we examined the effect of both MC080 and MC033 on MHC class I expression. MC033 has no obvious effect on the protein levels or glycosylation status of MHC-I HC (figure 4.3). In contrast, in the presence of MC080, the protein levels of MHC-I HC are diminished, and MHC-I HC become sensitive to Endo H, suggesting that MC080 retains MHC-I HC in the ER and reduces total MHC-I HC in the cell (figure 4.3).

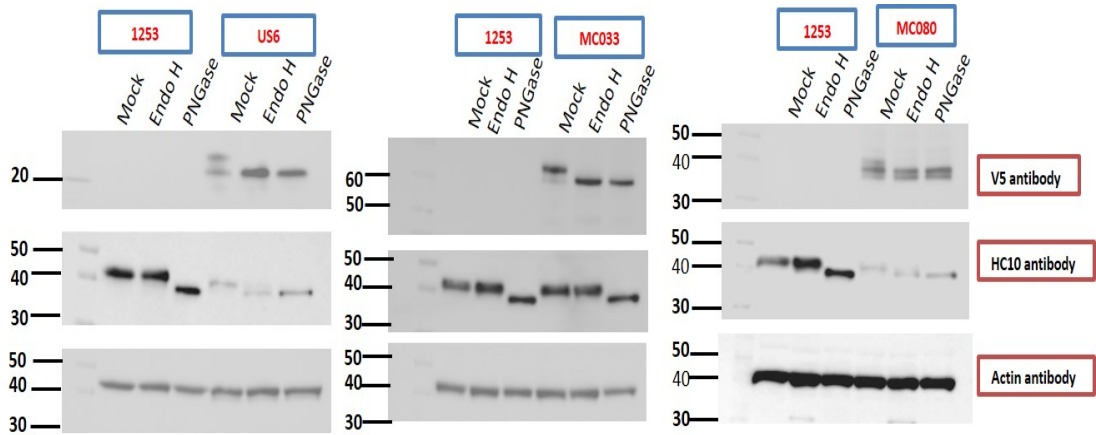


Figure 4.3: MC080 downregulates total MHC I. To investigate the intracellular localization of MC033 and MC080 and their effect on MHC-I, HF-CAR cells were infected with RAdmc033, RAdmc080, RAdUS6 (positive control) or RAd1253 (negative control) at an MOI 5 for 72 hs. Prior to Western blotting, denatured protein lysates were mock treated or were treated with either Endo H or PNGase F following the manufacturer's protocol, overnight at 37°C. The plotted membranes were immuno-probed with mouse monoclonal anti-V5 (1:10000), Heavy chain HC10 (1:600) or rabbit anti-actin antibody (1:3000).

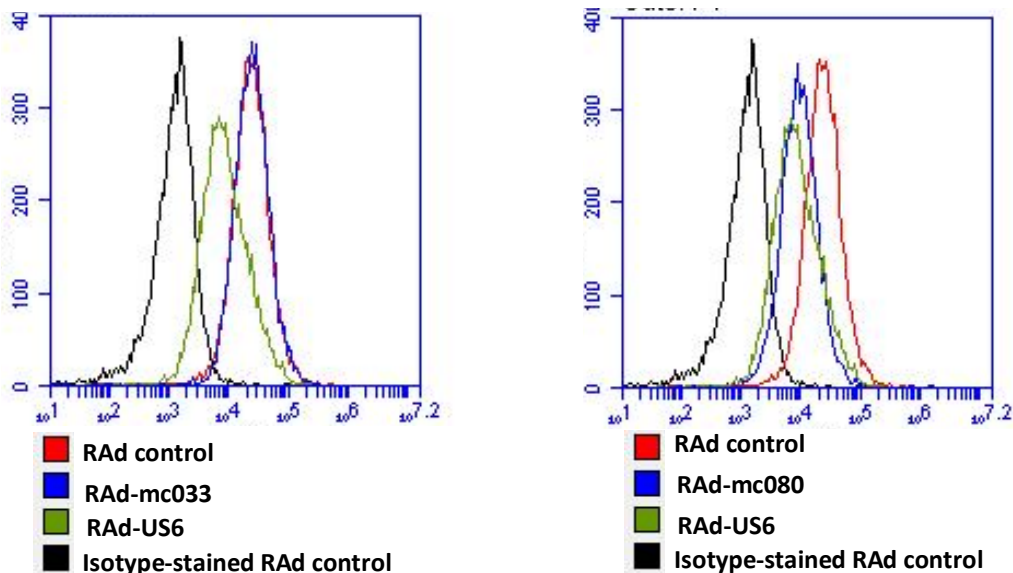


Figure 4.4: Flow cytometric analysis of effect of MC033 and MC080 on surface expression MHC-I. To investigate the surface expression of MHC-I, HF-CAR cells were infected with RAdmc033, RAdmc080, RAdUS6 or RAd1253 (Ad vector) at an MOI 5 for 72hs. The cells were stained using the APC conjugated W6/32 antibody (1:50), which detects the expression of MHC-I on the cell surface.

As the immunoblot data indicated that MC080 reduced total protein levels of MHC-I HC and rendered MHC-I HC susceptible to Endo-H digestion. Since immunofluorescence studies already indicated MC080 localised to the ER (Section 4.1), it was possible that MC080 could be retaining MHC-I in the ER. I therefore sought to investigate whether MC080 was able to downregulate MHC-I from the cell surface. Cell surface expression of MHC class I on HF-CAR cells infected with RAdmc080, RAdmc033, RAdUS6 or the appropriate Ad vector control was monitored by flow cytometry. MC080 reduced the levels of MHC class I surface expression at an equivalent efficacy through the time course to that observed with HCMV US6, a recognised inhibitor of TAP. MC033 did not exert an effect on the surface expression of MHC-I molecules (figure 4.4). Since only the EndoH-sensitive glycoform of MHC-1 can be detected in cells expressing MC080, it seems likely that MC080 is acting to retain MHC-I in the ER. The reduced levels of MHC-1 detected in the presence of MC080 suggests that it is being targeted for degradation rather than being retained as a stable complex (figure 4.3).

4.5 MC080 Downregulates HLA-E

Human histocompatibility leukocyte antigen-E (HLA-E), a non-classical MHC class Ib molecule, has limited sequence polymorphism. HLA-E normally binds a nonameric peptide derived from a conserved sequence present in the leader sequence of many conventional MHC HCs. Peptide binding is required for the maturation of HLA-E and its transit to the cell surface (Braud et al. 1997). Once the cell surface HLA-E binds the NK cell inhibitory receptor CD94/NKG2A and thus as a sensor of classical MHC-1 expression and an inhibitory ligand. To investigate the effect of MC080 on surface expression of HLA E, the HF-CARs were infected with RAd-mc080, RAd-mc033, RAd-US6 or RAd-1253 (control) with an MOI 5 PFU/cell. The level of HLA-E expression was analysed at 24, 48, 72 and 96 hours, the mAb 3D12 was used for flow cytometry, normal IgG1 was used as negative control. The flow cytometric data in figure 4.5 showed that, at all time points, low level of HLA-E were expressed on cell surface upon expression of MC080, in contrast, MC033 did not alter surface expression of HLA-E. Although the effect is consistent over the time course, the low level of HLA-E expression in human fibroblast makes the impact of mc080 on HLA-E difficult to resolve (figure 4.5), the US6 is known to block the

peptide transporter TAP as a result it downregulate HLA-E in a TAP dependent way (Braud et al. 1997; Tomasec 2000)

Efficient cell surface expression of HLA-E and classical MHC-I proteins require peptides to be loaded in a TAP dependent manner (Braud et al. 1997). Two herpesvirus proteins, HSV ICP47 and HCMV US6, have been shown to impede classical MHC-I expression by interfering with TAP and HHV-7 U21 downregulates HLA-E expression (Fruh et al. 1995; Hill et al. 1995; May et al. 2010) complex molecules from the cell surface. As our data indicated that MC080 and MC033 reside in the ER, where TAP primarily resides, and that MC080 can downregulate MHC-I and HLA-E, I sought to determine whether MC080 was able to hinder peptide loading by interfering with TAP and therefore reduce MHC-I and HLA-E surface expression. The NPi fibroblast cell line is derived from a patient with a genetic defect in TAP, and these cells exhibit extremely low levels of cells surface MHC class I and HLA-E expression. NPi cells were infected with Ad vector encoding HLA-A2 in conjunction with either RAd-mc080 or RAd-US6. The peptide binding groove in HLA-A2 binds hydrophobic peptides, many of which are able to reach the lumen of the ER in a TAP-independent manner. The HCMV inhibitor of TAP, US6, had no effect on HLA-A2 expression in TAP deficient cells while, in contrast, MC080 resulted in a striking reduction in HLA-A2 surface expression. This result implies that MC080, unlike US6, downregulates classical MHC-I via a TAP independent mechanism (figure 4.6). Next, we asked whether MC080 could interfere with cell surface expression of the non-classical MHC-I molecule HLA-E. NPi cells are negative for TAP and are therefore are not able to present HLA-E on their surface, therefore peptide was supplied from the HCMV strain Merlin UL40 protein which presents peptide to HLA-E in a TAP independent manner (Tomasec 2000). NPi cells were co-infected with recombinant adenoviruses expressing HLA-E*0101 (RAd-HLA-E) and UL40 (RAd-UL40) as well as RAdMC080 or RAdUS6. As previously reported, cell surface expression of HLA-E was increased in cells co-infected RAd-HLA-E and RAd-UL40 and here we show that co-infection of these cells with RAd-MC080 resulted in downregulation of HLA-E (FIG 4.6). These data indicate that MC080 downregulates classical MHC-I and HLA-E in a TAP independent manner.

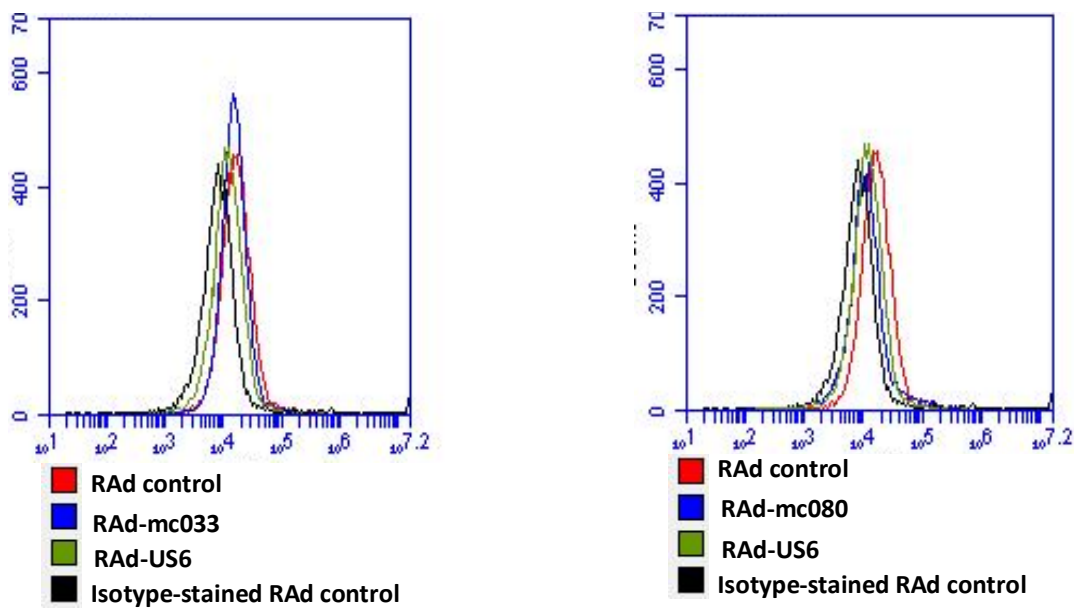


Figure 4.5: Flow cytometric analysis of effect of MC033 and MC080 on surface expression HLAE. To investigate the surface expression of HLAE, HF-CAR cells were infected with RAdmc033, RAdmc080, RAdUS6 or RAd1253 (vector control) at an MOI 5. 24, 48, 72 hours post infection, the HF-CAR cells were immune-stained using the PE conjugated 3D12 (1:50) antibody, which detects the expression of HLAE on the cell surface.

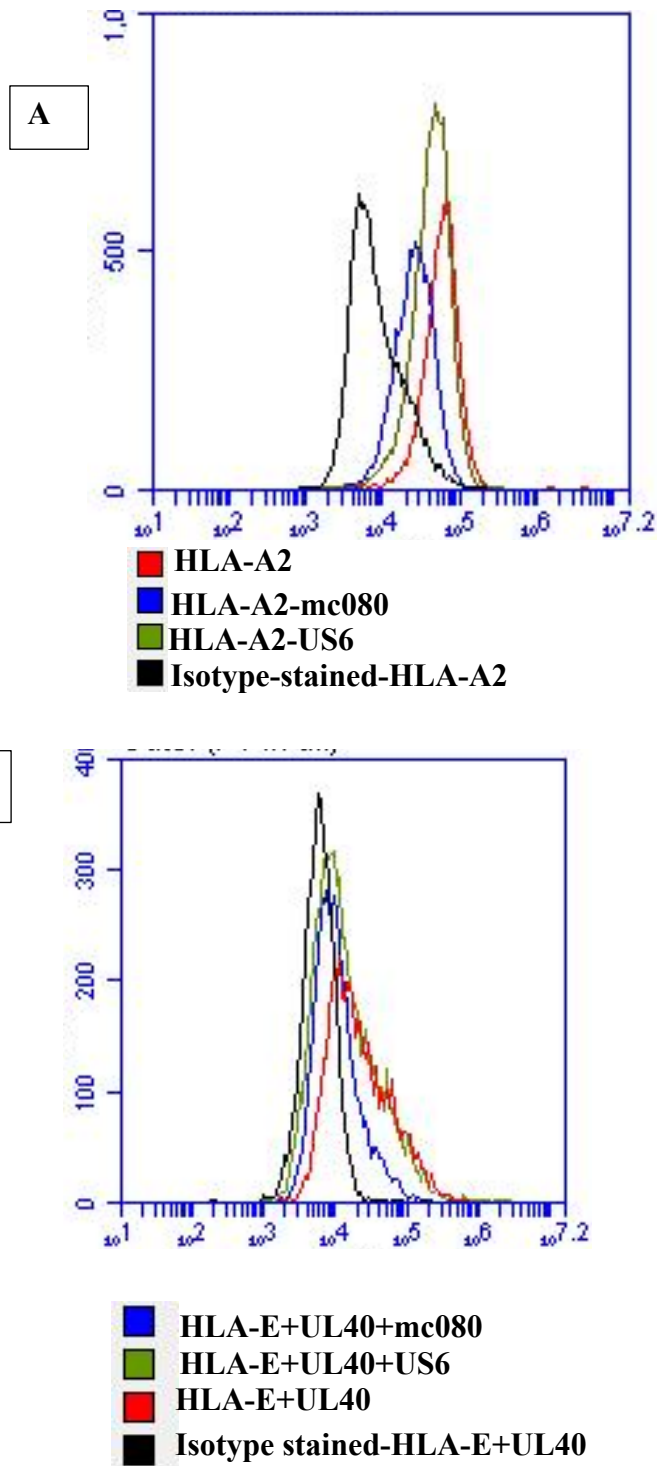


Figure 4.6: MC080 downregulate MHC I and HLA-E in a TAP independent way. (A) fibroblast from a TAP deficient patients (NPi) were co-infected at an MOI 350 with RAd control expression HLA-A2 and RAd-mc080 or RAd-US6 (control) or NPi cells infected with HLA-A2 only. After 72 hs from infection, the cells fixed and stained with APC conjugated W6/32 or isotype control IgG2a, then fixed and analysed using Accuri flow cytometry. (B) The NPi cells co-infected at MOI 350 with RAd expressing HLA-E*0101 and RAd-UL40 alone or in conjunction with either RAd-mc080 or RAd-US6. 72 hs p.i the cells fixed and stained with PE conjugated 3D12 or PE isotype control. The fixed cells analysed using Accuri flow cytometry.

4.6 Effect of mc080 on MICA

So far seven genes making the major histocompatibility complex class I chain-related molecule, they are from MICA to MICG. However, only MICA and MICB are functional genes, MICA looks very similar to its classical class I but does not bind β 2-microglobulin (β 2-m) (Bahram et al. 1996; Fodil et al. 1996; Li et al. 1999). More than 50 alleles of MICA have been described, the most common allele in North American Caucasoid with allele frequencies higher than 50% is MICA*008. The hallmark of this allele is that, it has an insertion that generates a premature stop codon in exon 5 which makes the transmembrane domain shorter, and also lacks the cytoplasmic tail (Petersdorf et al. 1999; Zhang et al. 2001; Stephens 2002). MICA is recognized by the C-type lectin NKG2D which is expressed on all NK cells, $\gamma\delta$ T cell and some $\alpha\beta$ T cells (Bauer et al. 1999). Since MC080 was capable of downregulating both MHC class I and HLA-E, the question was if it was able to have effect on expression MICA. MICA is a stress ligand; normal fibroblasts do not normally express significant amounts of MICA on the cell surface hence I used Chinese Hamster ovary (CHO)-CAR cells which lack endogenous MICA was used. To test the effect of MC080 on surface expression of MICA, CHO-CAR cells were infected at an MOI 50 with RAd-mc080 or RAd-control in combination with MOI 50 of full length MICA (RAd*002) or truncated MICA (RAd*008) all at an MOI of 50, for 72 hours. The cells were as stained with MICA antibody to test for surface expression of MICA, IgG2b was used as isotype control. It was noticed that MICA expression of MC080 was equal to expression MIC*002 or MIC*008, then it was concluded that MC080 had no effect on the cell surface expression of either full-length MICA*002 or truncated MIC*008 (Fig 4.7).

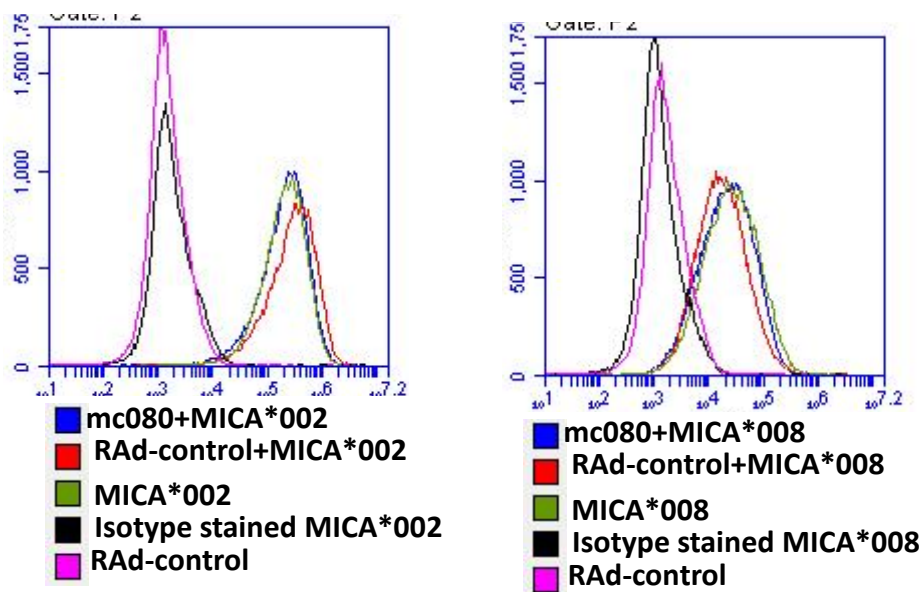


Figure 4.7: MC080 has no effect in surface expression MICA. CHO cells co-infected at MOI 50 with RAD vectors encoding the genotype MICA*002 or truncated MICA*008 genotype alone, or in combination with MOI 50 of either RAD-mc080 or a control RAD vector as indicated, CHO cells infected with MOI 50 of RAD control only was used as a control. After 72 hs cells were stained with PE conjugated anti-MICA or an PE conjugated IgG2b isotype control antibody analysed by flow cytometry.

4.7 Effect of MC080 on T-cell Activation

Cytotoxic CD8⁺ T lymphocytes (CTL) play a critical role in the immune control of viruses. CTL recognize cells presenting viral peptides bound to surface MHC class I molecules (Kagi et al. 1994). Since the number of cell surface, peptide loaded on MHC class I molecules required for CTL recognition is very low, the question is whether MC080 was capable of decreasing levels of MHC-I sufficiently to alter CTL recognition of MC080 expressing cells. HLA-A2-specific T cells lines from donor 007 specific for the HCMV IE1 -restricted VLEETSVML (VLE) epitope in the major IE1 protein and the NLVPMVATV (NLV) epitope in the tegument protein pp65 were kindly provided by Mihil Patel (Cardiff university). Both cell lines were expanded *in vitro*, before being used in CTL functional assays against peptide pulse target cells. Donor 007 HSF was infected with RAd-mc080, RAd control, RAd mc033 or RAd US6, Targets were coated with an appropriate concentration of peptide (VLE; 1.0µg/ml, 0.2µg/ml, 0.04µg/ml peptide and for NLV; 1.0µg/ml, 0.2µg/ml, 0.04µg/ml, 0.008µg/ml) for 1 hour. Excess peptide was washed, CD8⁺ T cells were incubated in triplicate with targets, with effector:target ratio of 10:1 and incubated for 5 h in a CD107a assay (section 2.16). CD8⁺ T cell degranulation was assessed by flow cytometry. For first time it was noticed that MC080 had the ability to protect against T-cell degranulation at a range of peptide concentrations and it was similar to US6 (the positive control). However, mc033 had no effect on CD8⁺ T activity. Also, it was found that lower peptide concentration has more impair of CD8⁺T cells activity. This is indicating that downregulation of MHC class I by MC080 provides MOCV with a mechanism for evading T-cells degranulation (figure 4.8).

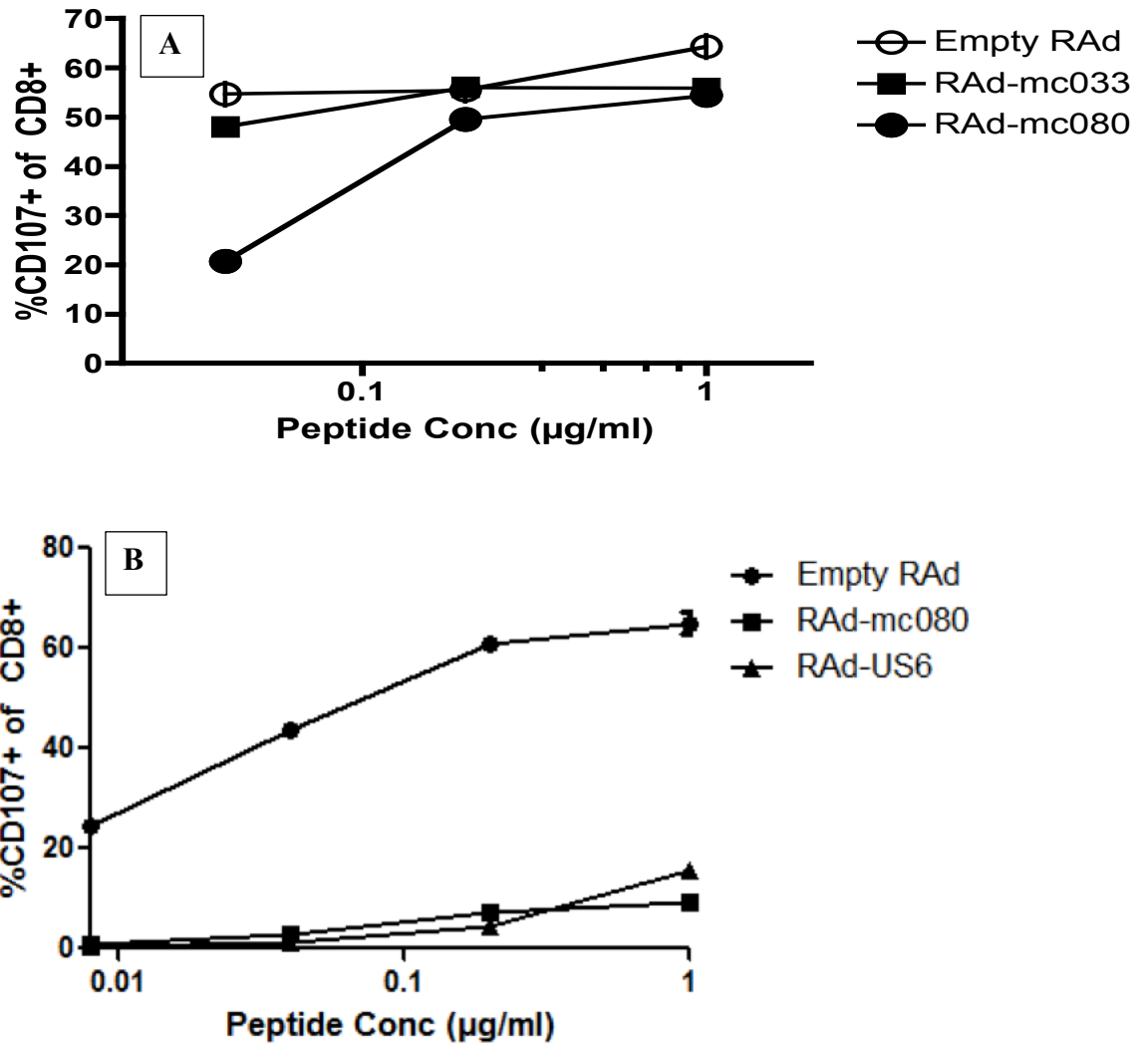


Figure 4.8: MC080 downregulate CD8⁺T cells. CD8⁺T cells lines generated from donor 007 restricted epitope (A)VLEETSVML (VLE) and (B) NLVPMVATV (NLV) were expanded. Autologous skin fibroblast cells were infected with at (A) RAd-mc080, RAd-mc033 and RAd-control; (B) RAd-mc080, RAd-US6 and RAd-control at MOI 500. 72 hours post infection, (A) the cells at were coated with VLE; 1.0µg/ml, 0.2µg/ml, 0.04µg/ml peptide, (B) the cells were coated with pp65;1.0µg/ml, 0.2µg/ml, 0.04µg/ml, 0.008µg/ml peptide for 1 hour at 37°C. Excess peptide was washed off, then CD8⁺ T cells were incubated in triplicate with targets, with effector:target ratio of 10:1. Following 5 hours incubation with FITC CD107a antibody or FITC IgG1 in presence of Golgi stop, then the cells were stained with PE/Cy7 conjugated CD3 and PE conjugated CD8. The cells fixed and then analysed using flow cytometry for CD3⁺ and CD8⁺.

4.8 Summary

Both MC033 and MC080 are glycoproteins sequestered in the ER. For first time, it was observed that MC080 is effective in suppressing NK cell activation in certain individuals and this difference NK cell responsiveness may be related to KIR/HLA genotype difference between individuals. Also, MC080 down regulates surface expression of MHC-I and total protein levels of MHC-I and may degrade or retain MHC-I in the ER. Furthermore, mc080 downregulates surface expression of HLA-E in a TAP independent way. In contrast, MC033 has no effect in MHC-I and HLA-E. MC080 has ability to protect against degranulation by CD8⁺ T cells.

5-Characterisation of HCMV MHC-I Homologues UL142.

5.1 Introduction

The HCMV UL18 ORF was first identified as a MHC class I homolog during analysis of the strain AD169 genome (Beck and Barrell 1988) and subsequently shown to encode for a 67-kDa endoglycosidase H-sensitive glycoprotein capable of forming a trimeric complex with β_2 -microglobulin and endogenous peptides (Browne et al. 1990). HCMV strain AD169 gpUL18 was shown to bind to the inhibitory receptor LILRB1 (LIR1) with 1,000-fold higher affinity than MHC class I; the affinity of UL18 in other strains may differ (Cosman et al. 1997; Bauer et al. 1999; Chapman et al. 1999; Cerboni et al. 2006; Chen et al. 2016). The role of gpUL18 in virus infection is complicated as while it inhibits LILRB1⁺ NK cells, it also activates LILRB1⁻ NK cells (Cosman et al. 1997; Bauer et al. 1999; Chapman et al. 1999; Davison et al. 2003b; Prod'homme et al. 2007). UL18 and UL142 together form the HCMV gene family of MHC I homologues (Davison et al. 2003b). UL142 also encodes a glycoprotein that exhibits amino acid sequence homology with MHC class I and secondary structure prediction delineate MHC class I alpha-1 and alpha-2 domains that in MHC class I play a role in binding to peptide and other ligands (Davison et al. 2003b; Wills et al. 2005). However, the alpha-3 domain which is necessary for MHC I stability, is truncated in UL142 (Davison et al. 2003b; Wills et al. 2005).

HCMV UL142 is contained within the *U₁/b'* gene region that is missing from commonly used high passage laboratory strains Towne and AD169. However, it is intact in the low passage strain Merlin (Tomasec et al. 2005; Stanton et al. 2010). HCMV strain Merlin, isolated in Cardiff, was initially sequenced at passage 3 and is genetically intact except for mutations identified in UL128L and RL13; these mutations are required for efficient growth in fibroblasts (Dolan et al. 2004; Stanton et al. 2010). UL142 is expressed late in infection and is heavily glycosylated in line with the prediction that it contains 17 potential N-linked glycosylation sites (Wills et al. 2005). Like UL18, HCMV UL142 has been demonstrated to be involved in NK cell evasion. However, unlike UL18, UL142 only inhibits NK cells in a proportion of donors (Wills et al. 2005). Current research demonstrates that HCMV UL142 can suppress NK cell activation by modulating expression of a ligand (MICA) for the ubiquitous NK cell activating receptor NKG2D (Wills et al. 2005). NKG2D is also

expressed on $\gamma\delta$ T cells and subsets of $\alpha\beta$ T cells (Bauer et al. 1999). NKG2D is remarkable in recognising at least 8 different ligands that are induced by cellular stress, such as virus infection or genotoxic shock. HCMV encodes multiple functions that retain and degrade NKG2D Ligands, thus preventing their presentation on the cell surface. HCMV UL16 targets MICB, ULBP1, ULBP2, and ULBP6 (Cosman et al. 2001; Chalupny et al. 2003; Bacon et al. 2004), while recently the US12 gene family, most notably US18 and US20, have been shown to reduce MICA expression extremely efficiently (Fielding et al. 2014; Fielding et al. 2017). HCMV UL142 has been shown to down regulate cell surface expression of MICA, re-localising and retaining MICA in the ER and the cis-Golgi apparatus (Chalupny et al. 2006; Ashiru et al. 2009). While MICA is highly polymorphic, there is particular interest in the MICA*008 allele. MICA*008 is found in 20% of the population and is C-terminally truncated such that it does not code for a transmembrane domain. Rather MICA*008 is expressed with a GPI anchor (Glycosyl-Phosphatidyl-Inositol) (Ashiru et al. 2013). MICA*008 appears to be immune from the attentions of UL142 and the US12 family. This led to the proposal that MICA*008 is an HCMV-resistant "escape variant" that has been selected during human evolution to circumvent the effects of HCMV UL142 and the US12 family. However, recently MICA*008 has been shown to be targeted by US9, indicating a dynamic co-evolution of the human immune system with HCMV infection (Seidel et al. 2015).

While more research has been conducted on the HCMV MHC-I homologues than on the comparable genes in *molluscum contagiosum*, our understanding of HCMV UL18 and UL142 is far from complete. The observation that the US12 family targets MICA post-dates the identification of UL142 as a gene that downregulates MICA. Although ectopically expressed gpUL142 had been shown to suppress MICA expression, this function of UL142 had not yet been investigated in the context of the virus genome. The observation that UL142 only functions in selected donors is not consistent with MICA being its target. The NKG2D-MICA interaction is a major and ubiquitous mechanism of NK cell recognition (Wills et al. 2005) and NKG2D is expressed on nearly all NK cells (Bauer et al. 1999). However, these disparities could potentially be attributed to MICA polymorphism. In light of the observation that the US12 family targeted MICA efficiently, my hypothesis was that MICA may not be

the primary target for UL142 in lytic infection and that gpUL142 may be suppressing NK cell activation by an independent mechanism.

In this chapter the expression of UL142 and the effect of UL142 on truncated MICA*008 and non-truncated MICA*002 expression was tested in isolation by expressing UL142 in an Ad vector. The effect of UL142 on MICA expression was also tested in the context of HCMV by studying the effect of the HCMV strain Merlin with deletion of UL142.

Table 5.1: The viruses used in this chapter

| Viruses | Information details |
|-------------------|--|
| RAd-UL141 | Strain Merlin UL141 ORF amplified by PCR with a C-terminal V5 tag and cloned in to AdZ vector system Constructed by Drs Sepehr Seirafian and James Davies |
| RAd-UL142-1A | Codon optimised versions of strain Merlin UL142 synthesised <i>de novo</i> to contain UL142 ORF with the signal peptide in the N terminus removed and replaced with a signal peptide from preprotrypsin (PPT). It has N terminal V5- epitope tag. Constructed by Dr Rebecca Aicheler |
| RAd-UL142-2A | Codon optimised versions of strain Merlin UL142 synthesised <i>de novo</i> to contain UL142 ORF with the signal peptide in the N terminus removed and replaced with a signal peptide from preprotrypsin (PPT). It has a C terminal V5- epitope tag. Constructed by Dr Rebecca Aicheler |
| RAd-UL142-3C | Codon optimised versions of strain Merlin UL142 synthesised <i>de novo</i> to contain the UL142 ORF with HCMV endogenous signal peptide. It has a C terminal V5- epitope tag. Constructed by Dr Rebecca Aicheler |
| RAd-Soluble UL142 | Codon optimised versions of strain Merlin UL142 synthesised <i>de novo</i> to contain UL142 ORF, the transmembrane part was cut and it has a C terminal V5- epitope tag linked to BirA. Constructed by Dr Sepehr Seirafian |

5.2 Expression of UL142 using an adenovirus vector

When the endogenous UL142 ORF with a V5 tag was cloned into the AdZ vector (RAd-UL142), gpUL142 expression could not be detected by immunofluorescence and was only weakly by western blot (Seirafian 2012). Optimisation of codon usage can be used to increase protein translation efficiency and changes in mRNA sequence can overcome issues with secondary structure and control signals in mRNA. Three codon optimised versions of UL142 designed by Dr Rebecca Aicheler were synthesised commercially and provided as PCR-amplified DNA fragments for the generation of RAd-UL142-1A, RAd-UL142-2A and RAd-UL142-3C (see Table 5.1). RAd-UL142-3C contains a codon optimised, full length version of UL142 with a C-terminal V5 tag. UL142 expression was previously shown to be more readily detectable when its endogenous signal peptide was replaced with the signal peptide from preprotrypsin (PPT) (Ashiru et al. 2009). To this end, the RAd-UL142-1A was made with the PPT signal peptide upstream of a N-terminal V5 tag; this construct was designed to test whether gpUL142 was expressed on the cell surface. Since signal sequences may help determine the cellular location of proteins, the PPT signal sequence could potentially target gpUL142 to a different cellular compartment. To control for this, RAd-UL142-2A was also produced with the PPT signal sequence but the V5 tag was inserted on the C-terminus. Any effects of the PPT signal sequence on UL142 localisation and expression levels can therefore be controlled for by comparing RAd-UL142-2A and RAd-UL142-3C.

The BAC DNA for three constructs (RAd-UL142-1A, RAd-UL142-2A and RAd-UL142-3C) was electroporated into *E. coli* SW102 then cultured on agar plates containing sucrose. The selective media ensures that bacteria where recombination did not happen failed to grow. For large scale plasmid preparation of transfection-quality DNA, maxi-preparations of the three constructs were performed. Fresh DNA for the BAC constructs were transfected into the 293TREX helper cell line to generate replication-deficient recombinant adenoviruses and the infections were then expanded into six tissue culture flasks (150 cm²) to produce a virus stock.

Dr Sepehr Seirafian also generated a soluble version of UL142 (RAd-Soluble UL142) in an AdZ vector in which the C-terminal transmembrane domain was

removed to encourage the protein secretion. A C terminal V5 epitope tag was added to allow for expression analysis and a recognition sequence for a biotin ligase BirA was inserted to enable biotinylation of UL142 with a view to generating tetramers or UL142 complexes for identifying potential binding partners. A BAC plasmid of this construct was sequenced for this project. DNA for the BAC construct was transfected into 293TREX cells to generate infectious virus RAd-soluble UL142 and the infection was then expanded into six tissue culture flasks (150 cm²) to produce a virus stock.

To test intracellular expression of gpUL142 from each of these constructs, human fibroblasts (HF-CAR) were infected with RAdUL142-1A, RAdUL142-2A, RAdUL142-3C, RAd-soluble UL142, or RAdUL18-V5 (served as positive control) at an MOI 10 PFU/cell for 72 h, then cells were fixed, permeabilized, stained for V5 and analysed by flow cytometry (figure 5.1). These data demonstrate that expression of gpUL142 could be detected from cells infected with RAdUL142-1A, RAdUL142-2A and RAdUL142-3C at levels similar to that observed for RAdUL18. Paradoxically, the version of UL142 (RAd-soluble UL142) engineered to be secreted gave the highest levels of intracellular expression.

Ashiru and co-workers claim that gpUL142 is predominantly localised to the ER and Golgi apparatus along with MICA, yet a small amount of protein did reach the cell surface (Ashiru et al. 2009). Since the cellular localisation of gpUL142 has implications for its function, I next sought to investigate surface expression of gpUL142 when expressed in the Ad vector. HF-CARs cells were infected with the RAd-UL142-1A construct (codon optimised, PPT signal peptide, V5 N-terminal tag), RAd-UL142-2A and RAd-control at an MOI 10 PFU/ml for 72 hours after which time, cells were stained with mouse V5 antibody or IgG1 isotype control (figure 5.2). By inserting the tag at the N-terminus of UL142 (downstream of the signal peptide), the tag should present externally rather than intracellularly. While expression could not be detected from RAd-control, the RAd-UL142-2A gave small shift in immunofluorescence compared to the RAd-control due to weak binding of V5 antibody to C terminal V5. When flow cytometry was performed on non-permeabilised cells, expression of gpUL142 was detected from the RAd-UL142-1A construct. This result is consistent with a proportion of gpUL142 being present on the surface of cells infected with RAd-UL142-1A.

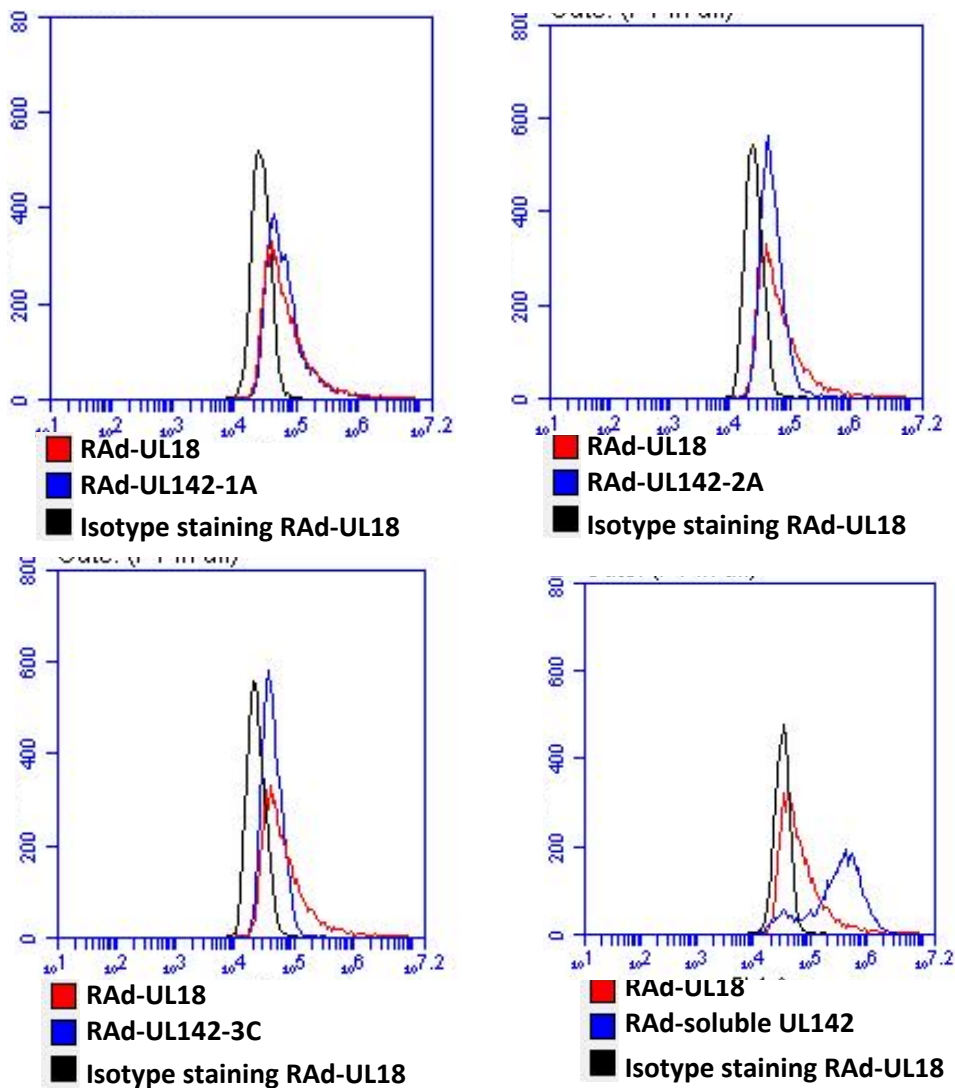


Figure 5.1: Intracellular Expression of UL142. HF-CARs cells were infected with RAD-UL142-1A, RAD-UL142-2A, RAD-UL142-3C, RAD-soluble-UL142 or RAD-UL18 (positive control) at an MOI 10 for 72 hs followed by permeabilization and intracellular staining for V5 using mouse monoclonal V5 antibody and IgG1 antibody was used as isotype control. Analysed by flow cytometry.

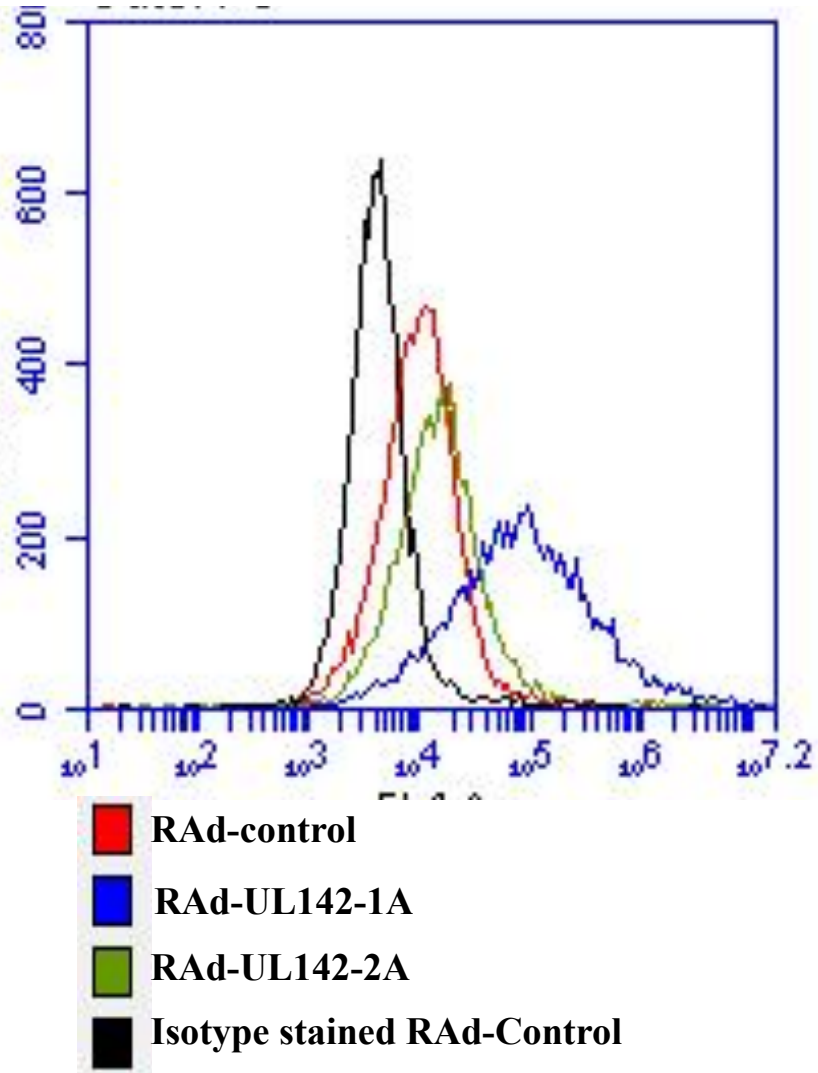


Figure 5.2: Surface Expression of UL142. HF-CARs cells were infected with RAd-UL142-1A, RAd-UL142-2A or RAd-control at an MOI 10 for 72 hs. Non permeabilised cells were stained with mouse monoclonal V5 antibody or IgG1 antibody, and analysed by flow cytometry.

5.3 Western blot Analysis of UL142 expression

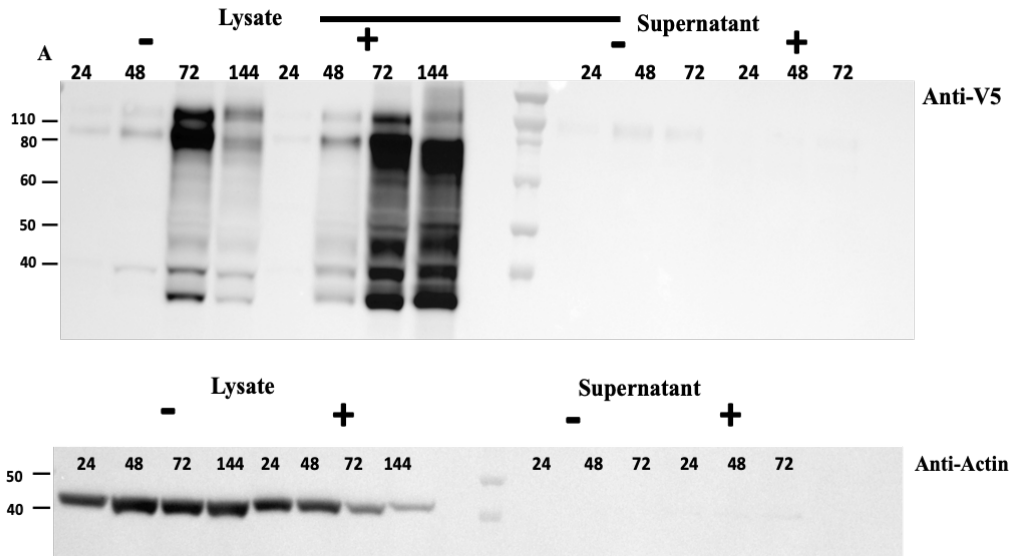
Western blot analysis was performed to further characterise UL142 expression from the Ad recombinants. Codon optimisation increased expression of gpUL142 to a level that could readily be detected by flow cytometry. In the Ad vector expression of UL142 is under the control of the constitutive HCMV major IE promoter. Forskolin is known to stimulate expression from the CMV IE promoter in the context of the Ad vector (Jacobs et al. 1992; Wilkinson and Akrigg 1992) and was thus used here in an attempt to further enhance the expression of gpUL142. Samples were prepared from infected-cell lysates and denatured prior to electrophoresis then analysed by Western blot. Supernatants from infected cells were also assessed for secretion of the “soluble” engineered version of gpUL142 and for release of the membrane-bound version (figure 5.3).

GpUL142 expression was readily detected from all four constructs and generally increased over time except where toxicity was observed in cells late in infection (72-144 h p.i.). Forskolin enhanced the expression of UL142 in the lysates of all constructs, except for RAd-UL142-soluble where expression was unexpectedly lower. Compared to the other recombinant viruses the RAd-soluble UL142 virus engineered to express soluble protein expressed higher levels of intracellular gpUL142 (figure 5.1). The increased intracellular expression of gpUL142 from the RAd-soluble UL142 virus is associated with increased toxicity as reflected by a decreased actin signal in the absence of forskolin which was further increased in the presence of forskolin (figure 5.3 D). High levels of gpUL142 expression appear to be associated with cytotoxicity (figure 5.3 A&D).

GpUL142 has 17 potential N-linked glycosylation sites and the N-linked glycans have been shown to account for approximately half the apparent molecular mass of the ~70-80kDa protein (Wills et al. 2005). GpUL142 expressed by RAd-UL142-1A and RAd-soluble UL142, consisted of multiple species with the heaviest form estimated to be around 105kDa whereas the fastest migrating form (~36kDa) may correspond to the immature ‘naked’ unglycosylated form (Figure 5.3 B & C); the calculated molecular weight for gpUL142 is 34,693 kDa.

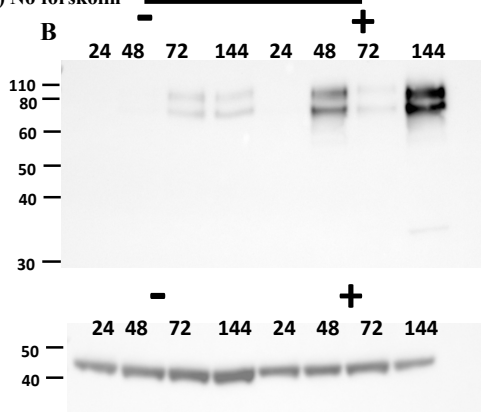
(+)Forskolin
 (-) No forskolin

UL142-1A

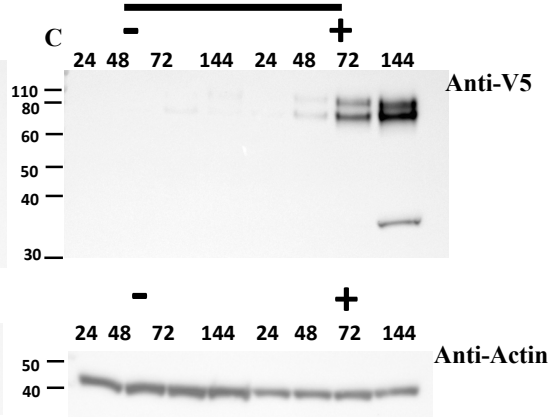


(+)Forskolin
 (-) No forskolin

UL142-2A



UL142-3C



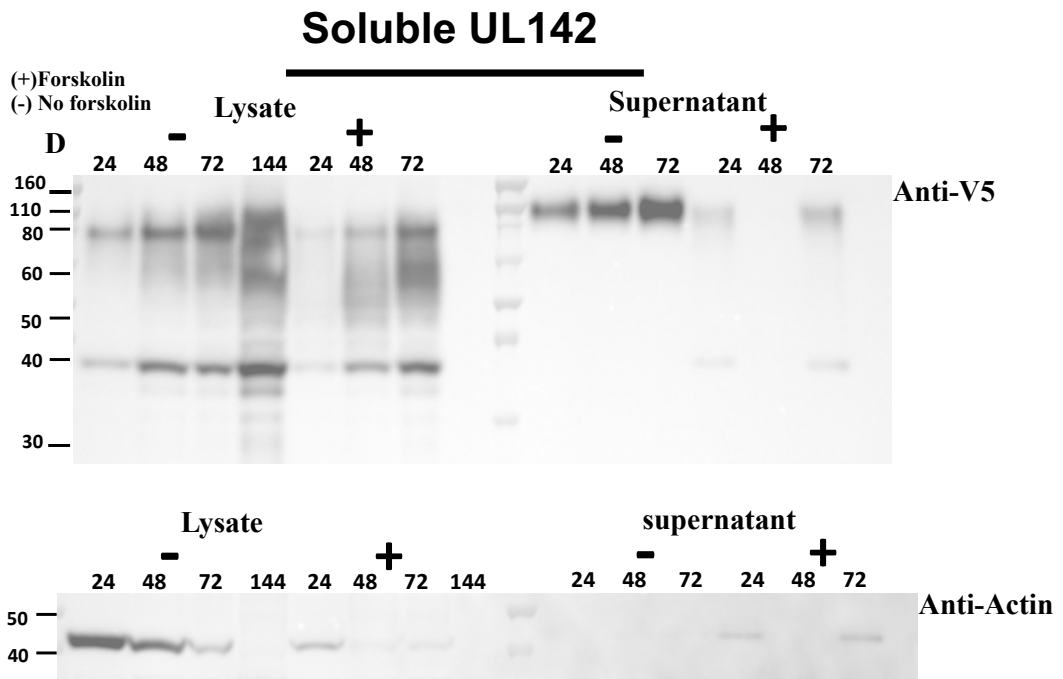


Figure 5.3: Western Blot of expression of UL142 expression from Ad recombinants. (A) HF-CARs cells were infected with RAd-UL142-1A at an MOI 10 for 24, 48, 72 and 144 hours for lysate. To analyse supernatants, the cells in T 25 flasks were washed twice with PBS, 72 hours post infection 2ml of DMEM was added to the flasks (with and without forskolin). Subsequently gpUL142 expression was examined at 24, 48 and 72 hs post wash. 20 μ l of lysate and 30 μ l of supernatant was applied into a 10% NuPAGE Bis-Tris gel, electroblotted to nitrocellulose membranes and probed with mouse monoclonal antiV5 (1:10000) for V5 tagged protein; then anti-mouse IgG HRP was applied. Membranes were washed twice with PBST, stripped and stained with anti-Actin antibody (1:3000(-)). (B) HF-CARs cells were infected with RAd-UL142-2A and cell but not secreted gpUL142 expression was analysed. (C) HF-CARs cells were infected with RAd-UL142-3C and cell extracts were analysed for expression. (D) HF-CARs cells were infected with RAd-Soluble UL142 as described above and UL142 expression in cell extract and supernatants was analysed. In each case, 20 μ l of lysate and 30 μ l of supernatant (where examined) was applied in sample buffer to a 10% NuPAGE Bis-Tris gel, electroblotted to nitrocellulose membranes and probed with mouse monoclonal anti-V5 (1:10000) then the anti-mouse IgG HRP. Subsequently membranes were washed using twice with PBST twice, stripped and stained with actin antibody.

GpUL142 produced in RAd-UL142-2A and RAd-UL142-3C infected cells had a molecular mass of around 105kDa. Higher levels of gpUL142 expression were detected in cells infected with RAd-UL142-1A and RAd-soluble UL142. This difference in expression was consistent (reproducible) as can be observed when the UL142-1A, UL142-2A and UL142-3C were run next to each other in figure 5.4A. The PPT leader peptide was selected because it has been reported to enhance expression of gpUL142, and this result is consistent with the observations of higher expression of the target protein from adenoviral vectors incorporating this leader sequence. It is also possible that anti-V5 antibody may detect N terminal V5 tagged proteins more readily than C-terminal tagged fusion proteins. The lower molecular weight proteins visible on long exposure of RAdUL142-1A and Rad-soluble UL142 suggest limited proteolytic degradation of these samples. An obvious limitation of using a C-terminal epitope tag to track expression is that the tag could be removed by post-translational processing. With RAdUL142-1A the N-terminal tag would escape C-terminal processing. The data is consistent with limited proteolysis of gpUL142 impacting detection of the C-terminal more than N-terminally tagged variants. With RAd-UL142-soluble, the cytosolic and transmembrane domains have been deleted and thus the truncated form of gpUL142 was released directly into the lumen of the ER, and thus this species would not be subjected to the same proteolytic processes.

Generally, forskolin stimulated gpUL142 expression levels, but there were exceptions. Most noticeably forskolin did not enhance expression of secreted gpUL142 from RAd-UL142-1A and RAd-soluble UL142 infected cells (figure 5.3a). It is possible that forskolin treatment may be suppressing the secretion of gpUL142, although this effect was not observed with other constructs (Jacobs et al. 1992). When membranes were stained for actin, the forskolin treated samples had lighter bands compared to non-treated samples. In these cells, the addition of forskolin dramatically reduced the levels of UL142 detectable in the supernatant. UL142 expression was readily detected in the supernatant and cell lysates of cells infected with RAd-soluble UL142 (figure 5.3d).

A high molecular weight UL142 glycoform was detected in the supernatant of RAd UL142-1A infected cells (around 105kDa) (figure 5.3A). Although the strength of

the signal in the supernatant fraction was less than with the cell lysate, it should be borne in mind that only 30µl of total 2ml (0.15%) supernatant was run in comparison with 20µl of 400µl (5%) for the cell lysate. The membrane was stripped and stained with actin as an assessment of cellular contamination. The faint actin bands just detectable in the forskolin-treated sample implied a low-level contamination with cellular proteins, possibly reflecting cytotoxicity. However, only gpUL142 was detected in the supernatant of cells and actin was not detectable in the supernatants of cells with no forskolin treatment. The results thus imply that gpUL142 was released/secreted from the cells. The size of gpUL142 in the cell supernatant match that of the highest band of lysate sample of UL142-1A (figure 5.3A); this result supports that protein is secreted as the molecular weight is comparable with mature glycosylated forms of UL142 expressed in cells. It is possible that gpUL142 could be secreted by exocytosis or a comparable process.

5.4 Glycosylation of secreted and cell-associated forms of gpUL142

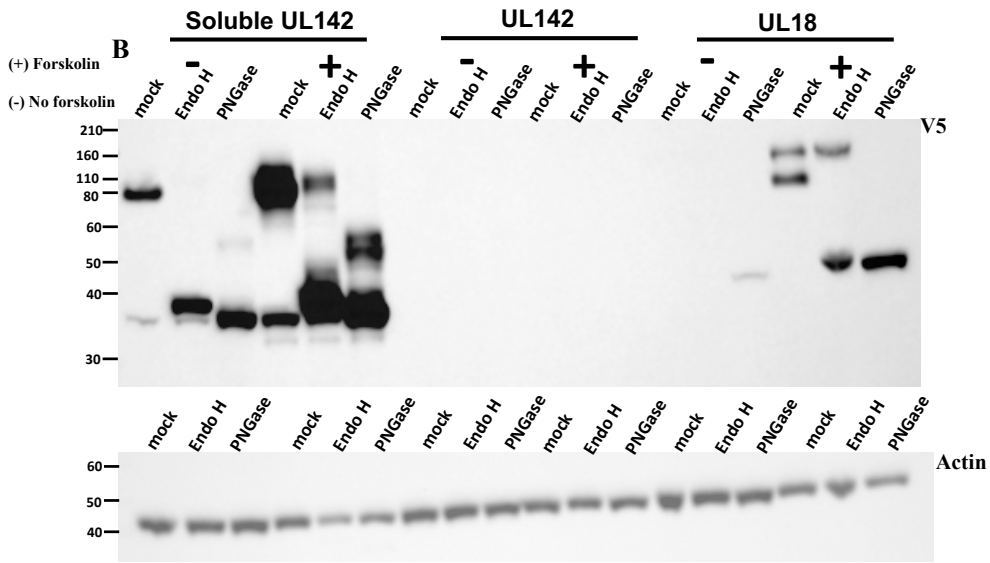
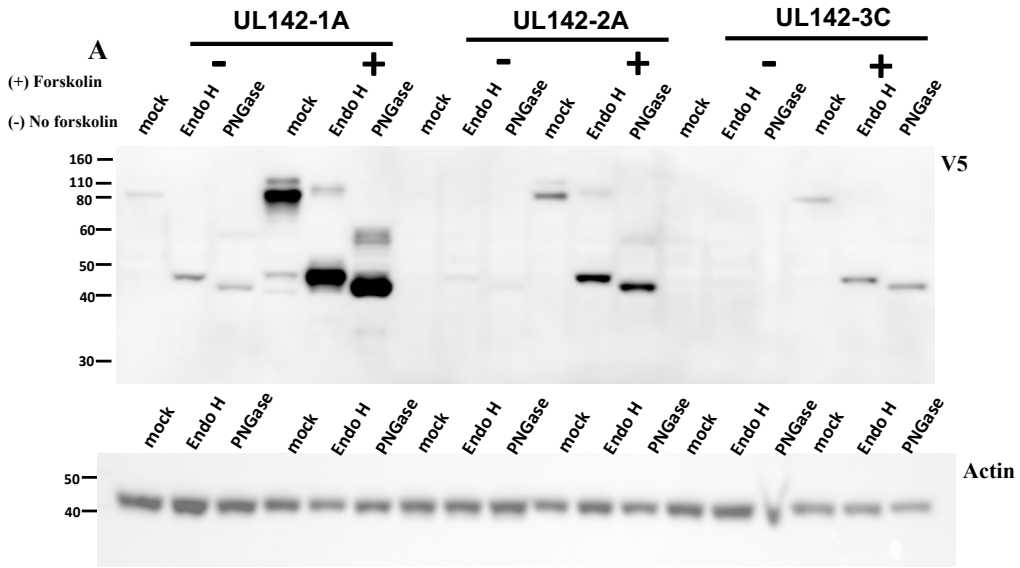
The data presented in figure 5.3 demonstrated that expression tended to be optimal at 72 h p.i and that forskolin was often able to enhance expression. I therefore selected this time point and conditions to investigate the glycosylation status of gpUL142 expressed from the various Ad recombinants detailed in Table 5.1 by EndoH and PNGaseF digestion. Lysates prepared from cells infected for 72 hs with each construct were treated with EndoH or PNGase F and analysed by Western blot, and the V5 tag was used to monitor gpUL142 expression. The absence of any toxicity under the conditions used is indicated by reproducibility of the actin loading control (figure 5.4). GpUL142 was detectable from RAd-UL142-1A infected cells in the absence of forskolin but, in contrast to the previous assay, was greatly enhanced by forskolin treatment (figure 5.4A). RAdUL142-1A infected cells expressed more gpUL142 than UL142-2A and UL142-3C which is in agreement with the previous experiment (Figure 5.3A). Also, RAdUL142-2A infected cells expressed more gpUL142 than UL142-3C, which indicates PPT enhances the expression of gpUL142. When comparing figure 5.3 with figure 5.4, one should bear in mind that the Western blot membranes had different exposure times in the gel imaging system. ‘Mock’ treatment in figure 5.4A refers to the control sample that did not receive

endoglycosidase treatment. A high molecular weight form of gpUL142 of approximately 105 kDa was detected in RAdUL142-1A, RAd UL142-2A and RAd UL142-3C infected cells. Endo H treated samples were detected at 40 kDa and PNGase treated samples were detected at 36 kDa, which is consistent with gpUL142 being highly glycosylated. The fact that the majority of gpUL142 expressed from all three viruses is EndoH sensitive implies that most of the proteins have not been processed by the Golgi apparatus, and thus are likely retained in the ER. However, the low abundance EndoH insensitive glycoforms detectable with RAd UL142-1A and RAd UL142-2A could represent a fraction that is fully processed and potentially presented on the cell surface (Figure 5.4A).

The cell lysate of RAd-soluble UL142 was run with non-codon optimized RAdUL142 and RAdUL18 on the same membrane as presented in figure 5.4B. All of the RAd-soluble UL142 expressed protein in the cell lysate was sensitive to EndoH and PNGase bands (Figure 5.4B). GpUL142 was not detectable in cells infected with the non-codon optimised version of UL142 (RAdUL142), a result consistent with previous findings (Seirafian 2012) and indicates codon optimization improves UL142 expression. RAdUL18 was included as a control to check EndoH and PNGase treatments. GpUL18 is highly glycosylated and is expressed in two glycoforms, one is susceptible to Endo H digestion and the other slower migrating form is resistant; the result was compatible with studies described by Griffin and co-worker (figure 5.4B) (Griffin et al. 2005). Forskolin significantly enhanced expression from RAdUL18. There are parallels between these HCMV MHC-I homologues: both are heavily glycosylated, both are expressed at low levels and although both are expressed at the cell surface, the majority of both proteins appears to be retained in the ER (as gauged by sensitivity to EndoH).

The gpUL142 version engineered to lack a transmembrane domain (RAd-soluble UL142) was Endo-H sensitive when present within the expressing cell, yet the form secreted into the supernatant was EndoH resistant (figure 5.4 C). EndoH appear to be able to trim some the glycans on this heavily glycosylated form but unlike the intracellular precursor, it was largely resistant. This result implies soluble gpUL142 is rapidly secreted once it transits the Golgi apparatus. In this experiment, forskolin stimulated expression of the secreted form of gpUL142.

The supernatant of RAd UL142-1A was tested because this version of gpUL142 has an N terminal V5 that allows the protein to be tracked if it is cleaved above the transmembrane domain and released; as indicated in figure 5.3A. Significant amounts of the N-terminally tagged version of gpUL142 were again detected in the supernatant. Actin could only be detected in samples treated with forskolin, indicating some cell toxicity. In the absence of forskolin actin was not detected, thus implying the low abundance gpUL142 detected in supernatants was not due to contamination by cell lysis. Moreover, the fact that it was completely EndoH resistant also argues against its presence being due to cellular contamination. The PNGase bands in supernatant UL142-1A and Soluble 142 run as two bands (more clearly in forskolin treated samples) ;the upper band at 46 kDa and the lower band at 36 kDa (figure 3.4C and D) may be related to N-glycans forms on unfolded/misfolded proteins which are more susceptible to PNGase than N-glycans on folded proteins (Ninagawa et al. 2015). In all samples from infected cell extracts, the EndoH treated bands were slightly lower than 40kDa indicating a loss of ~60-65 kDa of N-linked carbohydrate, implying that many of the predicted 17 glycosylation sites are functional. The presence of the fully glycosylated (EndoH-resistant) form of gpUL142 in the supernatant of AdUL142-1A-infected cells implies that it can be released from cells independently of any additional HCMV-encoded gene function. GpUL142 thus appears to be both expressed at the cell surface and released/secreted from cells.



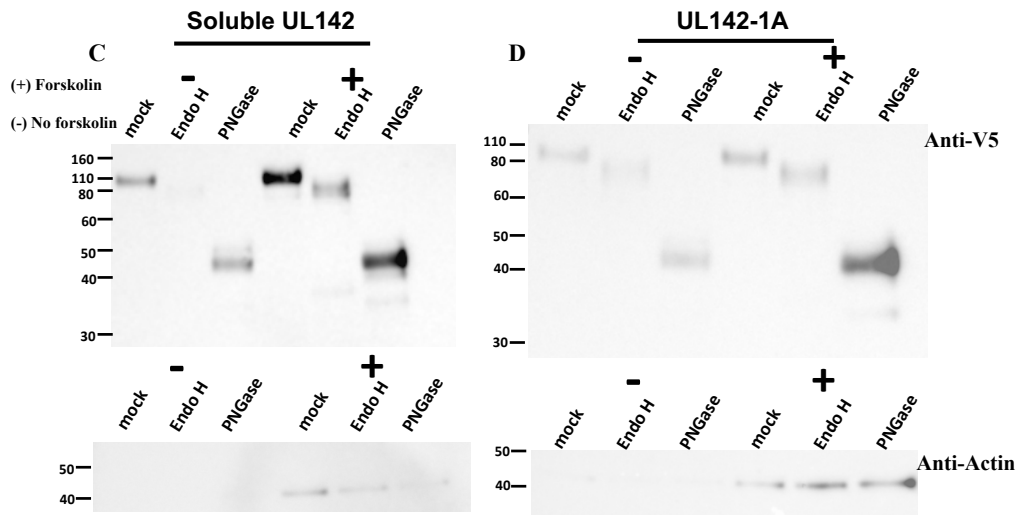


Figure 5.4: UL142 is highly glycosylated. Biochemical analysis of the intracellular localization and glycosylation status of UL142; (A) Samples from HF-CAR cells infected with RAD-UL142-1A, RAD-UL142-2A, RAD-UL142-3C at an MOI 10 PFU/ml for 72 hours were mock treated or treated with Endo H or PNGase F following the manufacturer's protocol, overnight at 37°C. Membranes were immuno-probed with mouse monoclonal anti-V5 (1:10000), subsequently membranes were stripped and treated with anti-Actin antibody (1:3000); (B) Samples from HF-CAR cells infected with RAD-solubleUL142-, RAD-UL142, RAD-UL18 (used as a control) at an MOI of 10 PFU/ml for 72 hours, were mock treated or treated with Endo H or PNGase F following the manufacturer's protocol, overnight at 37°C. Membranes were immuno-probed with mouse monoclonal anti-V5 (1:10000) , subsequently membranes were stripped and treated with anti-Actin (1:3000); (C) HF-CARs cells were infected with RAD-soluble UL142 at an MOI 10 PFU/ml for 72 hours. Cells in a T25 flask were washed twice with PBS then 2ml of DMEM media was added and cells were further incubated for 72, prior to Western blotting analysis. Supernatants were centrifuged twice then either mock treated or treated with Endo H or PNGase F following the manufacturer's protocol, overnight at 37°C before analysis. Membranes were immuno-probed with mouse monoclonal anti-V5 (1:10000) then stripped and treated with anti-Actin (1:3000); (D) HF-CARs cells were infected RAD-UL142-1A at an MOI 10 PFU/ml for 72 hours. Cells in a T25 flask were washed twice with PBS then incubated for a further 72 hours in 2ml DMEM media, prior to Western blotting analysis. Supernatants were centrifuged twice then either mock treated or treated with Endo H or PNGase F following the manufacturer's protocol, overnight at 37°C. Membranes were immuno-probed with mouse monoclonal anti-V5 (1:10000) then membranes were stripped and treated with anti-Actin (1:3000). (-) indicates treatment without forskolin; or (+) indicates treatment with forskolin.

5.5 UL142 and Surface Expression of MICA

I next sought to test whether UL142 expressed from any of the RAd constructs being characterised in this study was able to affect cell surface expression of MICA expression. MICA is a stress ligand and its expression levels in normal fibroblast culture is low even though Ad vector delivery is able to provide some stimulation of NKG2D Ligands (Tomasec et al. 2007). HF-CAR cells were infected with RAd-UL142-1A, RAd-UL142-3C, RAd-soluble UL142 or infected with both RAd-US18 and RAd-US20 together, which have been shown to act synergistically to inhibit MICA expression (positive control). The expression of surface MICA was analysed by flow cytometry (figure 5.5). UL142 expressed from both viruses RAd-UL142-1A and RAd-UL142-3C were able to reduce surface expression of MICA, in contrast, soluble UL142 did not alter surface expression of MICA. Ectopic expression of UL142 was able to downregulate cell surface expression of MICA but required the transmembrane/cytosolic domains of gpUL142.

Table 5.2: The HCMV viruses used in this chapter

| Viruses | Information details |
|----------------|--|
| RCMV1111 | The HCMV strain Merlin genome was cloned into a BAC at passage 5. Derived from the prototype RL13 ⁻ , UL128 ⁻ Merlin BAC described in Stanton et al (2010) |
| RCMV1656 | Deleted US18+US20 derived from MerinBAC1111 Constructed by Dr Ceri Fielding. |
| RCMV1812 | Deletion of UL142 in HCMV, derived from MerinBAC1111 Constructed by Dr Peter Tomasec |

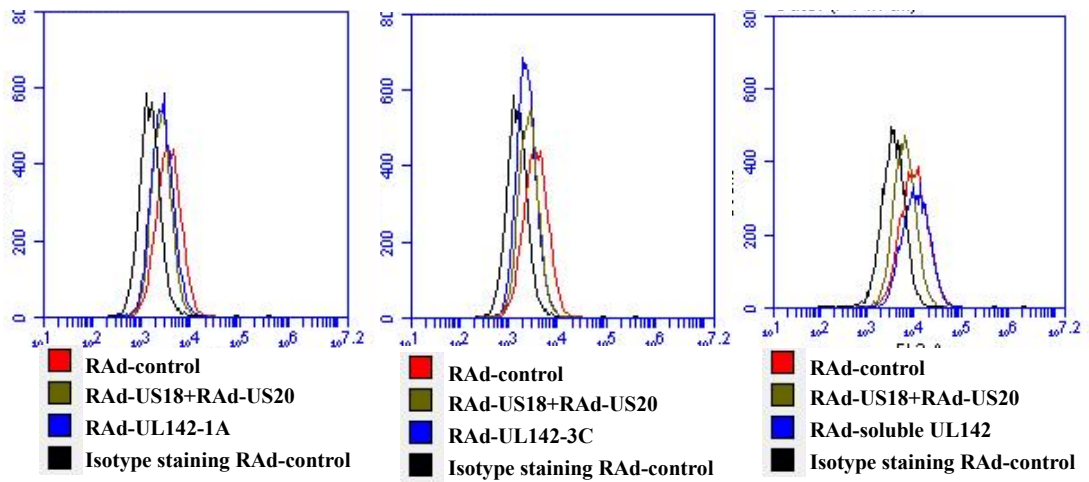


Figure 5.5: Effect of RAD UL142 on cell surface expression of MICA. HF-CARs cells were infected with RAD-UL142-1A, RAD-142-3C, RAD-soluble UL142, RAD1253 (vector control) or with RAD-US20 and RAD-US18 together (positive control) at an MOI 10. 72 p.i, the HF-CARs cells were immune-stained using the MICA-PE or isotype IgG2b-PE antibody.

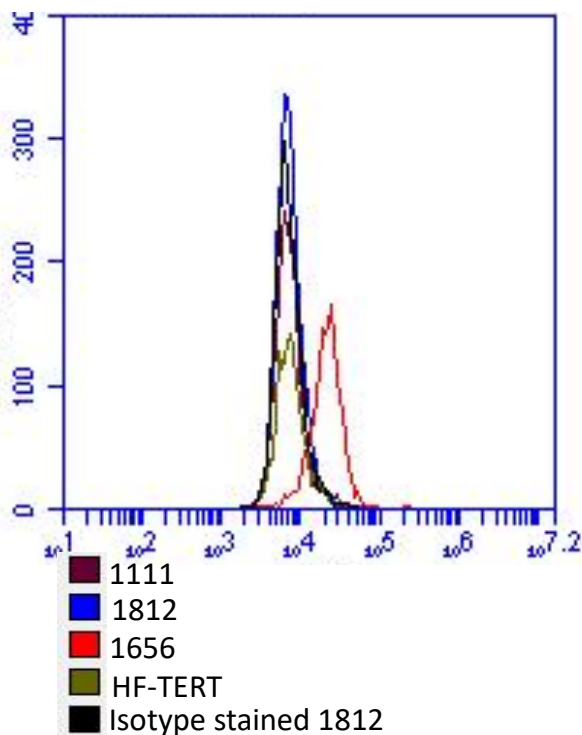


Figure 5.6: Effect of HCMV UL142 on surface expression of MICA. HF-TERTs were either mock infected or infected with Merlin Δ UL142 (RCMV 1812), Merlin Δ US18 Δ US20 (RCMV 1656) or HCMV strain Merlin (HCMV 1111) at an MOI of 10 for 72 h, then stained with MICA-PE or isotype IgG2b-PE antibody.

An advantage of working with HCMV, relative to molluscum contagiosum, is that gene functions can be assessed in the context of an active infection. The impact of a gene responsible for controlling MICA cell surface expression is likely to be more pronounced in the context of a productive HCMV infection where MICA is known to be induced. The effect of UL142 on MICA expression was therefore assessed using the HCMV strain Merlin. For this purpose, HCMV strain Merlin deletion mutant (Merlin Δ UL142; RCMV1812) virus was kindly provided by Dr Peter Tomasec. Since US18 and US20 have been previously shown to downregulate MICA expression, HCMV US18 and US20 double deletion mutant (Merlin Δ US18 Δ US20; HCMV 1656) was obtained from Dr Ceri Fielding for comparison. The ability of these mutant viruses to modulate MICA expression was compared to the parental virus, HCMV strain Merlin (HCMV 1111). Details of all HCMVs used are shown in table 5.2. Cell surface expression of MICA was assayed by flow cytometry in HF-TERTs at 72 hs p.i. (figure 5.6). Infection with the Merlin Δ US18 Δ US20 (RCMV 1656) mutant resulted in substantial upregulation of MICA on the cell surface whereas Merlin Δ UL142 (RCMV 1812) had no effect.

UL142 has been reported to downregulate full length alleles of MICA, but not the truncated MICA*008 allele (Chalupny et al. 2006; Ashiru et al. 2009). In order to test whether UL142 is able to target only full-length alleles of MICA, Chinese hamster ovary cells (CHO) – CAR were infected with adenovirus constructs encoding either truncated MICA*008 or the full-length MICA*002 in combination with the various RAdUL142 constructs described in Table 5.1. CHO-CAR were used for this study because they do not express endogenous MICA that could potentially confound the analysis of the experiment. The levels of MICA*002 and MICA*008 expression achieved by using the Ad vectors was not significantly altered by any of the UL142 variants (figure 5.7). Thus, expression of UL142 does not alter the surface expression levels of the full length (MICA*002) or truncated (MICA*008) alleles of MICA in CHO-CAR cells.

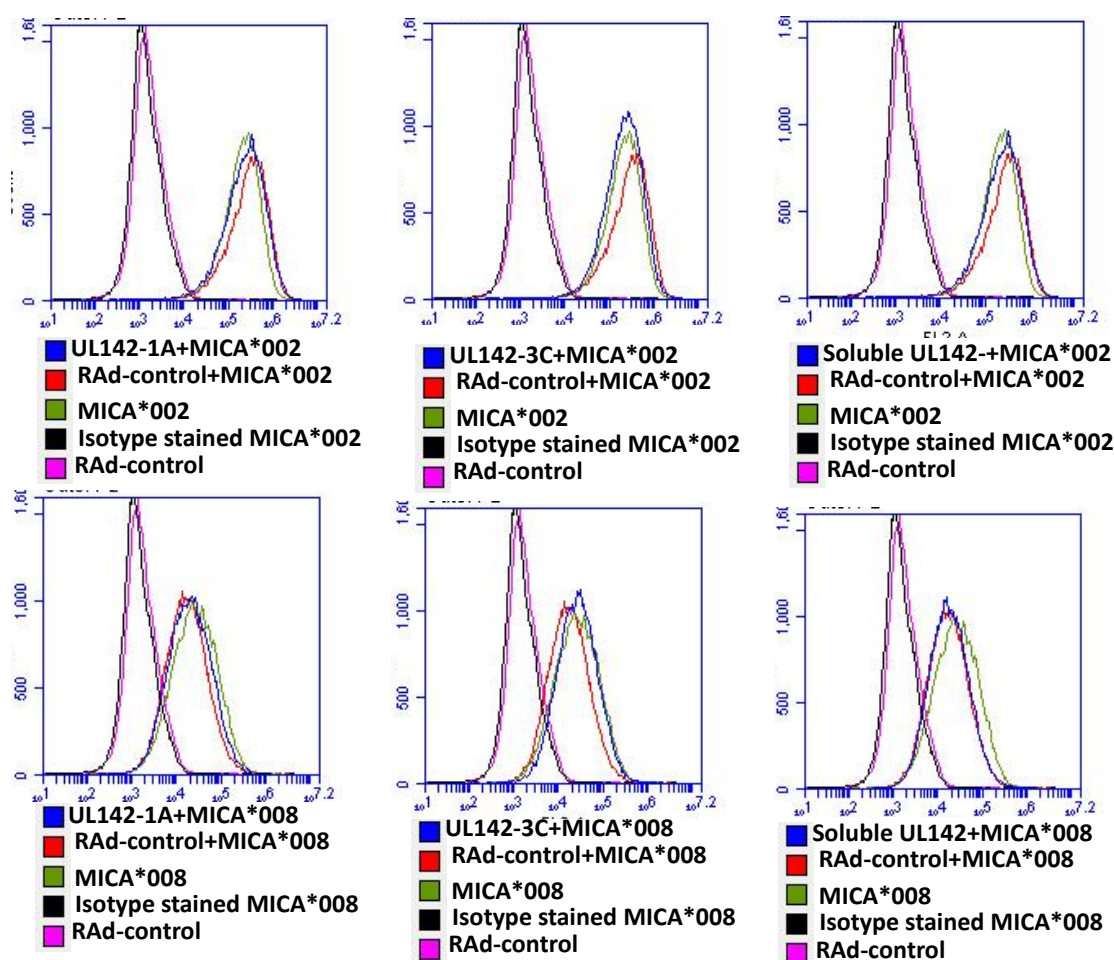


Figure 5.7: UL142 has no effect on surface expression of MICA in CHO cells. CHO cells were co-infected at an MOI 50 with RAd vectors encoding the MICA*002 and truncated MICA*008 genotype or RAd vector alone, or at an MOI 50 of RAd vectors encoding the genotype MICA*002, truncated MICA*008 genotype in combination with an MOI 50 of RAd-UL142-1A, RAd-UL142-2A, RAd-UL142-3C or RAd-soluble UL142 or control RAd vector as indicated. After 72 h, cells were stained with PE-conjugated anti-MICA or an PE conjugated IgG2b isotype control antibody analysed by flow cytometry.

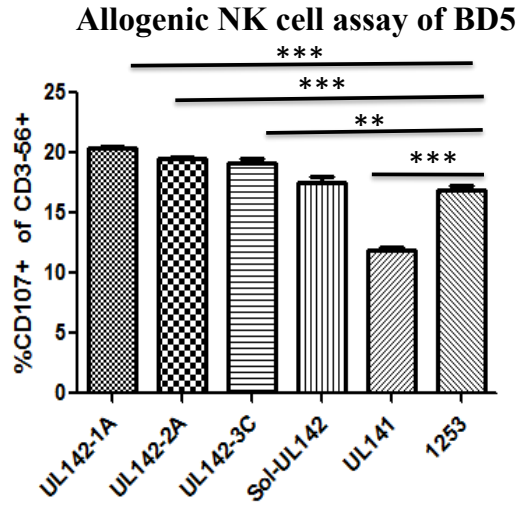
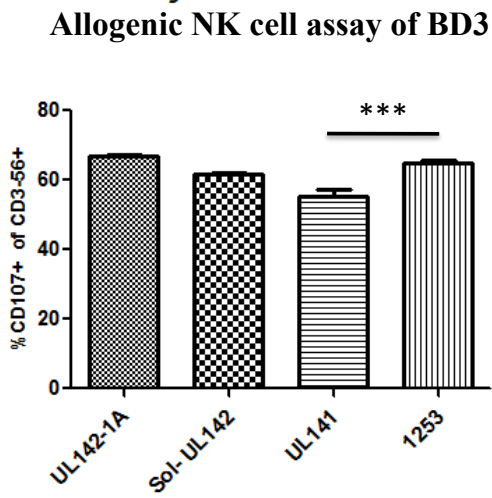
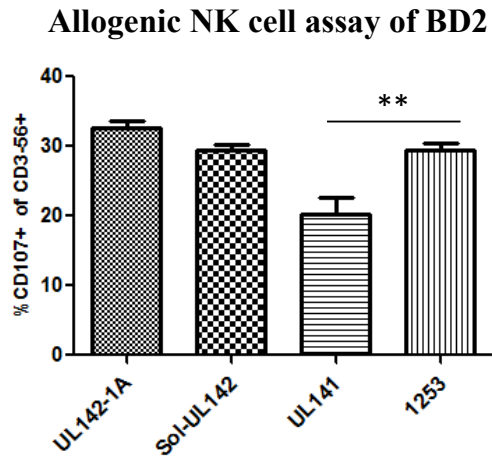
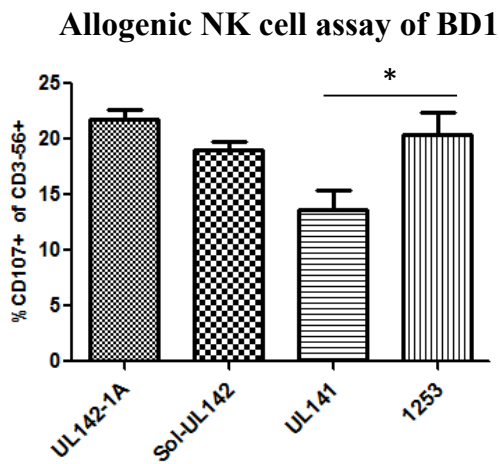
5.6 UL142 downregulates NK cell killing in an allogenic setting using a donor 007 NK line

Ectopic expression of UL142 has been shown to suppress NK cell activation, although interestingly only in a subset of donors (Wills et al. 2005; Prod'homme et al. 2007). In order to assess UL142 function, I sought to test whether I could recapitulate its function as an NK cell evasion molecule. Initial experiments involved harvesting PBMC from blood bags obtained from the Welsh Blood Transfusion service and generating NK cell lines from them. While blood bags provide an abundant source of PBMC, their quality can vary depending on how long they have been stored before being released for research. Functional variability is not only a limitation of blood bags but moreover the option does not exist to revisit donors with interesting responses. PBMCs donated by laboratory volunteers are therefore an invaluable source of fresh blood where the processing of bloods can be completely controlled, the HCMV serostatus has been determined, the responsiveness of NK cells tends to be well characterised from previous assays and the option exists to use matched skin fibroblasts, so experiments can be performed in an autologous setting. However, demand to access the donor pool is high and their availability is limited.

Consequently, the NK lines from blood donor 1 (BD1), blood donor 2 (BD2), blood donor 3 (BD3), and blood donor 005 (BD5) were generated and kindly provided by Dr Simone Forbes and Dr Virginia-Maria Vlachava and donor 007 (D007) was generated and kindly provided by Dr Rebecca Aicheler. HCMV UL141 elicits robust protection against NK cell activation and was therefore included as a positive control (Tomasec et al. 2005; Prod'homme et al. 2010; Smith et al. 2013b). In all assays UL141 was able to inhibit NK cell degranulation significantly (figure 5.8). Since the enhanced expression observed with the codon optimised versions of UL142 has the potential to influence the sensitivity of functional assays, the ability of different UL142 variants (Table 5.1) to modulate the NK cell responses was therefore compared. None of the UL142 constructs tested had an overt effect on NK cell function when cells from BD1, BD2 and BD3 were tested. Unexpectedly, UL142 significantly increased NK cell degranulation in BD5 when expressed from the RAd recombinants UL142-1A, UL142-2A and UL142-3C but not the construct expressing the soluble-UL142 form. This result implies that when expressed on the cell surface

gpUL142 may stimulate an activating signal receptor on BD5 NK cells, or impede signalling to an inhibitory receptor.

The NK cell line from D007 allows the function of UL142 to be assessed in both an autologous and an allogeneic setting. In an allogeneic setting, D007 NK cell degranulation was inhibited when target cells expressed either UL142-2A or soluble-UL142, but not when the cells expressed the UL142-1A and UL142-3C variants (figure 5.8). When assayed in an autologous system using the RAd-UL142-1A and RAd- soluble UL142 constructs stimulated NK cell activation. UL142 clearly had the capacity to modulate NK cell responses in lines derived from two out of the five donors tested. Interestingly, the same NK cell line was capable of being either being inhibited or activated depending on the properties of the target cell.



Allogenic NK assay of D007

Autologous NK assay D007

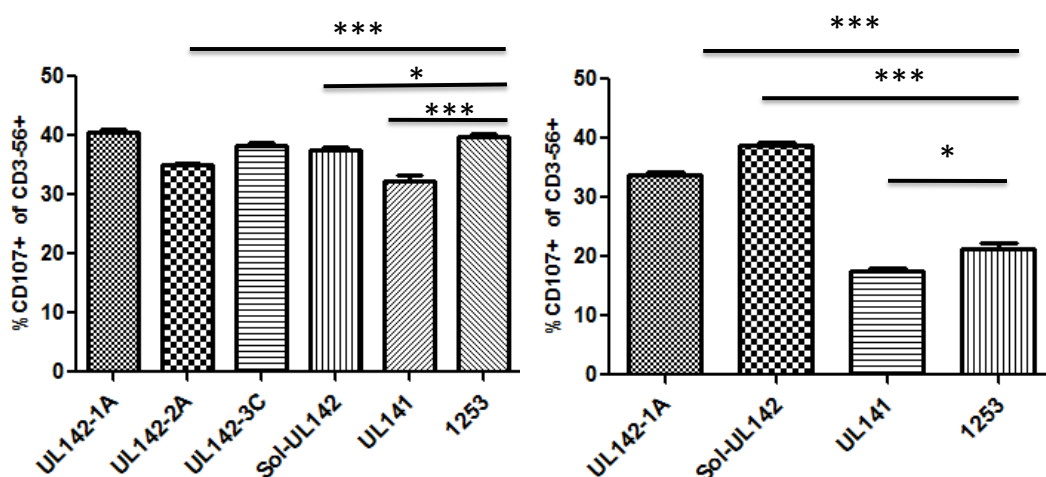


Figure 5.8: Effect of UL142 Expression of NK Cell Degranulation. The effect of UL142 on degranulation of NK cell lines was assessed by measuring the proportion of CD107a+ expression by CD3- and CD56+ NK cells. UL141 is a recognised HCMV NK cell evasion function that was included in the assays as a positive control. HF-CAR cells were infected at an MOI 10 with RAd-UL142-1A, RAd-UL142-2A, RAd-UL142-3C, RAd-soluble UL142, RAd UL141 or RAd 1253 (RAd-control) in allogenic setting for BD1, BD2, BD3, BD5 and D007 for 72h. D007 syngeneic fibroblasts were infected at an MOI of 500 with RAd-UL142-1A, RAd-soluble UL142, RAd UL141 or RAd 1253 (RAd-control) for 72 hs. Infected cells were incubated with D007 BD1, BD2, BD3, or BD5 NK cells 10:1 effector:target cell ratio for 5 h with FITC conjugated CD107a or FITC IgG1 isotype control antibody in the presence of Golgi stop. NK degranulation was assessed by measuring the %CD107a+ of CD3- CD56+ NK cells. The data was analysed statistically using one-way anova and a Dunnett test was used to compare NK cell responses with all the different RAd UL142 constructs and RAd UL141 versus the RAd-control (*P<0.05, **P<0.01, ***P<0.001).

5.7 Summary

The expression of RAd-UL142 was improved by codon optimization of RAd-UL142 constructs, and inclusion of a PPT leader peptide further enhanced expression of UL142. When expressed in isolation the majority of gpUL142 in the cell was detected in a highly glycosylated EndoH sensitive form, consistent with its association with the ER. Nevertheless, gpUL142 could readily be detected on the cell surface. Moreover, a mature Endo-H resistant form is released into the tissue culture supernatant, possibly as a result of proteolytic cleavage. These results indicate that gpUL142 has the potential to act either at the cell surface or remotely. By contrast with previous studies, Merlin UL142 had no effect on MICA expression when expressed by HCMV virus in infected fibroblasts or adenovirus in infected CHO-CAR cells coexpressing MICA. However, in agreement with previous observations, expression of UL142 by adenovirus in HF-CAR cells downregulated MICA expression. This observation may be due to the high levels of expression of gpUL142 by adenovirus in this system. UL142-2A and soluble-UL142 adenoviral constructs inhibited NK cell killing in in allogenic fibroblasts in a donor-specific fashion. However, by contrast, UL142-1A, UL142-2A and UL142-3C adenoviral constructs activated NK cells in autologous fibroblasts in a donor-specific fashion.

6-Discussion

6.1 Optimising expression of mc033L and mc080R using viral vectors

In order to analyse expression of the MOCV genes mc033L and mc080R, I sought to express these genes individually using appropriate mammalian expression vectors. VACV has proved to be a highly efficient virus vector that is able to accommodate extremely large inserts and, following the infection of mammalian cells, provides for the expression of recombinant proteins with appropriate posttranslational modifications (Perkus et al. 1985; Coupar et al. 1988). Being a poxvirus, VACV was a natural vector to attempt the expression of MOCV genes. Adenovirus vectors have been developed and used very extensively as gene delivery vehicles by the research group in Cardiff to analyse gene function (Stanton et al. 2008). Both vector system can readily be propagated to high titres and provide for efficient transgene delivery in both dividing and non-dividing cells. The AdZ vector allowed for direct insertion a transgene into the vector within *E.coli* with no requirement for a transfer vector. The DNA element encoding the transgene is introduced into recombineering bacteria that already carrying a BAC containing the AdZ vector (Stanton et al. 2008).

In preliminary investigations performed prior to the initiation of this study, the natural mc080 ORF was cloned into both the replication-competent VACV Western Reserve (WR) strain by Dr Subuhi Sherwani to produce the recombinant virus v293 (vWR293-mc080) and a replication-deficient Ad vector by Dr Rich Stanton to produce RAd961. Both recombinant viruses grew slowly and to low titres when propagated in vitro and critically, expression of MC080 could not be detected with either construct. Although the toxicity associated with these constructs was initially attributed to (low level) expression of the transgene, the later success with codon optimised versions of the gene makes it more likely that the extreme GC rich codon bias of the MOCV sequence may have been responsible for impeding vector propagation, inducing cytotoxicity and possibly also limited expression of the transgene.

Codon usage adapted versions of the mc033 and mc080 genes were synthesized with a view to optimising translation speed (Sorensen and Pedersen 1991; Tuller et al. 2010). Codon usage adapted version of the MOCV genes were not inserted in to the VACV vector as it was apparent from preliminary studies that the lytic infection

produced by the replication-competent VACV vector was going to complicate studies of transgene expression and function. In order to select a vector that caused minimal perturbation to the target cell in functional assays, the lentiviral donor plasmid pHAGE was also adopted for expression of the MOCV genes and neomycin resistance cassette used to select vector transduced cells. Since there was a major concern over cytotoxicity associated with expression of mc080, conditional expression of the transgene was sought using a tet regulated promoter (tetON). The pHAGE plasmid vector used to express codon-optimised MC033L ORF and MC080R ORF. The expression of MC033/MC080 from the stably transfected plasmids upon addition of the tet inducer was low and only small numbers of cells showed fluorescence in these experiments, indicating low induction efficiency or further toxicity in this system. The lentiviral gene expression system can be limited by the fact that expression tends to be limited to a small proportion of genes and the act of delivery can be cytopathic. The second-generation lentivirus system was used to express the MC033L and MC080R, these experiments were only conducted in preliminary fashion. While the expression of both genes by this approach was modest in immunofluorescence assays, there is clear potential to improve upon these levels, e.g by generating higher titre lentivirus stocks. These lentivirus recombinants could yet prove useful in future studies on the function of the MOCV genes.

Many of the assays available in Cardiff University to investigate the viral immunomodulatory genes were set up to tests functions of genes cloned in to Ad expression vectors. For examples, the HCMV immunomodulatory function of UL18, UL40, UL135, UL141 and UL142 were discovered and/or characterised by using Ad vector systems (Tomasec 2000; Tomasec et al. 2005; Wills et al. 2005; Prod'homme et al. 2007; Stanton et al. 2014). The AdZ vector system is robust, straightforward, and suited to both sporadic and high-throughput applications (Stanton et al. 2008). MC033 and MC080 were expressed highly efficiently from adenovirus constructs, indeed the signals were off the scale when they were first analysed by flow cytometry.

From a combination of immunofluorescence microscopy and western blot studies, MC033 and MC080 proteins were characterised as EndoH-sensitive glycoproteins that mainly co-localised with the ER marker calnexin. MC033 does not contain a

consensus ER localization signals; KDEL or K(X)KXX motifs that are frequently found in the cytoplasmic tail of ER resident proteins (Teasdale and Jackson 1996). The accumulation MC033 in ER may be mediated by a non-canonical ER retention signal, be a property of the transmembrane domain or MC033 may be retained through an interaction with another ER resident protein (Watson and Pessin 2001). My immunolocalization studies also detected the MC080 protein in the Golgi compartment, Senkevich and Moss also found MC080 protein accumulated in the Golgi compartments and ER (Senkevich and Moss 1998).

The fact that MC080 was only detected as an EndoH-sensitive form implies that the vast majority of the protein was retained within the cells. Interestingly, Senkevich and Moss were able to demonstrate that MC080 bound to β_2m in the ER, yet they were unable to detect MCO80R/ β_2m complexes on the cell surface (Senkevich and Moss 1998). The retention of MC080 within the cell argues against it acting as an HLA-I mimic, as is the case for HCMV UL18, which is known to reach the surface where it can interact with the NK cell inhibitory receptor LIR-1. However, it remains possible that MC080 is expressed on the cell surface at levels too low to be readily detected but sufficient to interact with immune cells. Moreover, care has to be taken in the interpretation data using virus genes expressed ectopically. It is possible that MC080 could require co-expression of (an) additional MOCV gene product(s) to reach the cell surface.

6.2 MC080 but not MC033 downregulated MHC I and HLA-E in a TAP independent way

MC080 was first shown to downregulate cell surface expression of HLA-I by flow cytometry when the MOCV gene was expressed in isolation from an Ad vector (Section 4.4). This function of MC080 was further characterised by western blot analysis that revealed that expression of MC080 was responsible for HLA-I remaining in an Endo-H sensitive form, consistent with HLA-I being retained in the ER. The abundance of HLA-I decreased over time in cells expressing either MC080 or HCMV US6 (a specific inhibitor of TAP), in both cases retention in the ER compartment was associated with a shorter half-life for HLA-I. These results thus

identify a novel immune evasion function for MC080 in suppressing MHC-I antigen presentation through its retention in ER.

Experimentally, mc080 acted in a similar fashion to the positive control HCMV US6. Both genes exhibited the capacity to retain the heavy chain of MHC-I in the ER and downregulate cell surface expression of classical MHC-I and HLA-E. HLA-E exhibits limited sequence polymorphism and binds a restricted set of peptides that are normally derived in a TAP-dependent manner from the leader sequences of HLA-I A, B, C and G (see section 1.9). HLA-E maturation is dependent on peptide binding, and results in its expression on the cell surface where HLA-E becomes available to bind the NK cell inhibitory receptor CD94/NKG2A. HLA-E thus inhibits NK cell-mediated cellular cytotoxicity (Tomasec 2000). HLA-A2 tends to bind hydrophobic proteins, and appears to be capable of presenting peptides capable of passive diffusion from the cytosol into the lumen of the ER independently of TAP, or derived directly from hydrophobic leader sequences (Lorente et al. 2011). In my experiments, US6 did not down regulate HLA-A2 in TAP-deficient cell whereas in contrast MC080 did. This result is consistent with US6 inhibiting TAP, and MC080 working by an alternative mechanism. HCMV UL40 is able to donate a peptide that upregulates HLA-E in a TAP-independent manner, and thereby reverses its downregulation by US6 (see section 1.9). MC080 was still able to downregulate HLA-E in TAP-deficient when UL40 was being used to rescue HLA-E expression. These results indicate that MC080 also targets HLA-E in a TAP-independent way.

Two MOCV MHC I homologues were studied in this thesis, MC033 had no obvious impact on the expression of either classical MHC I or HLA-E. It is possible MOCV may encode additional genes capable of acting in concert with MC080 to target MHC I. HCMV has at least four genes that act in concert to downregulate MHC-I (US2, US3, US6, US11) (see section 1.8). The HCMV MHC class I homologue gpUL18 both binds peptide and is presented on the surface while, in contrast, MC080 did not bind peptide and was not detectable on the surface (Senkevich and Moss 1998). MC080 and US6 were similar in that both localize to ER and downregulate MHC I and HLA-E, however MC080 has no apparent effect on TAP. MC080 must presumably use another mechanism to downregulate MHC I. HCMV US2 and US11 also localise to ER where they direct retrograde transport of MHC I to the cytosol after which it is rapidly degraded by proteasomes (Wiertz et al. 1996a; Wiertz et al.

1996b; Jones and Sun 1997) whereas US3 retains MHC I in the ER by binding the chaperon tapasin and inhibiting peptide loading of MHC I (Hegde et al. 2002; Chevalier and Johnson 2003; Noriega and Tortorella 2009). As an MHC-I homologue, it is possible MC080 enters the cellular pathway involved in processing the MHC-I complexes, only to sequester an essential factor. While MOCV is known to downregulate cell surface expression of $\beta 2m$ from the surface of MOCV lesions, it would be interesting now to look directly at cell surface expression of MHC-I in vivo. The downregulation of MHC I is associated with the diminution or abrogation of CTL recognition, and this allows viruses to persist and replicate more easily in the host. Since endogenous MHC-I and HLA-E are the chief ligands for NK cell inhibitory receptors, cells that downregulate these molecules tend to become targets for NK cells (Tortorella et al. 2000). Whilst the downregulation of MHC-I by HCMV may leave infected cells vulnerable to NK cell attack (see section 1.9) the virus compensates to some extent by UL40 rescuing HLA-E expression and gpUL18 acting as an MHC-I mimic by binding the NK cells inhibitory receptor LIR-1⁺ (Prod'homme et al. 2012). Since MOCV MC080 also suppresses cells surface expression of MHC-I, it is likely that MOCV may need to encode additional functions to help evade NK cells.

6.3 MC080 modulates NK cell activation

NK cell function is regulated by a fine balance of signals received by activating and inhibitory receptors. Interactions between endogenous HLA-I molecules and NK cell inhibitory receptors normally dominate over signals received from activating receptors. NK cell inhibitory receptors that recognise endogenous classical HLA-I molecules act to suppress killing by NK cells (Yokoyama et al. 2010). A proportion of human NK cells express a surface C-type lectin receptor, CD94/NKG2A, which delivers an inhibitory signal to NK cells (Braud et al. 1997). MC080 downregulates MHC I and HLA-E, and thus one would expect MC080 to render cells more vulnerable to NK cell attack. In this thesis, NK cell function was tested in autologous and allogenic assays using a CD107a degranulation assays and PBMCs obtained from local volunteer donors and blood transfusion service. NK lines were also established from D007 and the blood donor BD5; assays with the latter being restricted to an allogeneic setting. The NK assays unexpectedly gave different results

depending on whether they were performed in an autologous and allogenic setting for D007, D008 and D009. NK cell activation was variously associated with inhibition (in allogenic setting of D007, BD5 and autologous setting of D009), activation (in autologous setting of D008 and D007) or no effect (in allogenic setting of D008 and D009). The assays performed in an allogenic setting all used the same standard human foetal foreskin fibroblasts (HF-CAR) as targets, whereas the autologous assays were performed on skin fibroblasts taken from the donors by biopsy.

The effect of MC080 on MICA was discussed as the possible explanation to its NK cell effect. However, when investigated directly by ectopic expression in CHO-CAR cells, MC080 had no substantial effect on the expression of either a full-length MICA*002 allele or the truncated MICA*008 allele. While the downregulation of HLA-I would normally be expected to promote NK cell activation, NK inhibitory receptors are commonly paired with an activation receptor that recognises the same target, albeit with a different affinity. While HLA-E binds the inhibitory receptor CD94/NKG2A with high affinity, it can also bind the paired activating receptor CD94/NKG2C with low affinity. Although CD94/NKG2C is normally expressed on only a small subset of NK cell, during HCMV infection CD94/NKG2C⁺ cells expand in what can be considered akin to an adaptive response associated with memory. Likewise, NK cells are capable of expressing both inhibitory and activating KIRs capable of recognising endogenous HLA-I molecules. KIR genes are highly polymorphic, an important variation with respect to the activating KIR genes and humans may inherit multiple variants (Maxwell et al. 2004; Ahlenstiel et al. 2008). HF-CAR and autologous HSF each have individual HLA repertoires that react differently with the various KIRs expressed in NK cells. The downregulation of endogenous HLA molecules by MC080 may potentially either inhibit or activate NK cells depending on the KIR and HLA repertoires on the NK cell and HF respectively. Thus, it is possible that the downregulation of MHC-I by MC080 could result in NK cell inhibition when the NK cell functional assay is dominated by activating KIRs. However, it also possible that mc080 may yet have an additional effect on NK cells that is independent on MHC-I ligand recognition.

6.4 MC080 expression impair CD 8⁺ T cells activation

Cytotoxic CD8⁺ T lymphocytes recognise cells presenting viral peptides bound to surface MHC class I molecules. MC080 downregulated MHC-I rendering the number of cell surface, peptide loaded MHC class I molecules required for CTL recognition is very low. T cell epitopes have not been defined for MOCV. The functional effect of MC080 on CTL recognition were therefore investigated by using HLA-A2–restricted CD8⁺ CTL lines generated to HCMV-IE1 VLEETSMVL (VLE) and HCMV-pp65 NLVPMVATV (NLV) peptides using a range of peptide concentration. MC080 was able to protect against T-cell degranulation at a range of peptide concentrations, and with comparable efficacy to HCMV gpUS6 (Ahn et al. 1997). Interestingly, CD8⁺ T cells activation was impaired more when the cells were coated with lower peptide concentrations of VLE and pp65. The downregulation of MHC class I by MC080 provides MOCV with a mechanism for evading T-cells degranulation. MC080 interferes with the MHC class I antigen presentation pathway to prevent the presentation of processed viral peptides to CD8⁺ T cells. The MC080 protein is expressed early in MOCV infection (Senkevich et al. 1997) and it may be one of MOCV genes which are responsible for absence T cell at the site of MOCV infection (Viac and Chardonnet 1990). MC033 has no effect in MHC-I and HLA-E and did not have a significant effect on NK cell and T cell activity in this study. The Blast and Phyre of MC033 resulted with MHC-I homology. However, the homology was restricted to a very short region of the protein with an Ig-like fold. Phyre did not model MC033 on to MHC-I (data presented in the appendix). In view of the restricted extremely restricted nature of the homology detected, it may not be helpful to classify mc033 as an MHC-I homologue, indeed it may direct experimental enquiries away from its true function.

6.5 Optimizing expression of UL142

The non-codon optimized UL142 ORF with a V5 tag was cloned into the AdZ vector (RAd-UL142) as part of a project that generated an expression library of all canonical HCMV genes. However, using this construct gpUL142 expression could not be detected by immunofluorescence and only weakly by western blot (Seirafian 2012). Since UL142 expression was enhanced by substituting a preprotrypsin (PPT) signal

peptide for the normal leader peptide (Ashiru et al. 2009), Dr Rebecca Aicheler designed three codon-optimized UL142 constructs in AdZ vector with the purpose of improving expression (Table 5.1). I found that codon optimisation improved gpUL142 expression dramatically and PPT had mild increase on expression of gpUL142. The N-terminal signal peptide is a key factor in determining the efficiency of ER translocation from ribosome to ER membrane. Several studies have demonstrated that recombinant proteins can be produced with a high yield by replacing signal peptides (Olczak and Olczak 2006; Celinska et al. 2018). I also found that N terminal V5-tagged version of UL142 was much more readily detected than a comparable construct with a C terminal V5-tag. This is in agreement with a study carried by Park et al who observed that the C-terminal tag was associated with uneven expression of recombinant proteins and the N terminal tagged protein associated with over-expression of recombinant proteins (Park et al. 2015). To help investigate the function of UL142, Dr Sepehr Seirafian also produced a secreted form of UL142 by deleting transmembrane and cytoplasmic domains; this secreted version of gpUL142 was also expressed more efficiently.

In the AdZ vector system, the expression of UL142 was under the control of the constitutive HCMV major IE promoter. Forskolin is known to stimulate expression from the CMV IE promoter through its action on the multiple cAMP responsive elements in the enhancer in the context of the Ad vector (Jacobs et al. 1992; Wilkinson and Akrigg 1992) and was thus used here in an attempt to further enhance expression of gpUL142. By using time course to choose the best time point for gpUL142 expression (72h), expression was readily detected from all four constructs and generally increased over time except where cytotoxicity was observed in cells late in infection. Forskolin enhanced the expression of gpUL142 for all four constructs. However, in RAd-UL142-soluble supernatant samples the expressions were unexpectedly low, and is thought to relate to cytotoxicity induced by overexpression with time; in this experiment expression was measured after 96 h, 120 h and 144 h p.i. Cytotoxicity was reflected in reduced actin staining that was more extreme when forskolin was added to enhance soluble gpUL142 expression.

6.6 GpUL142 is expressed on the cell surface and may be released/secreted from the cells

Endoglycosidase H is a recombinant glycosidase which cleaves the chitobiose core of high mannose and some hybrid oligosaccharides from N-linked glycoproteins, a conversion that occurs in the medial Golgi region. When proteins are correctly processed through the endoplasmic reticulum (ER) and Golgi apparatus, they become resistant to EndoH, and sensitivity to EndoH indicates the presence of proteins that have not yet been processed beyond the ER.

GpUL142 is predicted to contain 17 glycosylation sites and has been shown experimentally to be highly glycosylated (Wills et al. 2005). Consistent with this observation, the apparent molecular mass of gpUL142 decreased by around 65kDa when treated with Endo-H (see section 5.4). The fact that the majority of all three forms of gpUL142 expressed by using Ad recombinants was EndoH-sensitive implies that most of the protein has not been processed by the Golgi apparatus, and thus are likely retained in the ER. This result is in agreement with Ashiru and co-workers report that gpUL142 is predominantly localised to the ER and Golgi apparatus along with MICA, yet a small amount of protein did reach the cell surface (Ashiru et al. 2009). However, the low abundance Endo-H resistance glycoforms detected with RAd UL142-1A and RAd UL142-2A could represent the fraction expressed on the cell surface. The soluble UL142 glycoprotein was Endo-H sensitive when expressed in the cell yet Endo-H resistant when supernatant samples were tested, which implies that 'soluble UL142' is rapidly secreted once it transits the Golgi apparatus.

Significant amounts of the N-terminally tagged version of gpUL142 were unexpectedly detected in the supernatant, and this result was consolidated when the samples were tested for glycosylation. The samples were analysed to determine whether gpUL142 is released due to spontaneous lysis of cells infected with AdUL142 recombinants. The cellular protein actin was only detectable in cells exhibiting significant cytotoxicity associated with treatment with certain preparations of forskolin. However, actin was not detectable in supernatant in the absence of forskolin, thus the low abundance gpUL142 detected in the absence of forskolin was therefore not likely to be caused by contamination associated with cell lysis.

Crucially, gpUL142 detected in the supernatant with the UL142-1A construct was completely Endo-H resistant. Thus, the secreted gpUL142-1A must have trafficked through Golgi compartments and is distinct from the predominant form associated with AdUL142-1A infected cells, which is EndoH sensitive. Even in the absence of any other HCMV gene product, a significant proportion of gpUL142 may be released from cells expressing the protein. Accordingly, gpUL142 may potentially be a secreted protein that modulates the immune response by affecting near and distant immune cells.

6.7 UL142 has no effect on MICA

HCMV IE1 upregulates NKG2DL ULBP2, and IE2 which upregulates MICA ligands. (Eagle et al. 2006; Venkataraman et al. 2007; Tavalai and Stamminger 2011) NKG2Ls are regarded as stress ligands so their expression tends to be extremely low, or absent, in cells cultured in vitro. It is thus really only following cell activation during productive infection that it is possible to fully evaluate viral evasion function that target NKG2DLs. While the impact of the US12 family on MICA had been examined in the context of HCMV lytic infection, the effect of UL142 on MICA has only been studied in ectopic expression.

Ashiru et al found that gpUL142 expressed using adenovirus vector was able to downregulate cell surface expression of full-length MICA variants to retain them in the ER and the cis-Golgi apparatus, yet UL142 had no effect on the truncated form MICA*008. UL142 luminal and transmembrane domains promote the recognition and intracellular sequestration of full-length MICA alleles (Chalupny et al. 2006; Ashiru et al. 2009). However, the HCMV laboratory strain AD169 lacks the *U_L/b'* region that contains the UL142 gene. Strain AD169 was reported to downregulate cell surface expression of full-length MICA alleles, but not MICA*008 (Zou et al. 2005). More recently, the US12 gene family was found to be primarily responsible for downregulating full-length MICA in productive infection (Fielding et al. 2014). The expression level of MICA ligands in normal fibroblast culture is low even though Ad vector delivery is able to provide some stimulation of NKG2DLs (Tomasec et al. 2007). In my results, all forms of gpUL142 expressed in context of adenovirus vector downregulates full length MICA, except for the soluble UL142 which had no effect

on either truncated or full-length MICA alleles. Thus, ectopic expression of UL142 was able to downregulate cell surface expression of full-length MICA, but the transmembrane/cytosolic domains of gpUL142 were required for this function. Unlike the situation in MOCV, with HCMV it is possible to investigate gene function in the context of a productive infection. The application of defined HCMV deletion mutants has supported the function of individual genes NK evasion functions, UL40 in the control of HLA-E, the control of MICB, ULBP1 and ULBP2 by UL16's, the interaction of gpUL18 with LIR1 plus MICA and B7H6 downregulation by the US12 family members US18 and US20 (Wang et al. 2002; Rolle et al. 2003; Fielding et al. 2014; Fielding et al. 2017). When I investigated the regulation of MICA in the context of productive HCMV infection, deletion of US18 and US20 associated with significant increase in MICA cell surface expression relative to HCMV-infected cells whilst deletion of UL142 has no overt affect. This indicates that the control of MICA expression during productive infection is primarily the responsibility of the US12 gene family and not UL142. Moreover, gpUL142 was unable to control the expression of either MICA*008 or MICA*002 when the genes were expressed in CHO-CAR cells; CHO cells lack an endogenous MICA homologue. UL142 is clearly capable of modulating the NK cells response. However, the data from the experiments performed in this thesis suggest that the primary mechanism of action of UL142 in productive HCMV may not be to target MICA, a result that is consistent with the US12 gene family (particularly US18 and US20) playing the predominant role in downregulation of full-length MICA (Fielding et al. 2014; Fielding et al. 2017).

6.8 UL142 modulate NK cell killing

The results obtained from these preliminary NK cells assays are intriguing. By using Ad vectors to deliver UL142, its function is being observed in the absence of any other HCMV immune evasion function, the absence of a virus induced stress response and also in an environment where gpUL142 over expression can be expected to down regulate MICA (see figure 5.5). HF-CARs express the full-length MIC-A*016 MICA*027 alleles (see table 2.3) so the downregulation of NK cell activation associated with the UL142-2A construct (see figure 5.8) could in this case be due to MICA sequestration within the cell. However, the secreted version of

gpUL142 over produced by RAd-soluble UL142 was not capable of suppressing cell surface MICA expression (see figure 5.5). Thus, it is likely that in this model that cell associated gpUL142 may be acting primarily via its effect on MICA but not the secreted form. Nevertheless, the secreted gpUL142 could theoretically possibly bind to MICA on the surface of target cells and thereby block its interaction with NKG2D (Chalupny et al. 2006; Ashiru et al. 2009).

D007, in contrast, are homozygous for the truncated MICA*008 allele (see table 2.3), so the strong NK cell functional effects of UL142 observed in the autologous setting are likely to be independent of any potential interaction between gpUL142 and MICA. An alternative explanation that is independent of MICA is therefore needed. A substantial proportion of NK cell receptors can be considered to be paired, where both an activating and an inhibitory receptor are capable of recognising the same ligand. As described in the introduction, HLA-E can be recognised by both the NK cell inhibitory receptor CD94:NKG2A and the NK cell activating receptor CD94:NKG2C. Over time in HCMV infected individuals a change in the NK cell repertoire is commonly observed due to an expansion in CD94:NKG2C⁺ NK cells and a compensatory decrease in CD94:NKG2A⁺ cells (Braud et al. 1997; Wilkinson et al. 2008). This effect extends to additional NK cell markers. Thus, there are expansion in HCMV carriers of unusual NK cell subsets, possibly to counter or circumvent HCMV immune evasion functions. Endogenous HLA-I molecules are the chief ligands for NK cell inhibitory receptors yet are downregulated by HCMV during productive infection. Many of the NK cell expansions seen in HCMV infection express multiple activating receptors balanced by expression of an inhibitory KIRs specific for self HLA molecules (see section 1.9). Downregulating endogenous HLA-I thus potentially comes at a cost. Donor D007 is known to be HCMV seropositive and to possess strong cellular immune response to HCMV. It would be interesting to evaluate the NK cell repertoire of D007 for evidence of specific NK cell expansions. HCMV UL18 is an HLA-I homologue that is known to bind LIR1. Since HCMV UL142 is also an HLA-I homologue expressed on the cell surface (see section 1.10), it is a strong candidate to bind an NK cell inhibitory receptor, possibly one or more KIR.

Whilst the NK cell functional data presented is too preliminary to define a mechanism, it may be useful as a basis for constructing a model to test

experimentally. Potentially gpUL142 expressed on the surface of infect cells may bind an NK inhibitory receptor at the immunological synapse (IS) to promote a negative signal and thereby suppress NK cell recognition. I show in this thesis that a significant proportion of gpUL142 appears to be cleaved and released from the cell surface. In the case of soluble gpUL142, the protein is only expressed in a secreted form. Overexpression of secreted form of gpUL142 could result in it binding an inhibitory receptor on NK cells outside the IS without inducing an inhibitory signal, i.e gpUL142 blocks its function as an inhibitory receptor and renders NK cells more susceptible to activation. In the context of a productive infection the secreted form of gpUL142 may serve to impair the capacity of NK cell to discriminate normal cells (including self), and this could be manifest by the enhanced killing of uninfected target cells, as observed in figure 5.8. The situation becomes more complex if gpUL142 is also recognised by a paired NK activating receptor (see section 1.8). It would clearly aid our understanding of HCMV pathogenesis to characterise the mechanism of action of UL142. If gpUL142 is specifically binding to an NK cell inhibitory receptor it should be possible to interrogate the mechanism in NK cell functional assays using characterised donors (e.g. D007). The KIR genotype of D007 is currently being determined to facilitate this process. It should be possible to determine whether specific NK cell inhibitory receptors correlate with reduced NK cell activation, an approach first applied to dissect the mechanism of action of UL18 (Prod'homme et al, 2007). Alternatively, the soluble form of gpUL142 was constructed with a BirA tag to enable the production of gpUL142 tetramers. I have shown that the codon optimised (soluble) form of gpUL142 is secreted in abundance and impacts NK cell function when expressed from the Ad recombinant. It should therefore now be possible to produce gpUL142 tetramers that can be used to sort NK cells expressing the receptor that recognises gpUL142. Immunophenotyping and/or proteomic analysis of this cell population may help define the mechanism of action of UL142.

6.9 The limitations and future plans of this thesis

As highlighted above, this study outlines several important new observations around the immune-evasion functions of HCMV/MOCV which are: For first time, it was

observed that MC080 is effective in suppressing NK cell activation in certain individuals, also, MC080 down regulates surface expression of MHC-I and HLA-E in a TAP independent way. Furthermore, MC080 has the ability to protect against degranulation by CD8⁺ T cells. In agreement with previous studies gpUL142 could readily be detected on the cell surface when Adenovirus expressing UL142 was used. However, for first time, I found the mature Endo-H resistant form is released into the tissue culture supernatant, possibly as a result of proteolytic cleavage. These results indicate that gpUL142 has the potential to act either at the cell surface or remotely. By contrast with previous studies, Merlin UL142 had no effect on MICA expression when expressed by HCMV. However, it is important to recognise and reflect upon some limitations of my thesis which might be addressed in future studies which are outlined below:

- 1 The MOI 1 that was used to infect HeLa cells with RAd961 and vaccinia virus v293 expressing MC080 was lower than would have been ideal (section 3.2). This was because the observations using a light microscope indicated that significant levels of cellular toxicity were associated with high MOI infection. We attempted to overcome this by designing coding optimized mc080 in subsequent experiments.
- 2 In chapter 3, we performed transfection of HeLa cells with pHAGE plasmids. However, these studies were lacking a suitable negative control. Future studies will therefore need to repeat these experiments with all appropriate controls.
- 3 In this study I generated second-generation lentiviruses expressing codon optimised mc033 and mc080. Future studies would optimise the expression of mc033 and mc080 from these vectors. Expression from the lentiviral vectors would then be used to confirm the results obtained using the adenoviral expression system.
- 4 Ideally, we would have performed additional biological replicates of the CD107a NK cell degranulation assays (section 4.3 and section 5.6). However, these were only performed to a limited *n* value since the assays require volunteer donors for blood which proved difficult to access. Future studies would therefore focus on increasing *n* values in these important studies to increase confidence in the findings presented.
- 5 Future studies may also seek to use NPi cells expressing human Coxsackie adenovirus receptor (hCAR) (section 4.5). Npi cells were used to determine whether MC080 is able to hinder peptide loading by interfering with TAP, and therefore reducing MHC-I and HLA-E surface expression (in section 4.5). In these experiments an MOI of 350 was used to infect NPi cells with either two or three adenoviruses (meaning for x3 adenoviral vectors, and overall MOI of 1050 was

used). This was necessary since the cells do not express the native Ad receptor, CAR, and therefore, to efficiently infect these cells, a very high MOI was required. In a study was performed by Tomasec et al, the NPi cell line was infected with a Rad expressing HLA-A2 using an MOI 50. In this study approximately 85% of cells were positive for HLA-A2 after infection with this virus. In my thesis an MOI 350 was used, this is seven times higher than that used in the study by Tomasec et al. Although not confirmed, in my assays this would suggest that approximately 100% of NPi cells were infected in the experiments using these cells in this thesis (section 4.5) (Tomasec et al. 2000). Also, Dr Rebecca Aicheler (nee Morris) found in her PhD thesis that increasing the MOI over 300 does not significantly increase the percentage of GFP positive cells when she infected a human skin fibroblast cell line, which does not express hCAR, with RAd-GFP (Morris 2005). Future studies may require an engineered NPi cell line that expresses the hCAR to facilitate adenovirus infection, and reduce the amount of virus required to efficiently transduce these cells, and limit potential toxicities associated with these techniques.

- 6 Future studies may also focus on the development of an N terminal V5 tagged mc080 to examine if MC080 is expressed on the surface of infected cells, as well as the C terminal V5 tag mc080 described here. I would have examined the possible expression of MC080 on the surface of infected cells using N terminal V5 tagged mc080.
- 7 Future studies may also seek to construct a HCMV Merlin viral genome deleted in UL142, US18 and US20. This triple deleted virus would allow a comparison with HCMV Merlin deleted UL142 virus and HCMV Merlin deleted US18 and US20 virus in MICA expression assay (section 5.5). you need to say why you want to do this.
- 8 Finally, the codon optimised (soluble) form of gpUL142 is secreted in abundance from the cells and it impacts NK cell function when expressed from the Ad recombinant (section 5.6). Future studies may utilise gpUL142 tetramers to identify and isolate NK cells expressing the receptor that recognises gpUL142. Immunophenotyping and proteomic analysis of this cell population may help define the mechanism of action of UL142.

7-References

Abele, R. and Tampe, R. 1999. Function of the transport complex TAP in cellular immune recognition. *Biochimica et Biophysica Acta* 1461(2), pp. 405-419.

Agromayor, M. et al. 2002. Molecular epidemiology of molluscum contagiosum virus and analysis of the host-serum antibody response in Spanish HIV-negative patients. *Journal of Medical Virology* 66(2), pp. 151-158.

Ahlenstiel, G. et al. 2008. Distinct KIR/HLA compound genotypes affect the kinetics of human antiviral natural killer cell responses. *Journal of Clinical Investigation* 118(3), pp. 1017-1026. doi: <https://dx.doi.org/10.1172/JCI32400>

Ahn, K. et al. 1996. Human cytomegalovirus inhibits antigen presentation by a sequential multistep process. *Proceedings of the National Academy of Sciences of the United States of America* 93(20), pp. 10990-10995.

Ahn, K. et al. 1997. The ER-luminal domain of the HCMV glycoprotein US6 inhibits peptide translocation by TAP. *Immunity* 6(5), pp. 613-621.

Alba, M. M. et al. 2001. Genomewide function conservation and phylogeny in the Herpesviridae. *Genome Research* 11(1), pp. 43-54.

Alcami, A. et al. 2000. The vaccinia virus soluble alpha/beta interferon (IFN) receptor binds to the cell surface and protects cells from the antiviral effects of IFN. *Journal of Virology* 74(23), pp. 11230-11239.

Androlewicz, M. J. P. 2001. Peptide generation in the major histocompatibility complex class I antigen processing and presentation pathway. *Current Opinion in Hematology January* 8(1), pp. 12-16.

Antoniou, A. N. et al. 2003. Assembly and export of MHC class I peptide ligands. *Current Opinion in Immunology* 15(1), pp. 75-81.

Ashiru, O. et al. 2009. NKG2D ligand MICA is retained in the cis-Golgi apparatus by human cytomegalovirus protein UL142. *Journal of Virology* 83(23), pp. 12345-12354. doi: <https://dx.doi.org/10.1128/JVI.01175-09>

Ashiru, O. et al. 2013. A GPI anchor explains the unique biological features of the common NKG2D-ligand allele MICA 008. *Biochemical Journal* 454(2), pp. 295-302. doi: <https://dx.doi.org/10.1042/BJ20130194>

Bacon, L. et al. 2004. Two human ULBP/RAET1 molecules with transmembrane regions are ligands for NKG2D. *Journal of Immunology* 173(2), pp. 1078-1084.

Bahram, S. 2000. MIC genes: from genetics to biology. *Advances in Immunology* 76, pp. 1-60.

- Bahram, S. et al. 1994. A second lineage of mammalian major histocompatibility complex class I genes. *Proceedings of the National Academy of Sciences of the United States of America* 91(14), pp. 6259-6263.
- Bahram, S. et al. 1996. Nucleotide sequence of the human MHC class I MICA gene. *Immunogenetics* 44(1), pp. 80-81.
- Barbanti-Brodano, G. et al. 1974. Abortive infection and transformation of human embryonic fibroblasts by *Molluscum contagiosum* virus. *Journal of General Virology* 24(2), pp. 237-246.
- Barel, M. T. et al. 2003a. Amino acid composition of alpha1/alpha2 domains and cytoplasmic tail of MHC class I molecules determine their susceptibility to human cytomegalovirus US11-mediated down-regulation. *European Journal of Immunology* 33(6), pp. 1707-1716.
- Barel, M. T. et al. 2003b. Human cytomegalovirus-encoded US2 differentially affects surface expression of MHC class I locus products and targets membrane-bound, but not soluble HLA-G1 for degradation. *Journal of Immunology* 171(12), pp. 6757-6765.
- Barkett, M. and Gilmore, T. D. 1999. Control of apoptosis by Rel/NF-kappaB transcription factors. *Oncogene* 18(49), pp. 6910-6924.
- Bartlett, N. W. et al. 2005. Murine interferon lambdas (type III interferons) exhibit potent antiviral activity in vivo in a poxvirus infection model. *Journal of General Virology* 86(Pt 6), pp. 1589-1596.
- Bauer, S. et al. 1999. Activation of NK cells and T cells by NKG2D, a receptor for stress-inducible MICA. *Science* 285(5428), pp. 727-729.
- Beattie, E. et al. 1991. Vaccinia virus-encoded eIF-2 alpha homolog abrogates the antiviral effect of interferon. *Virology* 183(1), pp. 419-422.
- Beck, S. and Barrell, B. G. 1988. Human cytomegalovirus encodes a glycoprotein homologous to MHC class-I antigens. *Nature* 331(6153), pp. 269-272.
- Becker, T. M. et al. 1986. Trends in molluscum contagiosum in the United States, 1966-1983. *Sexually Transmitted Diseases* 13(2), pp. 88-92.
- Benz, C. and Hengel, H. 2000. MHC class I-subversive gene functions of cytomegalovirus and their regulation by interferons-an intricate balance. *Virus Genes* 21(1-2), pp. 39-47.
- Biron, C. A. et al. 1989. Severe herpesvirus infections in an adolescent without natural killer cells. *New England Journal of Medicine* 320(26), pp. 1731-1735.

Birthing, K. and Carrington, D. 1997. Molluscum contagiosum virus. *Journal of Infection* 34(1), pp. 21-28.

Bjorkman, P. J. and Parham, P. 1990. Structure, function, and diversity of class I major histocompatibility complex molecules. *Annual Review of Biochemistry* 59, pp. 253-288.

Boeckh, M. and Boivin, G. 1998. Quantitation of cytomegalovirus: methodologic aspects and clinical applications. *Clinical Microbiology Reviews* 11(3), pp. 533-554.

Boeckh, M. et al. 1992. Cytomegalovirus antigen detection in peripheral blood leukocytes after allogeneic marrow transplantation. *Blood* 80(5), pp. 1358-1364.

Boeckh, M. and Geballe, A. P. 2011. Cytomegalovirus: pathogen, paradigm, and puzzle. *Journal of Clinical Investigation* 121(5), pp. 1673-1680. doi: <https://dx.doi.org/10.1172/JCI45449>

Boppana, S. B. and Fowler, K. B. 2007. Persistence in the population: epidemiology and transmission. *Cambridge University Press. Chapter 44,*

Borrego, F. et al. 1998. Recognition of human histocompatibility leukocyte antigen (HLA)-E complexed with HLA class I signal sequence-derived peptides by CD94/NKG2 confers protection from natural killer cell-mediated lysis. *Journal of Experimental Medicine* 187(5), pp. 813-818.

Borst, E. M. et al. 1999. Cloning of the human cytomegalovirus (HCMV) genome as an infectious bacterial artificial chromosome in *Escherichia coli*: a new approach for construction of HCMV mutants. *Journal of Virology* 73(10), pp. 8320-8329.

Bottino, C. et al. 2005. Cellular ligands of activating NK receptors. *Trends in Immunology* 26(4), pp. 221-226.

Bradley, A. J. et al. 2009. High-throughput sequence analysis of variants of human cytomegalovirus strains Towne and AD169. *Journal of General Virology* 90(Pt 10), pp. 2375-2380. doi: <https://dx.doi.org/10.1099/vir.0.013250-0>

Braud, V. et al. 1997. The human major histocompatibility complex class Ib molecule HLA-E binds signal sequence-derived peptides with primary anchor residues at positions 2 and 9. *European Journal of Immunology* 27(5), pp. 1164-1169.

Braud, V. M. et al. 1998. TAP- and tapasin-dependent HLA-E surface expression correlates with the binding of an MHC class I leader peptide. *Current Biology* 8(1), pp. 1-10.

Broder, C. C. and Earl, P. L. 1999. Recombinant vaccinia viruses. Design, generation, and isolation. *Molecular Biotechnology* 13(3), pp. 223-245.

- Browne, H. et al. 1990. A complex between the MHC class I homologue encoded by human cytomegalovirus and beta 2 microglobulin. *Nature* 347(6295), pp. 770-772.
- Bugert, J. J. et al. 1998. Chemokine homolog of molluscum contagiosum virus: sequence conservation and expression. *Virology* 242(1), pp. 51-59.
- Bugert, J. J. et al. 1999. Characterization of early gene transcripts of molluscum contagiosum virus. *Virology* 257(1), pp. 119-129.
- Bugert, J. J. et al. 2001. Molluscum contagiosum virus expresses late genes in primary human fibroblasts but does not produce infectious progeny. *Virus Genes* 22(1), pp. 27-33.
- Bugert, J. J. et al. 2000. Mapping of mRNA transcripts in the genome of molluscum contagiosum virus: transcriptional analysis of the viral slam gene family. *Virus Genes* 21(3), pp. 189-192.
- Buller, R. M. et al. 1995. Replication of molluscum contagiosum virus. *Virology* 213(2), pp. 655-659.
- Buller, R. M. and Palumbo, G. J. 1991. Poxvirus pathogenesis. *Microbiological Reviews* 55(1), pp. 80-122.
- Burnett, J. W. S., Jerry S. 1968. Molluscum contagiosum cytotoxicity for primary human amnion cells in vitro as studied by electron microscopy. *Journal of Investigative Dermatology*.
- Cannon, M. J. and Davis, K. F. 2005. Washing our hands of the congenital cytomegalovirus disease epidemic. *BMC Public Health* 5, p. 70.
- Cannon, M. J. et al. 2010. Review of cytomegalovirus seroprevalence and demographic characteristics associated with infection. *Reviews in Medical Virology* 20(4), pp. 202-213. doi: <https://dx.doi.org/10.1002/rmv.655>
- Celinska, E. et al. 2018. Robust signal peptides for protein secretion in *Yarrowia lipolytica*: identification and characterization of novel secretory tags. *Applied Microbiology & Biotechnology* 102(12), pp. 5221-5233. doi: <https://dx.doi.org/10.1007/s00253-018-8966-9>
- Carboni, C. et al. 2006. Spontaneous mutations in the human CMV HLA class I homologue UL18 affect its binding to the inhibitory receptor LIR-1/ILT2/CD85j. *European Journal of Immunology* 36(3), pp. 732-741.
- Cha, T. A. et al. 1996. Human cytomegalovirus clinical isolates carry at least 19 genes not found in laboratory strains. *Journal of Virology* 70(1), pp. 78-83.

Chalupny, N. J. et al. 2006. Down-regulation of the NKG2D ligand MICA by the human cytomegalovirus glycoprotein UL142. *Biochemical & Biophysical Research Communications* 346(1), pp. 175-181.

Chalupny, N. J. et al. 2003. ULBP4 is a novel ligand for human NKG2D. *Biochemical & Biophysical Research Communications* 305(1), pp. 129-135.

Chang, H. W. et al. 1992. The E3L gene of vaccinia virus encodes an inhibitor of the interferon-induced, double-stranded RNA-dependent protein kinase. *Proceedings of the National Academy of Sciences of the United States of America* 89(11), pp. 4825-4829.

Chapman, T. L. et al. 1999. The inhibitory receptor LIR-1 uses a common binding interaction to recognize class I MHC molecules and the viral homolog UL18. *Immunity* 11(5), pp. 603-613.

Charpak-Amikam, Y. et al. 2017. Human cytomegalovirus escapes immune recognition by NK cells through the downregulation of B7-H6 by the viral genes US18 and US20. *Scientific Reports* 7(1), p. 8661. doi: <https://dx.doi.org/10.1038/s41598-017-08866-2>

Chee, M. S. et al. 1990. Analysis of the protein-coding content of the sequence of human cytomegalovirus strain AD169. *Current Topics in Microbiology & Immunology* 154, pp. 125-169.

Chen, K. C. et al. 2016. Leukocyte Immunoglobulin-Like Receptor 1-Expressing Human Natural Killer Cell Subsets Differentially Recognize Isolates of Human Cytomegalovirus through the Viral Major Histocompatibility Complex Class I Homolog UL18. *Journal of Virology* 90(6), pp. 3123-3137.

Chen, X. et al. 2013. Molluscum contagiosum virus infection. *The Lancet Infectious Diseases* 13(10), pp. 877-888. doi: [http://dx.doi.org/10.1016/S1473-3099\(13\)70109-9](http://dx.doi.org/10.1016/S1473-3099(13)70109-9)

Chevalier, M. S. and Johnson, D. C. 2003. Human cytomegalovirus US3 chimeras containing US2 cytosolic residues acquire major histocompatibility class I and II protein degradation properties. *Journal of Virology* 77(8), pp. 4731-4738.

Compton, T. et al. 1993. Initiation of human cytomegalovirus infection requires initial interaction with cell surface heparan sulfate. *Virology* 193(2), pp. 834-841.

Cosman, D. et al. 1997. A novel immunoglobulin superfamily receptor for cellular and viral MHC class I molecules. *Immunity* 7(2), pp. 273-282.

- Cosman, D. et al. 2001. ULBPs, novel MHC class I-related molecules, bind to CMV glycoprotein UL16 and stimulate NK cytotoxicity through the NKG2D receptor. *Immunity* 14(2), pp. 123-133.
- Costantini, C. et al. 2010. Neutrophil activation and survival are modulated by interaction with NK cells. *International Immunology* 22(10), pp. 827-838. doi: <https://dx.doi.org/10.1093/intimm/dxq434>
- Coupar, B. E. et al. 1988. A general method for the construction of recombinant vaccinia viruses expressing multiple foreign genes. *Gene* 68(1), pp. 1-10.
- Cui, X. et al. 2009. The impact of genome length on replication and genome stability of the herpesvirus guinea pig cytomegalovirus. *Virology* 386(1), pp. 132-138. doi: <https://dx.doi.org/10.1016/j.virol.2008.12.030>
- Damon, I. et al. 1998. Broad spectrum chemokine antagonistic activity of a human poxvirus chemokine homolog. *Proceedings of the National Academy of Sciences of the United States of America* 95(11), pp. 6403-6407.
- Dargan, D. J. et al. 2010. Sequential mutations associated with adaptation of human cytomegalovirus to growth in cell culture. *Journal of General Virology* 91(Pt 6), pp. 1535-1546. doi: <https://dx.doi.org/10.1099/vir.0.018994-0>
- Das, S. and Pellett, P. E. 2007. Members of the HCMV US12 family of predicted heptaspanning membrane proteins have unique intracellular distributions, including association with the cytoplasmic virion assembly complex. *Virology* 361(2), pp. 263-273.
- Davison, A. J. et al. 2003a. Homology between the human cytomegalovirus RL11 gene family and human adenovirus E3 genes. *Journal of General Virology* 84(Pt 3), pp. 657-663.
- Davison, A. J. et al. 2003b. The human cytomegalovirus genome revisited: comparison with the chimpanzee cytomegalovirus genome. [Erratum appears in J Gen Virol. 2003 Apr;84(Pt 4):1053]. *Journal of General Virology* 84(Pt 1), pp. 17-28.
- Davison, A. J. et al. 2009. The order Herpesvirales. *Archives of Virology* 154(1), pp. 171-177. doi: <https://dx.doi.org/10.1007/s00705-008-0278-4>
- Dinarelli, C. A. 1999. IL-18: A TH1-inducing, proinflammatory cytokine and new member of the IL-1 family. *Journal of Allergy & Clinical Immunology* 103(1 Pt 1), pp. 11-24.
- Dohil, M. A. et al. 2006. The epidemiology of molluscum contagiosum in children. *Journal of the American Academy of Dermatology* 54(1), pp. 47-54.

Dolan, A. et al. 2004. Genetic content of wild-type human cytomegalovirus. *Journal of General Virology* 85(Pt 5), pp. 1301-1312.

Dollard, S. C. et al. 2007. New estimates of the prevalence of neurological and sensory sequelae and mortality associated with congenital cytomegalovirus infection. *Reviews in Medical Virology* 17(5), pp. 355-363.

Dugan, G. E. and Hewitt, E. W. 2008. Structural and Functional Dissection of the Human Cytomegalovirus Immune Evasion Protein US6. *Journal of Virology* 82(7), pp. 3271-3282. doi: <https://dx.doi.org/10.1128/JVI.01705-07>

Eagle, R. A. et al. 2006. Regulation of NKG2D ligand gene expression. *Human Immunology* 67(3), pp. 159-169.

Elliott, G. and O'Hare, P. 2000. Cytoplasm-to-nucleus translocation of a herpesvirus tegument protein during cell division. *Journal of Virology* 74(5), pp. 2131-2141.

Emery, V. C. et al. 1999. The dynamics of human cytomegalovirus replication in vivo. *Journal of Experimental Medicine* 190(2), pp. 177-182.

Escors, D. and Breckpot, K. 2010. Lentiviral vectors in gene therapy: their current status and future potential. *Archivum Immunologiae et Therapiae Experimentalis* 58(2), pp. 107-119. doi: <https://dx.doi.org/10.1007/s00005-010-0063-4>

Espinola, E. E. et al. 2017. Computational analysis of a species D human adenovirus provides evidence of a novel virus. *Journal of General Virology* 17, p. 17. doi: <https://dx.doi.org/10.1099/jgv.0.000947>

Fahnestock, M. L. et al. 1995. The MHC class I homolog encoded by human cytomegalovirus binds endogenous peptides. *Immunity* 3(5), pp. 583-590.

Farag, S. S. et al. 2003. Biology and clinical impact of human natural killer cells. *International Journal of Hematology* 78(1), pp. 7-17.

Feire, A. L. et al. 2004. Cellular integrins function as entry receptors for human cytomegalovirus via a highly conserved disintegrin-like domain. *Proceedings of the National Academy of Sciences of the United States of America* 101(43), pp. 15470-15475.

Ferlazzo, G. et al. 2004. Distinct roles of IL-12 and IL-15 in human natural killer cell activation by dendritic cells from secondary lymphoid organs. *Proceedings of the National Academy of Sciences of the United States of America* 101(47), pp. 16606-16611.

- Fielding, C. A. et al. 2014. Two novel human cytomegalovirus NK cell evasion functions target MICA for lysosomal degradation. *PLoS Pathogens* 10(5), p. e1004058. doi: <https://dx.doi.org/10.1371/journal.ppat.1004058>
- Fielding, C. A. et al. 2017. Control of immune ligands by members of a cytomegalovirus gene expansion suppresses natural killer cell activation. *eLife* 6(02), p. 10. doi: <https://dx.doi.org/10.7554/eLife.22206>
- Fields, B. N. et al. 2013. *Fields Virology*. Philadelphia ; London: Wolters Kluwer/Lippincott Williams & Wilkins Health.
- Fife, K. H. et al. 1996. Growth of molluscum contagiosum virus in a human foreskin xenograft model. *Virology* 226(1), pp. 95-101.
- Fischer, G. et al. 2000. Three novel MICB alleles. *Tissue Antigens* 55(2), pp. 166-170.
- Fitz-Gibbon, S. T. and House, C. H. 1999. Whole genome-based phylogenetic analysis of free-living microorganisms. *Nucleic Acids Research* 27(21), pp. 4218-4222.
- Fodil, N. et al. 1996. Allelic repertoire of the human MHC class I MICA gene. *Immunogenetics* 44(5), pp. 351-357.
- Freed, E. O. 2015. HIV-1 assembly, release and maturation. *Nature Reviews. Microbiology* 13(8), pp. 484-496. doi: <https://dx.doi.org/10.1038/nrmicro3490>
- Fruh, K. et al. 1995. A viral inhibitor of peptide transporters for antigen presentation. *Nature* 375(6530), p. 415.
- Fryer, J. F. et al. 2016. A collaborative study to establish the 1st WHO International Standard for human cytomegalovirus for nucleic acid amplification technology. *Biologicals* 44(4), pp. 242-251. doi: <https://dx.doi.org/10.1016/j.biologicals.2016.04.005>
- Gallego-Gomez, J. C. et al. 2003. Differences in virus-induced cell morphology and in virus maturation between MVA and other strains (WR, Ankara, and NYCBH) of vaccinia virus in infected human cells. *Journal of Virology* 77(19), pp. 10606-10622.
- Gandhi, M. K. and Khanna, R. 2004. Human cytomegalovirus: clinical aspects, immune regulation, and emerging treatments. *The Lancet Infectious Diseases* 4(12), pp. 725-738.
- Gatherer, D. et al. 2011. High-resolution human cytomegalovirus transcriptome. *Proceedings of the National Academy of Sciences of the United States of America* 108(49), pp. 19755-19760. doi: <https://dx.doi.org/10.1073/pnas.1115861108>

- Gazit, R. et al. 2004. Expression of KIR2DL1 on the entire NK cell population: a possible novel immunodeficiency syndrome. *Blood* 103(5), pp. 1965-1966.
- Geraghty, D. E. et al. 1990. Human leukocyte antigen F (HLA-F). An expressed HLA gene composed of a class I coding sequence linked to a novel transcribed repetitive element. *Journal of Experimental Medicine* 171(1), pp. 1-18.
- Gerna, G. et al. 1992. Comparison of different immunostaining techniques and monoclonal antibodies to the lower matrix phosphoprotein (pp65) for optimal quantitation of human cytomegalovirus antigenemia. *Journal of Clinical Microbiology* 30(5), pp. 1232-1237.
- Gerna, G. et al. 1990. Quantification of human cytomegalovirus viremia by using monoclonal antibodies to different viral proteins. *Journal of Clinical Microbiology* 28(12), pp. 2681-2688.
- Gerosa, F. et al. 2002. Reciprocal activating interaction between natural killer cells and dendritic cells. *Journal of Experimental Medicine* 195(3), pp. 327-333.
- Gewurz, B. E. et al. 2001. Antigen presentation subverted: Structure of the human cytomegalovirus protein US2 bound to the class I molecule HLA-A2. *Proceedings of the National Academy of Sciences of the United States of America* 98(12), pp. 6794-6799.
- Gilbert, G. L. et al. 1989. Prevention of transfusion-acquired cytomegalovirus infection in infants by blood filtration to remove leucocytes. Neonatal Cytomegalovirus Infection Study Group. *Lancet* 1(8649), pp. 1228-1231.
- Gillet, J. P. et al. 2009. The development of gene therapy: from monogenic recessive disorders to complex diseases such as cancer. *Methods in molecular biology* 542(pp 5-54), doi: http://dx.doi.org/10.1007/978-1-59745-561-9_1
- Goldszmid, R. S. et al. 2012. NK cell-derived interferon-gamma orchestrates cellular dynamics and the differentiation of monocytes into dendritic cells at the site of infection. *Immunity* 36(6), pp. 1047-1059. doi: <https://dx.doi.org/10.1016/j.immuni.2012.03.026>
- Gomez, C. E. et al. 2011. MVA and NYVAC as vaccines against emergent infectious diseases and cancer. *Current Gene Therapy* 11(3), pp. 189-217.
- Gompels, U. A. and Macaulay, H. A. 1995. Characterization of human telomeric repeat sequences from human herpesvirus 6 and relationship to replication. *Journal of General Virology* 76(Pt 2), pp. 451-458.
- Graham, F. L. et al. 1977. Characteristics of a human cell line transformed by DNA from human adenovirus type 5. *Journal of General Virology* 36(1), pp. 59-74.

Grey, F. et al. 2007. A human cytomegalovirus-encoded microRNA regulates expression of multiple viral genes involved in replication. *PLoS Pathogens* 3(11), p. e163.

Griffin, C. et al. 2005. Characterization of a highly glycosylated form of the human cytomegalovirus HLA class I homologue gpUL18. *Journal of General Virology* 86(Pt 11), pp. 2999-3008.

Groh, V. et al. 1996. Cell stress-regulated human major histocompatibility complex class I gene expressed in gastrointestinal epithelium. *Proceedings of the National Academy of Sciences of the United States of America* 93(22), pp. 12445-12450.

Hahn, G. et al. 1998. Cytomegalovirus remains latent in a common precursor of dendritic and myeloid cells. *Proceedings of the National Academy of Sciences of the United States of America* 95(7), pp. 3937-3942.

Halenius, A. et al. 2015. Classical and non-classical MHC I molecule manipulation by human cytomegalovirus: so many targets-but how many arrows in the quiver? *Cellular & Molecular Immunology* 12(2), pp. 139-153. doi: <https://dx.doi.org/10.1038/cmi.2014.105>

Hegde, N. R. et al. 2002. Inhibition of HLA-DR assembly, transport, and loading by human cytomegalovirus glycoprotein US3: a novel mechanism for evading major histocompatibility complex class II antigen presentation. *Journal of Virology* 76(21), pp. 10929-10941.

Hernaez, B. et al. 2018. A virus-encoded type I interferon decoy receptor enables evasion of host immunity through cell-surface binding. *Nature communications* 9(1), p. 5440. doi: <https://dx.doi.org/10.1038/s41467-018-07772-z>

Hewitt, E. W. 2003. The MHC class I antigen presentation pathway: strategies for viral immune evasion. *Immunology* 110(2), pp. 163-169.

Hill, A. et al. 1995. Herpes simplex virus turns off the TAP to evade host immunity. *Nature* 375(6530), p. 411.

Hoglund, P. and Brodin, P. 2010. Current perspectives of natural killer cell education by MHC class I molecules. *Nature Reviews. Immunology* 10(10), pp. 724-734. doi: <https://dx.doi.org/10.1038/nri2835>

Hook, L. et al. 2014. Cytomegalovirus microRNAs. *Current Opinion in Virology* 7, pp. 40-46. doi: <https://dx.doi.org/10.1016/j.coviro.2014.03.015>

Hsu, J. L. et al. 2015. Plasma Membrane Profiling Defines an Expanded Class of Cell Surface Proteins Selectively Targeted for Degradation by HCMV US2 in Cooperation with UL141. *PLoS Pathogens* 11 (4) (no pagination)(e1004811), doi: <http://dx.doi.org/10.1371/journal.ppat.1004811>

http://www.clontech.com/US/Products/Inducible_Systems/TetSystems_Product_Overview/Tet-One_Overview. 12/02/2018. Lentiviral Guide.

http://www.clontech.com/US/Products/Inducible_Systems/TetSystems_Product_Overview/Tet-One_Overview.

<https://www.addgene.org/viral-vectors/lentivirus/lenti-guide/>. 12/02/2018.

Lentiviral Guide. <https://www.addgene.org/viral-vectors/lentivirus/lenti-guide/>.

Husar, K. and Skerlev, M. 2002. Molluscum contagiosum from infancy to maturity. *Clinics in Dermatology* 20(2), pp. 170-172.

Isacson, M. K. and Compton, T. 2009. Human cytomegalovirus glycoprotein B is required for virus entry and cell-to-cell spread but not for virion attachment, assembly, or egress. *Journal of Virology* 83(8), pp. 3891-3903. doi:

<https://dx.doi.org/10.1128/JVI.01251-08>

Ishikawa-Mochizuki, I. et al. 1999. Molecular cloning of a novel CC chemokine, interleukin-11 receptor alpha-locus chemokine (ILC), which is located on chromosome 9p13 and a potential homologue of a CC chemokine encoded by molluscum contagiosum virus. *FEBS Letters* 460(3), pp. 544-548.

Jacobs, S. C. et al. 1992. High-level expression of the tick-borne encephalitis virus NS1 protein by using an adenovirus-based vector: protection elicited in a murine model. *Journal of Virology* 66(4), pp. 2086-2095.

Jaeger, B. N. et al. 2012. Neutrophil depletion impairs natural killer cell maturation, function, and homeostasis. *Journal of Experimental Medicine* 209(3), pp. 565-580. doi: <https://dx.doi.org/10.1084/jem.20111908>

Jarvis, M. A. and Nelson, J. A. 2007. Human cytomegalovirus tropism for endothelial cells: not all endothelial cells are created equal. *Journal of Virology* 81(5), pp. 2095-2101.

Jean Beltran, P. M. and Cristea, I. M. 2014. The life cycle and pathogenesis of human cytomegalovirus infection: lessons from proteomics. *Expert Review of Proteomics* 11(6), pp. 697-711. doi:

<https://dx.doi.org/10.1586/14789450.2014.971116>

Jin, Q. et al. 2011. Role for the conserved N-terminal cysteines in the anti-chemokine activities by the chemokine-like protein MC148R1 encoded by Molluscum contagiosum virus. *Virology* 417(2), pp. 449-456. doi:

<http://dx.doi.org/10.1016/j.virol.2011.07.001>

Jones, E. Y. 1997. MHC class I and class II structures. *Current Opinion in Immunology* 9(1), pp. 75-79.

- Jones, T. R. and Sun, L. 1997. Human cytomegalovirus US2 destabilizes major histocompatibility complex class I heavy chains. *Journal of Virology* 71(4), pp. 2970-2979.
- Jun, Y. et al. 2000. Human cytomegalovirus gene products US3 and US6 down-regulate trophoblast class I MHC molecules. *Journal of Immunology* 164(2), pp. 805-811.
- Just-Nubling, G. et al. 2003. Primary cytomegalovirus infection in an outpatient setting--laboratory markers and clinical aspects. *Infection* 31(5), pp. 318-323.
- Kagan, K. O. and Hamprecht, K. 2017. Cytomegalovirus infection in pregnancy. *Archives of Gynecology & Obstetrics* 296(1), pp. 15-26. doi: <https://dx.doi.org/10.1007/s00404-017-4380-2>
- Kagi, D. et al. 1994. Fas and perforin pathways as major mechanisms of T cell-mediated cytotoxicity. *Science* 265(5171), pp. 528-530.
- Kaiser, B. K. et al. 2008. Structural basis for NKG2A/CD94 recognition of HLA-E. *Proceedings of the National Academy of Sciences of the United States of America* 105(18), pp. 6696-6701. doi: <https://dx.doi.org/10.1073/pnas.0802736105>
- Kalejta, R. F. 2008. Tegument proteins of human cytomegalovirus. *Microbiology & Molecular Biology Reviews* 72(2), pp. 249-265, table of contents. doi: <https://dx.doi.org/10.1128/MMBR.00040-07>
- Kenneson, A. and Cannon, M. J. 2007. Review and meta-analysis of the epidemiology of congenital cytomegalovirus (CMV) infection. *Reviews in Medical Virology* 17(4), pp. 253-276.
- Kim, S. et al. 2015. Temporal Landscape of MicroRNA-Mediated Host-Virus Crosstalk during Productive Human Cytomegalovirus Infection. *Cell Host & Microbe* 17(6), pp. 838-851. doi: <https://dx.doi.org/10.1016/j.chom.2015.05.014>
- Koller, B. H. et al. 1988. HLA-E. A novel HLA class I gene expressed in resting T lymphocytes. *Journal of Immunology* 141(3), pp. 897-904.
- Kotenko, S. V. et al. 2000. Human cytomegalovirus harbors its own unique IL-10 homolog (cmvIL-10). *Proceedings of the National Academy of Sciences of the United States of America* 97(4), pp. 1695-1700.
- Kotwal, G. J. and Moss, B. 1988. Vaccinia virus encodes a secretory polypeptide structurally related to complement control proteins. *Nature* 335(6186), pp. 176-178.
- Krathwohl, M. D. et al. 1997. Functional characterization of the C---C chemokine-like molecules encoded by molluscum contagiosum virus types 1 and 2.

Proceedings of the National Academy of Sciences of the United States of America 94(18), pp. 9875-9880.

Kubin, M. et al. 2001. ULBP1, 2, 3: novel MHC class I-related molecules that bind to human cytomegalovirus glycoprotein UL16, activate NK cells. *European Journal of Immunology* 31(5), pp. 1428-1437.

Kulski, J. K. et al. 2002. Comparative genomic analysis of the MHC: the evolution of class I duplication blocks, diversity and complexity from shark to man. *Immunological Reviews* 190, pp. 95-122.

Lanier, L. L. 2005. NK cell recognition. *Annu. Rev. Immunol.* 23, pp. 225-274.

Lavrik, I. N. and Krammer, P. H. 2012. Regulation of CD95/Fas signaling at the DISC. *Cell Death & Differentiation* 19(1), pp. 36-41. doi: <https://dx.doi.org/10.1038/cdd.2011.155>

LeDuc, J. W. and Becher, J. 1999. Current status of smallpox vaccine. *Emerging Infectious Diseases* 5(4), pp. 593-594.

Lee, N. et al. 1998. HLA-E surface expression depends on binding of TAP-dependent peptides derived from certain HLA class I signal sequences. *Journal of Immunology* 160(10), pp. 4951-4960.

Lefkowitz, E. J. et al. 2006. Poxviruses: past, present and future. *Virus Research* 117(1), pp. 105-118.

Lehner, P. J. et al. 1997. The human cytomegalovirus US6 glycoprotein inhibits transporter associated with antigen processing-dependent peptide translocation. *Proceedings of the National Academy of Sciences of the United States of America* 94(13), pp. 6904-6909. doi: <http://dx.doi.org/10.1073/pnas.94.13.6904>

Lemberg, M. K. et al. 2001. Intramembrane proteolysis of signal peptides: an essential step in the generation of HLA-E epitopes. *Journal of Immunology* 167(11), pp. 6441-6446.

Leong, C. C. et al. 1998. Modulation of natural killer cell cytotoxicity in human cytomegalovirus infection: the role of endogenous class I major histocompatibility complex and a viral class I homolog.[Erratum appears in J Exp Med 1998 Aug 3;188(3):following 614]. *Journal of Experimental Medicine* 187(10), pp. 1681-1687.

Lesniewski, M. et al. 2006. Primate cytomegalovirus US12 gene family: a distinct and diverse clade of seven-transmembrane proteins. *Virology* 354(2), pp. 286-298.

Leung, A. K. C. et al. 2017. Molluscum Contagiosum: An Update. *Recent Patents on Inflammation & Allergy Drug Discovery* 11(1), pp. 22-31.

- Li, P. et al. 1999. Crystal structure of the MHC class I homolog MIC-A, a gammadelta T cell ligand. *Immunity* 10(5), pp. 577-584.
- Lilley, B. N. et al. 2003. Dislocation of a type I membrane protein requires interactions between membrane-spanning segments within the lipid bilayer. *Molecular Biology of the Cell* 14(9), pp. 3690-3698.
- Liu, W. et al. 2002. Analysis of human cytomegalovirus US3 gene products. *Virology* 301(1), pp. 32-42.
- Long, E. O. 1999. Regulation of immune responses through inhibitory receptors. *Annual Review of Immunology* 17, pp. 875-904.
- Lorente, E. et al. 2011. Allele-dependent processing pathways generate the endogenous human leukocyte antigen (HLA) class I peptide repertoire in transporters associated with antigen processing (TAP)-deficient cells. *Journal of Biological Chemistry* 286(44), pp. 38054-38059. doi: <https://dx.doi.org/10.1074/jbc.M111.281808>
- Lubeck, P. R. et al. 2010. Epidemiology of human cytomegalovirus (HCMV) in an urban region of Germany: what has changed? *Medical Microbiology & Immunology* 199(1), pp. 53-60. doi: <https://dx.doi.org/10.1007/s00430-009-0136-3>
- Luttichau, H. R. et al. 2001. MC148 encoded by human molluscum contagiosum poxvirus is an antagonist for human but not murine CCR8. *Journal of Leukocyte Biology* 70(2), pp. 277-282.
- Luttichau, H. R. et al. 2000. A highly selective CC chemokine receptor (CCR)8 antagonist encoded by the poxvirus molluscum contagiosum. *Journal of Experimental Medicine* 191(1), pp. 171-180.
- Magee, W. C. et al. 2005. Mechanism of inhibition of vaccinia virus DNA polymerase by cidofovir diphosphate. *Antimicrobial Agents & Chemotherapy* 49(8), pp. 3153-3162.
- Maidji, E. et al. 2002. Transmission of human cytomegalovirus from infected uterine microvascular endothelial cells to differentiating/invasive placental cytotrophoblasts. *Virology* 304(1), pp. 53-69.
- Mann, B. A. et al. 2008. Vaccinia virus blocks Stat1-dependent and Stat1-independent gene expression induced by type I and type II interferons. *Journal of Interferon & Cytokine Research* 28(6), pp. 367-380. doi: <https://dx.doi.org/10.1089/jir.2007.0113>
- Martin, A. M. et al. 2004. Comparative genomic analysis, diversity and evolution of two KIR haplotypes A and B. *Gene* 335, pp. 121-131.

Maxwell, L. D. et al. 2004. Investigation of killer cell immunoglobulin-like receptor gene diversity: II. KIR2DS4. *Human Immunology* 65(6), pp. 613-621.

May, N. A. et al. 2010. Human herpesvirus 7 u21 downregulates classical and nonclassical class I major histocompatibility complex molecules from the cell surface. *Journal of virology* 84(8), pp. 3738-3751.

Mayr, A. et al. 1978. [The smallpox vaccination strain MVA: marker, genetic structure, experience gained with the parenteral vaccination and behavior in organisms with a debilitated defence mechanism (author's transl)]. *Zentralblatt fur Bakteriologie, Parasitenkunde, Infektionskrankheiten und Hygiene - Erste Abteilung Originale - Reihe B: Hygiene, Betriebshygiene, Praventive Medizin* 167(5-6), pp. 375-390.

McConnell, M. J. and Imperiale, M. J. 2004. Biology of adenovirus and its use as a vector for gene therapy. *Human Gene Therapy* 15(11), pp. 1022-1033.

McFadden, G. et al. 1979. Biogenesis of poxviruses: Transitory expression of Molluscum contagiosum early functions. *Virology* 94(2), pp. 297-313.

McGeoch, D. J. et al. 1995. Molecular phylogeny and evolutionary timescale for the family of mammalian herpesviruses. *Journal of Molecular Biology* 247(3), pp. 443-458.

McGeoch, D. J. et al. 2000. Toward a comprehensive phylogeny for mammalian and avian herpesviruses. *Journal of Virology* 74(22), pp. 10401-10406.

McGeoch, D. J. et al. 2006. Topics in herpesvirus genomics and evolution. *Virus Research* 117(1), pp. 90-104.

McKenzie, R. et al. 1992. Regulation of complement activity by vaccinia virus complement-control protein. *Journal of Infectious Diseases* 166(6), pp. 1245-1250.

McSharry, B. P. et al. 2001. Human telomerase reverse transcriptase-immortalized MRC-5 and HCA2 human fibroblasts are fully permissive for human cytomegalovirus. *Journal of General Virology* 82(Pt 4), pp. 855-863.

Melquiot, N. V. and Bugert, J. J. 2004. Preparation and use of molluscum contagiosum virus from human tissue biopsy specimens. *Methods in Molecular Biology* 269, pp. 371-384.

Mendelson, M. et al. 1996. Detection of endogenous human cytomegalovirus in CD34+ bone marrow progenitors. *Journal of General Virology* 77(Pt 12), pp. 3099-3102.

Meshesha, M. K. et al. 2016. In vivo expression of human cytomegalovirus (HCMV) microRNAs during latency. *Gene* 575(1), pp. 101-107. doi: <https://dx.doi.org/10.1016/j.gene.2015.08.040>

Messerle, M. et al. 1997. Cloning and mutagenesis of a herpesvirus genome as an infectious bacterial artificial chromosome. *Proceedings of the National Academy of Sciences of the United States of America* 94(26), pp. 14759-14763.

Michel, T. et al. 2012. Consequences of the crosstalk between monocytes/macrophages and natural killer cells. *Frontiers in Immunology* 3, p. 403. doi: <https://dx.doi.org/10.3389/fimmu.2012.00403>

Miyoshi, H. et al. 1997. Stable and efficient gene transfer into the retina using an HIV-based lentiviral vector. *Proceedings of the National Academy of Sciences of the United States of America* 94(19), pp. 10319-10323. doi: <http://dx.doi.org/10.1073/pnas.94.19.10319>

Mocarski, E. S. et al. 1988. Human cytomegalovirus ICP22, the product of the HWLF1 reading frame, is an early nuclear protein that is released from cells. *Journal of General Virology* 69(Pt 10), pp. 2613-2621.

Mocsai, A. 2013. Diverse novel functions of neutrophils in immunity, inflammation, and beyond. *Journal of Experimental Medicine* 210(7), pp. 1283-1299. doi: <https://dx.doi.org/10.1084/jem.20122220>

Mohr, S. et al. 2008. Targeting the retinoblastoma protein by MC007L, gene product of the molluscum contagiosum virus: detection of a novel virus-cell interaction by a member of the poxviruses. *Journal of Virology* 82(21), pp. 10625-10633. doi: <https://dx.doi.org/10.1128/JVI.01187-08>

Montanuy, I. et al. 2011. Glycosaminoglycans mediate retention of the poxvirus type I interferon binding protein at the cell surface to locally block interferon antiviral responses. *FASEB Journal* 25(6), pp. 1960-1971. doi: <https://dx.doi.org/10.1096/fj.10-177188>

Morandi, B. et al. 2006. NK cells of human secondary lymphoid tissues enhance T cell polarization via IFN-gamma secretion. *European Journal of Immunology* 36(9), pp. 2394-2400.

Moretta, A. et al. 2001. Activating receptors and coreceptors involved in human natural killer cell-mediated cytotoxicity. *Annual Review of Immunology* 19, pp. 197-223.

Morris, R. 2005. *Immunomodulation of the cellular immune response by Human cytomegalovirus* Cardiff University, .

Murao, L. E. and Shisler, J. L. 2005. The MCV MC159 protein inhibits late, but not early, events of TNF-alpha-induced NF-kappaB activation. *Virology* 340(2), pp. 255-264.

Murphy, E. et al. 2003. Coding potential of laboratory and clinical strains of human cytomegalovirus. *Proceedings of the National Academy of Sciences of the United States of America* 100(25), pp. 14976-14981.

Murrell, I. et al. 2013. Impact of sequence variation in the UL128 locus on production of human cytomegalovirus in fibroblast and epithelial cells. *Journal of Virology* 87(19), pp. 10489-10500. doi: <https://dx.doi.org/10.1128/JVI.01546-13>

Naldini, L. et al. 1996. In vivo gene delivery and stable transduction of nondividing cells by a lentiviral vector. *Science* 272(5259), pp. 263-267.

Nicholas, J. 1996. Determination and analysis of the complete nucleotide sequence of human herpesvirus. *Journal of Virology* 70(9), pp. 5975-5989.

Niizeki, K. et al. 1984. An epidemic study of molluscum contagiosum. Relationship to swimming. *Dermatologica* 169(4), pp. 197-198.

Ninagawa, S. et al. 2015. Forcible destruction of severely misfolded mammalian glycoproteins by the non-glycoprotein ERAD pathway. *Journal of Cell Biology* 211(4), pp. 775-784. doi: <https://dx.doi.org/10.1083/jcb.201504109>

Noriega, V. M. and Tortorella, D. 2008. A bipartite trigger for dislocation directs the proteasomal degradation of an endoplasmic reticulum membrane glycoprotein. *Journal of Biological Chemistry* 283(7), pp. 4031-4043.

Noriega, V. M. and Tortorella, D. 2009. Human cytomegalovirus-encoded immune modulators partner to downregulate major histocompatibility complex class I molecules. *Journal of Virology* 83(3), pp. 1359-1367. doi: <https://dx.doi.org/10.1128/JVI.01324-08>

Olczak, M. and Olczak, T. 2006. Comparison of different signal peptides for protein secretion in nonlytic insect cell system. *Analytical Biochemistry* 359(1), pp. 45-53.

Pahl, H. L. 1999. Activators and target genes of Rel/NF-kappaB transcription factors. *Oncogene* 18(49), pp. 6853-6866.

Palu, G. et al. 2000. Progress with retroviral gene vectors. *Reviews in Medical Virology* 10(3), pp. 185-202.

Pamer, E. and Cresswell, P. 1998. Mechanisms of MHC class I--restricted antigen processing. *Annual Review of Immunology* 16, pp. 323-358.

Parham, P. 2005. MHC class I molecules and KIRs in human history, health and survival. *Nature Reviews Immunology* 5(3), pp. 201-214.

Paslin, D. et al. 1997. Molluscum contagiosum virus grows in human skin xenografts. *Archives of Dermatological Research* 289(8), pp. 486-488.

Pegram, H. J. et al. 2011. Activating and inhibitory receptors of natural killer cells. *Immunology & Cell Biology* 89(2), pp. 216-224. doi: <https://dx.doi.org/10.1038/icb.2010.78>

Penfold, M. E. et al. 1999. Cytomegalovirus encodes a potent alpha chemokine. *Proceedings of the National Academy of Sciences of the United States of America* 96(17), pp. 9839-9844.

Perkus, M. E. et al. 1985. Recombinant vaccinia virus: immunization against multiple pathogens. *Science, USA* 229(Sep. 6), pp. 981-984.

Petersdorf, E. W. et al. 1999. Population study of allelic diversity in the human MHC class I-related MIC-A gene. *Immunogenetics* 49(7-8), pp. 605-612.

Placa, M. 1966. On the mechanism of the cytopathic changes produced in human amnion cell **cultures** by the **molluscum contagiosum virus**. *Archiv für die gesamte Virusforschung*.

Plotkin, S. A. et al. 1975. Candidate cytomegalovirus strain for human vaccination. *Infection & Immunity* 12(3), pp. 521-527.

Plotkin, S. A. et al. 1989. Protective effects of Towne cytomegalovirus vaccine against low-passage cytomegalovirus administered as a challenge. *Journal of Infectious Diseases* 159(5), pp. 860-865.

Porter, C. D. et al. 1989. Molluscum contagiosum virus types in genital and non-genital lesions. *British Journal of Dermatology* 120(1), pp. 37-41.

Prod'homme, V. et al. 2010. Human cytomegalovirus UL141 promotes efficient downregulation of the natural killer cell activating ligand CD112. *Journal of General Virology* 91(8), pp. 2034-2039. doi: <http://dx.doi.org/10.1099/vir.0.021931-0>

Prod'homme, V. et al. 2012. Human cytomegalovirus UL40 signal peptide regulates cell surface expression of the NK cell ligands HLA-E and gpUL18. *Journal of Immunology* 188(6), pp. 2794-2804. doi: <http://dx.doi.org/10.4049/jimmunol.1102068>

- Prod'homme, V. et al. 2007. The human cytomegalovirus MHC class I homolog UL18 inhibits LIR-1+ but activates LIR-1- NK cells. *The Journal of Immunology* 178(7), pp. 4473-4481.
- Quinnan, G. V., Jr. et al. 1984. Comparative virulence and immunogenicity of the Towne strain and a nonattenuated strain of cytomegalovirus. *Annals of Internal Medicine* 101(4), pp. 478-483.
- Randall, C. M. H. et al. 2014. Inhibition of interferon gene activation by death-effector domain-containing proteins from the molluscum contagiosum virus. *Proceedings of the National Academy of Sciences of the United States of America* 111(2), pp. E265-E272. doi: <http://dx.doi.org/10.1073/pnas.1314569111>
- Randolph-Habecker, J. R. et al. 2002. The expression of the cytomegalovirus chemokine receptor homolog US28 sequesters biologically active CC chemokines and alters IL-8 production. *Cytokine* 19(1), pp. 37-46.
- Rath, A. et al. 2009. Detergent binding explains anomalous SDS-PAGE migration of membrane proteins. *Proceedings of the National Academy of Sciences of the United States of America* 106(6), pp. 1760-1765. doi: <https://dx.doi.org/10.1073/pnas.0813167106>
- Reeves, M. and Sinclair, J. 2008. Aspects of human cytomegalovirus latency and reactivation. *Current Topics in Microbiology & Immunology* 325, pp. 297-313.
- Reyburn, H. T. et al. 1997. The class I MHC homologue of human cytomegalovirus inhibits attack by natural killer cells. *Nature* 386(6624), pp. 514-517.
- Rice, G. P. et al. 1984. Cytomegalovirus infects human lymphocytes and monocytes: virus expression is restricted to immediate-early gene products. *Proceedings of the National Academy of Sciences of the United States of America* 81(19), pp. 6134-6138.
- Robinson, J. et al. 2001. MICA sequences 2000. *Immunogenetics* 53(2), pp. 150-169.
- Rolle, A. et al. 2003. Effects of human cytomegalovirus infection on ligands for the activating NKG2D receptor of NK cells: up-regulation of UL16-binding protein (ULBP)1 and ULBP2 is counteracted by the viral UL16 protein. *Journal of Immunology* 171(2), pp. 902-908.
- S., N. and R., K. 1997. Simian immunodeficiency virus as a model of HIV pathogenesis. *Springer Seminars in Immunopathology* 18(3), pp. 391-405. doi: <http://dx.doi.org/10.1007/BF00813505>

- Santoli, D. et al. 1978. Cell-mediated cytotoxicity against virus-infected target cells in humans. II. Interferon induction and activation of natural killer cells. *Journal of Immunology* 121(2), pp. 532-538.
- Sarker, S. et al. 2018. Molecular characterization of the first saltwater crocodilepox virus genome sequences from the world's largest living member of the Crocodylia. *Scientific Reports* 8(1), p. 5623.
- Scaffidi, C. et al. 1999. The role of c-FLIP in modulation of CD95-induced apoptosis. *Journal of Biological Chemistry* 274(3), pp. 1541-1548.
- Scapini, P. and Cassatella, M. A. 2014. Social networking of human neutrophils within the immune system. *Blood* 124(5), pp. 710-719. doi: <https://dx.doi.org/10.1182/blood-2014-03-453217>
- Schneider, W. M. et al. 2014. Interferon-stimulated genes: a complex web of host defenses. *Annual Review of Immunology* 32, pp. 513-545. doi: <https://dx.doi.org/10.1146/annurev-immunol-032713-120231>
- Scholz, J. et al. 1989. Epidemiology of molluscum contagiosum using genetic analysis of the viral DNA. *Journal of Medical Virology* 27(2), pp. 87-90.
- Scholz, M. et al. 2003. Human cytomegalovirus retinitis: pathogenicity, immune evasion and persistence. *Trends in Microbiology* 11(4), pp. 171-178.
- Scholz, M. et al. 2004. Supernatants from human cytomegalovirus (HCMV)-infected retinal glial cells increase transepithelial electrical resistance in a cell culture model: evidence of HCMV immune escape in the eye? *Medical Microbiology & Immunology* 193(4), pp. 205-208.
- Schriewer, J. et al. 2004. Mouse models for studying orthopoxvirus respiratory infections. *Methods in Molecular Biology* 269, pp. 289-308.
- Seidel, E. et al. 2015. Dynamic co-evolution of host and pathogen: HCMV downregulates the prevalent allele MICA* 008 to escape elimination by NK cells. *Cell reports* 10(6), pp. 968-982.
- Seirafian, S. 2012. *an analysis of human cytomegalovirus gene usage*. Cardiff University.
- Sen, G. C. and Sarkar, S. N. 2007. The interferon-stimulated genes: targets of direct signaling by interferons, double-stranded RNA, and viruses. *Current Topics in Microbiology & Immunology* 316, pp. 233-250.
- Senkevich, T. G. et al. 1996. Genome sequence of a human tumorigenic poxvirus: prediction of specific host response-evasion genes. *Science* 273(5276), pp. 813-816.

Senkevich, T. G. et al. 1997. The genome of molluscum contagiosum virus: analysis and comparison with other poxviruses. *Virology* 233(1), pp. 19-42.

Senkevich, T. G. and Moss, B. 1998. Domain structure, intracellular trafficking, and beta2-microglobulin binding of a major histocompatibility complex class I homolog encoded by molluscum contagiosum virus. *Virology* 250(2), pp. 397-407.

Shchelkunov, S. N. et al. 2000. Alastrim smallpox variola minor virus genome DNA sequences. *Virology* 266(2), pp. 361-386.

Shisler, J. L. et al. 1998. Ultraviolet-induced cell death blocked by a selenoprotein from a human dermatotropic poxvirus. *Science* 279(5347), pp. 102-105. doi: <http://dx.doi.org/10.1126/science.279.5347.102>

Shizuya, H. et al. 1992. Cloning and stable maintenance of 300-kilobase-pair fragments of human DNA in *Escherichia coli* using an F-factor-based vector. *Proceedings of the National Academy of Sciences of the United States of America* 89(18), pp. 8794-8797.

Sijmons, S. et al. 2014. Genomic and functional characteristics of human cytomegalovirus revealed by next-generation sequencing. *Viruses* 6(3), pp. 1049-1072. doi: <https://dx.doi.org/10.3390/v6031049>

Sinclair, J. and Sissons, P. 2006. Latency and reactivation of human cytomegalovirus. *Journal of General Virology* 87(Pt 7), pp. 1763-1779.

Sindre, H. et al. 1996. Human cytomegalovirus suppression of and latency in early hematopoietic progenitor cells. *Blood* 88(12), pp. 4526-4533.

Sinzger, C. et al. 1995. Fibroblasts, epithelial cells, endothelial cells and smooth muscle cells are major targets of human cytomegalovirus infection in lung and gastrointestinal tissues. *Journal of General Virology* 76(Pt 4), pp. 741-750.

Sinzger, C. et al. 2000. Tropism of human cytomegalovirus for endothelial cells is determined by a post-entry step dependent on efficient translocation to the nucleus. *Journal of General Virology* 81(Pt 12), pp. 3021-3035.

Skaletskaya, A. et al. 2001. A cytomegalovirus-encoded inhibitor of apoptosis that suppresses caspase-8 activation. *Proceedings of the National Academy of Sciences of the United States of America* 98(14), pp. 7829-7834.

Smee, D. F. and Sidwell, R. W. 2003. A review of compounds exhibiting anti-orthopoxvirus activity in animal models. *Antiviral Research* 57(1-2), pp. 41-52.

- Smith, G. L. et al. 2013a. Vaccinia virus immune evasion: mechanisms, virulence and immunogenicity. *Journal of General Virology* 94(Pt 11), pp. 2367-2392. doi: <https://dx.doi.org/10.1099/vir.0.055921-0>
- Smith, K. A. 2011. Edward Jenner and the smallpox vaccine. *Frontiers in Immunology* 2, p. 21. doi: <https://dx.doi.org/10.3389/fimmu.2011.00021>
- Smith, R. M. et al. 2014. Role of human cytomegalovirus tegument proteins in virion assembly. *Viruses* 6(2), pp. 582-605. doi: <https://dx.doi.org/10.3390/v6020582>
- Smith, W. et al. 2013b. Human cytomegalovirus glycoprotein UL141 targets the TRAIL death receptors to thwart host innate antiviral defenses. *Cell Host and Microbe* 13(3), pp. 324-335. doi: <http://dx.doi.org/10.1016/j.chom.2013.02.003>
- Snel, B. et al. 1999. Genome phylogeny based on gene content. *Nature Genetics* 21(1), pp. 108-110.
- Soetandyo, N. and Ye, Y. 2010. The p97 ATPase dislocates MHC class I heavy chain in US2-expressing cells via a Ufd1-Npl4-independent mechanism. *Journal of Biological Chemistry* 285(42), pp. 32352-32359. doi: <https://dx.doi.org/10.1074/jbc.M110.131649>
- Sorensen, M. A. and Pedersen, S. 1991. Absolute in vivo translation rates of individual codons in *Escherichia coli*. The two glutamic acid codons GAA and GAG are translated with a threefold difference in rate. *Journal of Molecular Biology* 222(2), pp. 265-280.
- Spiliotis, E. T. et al. 2000. Selective export of MHC class I molecules from the ER after their dissociation from TAP. [Erratum appears in *Immunity* 2001 Feb;14(2):following 204]. *Immunity* 13(6), pp. 841-851.
- Spreu, J. et al. 2006. Human cytomegalovirus-encoded UL16 discriminates MIC molecules by their alpha2 domains. *Journal of Immunology* 177(5), pp. 3143-3149.
- Stam, N. J. et al. 1986. Monoclonal antibodies raised against denatured HLA-B locus heavy chains permit biochemical characterization of certain HLA-C locus products. *Journal of Immunology* 137(7), pp. 2299-2306.
- Stanton, R. J. et al. 2010. Reconstruction of the complete human cytomegalovirus genome in a BAC reveals RL13 to be a potent inhibitor of replication. *Journal of Clinical Investigation* 120(9), pp. 3191-3208.
- Stanton, R. J. et al. 2008. Re-engineering adenovirus vector systems to enable high-throughput analyses of gene function. *BioTechniques* 45(6), pp. 659-668. doi: <http://dx.doi.org/10.2144/000112993>

Stanton, R. J. et al. 2007. Cytomegalovirus destruction of focal adhesions revealed in a high-throughput Western blot analysis of cellular protein expression. *Journal of Virology* 81(15), pp. 7860-7872.

Stanton, R. J. et al. 2014. HCMV pUL135 remodels the actin cytoskeleton to impair immune recognition of infected cells. *Cell Host & Microbe* 16(2), pp. 201-214. doi: <https://dx.doi.org/10.1016/j.chom.2014.07.005>

Stephens, H. A. 2002. MHC haplotypes, MICA genes and the 'wonderland' of NK receptor polymorphism. *Trends in Immunology* 23(8), pp. 385-386.

Stern-Ginossar, N. et al. 2007. Host immune system gene targeting by a viral miRNA. *Science* 317(5836), pp. 376-381.

Tavalai, N. and Stamminger, T. 2011. Intrinsic cellular defense mechanisms targeting human cytomegalovirus. *Virus Research* 157(2), pp. 128-133. doi: <https://dx.doi.org/10.1016/j.virusres.2010.10.002>

Taylor-Wiedeman, J. et al. 1993. Polymorphonuclear cells are not sites of persistence of human cytomegalovirus in healthy individuals. *Journal of General Virology* 74(Pt 2), pp. 265-268.

Taylor-Wiedeman, J. et al. 1991. Monocytes are a major site of persistence of human cytomegalovirus in peripheral blood mononuclear cells. *Journal of General Virology* 72(Pt 9), pp. 2059-2064.

Teasdale, R. D. and Jackson, M. R. 1996. Signal-mediated sorting of membrane proteins between the endoplasmic reticulum and the golgi apparatus. *Annual Review of Cell & Developmental Biology* 12, pp. 27-54.

Thanos, D. and Maniatis, T. 1995. NF-kappa B: a lesson in family values. *Cell* 80(4), pp. 529-532.

Thoren, F. B. et al. 2012. Human NK Cells induce neutrophil apoptosis via an NKp46- and Fas-dependent mechanism. *Journal of Immunology* 188(4), pp. 1668-1674. doi: <https://dx.doi.org/10.4049/jimmunol.1102002>

Tomasec, P. 2000. Surface expression of HLA-E, an inhibitor of natural killer cells, enhanced by human cytomegalovirus gpUL40. *Science* 287(5455), pp. 1031-1033. doi: <http://dx.doi.org/10.1126/science.287.5455.1031>

Tomasec, P. et al. 2007. Adenovirus vector delivery stimulates natural killer cell recognition. *Journal of General Virology* 88(Pt 4), pp. 1103-1108.

Tomasec, P. et al. 2005. Downregulation of natural killer cell-activating ligand CD155 by human cytomegalovirus UL141. *Nature Immunology* 6(2), pp. 181-188.

- Tomazin, R. et al. 1999. Cytomegalovirus US2 destroys two components of the MHC class II pathway, preventing recognition by CD4+ T cells. *Nature Medicine* 5(9), pp. 1039-1043.
- Trinchieri, G. et al. 1978. Spontaneous cell-mediated cytotoxicity in humans: role of interferon and immunoglobulins. *Journal of Immunology* 120(6), pp. 1849-1855.
- Tuller, T. et al. 2010. An evolutionarily conserved mechanism for controlling the efficiency of protein translation. *Cell* 141(2), pp. 344-354. doi: <https://dx.doi.org/10.1016/j.cell.2010.03.031>
- Tyring, S. K. 2003. Molluscum contagiosum: the importance of early diagnosis and treatment. *American Journal of Obstetrics & Gynecology* 189(3 Suppl), pp. S12-16.
- Ulbrecht, M. et al. 2000. Cutting edge: the human cytomegalovirus UL40 gene product contains a ligand for HLA-E and prevents NK cell-mediated lysis. *Journal of Immunology* 164(10), pp. 5019-5022.
- van den Broek, M. F. et al. 1995. Antiviral defense in mice lacking both alpha/beta and gamma interferon receptors. *Journal of Virology* 69(8), pp. 4792-4796.
- van der Bij, W. et al. 1988. Rapid immunodiagnosis of active cytomegalovirus infection by monoclonal antibody staining of blood leucocytes. *Journal of Medical Virology* 25(2), pp. 179-188.
- Vanarsdall, A. L. and Johnson, D. C. 2012. Human cytomegalovirus entry into cells. *Current Opinion in Virology* 2(1), pp. 37-42. doi: <https://dx.doi.org/10.1016/j.coviro.2012.01.001>
- Vanderplasschen, A. et al. 1998. Extracellular enveloped vaccinia virus is resistant to complement because of incorporation of host complement control proteins into its envelope. *Proceedings of the National Academy of Sciences of the United States of America* 95(13), pp. 7544-7549.
- Venkataraman, G. M. et al. 2007. Promoter region architecture and transcriptional regulation of the genes for the MHC class I-related chain A and B ligands of NKG2D. *Journal of Immunology* 178(2), pp. 961-969.
- Viac, J. and Chardonnet, Y. 1990. Immunocompetent cells and epithelial cell modifications in molluscum contagiosum. *Journal of Cutaneous Pathology* 17(4), pp. 202-205.
- Vivier, E. et al. 2011. Innate or adaptive immunity? The example of natural killer cells. *Science* 331(6013), pp. 44-49. doi: <https://dx.doi.org/10.1126/science.1198687>

- Volz, A. and Sutter, G. 2013. Protective efficacy of Modified Vaccinia virus Ankara in preclinical studies. (Special Issue: Poxvirus vectors.). *Vaccine* 31(39), pp. 4235-4240. doi: <http://dx.doi.org/10.1016/j.vaccine.2013.03.016>
- Wang, E. C. Y. et al. 2002. UL40-mediated NK evasion during productive infection with human cytomegalovirus. *Proceedings of the National Academy of Sciences* 99(11), pp. 7570-7575.
- Watson, R. T. and Pessin, J. E. 2001. Transmembrane domain length determines intracellular membrane compartment localization of syntaxins 3, 4, and 5. *American Journal of Physiology - Cell Physiology* 281(1), pp. C215-223.
- Weekes, M. P. et al. 2014. Quantitative temporal viromics: an approach to investigate host-pathogen interaction. *Cell* 157(6), pp. 1460-1472. doi: <https://dx.doi.org/10.1016/j.cell.2014.04.028>
- Wei, P. et al. 1998. A novel CDK9-associated C-type cyclin interacts directly with HIV-1 Tat and mediates its high-affinity, loop-specific binding to TAR RNA. *Cell* 92(4), pp. 451-462.
- Weihofen, A. et al. 2003. Targeting presenilin-type aspartic protease signal peptide peptidase with gamma-secretase inhibitors. *Journal of Biological Chemistry* 278(19), pp. 16528-16533.
- Wiertz, E. J. et al. 1996a. The human cytomegalovirus US11 gene product dislocates MHC class I heavy chains from the endoplasmic reticulum to the cytosol. *Cell* 84(5), pp. 769-779.
- Wiertz, E. J. et al. 1996b. Sec61-mediated transfer of a membrane protein from the endoplasmic reticulum to the proteasome for destruction. *Nature* 384(6608), pp. 432-438.
- Wilkinson, G. W. and Akrigg, A. 1992. Constitutive and enhanced expression from the CMV major IE promoter in a defective adenovirus vector. *Nucleic Acids Research* 20(9), pp. 2233-2239.
- Wilkinson, G. W. et al. 2015. Human cytomegalovirus: taking the strain. *Medical Microbiology & Immunology* 204(3), pp. 273-284. doi: <https://dx.doi.org/10.1007/s00430-015-0411-4>
- Wilkinson, G. W. G. et al. 2008. Modulation of natural killer cells by human cytomegalovirus. *Journal of Clinical Virology* 41(3), pp. 206-212. doi: <http://dx.doi.org/10.1016/j.jcv.2007.10.027>
- Willcox, B. E. et al. 2003. Crystal structure of HLA-A2 bound to LIR-1, a host and viral major histocompatibility complex receptor. *Nature Immunology* 4(9), pp. 913-919.

- Williams, A. P. et al. 2002. Optimization of the MHC class I peptide cargo is dependent on tapasin. *Immunity* 16(4), pp. 509-520.
- Wills, M. R. et al. 2005. Human cytomegalovirus encodes an MHC class I-like molecule (UL142) that functions to inhibit NK cell lysis. *Journal of Immunology* 175(11), pp. 7457-7465.
- Wu, J. et al. 1999. An activating immunoreceptor complex formed by NKG2D and DAP10. *Science* 285(5428), pp. 730-732.
- Xiang, Y. and Moss, B. 2001. Correspondence of the functional epitopes of poxvirus and human interleukin-18-binding proteins. *Journal of Virology* 75(20), pp. 9947-9954. doi: <http://dx.doi.org/10.1128/JVI.75.20.9947-9954.2001>
- Xiang, Y. and Moss, B. 2003. Molluscum contagiosum virus interleukin-18 (IL-18) binding protein is secreted as a full-length form that binds cell surface glycosaminoglycans through the C-terminal tail and a furin-cleaved form with only the IL-18 binding domain. *Journal of Virology* 77(4), pp. 2623-2630.
- Yeager, A. S. et al. 1981. Prevention of transfusion-acquired cytomegalovirus infections in newborn infants. *Journal of Pediatrics* 98(2), pp. 281-287.
- Yokoyama, W. M. et al. 2010. Natural killer cells: tolerance to self and innate immunity to viral infection and malignancy. *Biology of Blood & Marrow Transplantation* 16(1 Suppl), pp. S97-S105. doi: <https://dx.doi.org/10.1016/j.bbmt.2009.10.009>
- Zhang, Y. et al. 2001. Typing for all known MICA alleles by group-specific PCR and SSOP. *Human Immunology* 62(6), pp. 620-631.
- Zou, Y. et al. 2005. Effect of human cytomegalovirus on expression of MHC class I-related chains A. *Journal of Immunology* 174(5), pp. 3098-3104.
- Zwirner, N. W. et al. 1999. Differential surface expression of MICA by endothelial cells, fibroblasts, keratinocytes, and monocytes. *Human Immunology* 60(4), pp. 323-330.

8-Appendix

The Optimized mc080R

Not-kozak-atg- optimized gene- mycTAG- stop- bamHI

GCGGCCGCGCCACC ATG ACC GGT ACC CTC ATT CTG CTC CTG GCA
TGC GTA CTG AAC GCC ATG GCG CAG TTG CTT GCC CGG GTT TGC
ATG GCT GCC GCT ACA CTC GCA CGC ATG CTC GCC CTT AGC GTG
GCG TTT CTG CTG GCT CTT GCC AGG ACA CGG ACC GGA CTG AGG
GCC ATC CTG GTT GCC CTG CTG CTG CGA GCC TTG CTT AGA GCA
CTG CTG GCC CAC GCA CAT GCG CAC ACA CTG TCC TAC GTA GCT
GCT GTC GTG TAC ACA CCC GGG AAT GCA CAG CCC TTG CTT CTG
GCG GAA GGC TCA ATC AAC GAC CTG GTG TTC ATG CGG TAT CAC
AGA CAA AGC GGC TCA GTG CTG CCA AGT CCC GAA TGG GCT CCA
AGC GTG TAC TTC CAC GAC GAG CTC TGG ATG CTG AAT GCC CGC
GTT GAT GCC CTT CGG TCC CTG AGT GTG CCT GGT GCA CGA CTG
GGG AAT GGC ACC TTG GGT GCT AGA TCT CTC CAA CTC GCA GTG
GGC TGC GAA AAG GTG GCA GGG GAT GCC AGC TTT TGG GAT CTG
GTG TAT GAT GGG ACT GAG CAG ATC TGT ATG CAC GCT GAT GCC
ACC GAG TGT GAG CCT GGA CTC CCC GTT CAT GCC AGG CTG GCC
AAA GAG CGG TGG ACA AGA CTC GGA GCT CAC AGT CAT GCG CTC
GAG CAG CGT TGT CTG CAG TGG TTG GAA AGG CAT CTG GGA GCA
AGG ACC AAC CGA CCG GTG GTG TCT GTT CCG CTG TTG AGC GTC
GTC GCC TAT GCC GAC GGC TCT GGC ACT CGC CTG CGT TGT ACT
GCT TCA GGC TTC TCT CCC CGA GAT GTG CGG CTG CTG TGG ACT
CGC GAT GGA ATT CCA GGA CCA GAC TAC GAC TTC GTG GAA CCT
CGC CCA TCT GGG GAC GGC AGC TTT CAG CAG TGG GCA GAG CTG
GTC GTA GCC GCT GGC TTG GAG ACA CAC TAT GTC TGC GTA GCC
TCC CAT GAC TCC TGG AAG TCA TCC TGG CGG GCT AGA TGG GAA
GAG GGG AAA CGC AGG GTC GCT ACC AGT GCG AGA GTG GCA CCC
TTG GCA ACG ATA GCC GAG ATG CTT GTC GCC CTG GAA CTC ATG
CTG ATT CTG AGG GAA CGT CGC CTT ACT CTG GGT GCC CTG GCA
ACG ATG CTG GCT TGC AGC ATG CCT AAC CTC CTG CCT CAA GCC
CTC AGA GAG AGA GCT GGA
TTTGAACAAAACTCATCTCAGAAGAGGATCTG TGAGGATCC

MC080 amino acid sequence

GRATMTGTLILLLACVLNAMAQLLARVCM AATLARM LALSVAFL LALARTRTGLR
AILVALLLRALLRALLAH AHAHTLSYVA AVVYTPGNAQPLLLAEGSINDLVFMR YH
RQSGSVLPSP EWAPSVYFHDELWMLNARVDALRSLSVPGARLGNGTLGARSLQLAV
GCEKVAGDASFWDLVYDGTEQICMHADATECEPGLPVHARLAKERWTRLGAHSHAL
EQRCLQWLERHLGARTNRPVVSVP LLSV VAYADGSGTRLRCTASGFSPRDVRL LWT
RDGIPGPDYDFVEPRPSGDGSFQQWAE LVVAAGLETHYVCVASHDSWKSSWRARWE
EGKRRVATSARVAPLATIAEMLVALELMLILRERRLTLGALATMLACSM PNL L PQA
LRERAGFEQKLI SEEDL*GSX

The Optimized mc033L

Not-kozak-atg- optimized MC033gene- ha TAG- stop- bamHI

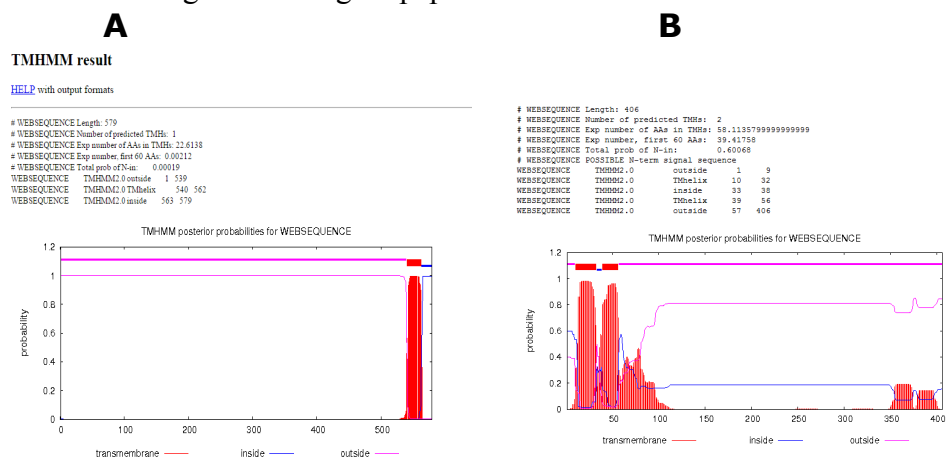
GCGGCCGC**GCCACC**ATG AGG CCC CAC GTG CTG ATC ACC CTG GCC
ACT TGT GCC TTG CGG GCT CTT GCC CAG GTG ATA GAC GAA CAC
GAG CAC TCT GAA CCA CCA GTT TCA ACA TGG CCC GAC ATG TCC
TAC CTG GTC GCA GAG ATG CGG TCT GAT AGC GTA CTG ATG CGG
GGC ATG CTG GAT GGC CAT GAG CAC GTG CGC TGT ACT TGC GTG
CCA AAG TGC GCC TGC TTG GAG CCC ACC CTT CCA CGA GCC GCT
CTG GAA CAA GCC CGC TCA CGG GTA CTG GAT GCC CAT GCT GGT
CGT GTG CCC GGA CTG AGA GCC CCT AGC AGG GCA GCA CAT CGC
AGA GTC GTG CTC ACT GCC GGG TGT CGC TTC ACT CAG GGC TTT
CCG GAG CCC TTT GAG GGC CTC TGG GTC GCC AGC GCT GAA CCA
GGT GCT CAC GAC GAG TTC TTT TGT GTC GGT GAG CAC TGT GAC
GCA CAC CTG TCC TCC ATC TTT TGC CAC GCA GCA TCC ACC ATG
CCC CTG GCC AGA GCC CCT CAT AGC CCT CCC ATG GTG ACG TTC
AGT GCC CTG TCA GCC GGC GAA AAC TAC CTC AGG CTG GTT TGC
CGG GCG TCT GGA GCC TAT CCT CCT GTT GAC ACT CTG ACC CTC
GTG AGC CAG CCT CAA CAG CCA GAA GAT GCC CCT TGC GAG ACA
TAC GCC GGA ACA AAC GCT GAC AGC ACC GGC CAC GTC GGA ATG
GCT TGC GTC CGT TCT GAC GCG CTC GCT GGG GCA GCG TGT GCA
GTC CAG CAT AGA GGC GTG ACA ACC AGC GCC CGG ATT GTG CTT
GTG CCG GCA AAT GAT GGG GCC AAA GTC GGA GCC TAT GCT GAT
GTC GAT GCC GAT TTC TAT GCC GAC GTT CCG CCT CTC CCC GAA
CCC GAG TCC GAC AGC TTG GCT GTA CAC GCA CTG TTC GTA GCC
GGG AAC ACT GAG CTG TAT GTT CAC GGG ACA GCG GCT GGC GTA
CCA TCT GCC TCC TGT AGG TGT GAC ACC AGG AGA TGC ACA TGC
GTG CTG GCT CCC GCC ACA TGG ACT GCC GGA GTG GTG CGA GAA
CTG GCG AGA GCG GCT GCT CAT GAC CTT CTG CTT GCT GTG CTG
GAC GTT CAT GCC TCA GGC CTC GCT CTC AAC CGA TCA TCC ATG
CAA GTG TAT GCC GAA TGT GGG CCT GCA GGG AGG AGA CTT CGG
GTT CAC AAT ACC GGT ACC CGG CGA CAG CGC GTG TGC GCA CGC
GGA GCT TGC GAG CCG GCT TAT CTG GTG GCA TGT GAG CTG TTG
CGG ACG GAC ACC CCA GCA CCT CGG CGA CCT CGC ATG AGT GTT
CAG CAC AGA CGG GAT AGT AGC GGG CAT TAC TAC GTG TGC TCT
GCC TAC GGC TTT TAC CCC AAG GAG ATT GTG CTG GAG ATG AGA
GCA AAT CGC AGC TGT GAT GAG CGC GCA CGC CTG TCT GGT TTC
TGG TGC AGA CAC GAT CCA CCC GCA CCT AAT GCC GAT GGC ACC
TTC TTT GCG AGG GTG TTC TGC AAA GCG CCA GAA AAC GCC CTT
CTG ATG ACC TGT GTT ACA CGT CAT GCC AGT CGC CCA CGG GCC
CTG GCC GTA CCA TGT CCC CGA CGA GCT CGT ACT CCT AGG GAA
AGA TGG GCC GCA CTG CTC ACG GTG TTG GCA CGC GTC CCC TGG
AGT GCT GTG CTG TTG GCG CTG GCC ATG GGA GCA GCA CCG TTG
GCT TGC GCT AGG CTC GTC CAT GCT AGG TCC ACA AGG ACG GCC
CGG AGA GCT AGG CGT GCT AGG AGA GCG TAC CCA TAC GAT GTT
CCA GAT TAC GCT TGA GGATCC

MC033 amino acid sequence

GRATMRPHVLIITLATCALRALAQVIDEHEHSEPPVSTWPDMSYLV AEMRSDSVLMR
GMLDGHEHVRCTCVPKCACLEPTLPRAALEQARSRVLDAHAGRV PGLRAPSRAAHR
RVVLTAGCRFTQGFPEPFEGWLWASAEPGAHDEFFCVGEHCDAHLSSI FCHAASTM
PLARAPHSPPMVTFSALSAGENYLRLLVCRASGAYPPVDTLTLVSQPQQPEDAPCET
YAGTNADSTGHVGMACVRS DALAGAACAVQHRGVTT SARIVLVPANDGAKVGAYAD
VDADFYADV PPLPEPESDSLAVHALFVAGNTELYVHGTAAGVPSASCRCDTRRCTC
VLAPATWTAGVVRELARAAHDL LLAVLVDVHASGLALNRRSSMQVYAE CGPAGRRLR
VHNTGTRRQRCARGACEPAYLVACELLRTDTPAPRRPRMSVQHRRDSSGHYYVCS
AYGFYPKEIVLEMRANRSCDERARLSGFWCRHDP PAPANADGTF FARVFCKAPENAL
LMTCVTRHASRPRALAVPCPRRARTPRERWAALLTVLARVPWSAVLLALAMGAAPL
ACARLVHARSTRTARRARRARRAYPYDVPDYA*GSX

Prediction of transmembrane part and signal peptide

MC080 and MC033 were analyzed using TMHH software to predict transmembrane regions and signal peptides

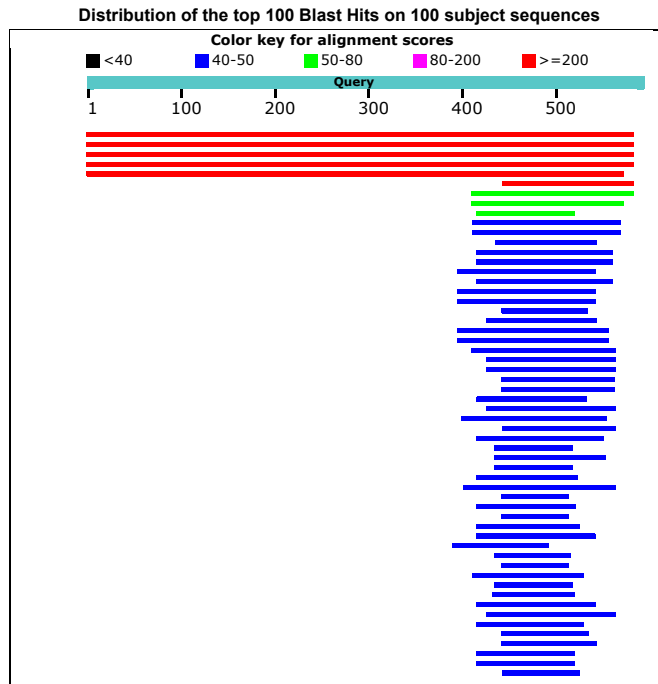
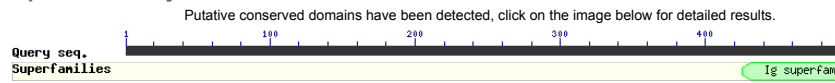


Transmembrane plot (TMHH software) was used to predict transmembrane region and signal peptide, (A) MC033; (B) MC080 <http://www.cbs.dtu.dk/services/TMHMM>

MC033 MHC-I homology using BlastT and Phyre

MC033 [Molluscum contagiosum virus subtype 1]

Graphic Summary



| Description | Max score | Total score | Query cover | E value | Ident | Accession |
|--|-----------|-------------|-------------|---------|-------|--------------------------------|
| MC033 [Molluscum contagiosum virus subtype 1] | 1161 | 1161 | 100% | 0.0 | 100% | AYO87489.1 |
| MC033 [Molluscum contagiosum virus subtype 1] | 1159 | 1159 | 100% | 0.0 | 99% | AQY17137.1 |
| MC033L [Molluscum contagiosum virus subtype 1] | 1159 | 1159 | 100% | 0.0 | 99% | NP_043984.1 |
| MC033 [Molluscum contagiosum virus subtype 1] | 1154 | 1154 | 100% | 0.0 | 99% | AQY16957.1 |
| MC033 [Molluscum contagiosum virus subtype 2] | 1041 | 1041 | 98% | 0.0 | 94% | AQY16606.1 |
| unknown [Molluscum contagiosum virus subtype 1] | 271 | 271 | 23% | 1e-85 | 100% | AAB57948.1 |
| major histocompatibility complex class I-related gene protein-like isoform X1 [Phascolarctos cinereus] | 52.4 | 52.4 | 29% | 0.002 | 26% | XP_020856818.1 |
| major histocompatibility complex class I-related gene protein-like isoform X2 [Phascolarctos cinereus] | 52.0 | 52.0 | 27% | 0.002 | 27% | XP_020856819.1 |
| patr class I histocompatibility antigen, A-2 alpha chain-like [Python bivittatus] | 50.8 | 50.8 | 17% | 0.006 | 34% | XP_025029032.1 |
| PREDICTED: zinc-alpha-2-glycoprotein-like [Monodelphis domestica] | 49.7 | 49.7 | 26% | 0.012 | 26% | XP_007477530.2 |
| zinc-alpha-2-glycoprotein-like [Monodelphis domestica] | 49.7 | 49.7 | 26% | 0.015 | 26% | NP_001311360.1 |
| LOW QUALITY PROTEIN: uncharacterized protein LOC105749203 [Sarcophilus harrisii] | 49.7 | 49.7 | 18% | 0.018 | 33% | XP_023351330.1 |
| RLA class I histocompatibility antigen, alpha chain 11/11-like isoform X2 [Phascolarctos cinereus] | 48.5 | 48.5 | 24% | 0.031 | 28% | XP_020856787.1 |
| zinc-alpha-2-glycoprotein-like isoform X1 [Phascolarctos cinereus] | 48.5 | 48.5 | 24% | 0.031 | 28% | XP_020856786.1 |
| PREDICTED: zinc-alpha-2-glycoprotein-like isoform X2 [Monodelphis domestica] | 48.9 | 48.9 | 24% | 0.036 | 25% | XP_007477543.1 |
| alpha-2-glycoprotein 1 zinc-binding protein [Phascolarctos cinereus] | 48.1 | 48.1 | 24% | 0.036 | 29% | ALX81643.1 |
| PREDICTED: uncharacterized protein LOC103096009 isoform X1 [Monodelphis domestica] | 48.5 | 48.5 | 24% | 0.041 | 25% | XP_007477542.1 |
| MHC class I antigen [Monodelphis domestica] | 48.1 | 48.1 | 24% | 0.044 | 25% | AJT46737.1 |
| major histocompatibility complex class I-related gene protein-like [Notechis scutatus] | 46.6 | 46.6 | 15% | 0.054 | 27% | XP_026546790.1 |
| zinc-alpha-2-glycoprotein-like [Phascolarctos cinereus] | 47.8 | 47.8 | 19% | 0.060 | 29% | XP_020856856.1 |
| hypothetical protein XENTR_v90022327mg [Xenopus tropicalis] | 47.0 | 47.0 | 27% | 0.078 | 24% | OCA27275.1 |

Blast Alignment of MC033: MC033 has 26 % homology to MHC I and it is restricted to a very short region of the protein with Ig-like fold

<https://blast.ncbi.nlm.nih.gov/Blast.cgi>

| | |
|---------------|---|
| Description | MC033 |
| Date | Fri Nov 9 14:13:51 GMT 2018 |
| Unique Job ID | 08d12977476c9231 |
| Sequence | MRPHVLITLA ... Download FASTA |
| Job Type | normal |

| # | Template | Alignment Coverage | MS Score | Confidence | % Id. | Template Information |
|----|------------------------|--------------------|----------|------------|-------|---|
| 1 | c3dbxA | Alignment | | 98.7 | 27 | PDB header: immune system Chain: A: PDB Molecule: cd1-2 antigen; PDBTitle: structure of chicken cd1-2 with bound fatty acid |
| 2 | c3dbxA | Alignment | | 98.7 | 26 | PDB header: immune system Chain: A: PDB Molecule: cd1-2 antigen; PDBTitle: crystal structure of the chicken pcd1-2 molecule |
| 3 | c3dbxA | Alignment | | 98.7 | 24 | PDB header: immune system Chain: A: PDB Molecule: cd1-2 antigen; PDBTitle: structure of chicken cd1-2 with bound fatty acid |
| 4 | c3dbxA | Alignment | | 98.6 | 30 | PDB header: immune system Chain: A: PDB Molecule: cd1-2 antigen; PDBTitle: crystal structure of the chicken pcd1-2 molecule |
| 5 | c3dbxA | Alignment | | 98.6 | 24 | PDB header: immune system Chain: A: PDB Molecule: cd1-2 antigen; PDBTitle: structure of chicken cd1-2 with bound fatty acid |
| 6 | c3dbxA | Alignment | | 98.6 | 26 | PDB header: immune system Chain: A: PDB Molecule: cd1-2 antigen; PDBTitle: crystal structure of the chicken pcd1-2 molecule |
| 7 | c3dbxA | Alignment | | 98.6 | 25 | PDB header: immune system Chain: A: PDB Molecule: cd1-2 antigen; PDBTitle: structure of chicken cd1-2 with bound fatty acid |
| 8 | c3dbxA | Alignment | | 98.6 | 26 | PDB header: immune system Chain: A: PDB Molecule: cd1-2 antigen; PDBTitle: crystal structure of the chicken pcd1-2 molecule |
| 9 | c3dbxA | Alignment | | 98.6 | 24 | PDB header: immune system Chain: A: PDB Molecule: cd1-2 antigen; PDBTitle: structure of chicken cd1-2 with bound fatty acid |
| 10 | c3dbxA | Alignment | | 98.6 | 26 | PDB header: immune system Chain: A: PDB Molecule: cd1-2 antigen; PDBTitle: crystal structure of the chicken pcd1-2 molecule |
| 11 | c3dbxA | Alignment | | 98.6 | 25 | PDB header: immune system Chain: A: PDB Molecule: cd1-2 antigen; PDBTitle: structure of chicken cd1-2 with bound fatty acid |

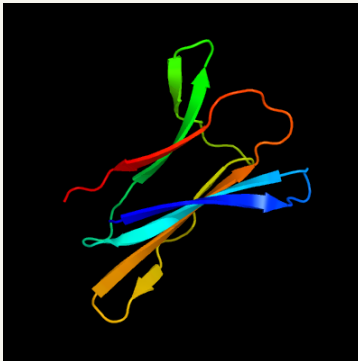


Image coloured by rainbow N → C terminus
Model dimensions (Å): X:30.599 Y:31.048 Z:46.368

Top model

Model (left) based on template [c3dbxA](#)

Top template information

PDB header:immune system
Chain: A: **PDB Molecule:**cd1-2 antigen;
PDBTitle: structure of chicken cd1-2 with bound fatty acid

Confidence and coverage

Confidence: **98.7%** Coverage: **14%**

82 residues (14% of your sequence) have been modelled with 98.7% confidence by the single highest scoring template.



You may wish to submit your sequence to [Phyre2](#). This will automatically scan your sequence every week for new potential templates as they appear in the Phyre2 library.

3D viewing

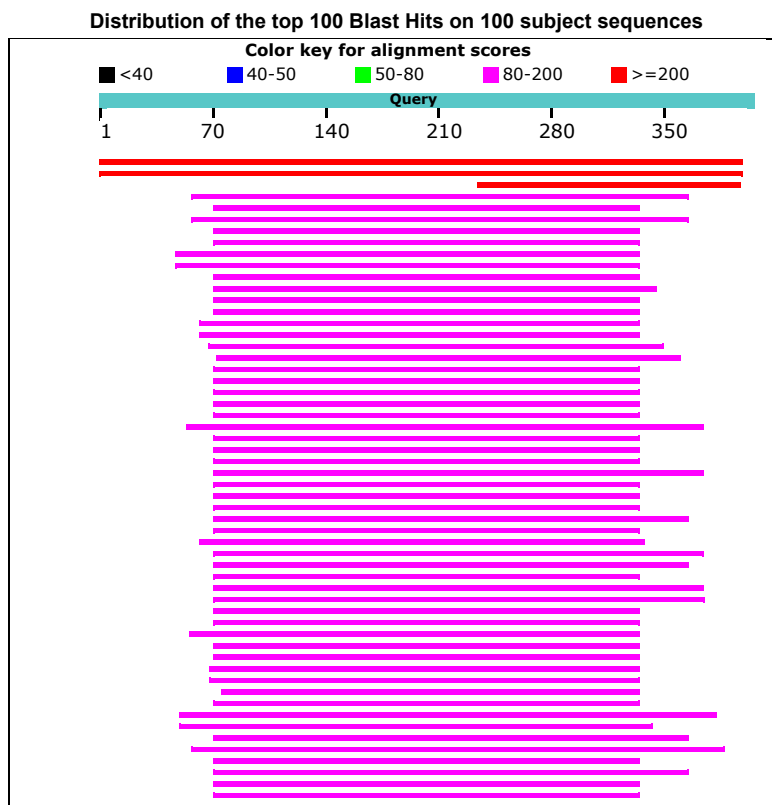
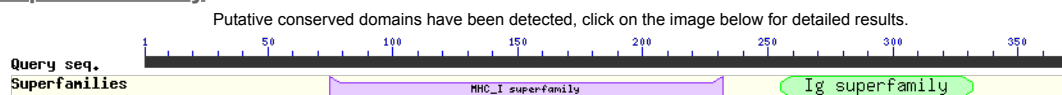
[Interactive 3D view in JSmol](#)

For other options to view your downloaded structure offline see the [FAQ](#)

The Phyre2 study of MC033: The Phyre does not model it on to MHC-I. No evidence that it is MHC-1 functional mimic. Indeed, highly questionable that it is an MHC-I homologue
<http://www.sbg.bio.ic.ac.uk/~phyre2/html/page.cgi?id=index>

MC080 MHC-I homology using BlastT and Phyre

Graphic Summary



| Description | Max score | Total score | Query cover | E value | Ident | Accession |
|---|-----------|-------------|-------------|---------|-------|--------------------------------|
| MC080R [Molluscum contagiosum virus subtype 1] | 789 | 789 | 100% | 0.0 | 100% | NP_044031.1 |
| MC080R [Molluscum contagiosum virus subtype 2] | 660 | 660 | 100% | 0.0 | 90% | AAC72821.1 |
| hypothetical protein DDJ49_30250 [Klebsiella pneumoniae] | 294 | 294 | 40% | 2e-96 | 92% | RFC01606.1 |
| SLA-11 histocompatibility antigen, class I [Sus scrofa] | 124 | 124 | 77% | 2e-28 | 29% | BAG82704.1 |
| MHC class I antigen [Ovis aries] | 122 | 122 | 66% | 8e-28 | 30% | CAJ57269.1 |
| histocompatibility antigen, class I [Sus scrofa] | 122 | 122 | 77% | 9e-28 | 29% | BBE49437.1 |
| non-MHC class I antigen [Bos taurus] | 122 | 122 | 66% | 1e-27 | 34% | ANG83508.1 |
| non-classical MHC class I antigen [Bos taurus] | 122 | 122 | 66% | 1e-27 | 34% | AAZ74695.1 |
| HLA class I histocompatibility antigen, B-40 alpha chain-like isoform X1 [Trichechus manatus latirostris] | 122 | 122 | 72% | 1e-27 | 30% | XP_023581056.1 |
| HLA class I histocompatibility antigen, B-40 alpha chain-like isoform X2 [Trichechus manatus latirostris] | 122 | 122 | 72% | 1e-27 | 30% | XP_023581057.1 |
| BOLA class I histocompatibility antigen, alpha chain BL3-7-like isoform X1 [Bos taurus] | 122 | 122 | 66% | 1e-27 | 33% | XP_005223758.1 |
| BOLA class I histocompatibility antigen, alpha chain BL3-7-like isoform X3 [Bos taurus] | 121 | 121 | 68% | 2e-27 | 33% | XP_024839906.1 |
| non-MHC class I antigen [Bos taurus] | 121 | 121 | 66% | 2e-27 | 33% | ANG83507.1 |

alignment of MC080 using BlastT: The BlastT reveals that MC080 is MHC-I like molecule

<https://blast.ncbi.nlm.nih.gov/Blast.cgi>

| | |
|---------------|--|
| Description | Mc080 |
| Date | Sat Nov 10 00:20:38 GMT 2018 |
| Unique Job ID | 6d71f704c4e18f42 |
| Sequence | MTGTLILLA ... Download FASTA |
| Job Type | normal |

| | | | | | |
|---|---|---|-------|----|--|
| 1 |  |  | 100.0 | 22 | PDB header: immune system Chain: A; PDB Molecule: rfp-y class I PDBTitle: crystal structure of the ribonuclease P |
| 2 |  |  | 100.0 | 24 | PDB header: immune system Chain: A; PDB Molecule: major histocompatibility complex PDBTitle: complex of a b2i chicken mhc class II molecule peptide |
| 3 |  |  | 100.0 | 24 | PDB header: lipid binding protein Chain: A; PDB Molecule: alpha-2-glycosylase PDBTitle: an alpha-2-glycosylase; cho-tag |
| 4 |  |  | 100.0 | 28 | PDB header: immune system Chain: H; PDB Molecule: 2ab mhc class I PDBTitle: mhc class I h-2b molecule complex |
| 5 |  |  | 100.0 | 28 | PDB header: immune system Chain: A; PDB Molecule: 2 class I histocompatibility PDBTitle: crystal structure of the liver derived h2c mouse mhc class I h-2 kb |
| 6 |  |  | 100.0 | 28 | PDB header: immune system Chain: A; PDB Molecule: 2 class I histocompatibility PDBTitle: mhc class I natural region h-2ba beta 22 microglobulin and jbeta8 peptide |

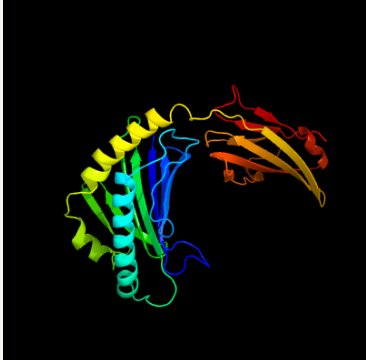


Image coloured by rainbow N → C terminus
Model dimensions (Å): X:54.822 Y:65.785 Z:60.084

Model (left) based on template [c3p73A](#)

Top template information

PDB header:immune system
Chain: A; **PDB Molecule:**mhc rfp-y class i alpha chain;
PDBTitle: crystal structures of the chicken yf1*7.1 molecule

Confidence and coverage

Confidence: **100.0%** Coverage: **66%**

261 residues (66% of your sequence) have been modelled with 100.0% confidence by the single highest scoring template.



You may wish to submit your sequence to [Phyrealarm](#). This will automatically scan your sequence every week for new potential templates as they appear in the Phyre2 library.

[3D viewing](#)

[Interactive 3D view in JSmol](#)

For other options to view your downloaded structure offline see the [FAQ](#)

The Phyre2 study of MC080: The Phyre provides that MC080 has homology to MHC-I

Primers to produce RAdmc033 and RAdmc080

were ordered from Eurofins MWG

mc033-Forward primer:

TGAACCGTCAGATCGCCTGGAGACGCCATCCACGCTGTTTTGACCTCCATAGAAGA
CACCGGGACCGATCCAGCCTGGATCCGCCACCATGAGGCCCCAC

mc033-Reverse primer:

TAGAGTATACAATAGTGACGTGGGATCCTTACGTAGAATCAAGACCTAGGAGCGGG
TTAGGGATTGGCTTACCAGCGCTCGCTCTCCTAGCACGCCTAGC

mc080-Forward primer:

ACCGTCAGATCGCCTGGAGACGCCATCCACGCTGTTTTGACCTCCATAGAAGACAC
CGGGACCGATCCAGCCTGGATCCGCCACCATGACCGGTACCCTC

mc080-Reverse primer:

AGTATACAATAGTGACGTGGGATCCTTACGTAGAATCAAGACCTAGGAGCGGGTTA
GGGATTGGCTTACCAGCGCTAAATCCAGCTCTCTCTGAGGGC

The green letters are V5, the red letters are the actual primer of gene, the blue letters are the link and the black letters are the region of homology.

Primer used to Confirm the sequence of the insert of RAdmc033 and RAdmc08:

Forward primer:

5-CCA TGG TGA TGC GGT TTT G-3

Reverse primer:

5- AAC TAC ATA AGA CC CCA CC-3

PCR using Phusion® High-Fidelity DNA Polymerase

(M0530L, New England Biolabs) kit

Sample PCR reaction mixture for 50 µl total volum

5x Buffer: 10 µl

DNA: 1 µl

Primers (F+R): 2.5 µl of 100 µM each

DMSO: 1.5 µl

Enzyme: 0.5 µl

dNTPs: 1 µl

dH₂O 33.5 µl

PCR program

Initial denaturation 98°C for 45 seconds then

Denaturation: 98°C for 12 seconds
Annealing: 55°C for 40 seconds 36 cycles
Extension: 72°C for 2 minutes

Final extension 72°C for 12 minutes

Expand High fidelity (HIFI, 11732 641001, Roche)/Taq polymerase

Sample PCR reaction mixture for 50 µl total volume

10x Buffer: 5 µl
DNA: 1 µl
Primers (F+R): 2.5 µl of 100 µM each
DMSO: 1.5 µl
Enzyme: 0.5 µl
dNTPs: 1 µl
dH₂O 38.5 µl

PCR program

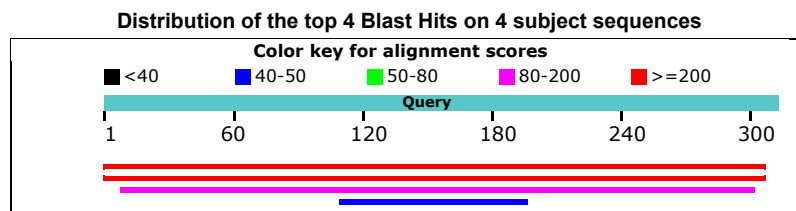
Initial denaturation 94°C for 2 minutes then

Denaturation: 94°C for 15 seconds
Annealing: 55°C for 30 seconds 9 cycles
Extension: 72°C for 2 minutes

Denaturation: 98°C for 15 seconds
Annealing: 55°C for 30 seconds 24 cycles
Extension: 72°C for 2 minutes + 5 seconds (increase 5 seconds every cycle)

Final extension 72°C for 7 minutes

UL142 MHC-I homology using BlastT and Phyre



| Description | Max score | Total score | Query cover | E value | Ident | Accession |
|---|-----------|-------------|-------------|---------|-------|--------------------------------|
| membrane glycoprotein UL142 [synthetic human betaherpesvirus 5] | 621 | 621 | 100% | 0.0 | 100% | AVT50373.1 |
| membrane glycoprotein UL142 [synthetic human betaherpesvirus 5] | 580 | 580 | 100% | 0.0 | 95% | ATP76408.1 |
| membrane glycoprotein UL142 [Panine betaherpesvirus 2] | 82.8 | 82.8 | 95% | 3e-14 | 23% | NP_612759.2 |
| PREDICTED: LOW QUALITY PROTEIN: class I histocompatibility antigen, F10 alpha chain-like [Anser cygnoides domesticus] | 40.0 | 40.0 | 28% | 4.0 | 31% | XP_013026254.1 |

The alignment of UL142 using BlastT : UL142 is MHC I homologue

| | |
|---------------|--|
| Description | UL142_____ |
| Date | Fri Nov 9 15:04:30 GMT 2018 |
| Unique Job ID | b07652a172cd14b5 |
| Sequence | MRIEWACWLF ... Download FASTA |
| Job Type | normal |

Top model

Model (left) based on template [c4gupA](#)

[Top template information](#)

PDB header: immune system
Chain: A: **PDB Molecule:** major histocompatibility complex class i-related gene
PDBTitle: structure of mhc-class i related molecule mr1

Confidence and coverage:
Confidence: **100.0%** Coverage: **78%**

238 residues (78% of your sequence) have been modelled with 100.0% confidence by the single highest scoring template.

[3D viewing](#)

[Interactive 3D view in JSmol](#)

For other options to view your downloaded structure offline see the [FAQ](#)

Image coloured by rainbow N → C terminus
Model dimensions (Å): X:66.411 Y:56.353 Z:56.842

1 [c4gupA](#) Alignment

The Phyre2 study of UL142: structural prediction (Phyre 2) clearly show UL142 to be a Class I like protein with evidence of a peptide binding groove and similarity across the molecule. It probably does not bind β 2m